

AD-A155 024

SEAT EXPERIMENTS FOR THE FULL-SCALE TRANSPORT AIRCRAFT  
CONTROLLED IMPACT. (U) RMS TECHNOLOGIES INC TREVOSE PA  
M R CANNON ET AL. MAR 85 DOT/FAR/CT-84/10

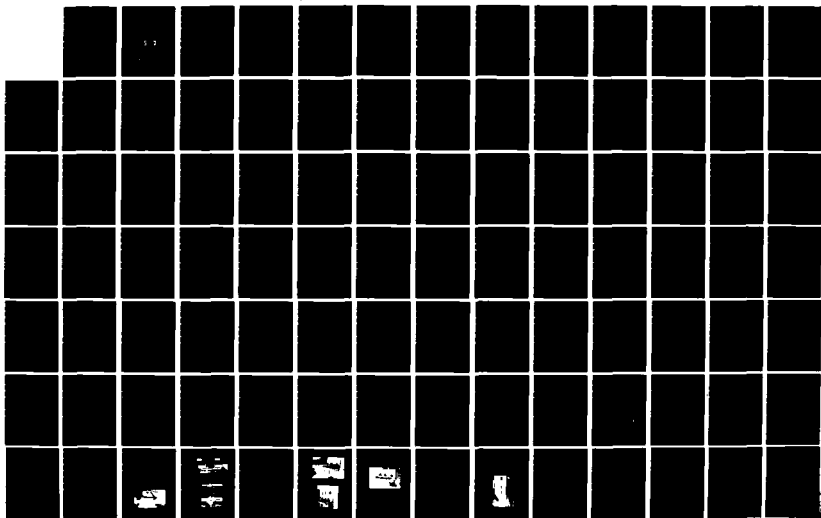
1/3

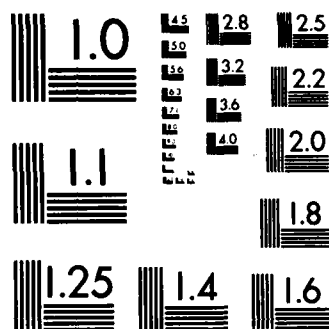
UNCLASSIFIED

DTFA03-81-C-00040

F/G 1/3

NL





MICROCOPY RESOLUTION TEST CHART  
NATIONAL BUREAU OF STANDARDS-1963-A

85 02 9 98

85 520 052

2

DOT/FAA/CT-84/10

# Seat Experiments for the Full-Scale Transport Aircraft Controlled Impact Demonstration

AD-A155 024

Mark R. Cannon  
Richard E. Zimmermann

RMS Technologies, Inc./Simula Inc.  
Trevose, PA/Tempe, AZ



March 1985  
Final Report

This document is available to the U.S. public  
through the National Technical Information  
Service, Springfield, Virginia 22161.

DTIC FILE COPY



US Department of Transportation  
**Federal Aviation Administration**  
Technical Center  
Atlantic City Airport, N.J. 08405

#### NOTICE

This document is disseminated under the sponsorship of the Department of Transportation in the interest of information exchange. The United States Government assumes no liability for the contents or use thereof.

The United States Government does not endorse products or manufacturers. Trade or manufacturer's names appear herein solely because they are considered essential to the object of this report.



# PREFACE

This report describes the transport seat crashworthiness project conducted by RMS Technologies, Inc. (RMS) and Simula Inc. under Federal Aviation Administration (FAA) Technical Center Contract DTFA03-81-C-00040. This was a combined effort to design and fabricate experimental passenger seats to be included as test specimens in the joint FAA and National Aeronautics and Space Administration (NASA) Full-Scale Transport Aircraft Controlled Impact Demonstration (CID). Technical monitor for the FAA Technical Center was Mr. Dick Johnson, FAA Transport Program Manager. The contractor's technical monitor was Mr. Roger Lloyd, Program Manager.

Accession For	
NTIS GRA&I	<input checked="" type="checkbox"/>
DTIC TAB	<input checked="" type="checkbox"/>
Unannounced	<input type="checkbox"/>
Justification	
By	
Distribution/	
Availability Codes	
Dist	Avail and/or Special
A/1	



## EXECUTIVE SUMMARY

As part of the FAA/NASA Controlled Impact Demonstration (CID) with a four-engine jet transport, 22 experimental seats have been placed on the aircraft by the contractor for the FAA. Four additional experimental seats have been directly installed by NASA and the FAA. Also, an originally installed pilot seat was included in the overall series of 27 seat experiments. Of the 22 seats installed by the contractor, 13 have been modified for the intent of improving their structural crashworthiness. These include 12 triple-occupant passenger seats and one flight attendant seat.

The modification process was supported by extensive testing and analysis. Initially, identical seats were subjected to both static and dynamic destructive tests. From these tests, much was learned about the failure modes of the seat structure and the loads at which they would occur. Using these data, a design effort (supported by NASTRAN finite element models of the seats) produced methods for improving the capability of the seat structure to sustain crash loads. Prototypes of the designs were fabricated and subjected to identical static and dynamic testing sequences. Where necessary, design improvements were made and retested. Modified experimental seats were then fabricated for installation on the test aircraft.

While final conclusions must await the completion of the CID findings, development tests have shown that a great improvement in crashworthiness can be achieved with only a small percentage in weight increase. This weight increase is representative of prototype construction, and could be reduced in a production design.

## TABLE OF CONTENTS

	<u>Page</u>
PREFACE. . . . .	iii
EXECUTIVE SUMMARY. . . . .	iv
LIST OF TABLES . . . . .	xi
INTRODUCTION . . . . .	1
CRITERIA . . . . .	2
ASSUMPTIONS. . . . .	4
PRIOR DEVELOPMENT. . . . .	6
RESEARCH AND DEVELOPMENT. . . . .	6
AVSER. . . . .	6
NASA . . . . .	6
THE BOEING COMPANY . . . . .	6
NAVAL AIR DEVELOPMENT CENTER (NADC). . . . .	6
MANUFACTURED SEATS. . . . .	6
HARDMAN. . . . .	7
GENERAL DYNAMICS CORPORATION, CONVAIR DIVISION . . . . .	7
DOUGLAS AIRCRAFT COMPANY . . . . .	7
TECO . . . . .	7
AEROTHERM (UOP INC., AEROSPACE DIVISION) . . . . .	8
THE WEBER CORPORATION. . . . .	8
FAIRCHILD BURNS COMPANY. . . . .	8
OTHER MANUFACTURED SEATS . . . . .	9
OTHER CRASHWORTHY FEATURES . . . . .	9
INJURY MECHANISMS. . . . .	10
SEAT/RESTRAINT FAILURE. . . . .	10
ADJACENT SEAT FAILURE . . . . .	10
FLAILING. . . . .	10
FIRE. . . . .	11
CRASH TEST AIRCRAFT EXPERIMENTAL SEATS. . . . .	11
CAMI DYNAMIC TESTS . . . . .	12

## TABLE OF CONTENTS (CONTD)

	<u>Page</u>
MODIFICATION PROCEDURE . . . . .	13
SEAT PROCUREMENT . . . . .	13
DESTRUCTIVE TESTS . . . . .	13
STATIC TESTS . . . . .	14
DYNAMIC TESTS . . . . .	14
MODIFICATION PROCESS . . . . .	14
STATIC VERIFICATION TESTS . . . . .	15
DYNAMIC VERIFICATION TESTS . . . . .	16
ADDITIONAL SEAT MODIFICATIONS . . . . .	16
TRACK FITTINGS . . . . .	17
EXISTING FITTINGS . . . . .	17
BROWNLIN FITTING . . . . .	17
ANCRA FITTING . . . . .	17
SABRE FITTING . . . . .	17
UOP FITTING . . . . .	17
TRACK FITTING STRENGTHS AND WEIGHTS . . . . .	17
CONCEPTS FOR NEW FITTINGS . . . . .	18
FIRST PROTOTYPE FITTING . . . . .	19

## TABLE OF CONTENTS (CONTD)

	<u>Page</u>
PLASTIC HINGE CONCEPT . . . . .	20
SECOND PROTOTYPE FITTING. . . . .	20
MODIFICATION CONCEPTS. . . . .	22
ROTATING AND TRANSLATING SEATS. . . . .	23
ENERGY-ABSORBING RESTRAINT SYSTEMS. . . . .	25
LOAD PATHS. . . . .	25
TORSIONAL RIGIDITY. . . . .	26
LATERAL BRACING . . . . .	26
AFT-FACING SEATS. . . . .	27
SEAT MODIFICATIONS . . . . .	29
STANDARD WEBER SEAT . . . . .	29
SEAT DESCRIPTION . . . . .	29
RESULTS OF FORWARD STATIC TEST . . . . .	30
RESULTS OF FORWARD DYNAMIC TEST. . . . .	30
WEBER MOD I SEAT. . . . .	30
MODIFICATION CONCEPT . . . . .	30
MODIFICATION DETAILS . . . . .	30
ENERGY ABSORBERS . . . . .	31
RESULTS OF FORWARD STATIC TEST . . . . .	31
RESULTS OF LATERAL STATIC TEST . . . . .	31
RESULTS OF DYNAMIC TEST. . . . .	31
WEIGHT DISCUSSION. . . . .	32
WEBER MOD II SEAT . . . . .	32
MODIFICATION CONCEPT . . . . .	32
MODIFICATION DETAILS . . . . .	32
ENERGY ABSORBERS . . . . .	32
RESULTS OF FORWARD STATIC TEST . . . . .	33
RESULTS OF LATERAL STATIC TEST . . . . .	33
RESULTS OF DYNAMIC TEST. . . . .	33
WEIGHT DISCUSSION. . . . .	34

## TABLE OF CONTENTS (CONTD)

	<u>Page</u>
STANDARD UOP SEAT . . . . .	34
SEAT DESCRIPTION . . . . .	34
RESULTS OF FORWARD STATIC TEST . . . . .	35
RESULTS OF FORWARD DYNAMIC TEST. . . . .	35
UOP MOD I SEAT. . . . .	35
MODIFICATION CONCEPT . . . . .	35
MODIFICATION DETAILS . . . . .	36
ENERGY ABSORBERS . . . . .	36
RESULTS OF FORWARD STATIC TEST . . . . .	37
RESULTS OF LATERAL STATIC TEST . . . . .	37
RESULTS OF DYNAMIC TEST. . . . .	37
WEIGHT DISCUSSION. . . . .	38
UOP MOD II SEAT . . . . .	38
MODIFICATION CONCEPT . . . . .	38
MODIFICATION DETAILS . . . . .	38
ENERGY ABSORBERS . . . . .	39
RESULTS OF STATIC TEST . . . . .	39
RESULTS OF LATERAL TEST. . . . .	39
RESULTS OF DYNAMIC TEST. . . . .	39
WEIGHT DISCUSSION. . . . .	40
STANDARD WEBERLITE SEAT . . . . .	40
SEAT DESCRIPTION . . . . .	40
RESULTS OF FORWARD STATIC TEST . . . . .	41
RESULTS OF FORWARD DYNAMIC TEST. . . . .	42
WEBERLITE MOD SEAT. . . . .	42
MODIFICATION CONCEPT . . . . .	42
MODIFICATION DETAILS . . . . .	42
ENERGY ABSORBERS . . . . .	43
RESULTS OF FORWARD STATIC TEST . . . . .	43
RESULTS OF LATERAL STATIC TEST . . . . .	43
RESULTS OF DYNAMIC TEST. . . . .	43
WEIGHT DISCUSSION. . . . .	44
WEBER AFT-FACING MOD SEAT . . . . .	44
MODIFICATION DETAILS . . . . .	44
ENERGY ABSORBERS . . . . .	45
RESULTS OF FORWARD STATIC TEST . . . . .	45
RESULTS OF LATERAL STATIC TEST . . . . .	45
RESULTS OF DYNAMIC TEST. . . . .	46
WEIGHT DISCUSSION. . . . .	46

## TABLE OF CONTENTS (CONTD)

	<u>Page</u>
STANDARD TRANS-AERO FLIGHT ATTENDANT SEAT . . . . .	47
SEAT DESCRIPTION . . . . .	47
RESULTS OF DOWNWARD STATIC TEST . . . . .	48
MODIFIED TRANS-AERO FLIGHT ATTENDANT SEAT . . . . .	48
MODIFICATION CONCEPT . . . . .	49
MODIFICATION DETAILS . . . . .	49
RESULTS OF DOWNWARD STATIC TEST . . . . .	50
WEIGHT DISCUSSION . . . . .	50
AIRCRAFT TEST SETUP. . . . .	51
FLOOR PLAN . . . . .	51
ANTHROPOMORPHIC DUMMIES . . . . .	51
INSTRUMENTATION . . . . .	53
ACCELEROMETERS . . . . .	53
LAP BELT TENSIO METERS . . . . .	53
SECONDARY RESTRAINT . . . . .	54
FLIGHT ATTENDANT SEATS INSTALLATION . . . . .	54
DISCUSSION . . . . .	55
CONCLUSIONS . . . . .	60
REFERENCES . . . . .	63
ILLUSTRATIONS AND PHOTOGRAPHS . . . . .	68
APPENDIX A - CRASH ENVIRONMENT AND DESIGN PULSES FOR TRANSPORT CATEGORY AIRCRAFT . . . . .	198
APPENDIX B - FINITE ELEMENT STRUCTURAL ANALYSIS OF SEATS . . . . .	202
APPENDIX C - FLOOR TRACK STRENGTH . . . . .	215

TABLE OF CONTENTS (CONTD)

	<u>Page</u>
APPENDIX D - LONGITUDINAL LOAD LIMITING . . . . .	218
APPENDIX E - LAP BELT ENERGY ABSORBERS . . . . .	221
APPENDIX F - LEG BRACING OPTIONS . . . . .	229
APPENDIX G - LAP BELT ENERGY ABSORBER COMPONENT TESTS . . . . .	232



## LIST OF TABLES

<u>Table</u>		<u>Page</u>
1	Floor Reactions as a Function of Occupancy . . . . .	5
2	Track Fitting Test Results . . . . .	18
3	First Prototype Track Fitting Test Results . . . . .	19
4	Second Prototype Track Fitting Test Results. . . . .	21
5	Breakdown of Weight Increases for the Weber MOD I Seat . . .	32
6	Breakdown of Weight Increases for the Weber MOD II Seat. . .	34
7	Breakdown of Weight Increases for the UOP MOD I Seat . . . .	38
8	Breakdown of Weight Increases for the UOP MOD II Seat. . . .	40
9	Breakdown of Weight Increases for the Weberlite MOD Seat . .	44
10	Breakdown of Weight Increases for the Weber Aft-Facing MOD Seat . . . . .	47
11	Locations and Quantities of Seat and Dummy Accelerometers. .	52
12	Relative Transport Sizes . . . . .	56

## INTRODUCTION

The purpose of this project was to design and fabricate experimental passenger seats to be included in the joint FAA/NASA Controlled Impact Demonstration of a four-engine, commercial transport aircraft. This test was conducted in December 1984, at the NASA Dryden Flight Research Facility at Edwards Air Force Base, California.

The experiments were centered around existing transport seats and modifications. Both used and new seats were purchased and subjected to destructive static and dynamic tests. In the static tests, the loads were applied slowly, so that deformations and failures could be observed as they occurred. In the dynamic tests, seats (with dummies) were installed on a sled which was abruptly decelerated in a controlled manner, to approximate a survivable crash environment in a transport aircraft.

Using the data gathered from the destructive tests, concepts were developed for improving the crashworthiness of the seats. In this project, the emphasis was on modifying the seat to prevent structural failure. The experiments did not deal with the delethalization (padding, rounding, and blunting of structural components to reduce injury due to seat-occupant impact) of the seats, and only a limited effort was applied toward reducing the combustibility of the seats. The structural modifications included reinforcement, pinned joints and other releases to prevent the development of destructive bending or torsional stresses, and sufficient energy-absorbing capability to enhance the ability of the structure to survive a crash environment as efficiently as possible.

After the seats were modified, they were again subjected to the same static and dynamic tests to verify that the modifications had achieved their intended results. Then, additional identical seats were modified for use as test specimens aboard the test aircraft.

Except in certain cases involving individual seat installations, a modified and an unmodified seat configuration were placed on the aircraft. The seats were placed in a forward-facing position, except for three seats, which were placed in an aft-facing position. The seats are occupied by anthropomorphic dummies. Selected dummies and seats were instrumented with accelerometers and lap belt tensiometers.

After the crash test, the performance of the various modification concepts will be evaluated. Evaluations will be performed visually, by examination of high-speed photographic coverage, and by analysis of the accelerometer and tension-meter data. The data will also be correlated with computer simulations, and the results used to extrapolate further data and to assess injury potential.

reference 11. Critical structural interfaces were released from bending and torsional moments so that deformation could occur without developing destructive stresses, and energy-absorbing features were employed to limit the loads acting on the structure.

The design goals for each of the modifications were based on the criteria from Appendix A. Specifically, the modified seats were designed to survive a forward 18-G, 35-ft/sec triangular acceleration pulse. (For reasons discussed in Appendix D, this was reduced from the 50-ft/sec velocity change recommended in Appendix A.) In most cases, the seats were designed to withstand static loads of 10 G in the lateral and downward directions. These requirements are not as extensive as the full design test criteria in Appendix A. However, they demonstrate improvements in crash survivability relative to existing standards. Lateral energy absorption was not included because it was assumed that encroachment into the aisle would be undesirable. Lateral dynamic tests were not conducted because test samples were limited.

Finite element models were used to support a design process resulting in structures which would meet these criteria with a minimum of additional weight. Modified or replacement parts were designed based largely on the computer models, and stress analyses of fittings and fasteners were conducted to assure structural integrity. Appendix B describes the finite element techniques which were used.

After design and fabrication, the modification components were installed on the standard seat structure. Some were replacement parts, while others reinforced existing components. For some of the seats, the modification could possibly be a retrofit kit. For other seats, retrofitting would not be feasible, but the modifications would demonstrate a means by which newly built seats could be fabricated to improve crashworthiness.

#### STATIC VERIFICATION TESTS.

After the seats were modified, they were statically tested. The tests were done to assure that the seat had the strength characteristics predicted by the design and analysis effort. The same test procedure previously featured in the destructive static tests was used. However, if the seat successfully sustained the design loads, it was not necessarily pulled to destruction. This allowed the seat to be used in other static tests (No dynamic test specimen was subjected to prior tests.)

During the initial destructive tests, forward, downward, and lateral tests were conducted. It was found that lateral failure occurred at the location of the maximum bending moment in the legs. When new seats were purchased for further testing, it was decided not to purchase seats for a lateral test because the ultimate loads were relatively low and reasonably predictable. Also, during the downward tests, it was found that the seats tended to be stronger than required in this direction. In some cases, the seats approached or exceeded the desired 10-G strength in the unmodified condition.

When the modified seats were tested, it was decided that the forward and lateral tests were of the most concern. The lateral tests were of particular interest because changes had been made to greatly increase the lateral strength; it was desired to determine what the modified ultimate strength was. Downward

STATIC TESTS. The destructive static tests were conducted at Simula Inc. Sections of heavy-duty Browline floor track having the same critical dimensions as the track in the test aircraft were attached to a rigid fixture mounted in a rigid loading frame. No attempt was made to simulate the flexibility of an aircraft floor. The seat was placed on the fixture, and body blocks approximately in accordance with NAS 809, were then secured to the seats with the lap belts. The blocks were slightly modified to better approximate the actual geometry of an occupant under loaded conditions (see figure 11).

Hydraulic cylinders were connected to each of the body blocks, with load cells at the interface. The cylinders were connected to a common hydraulic power unit so that the same pressure would be applied to each cylinder and approximately the same load would be applied to each body block. The presence of three load cells permitted recording the exact load applied to each of the body blocks.

The cylinders were used to apply loads in the three most critical directions, as is illustrated in figures 12 through 14. String potentiometers were connected to points of interest on the structure to record displacement as deformation occurred. In most cases, the motion of the rear transverse seat pan tube was measured in the forward and downward directions at the center of each seat position while the lateral displacement was measured at one end of the tube.

Force and deflection data were recorded on magnetic tape as the load was increased to ultimate failure. Later, these data were digitized, processed, and plotted in the form of applied force versus deflection curves for the different seat positions. Numerous pretest and posttest photographs of the seat were taken.

DYNAMIC TESTS. Dynamic tests were conducted at the FAA/CAMI facility in Oklahoma City, Oklahoma. The seats were mounted on a sled which is accelerated by a falling weight. The sled impacts an array of wires which are pulled through a selected arrangement of pins and absorb the energy necessary to stop the sled with the desired deceleration. Redundant tiedown straps are attached to the dummies in case of ultimate seat failure.

The seats were installed on sections of floor track which were mounted on load cells so the floor reaction forces could be measured. The tracks could also be pitched and rolled 10 degrees to simulate floor warpage. One track was pitched, and the other was rolled.

Instrumented anthropomorphic dummies were installed in the seats and secured with lap belts. The belts were instrumented with tensiometers. High-speed motion pictures were taken during the test, while still photographs were taken before and after the test. The tests were conducted with a 9-G 50-ft/sec pulse equivalent to that used by CAMI in prior seat testing.

#### MODIFICATION PROCESS.

The modification process began with careful examination of the results of the destructive tests. From the mode of failure, ideas for improving structural integrity were generated. Also, a finite element model of the seat was used to identify areas where reinforcement would be most useful, and to evaluate the effectiveness of reinforcement concepts. Basic principles of crashworthiness were applied in accordance with the design philosophy provided under

## MODIFICATION PROCEDURE

Seats were modified in a multi-step process. First, the selected seats were subjected to both static and dynamic destructive testing to determine the ultimate structural strengths and failure modes. Then, concepts for improving the structural integrity in a crash were developed. Layouts of promising concepts were prepared to examine their feasibility, and finite element models were used to analyze the structural stresses resulting in the proposed modification. Detailed designs for the modification components were then prepared. The necessary parts were fabricated, the seats modified accordingly, and static verification tests conducted to show that the modified structure performed as anticipated. Dynamic verification tests were also conducted to further establish confidence in the design. Finally, additional identical seats were modified and installed on the test aircraft.

### SEAT PROCUREMENT.

The following seats were selected and procured for the modification program:

- Weber P/N 819493, triple-occupant seat - 20 ea.
- Weberlite 4000, triple-occupant seat - 10 ea.
- UOP Model 901, triple-occupant seat - 14 ea.
- Trans-Aero Model 90835-4, flight attendant seat - 4 ea.

In each case, equal quantities of right- and left-hand passenger seats were purchased.

The Weber P/N 819493 seat was selected because it was representative of seat designs on early, narrow-body aircraft, such as the Boeing 707/720 and Douglas DC-8 aircraft, and presented a baseline consistent with the airframe. The seat has a tubular steel leg structure typical of many transport seats. As a later design, the Weberlite 4000 is very similar to the Weber P/N 819493 in appearance, but is approximately 30 lb lighter. Therefore, it was chosen as a sample of a modern lightweight structure with a design similar to the older seats. The UOP Model 901 seat was selected because it is also a modern lightweight seat but the leg construction uses built-up sheet metal members rather than steel tubing. The Trans-Aero Model 90835-4 flight attendant seat is used on the Boeing 737, and was selected as a representative of present day flight attendant seats. Flight attendant seats from the era of the Boeing 727 were not included because there was not enough space available to mount more flight attendant seats.

### DESTRUCTIVE TESTS.

Two destructive tests were run: static and dynamic. The static tests permitted the application of loads at controlled rates so that the sequence and mode of failure could be easily observed. The dynamic tests were conducted to observe the effects of an actual crash condition.

## CAMI DYNAMIC TESTS

The results of some of the numerous dynamic tests of commercial transport seats conducted by CAMI are reported in reference 9. These tests were conducted with fixtures which could pitch and roll the floor tracks in accordance with reference 11, to simulate warpage of the aircraft floor. Just prior to the test, one track was pitched 10 degrees and the other was rolled 10 degrees.

The seats were subjected to rectangular dynamic deceleration pulses of 6, 9, and 12 G with a 50-ft/sec velocity change. Instrumented anthropomorphic dummies were installed in the seats, and the floor track segments which the seat was attached to were mounted on load cells. High-speed photographs of the test were also taken.

First, the CAMI tests showed that many seats fail when floor distortion is introduced, and before any inertial loads are applied. Either the fittings fail, or the overall structure fails because it is too rigid to accommodate any distortion of the floor.

Secondly, the CAMI tests demonstrated that the typical transport seat, designed and certified for a 9-G longitudinal static load, cannot withstand a 9-G dynamic pulse with appreciable velocity change. Many seats were already highly stressed because of the floor warpage, but almost none of them survived a 9-G, 50-ft/sec pulse. None survived a 12-G, 50-ft/sec pulse. The results were usually catastrophic, with the restraints separating from the seat, the seat separating from the legs, or the legs separating from the floor tracks.

The load cells under the floor track segments showed the magnitude of the dynamic overshoot effects which cause a seat certified at 9 G statically to fail catastrophically in a 9-G dynamic test. Peak reaction forces on the seat legs were as much as 70 percent greater than they would have been if a 9-G load were applied statically.

the backs which will deform upon head impact (reference 9). The armrest is also a potential point of head impact, and should be designed accordingly (reference 34).

According to reference 35, impact of the occupant's leg with the rear of the seat can cause fracture, and thus make egress from the aircraft impossible. Such impacts place additional stress on the seat ahead, and may increase the probability of its failure.

The lap belt itself can cause injury to the occupant as it applies load to restrain him (reference 36). Generally, the looser the belt is worn the greater the probability of injury. The anchorage location of the belt is also related to the belt's injury potential (reference 11). However, the anchorage location is acceptable on most present day transport seats.

#### FIRE.

Seat failures may cause the death of occupants who survived the crash with minor or no injury if the failure of other seats blocks their egress from the aircraft. In accidents involving high lateral impact loads, there is a relatively high risk of this because seats presently have no lateral bracing because of the minimum lateral load requirements. The failed seats are therefore likely to block the aisle (Appendix A).

Seats can also pose a hazard by providing a source of combustible materials (cushions and upholstery) which can burn rapidly and produce toxic fumes. Considerable research has been done in this area by the FAA Technical Center in Atlantic City, New Jersey.

#### CRASH TEST AIRCRAFT EXPERIMENTAL SEATS.

The experimental seats involved only the first hazard discussed previously: catastrophic failure of the seat/restraint structure. The experiments were prepared by modifying commercial transport seats instead of creating new ones, due to time and funding limitations. The seats were modified in various ways to explore means of solving the most serious problem in a severe crash: collapse of the seat structure or separation of the seat structure from the floor. Improved delethalization would be difficult to accomplish in a modification effort. Therefore, delethalization of the seat was not addressed. Neither was the risk due to fire, except for covering some of the existing seat cushions with a fire-retardant fabric.

## INJURY MECHANISMS

An occupant in a transport crash is subjected to a number of injury-causing hazards related to his own seat or adjacent seats. These include impact with other objects due to seat or restraint failure, impact by other failed seats, and impact with other objects or himself due to flailing of the body. Injuries may also result from fire due to entrapment.

### SEAT/RESTRAINT FAILURE.

If the seat or restraint system experiences an ultimate failure, the occupant continues to travel at or near his initial velocity while the surrounding aircraft structure is being decelerated. Eventually, he impacts some object and loses his relative velocity to the aircraft in a very short distance. This secondary deceleration is frequently more injurious than the primary one the occupant would have experienced had the seat or restraint system not failed. The reason for this is that the second deceleration is sometimes higher, and can involve impacts with sharp objects.

Secondary impact problems can occur with or without the mass of the seat. The occupant may break free from the seat if the restraint or its anchorage fails, or the entire seat or some portion of it may break free from the floor. Current regulations call for a 33 percent fitting factor (margin of safety) in restraint anchorages and seat track fittings, so a probable failure is for the seat to break away without its legs. The occupant striking other objects with the seat still strapped to him obviously is more likely to be injured due to the mass of the seat applying additional inertial load.

Seat failure in the downward direction can also be extremely hazardous to the occupant. When he is finally decelerated due to impact with the floor, he may very likely experience higher vertical acceleration than he would ever have experienced had he been seated on a rigid seat which did not fail. Uncontrolled seat failure does not benefit the occupant under any circumstances.

### ADJACENT SEAT FAILURE.

An occupant remaining in his position can still be subjected to secondary impacts by seats adjacent to him, or most likely, seats immediately behind him. In the extreme case where he is the sole occupant of a triple-occupant seat and the one to his rear is full, that seat could experience ultimate failure, impact his seat and cause it to fail. The worst case would be a domino effect resulting in the seats piling up in the front of the aircraft.

### FLAILING.

If the occupant is restrained by the seat structure, he may still be injured by impact with the seats as the legs and upper body flail into them. This would primarily involve the seat directly to the front. The flailing envelope of the body is illustrated in reference 11. The most serious injuries will result from head impact with the seat backs. As discussed previously, transport seats have been designed with "breakaway" backs, which allow the backs to move forward when struck from behind. A practice encouraged by ARP 767A (reference 33) and followed by some manufacturers is to incorporate ductile structure in



This seat is the recently introduced "ultra high density" model, which permits a 29-in. seat spacing.

OTHER MANUFACTURED SEATS. Dynamic and static testing on a seat with energy-absorbing features is reported in NAFEC NA-69-5 (reference 24). This was a triple-occupant seat which was floor-mounted on one end and wall-mounted on the other. The leg assembly on the floor-mounted end had energy-absorbing characteristics, apparently similar to that of the Palomar seat. However, the manufacturer of the seat is not identified.

OTHER CRASHWORTHY FEATURES. Many seats incorporated a "breakover" feature in the seat backs which limits the force required to move the seat back forward. This represents an effort at delethalization, and is intended to reduce the probability of severe injury when an occupant impacts the seat ahead of him. All seats examined during the conduct of this program had such a feature. (A number of other seat and restraint concepts are presented in reference 32).

In view of the extensive activity involving energy-absorbing design features which took place in the 1960's, it is quite possible that other seats with such features were designed and placed aboard transport aircraft. This summary includes those seats encountered during the course of this study, but should not be considered an exhaustive literature search.

slot in the ductile steel plate as the seat rotated. Seats of this type were tested at CAMI in 1981 (reference 9). The cited reference also includes further discussion and references on seat development.

AEROTHERM (UOP INC., AEROSPACE DIVISION). This company has designed and manufactured a number of seats with energy-absorbing features. Early work was done for the Navy (reference 25), and energy-absorbing transport seats were also designed (reference 26). The model 587 and 588 seats, manufactured under the Aerotherm name and used aboard the Boeing 727 by Pan Am and others, had energy absorbers of the contracting tube type in the two rear legs so that the seat could rock forward. Test results on these devices are described in AvSER Memorandum Report M69-2 (reference 27). Some of these seats may still be in operation today aboard Boeing 727 aircraft.

According to Aerotherm brochure AOT 502, the "spacesaver" seat for the Boeing 707, 720, and 727 had energy-absorbing rear legs using a tube pulled through a die. According to brochure AOT 503 for the Zephyr II seat for the same Boeing aircraft, energy-absorbing features were optional (reference 28).

Pages 10 and 11 of the 1961-62 winter issue of the Aerotech Industries Review (reference 29) describe an aft-facing, energy-absorbing seat for the Air Force. This seat had energy-absorbing front (relative to the seat) legs which stretched as the seat rocked to the rear (relative to the seat). The seat was designed to stroke at 20 G.

Seats utilizing similar energy-absorbing mechanisms were later developed for Pan Am for use aboard the Boeing 747. However, rather than two energy-absorbing devices, these seats featured six. Each seat pan in the triple-occupant seat was connected to a floor-mounted spreader bar by a pair of energy absorbers. This seat, designated the model 723, was manufactured under the UOP Aerospace Division name, and Pan Am had thirty 747 aircraft fitted with a full complement of these seats. Side and rear views of the seat are shown in figures 8 and 9. A closeup of two of the energy absorbers is shown in figure 10.

The model 723 seats were used aboard Boeing 747 aircraft until a few years ago, when they were replaced by lighter seats. The replacement seats weigh only 55 lb each, and have some provision for energy absorption: the front legs are designed to collapse in a controlled manner.

THE WEBER CORPORATION. A triple-occupant seat with energy-absorbing devices in the rear legs (allowing rotation about the lower ends of the front legs), was developed by Weber and tested for Trans World Airlines (TWA) in 1962 in accordance with TWA specifications (reference 30). The test pulse was a 30-G half sine pulse with a 30- to 50-msec duration. Longitudinal testing was conducted with one, two, and three occupants to verify that the seat would function in spite of the highly asymmetric loading conditions that might be placed upon it. The test was also conducted with three occupants and 20 degrees of yaw.

Weber also designed and dynamically tested aft-facing seats for the Air Force (reference 31).

FAIRCHILD BURNS COMPANY. Literature on the Airstead UHD 2000 seat received from the Fairchild Burns Company (a subsidiary of Fairchild Industries, Germantown, Maryland), indicates that optional energy-absorbing front legs are available.

were all initiated by either the manufacturer or the user. In all cases, the energy absorption features were designed to reduce the loads on the structure in the forward direction. Most of this activity was initiated approximately 20 years ago, and many of the features have been abandoned over the years, presumably in the interest of reducing weight and cost. However, some of these seats are believed to still be in service, and some newly manufactured seats give some consideration to crash conditions.

HARDMAN. A lap belt energy absorption system was developed by Hardman in 1961. It utilized 304 stainless steel tension rods which were stretched by a cable and pulley arrangement. The configuration of the device and its installation are illustrated in figures 4 and 5. (Figure 4 shows only one of the two identical mechanisms). According to pages 648 and 649 of reference 23, extensive testing was conducted to establish that the device would provide adequate protection for a 35-G half sine pulse with a 30-msec duration.

Notations on various drawings suggest that the seat with the lap belt energy absorber was placed into service on transport aircraft. Hardman drawing No. 8910 identifies part numbers for double- and triple-occupant seats for American Airlines and Braniff 720 aircraft. Boeing print No. 65-14534 shows seats with this device aboard Western Airlines' 720 aircraft. The seat on the Western Airlines aircraft was identified as Part No. 7485.

The Hardman Model 8727 seat also incorporated features which enhanced its performance in a crash environment. The lap belt anchorages could travel forward as the sheet metal seat pan crushed and the rear leg rotated on its attachment points. The before and after configuration of the window-side leg assembly from a test of the seat is shown in figure 6, and the load-deformation characteristics are shown in figure 7. Considerable dynamic testing in both the forward and vertical directions was conducted on this seat by the National Aviation Facilities Experimental Center (NAFEC), and is reported in reference 24. The performance of a Hardman Model 8727 seat was also evaluated as part of the FAA Technical Center full-scale test of a RB-66 aircraft (1983).

Both types of Hardman seats described above were also found aboard the Boeing 720 test aircraft. They were apparently installed when the aircraft was purchased new.

GENERAL DYNAMICS CORPORATION, CONVAIR DIVISION. Seats designed and manufactured by Convair, and presumably used on the Convair 880, had a lap belt energy-absorbing system in which a square die on a cable was pulled through a round aluminum tube. Some of these seats have been tested at Civil Aeromedical Institute (CAMI), and others are in storage there at this time.

DOUGLAS AIRCRAFT COMPANY. A seat designed by the Douglas Aircraft Company for the Series 50 DC-8 was claimed to have some energy absorption capability. The seat was attached to the wall on one end, and had only one leg assembly. This leg assembly was made of sheet metal, and was presumably designed to absorb some energy when deformed in the forward direction. This seat was marketed under the Palomar tradename, and was manufactured for Douglas by the Hardman Company.

TECO. A seat manufactured by TECO, formerly of Burbank, California, rotated about a single cross tube under the seat pan. The energy absorber deformed a

## PRIOR DEVELOPMENT

While a comprehensive literature search was not a part of this project, readily available reports were reviewed to determine what efforts had been made to improve the crashworthiness of transport seats. During the 1960's, considerable effort was directed toward the development of improved transport seats with crashworthy features. Some projects went no further than design studies or development testing, but a number of systems were certified and placed into service.

### RESEARCH AND DEVELOPMENT.

Research and development programs pertaining to transport seats were conducted by Aviation Safety Engineering and Research (AvSER) and by the National Aeronautics and Space Administration (NASA). AvSER, a Flight Safety Foundation test facility, later became Dynamic Science, a division of Marshall Industries. The AvSER work was directed toward the conventional triple-occupant seat configuration, while the NASA work pursued a more unconventional approach.

AVSER. A program devoted to the study of transport seats was conducted under the sponsorship of NASA and the armed services. The program included design studies, computer modeling of seat-occupant systems, and dynamic testing of the seat-occupant systems. As part of this program, the front legs of a Hardman seat were replaced with inversion tube energy absorbers, and the seat was subsequently tested (reference 12). Arizona State University (ASU) participated in this program, and a design study conducted there proposed a transport seat load-limited at the floor tracks. The seat concept is shown in figure 1, with an enlarged view of the energy-absorbing floor track. The ASU work is reported in reference 13.

Additional testing conducted on transport seats at AvSER is reported in references 14 through 18.

NASA. A single-occupant transport seat was developed with the seat bucket suspended on frangible mounts and stainless steel wires. The wires were arranged to provide energy absorption in both the vertical and longitudinal directions. Figures 2 and 3 illustrate this concept, and the design and test results are described in reference 19. Earlier work explored the performance of rear-facing seats mounted on a base with a nonlinear spring characteristic (reference 20).

THE BOEING COMPANY. In 1978, The Boeing Company conducted a study of flight attendant restraint systems. The intent of the effort was to evaluate present configurations and recommend guidelines for improvement (reference 21).

NAVAL AIR DEVELOPMENT CENTER (NADC). NADC sponsored development of two different rear-facing energy-absorbing double-occupant transport seats. One design featured wire benders, and the other used Torshocks. The results are discussed in reference 22.

### MANUFACTURED SEATS.

Various seat manufacturers have developed transport seats with some provision for energy absorption. Apparently, these efforts at improving crashworthiness

The preceding argument concerning user acceptance also dismissed the development of designs using shoulder restraints, which would reduce head and neck injuries by providing upper torso restraint. The use of shoulder belts is also incompatible with the present delethalization "breakover" feature of transport seats. Such a change was also somewhat beyond the scope of the modification effort, since the existing seat backs cannot support the required loads. However, it is believed that a feasible structure for utilizing shoulder belts on transport seats could be developed. The primary question is whether they would be used.

It was assumed that compatibility with existing seat tracks and airframes was highly desirable. While a greater degree of crashworthiness would be obtained if the floor and tracks were reinforced, such reinforcement might be quite expensive; a design which could be used with the existing airframe structures would have a much higher probability of being placed into service.

Crashworthiness could also be improved if the floor tracks were symmetric with respect to the passenger seating position. The current asymmetry of the tracks causes the window-side legs of the triple-passenger seat to support twice as much load as the aisle-side legs. Consequently, under loading conditions the window-side seat experiences greater deformation, and, as tests have shown, is the first to fail. Due to the asymmetry, three occupants in the seat do not necessarily constitute the worst loading condition on the seat legs. Under a forward load, even more load is transferred to the window-side legs if the aisle-side seat is empty. This is illustrated by table 1, which shows that two occupants seated next to one another can cause higher floor reactions than three occupants. It was assumed that many new seats would still need to be designed in the present fashion, since the new generation aircraft such as the Boeing 757 and 767 use this asymmetric track configuration, and will probably be in service for 10 to 20 years. Therefore, no changes in leg location were made on any of the experimental seats.

TABLE 1. FLOOR REACTIONS AS A FUNCTION OF OCCUPANCY\*

Seat			Longitudinal floor Reactions (lb/G)	
			Window-side Leg	Aisle-side Leg
Window	Center	Aisle		
V	V	O	50	200
V	O	O	140	280
O	O	O	400	190
O	O	V	435	-15
O	V	V	320	-70
O	V	O	170	80
V	O	V	290	130

O = Occupied, V = Vacant

\*For a 1-G forward load applied to a triple-occupant transport seat with dimensions typical of those discussed in this report.

## ASSUMPTIONS

Assumptions were established during the conceptual design of the seat modifications to ensure that changes made would not render the seat incompatible or unreasonable in terms of general configuration, weight, cost, and comfort. It was assumed that the envelope of any seat must be reasonably similar to that of existing transport seats: it must permit the same seating density and provide the same amount of space for the occupant and carry-on luggage. Most significantly, the space beneath the seat must remain available for luggage and for the feet of an occupant in the seat to the rear.

Another assumed requirement was that of minimal weight increase. This is implied by the current trend of weight reductions in transport seats to reduce operating costs. Earlier triple-occupant seats such as the Weber P/N 819493 and Hardman Model 8727 seats weigh between 80 and 90 lb. The Weberlite 4000, a more recent seat, weighs 55 lb, and the latest UOP 910 composite seat is advertised as weighing 42 lb.

In view of this trend, considerable opposition can be expected to any design change which would require increased seat weights. Therefore, it was concluded that design concepts involving appreciable weight increases were not worth pursuing. This did not prevent modifying the seats to comply with design criteria, but emphasis had to be placed on energy-absorbing (load limiting) capability rather than on rigid structural strength.

A similar situation was assumed to exist relative to cost. It was therefore determined that design concepts be limited to those which could be mass produced using conventional materials.

It was assumed that a survivable crash need not be limited to one in which no serious rupture or breakage occurs. In a large transport aircraft, survivable volumes for a large percentage of the occupants could be maintained even if the fuselage separated completely. Therefore, design criteria which exceed existing criteria were considered applicable.

The degree of passenger comfort was not an objective of this project, but it was assumed that any changes made to the seat cushion, backrest cushion, or their respective angles and heights which would appreciably reduce comfort were impermissible. The lap belt anchorage point was also unchanged. Although the current belt angle approaches 70 degrees, it probably lies within the 45- to 55-degree recommended envelope occurring while the crash loads act on the occupant (reference 11). There also appears to be no way of reducing the belt angle without increasing the seat spacing.

Although aft-facing, energy-absorbing seats increase impact tolerances and reduce flailing injuries, it was assumed that airlines and passengers would be reluctant to accept such seats. Also, the recommended criteria are within human tolerance in the forward direction, providing secondary impacts do not induce too severe injuries. Emphasis was placed on developing forward-facing concepts, although one rear-facing, energy-absorbing seat modification was designed and tested to prove its feasibility. (On-board seat experiments also included the installation of an additional pair of standard in-service aft-facing seats.)

For an occupant to survive exposure to the above mentioned G loads and related environment, the seat must either have sufficient strength to sustain the loads, or be designed to deform, and thereby limit the forces acting on it. The latter approach is preferable, to the extent that existing seat tracks and perhaps the floor structures in transport aircraft usually cannot support these loads, and increasing the floor strength of the aircraft would not be an acceptable solution because of the expense. Since none of the loads contained in the proposed seat design criteria exceed human tolerance levels (reference 5), the only purpose of energy absorption is to limit the loads imposed on the structure and thus avoid the additional weight associated with a design that could sustain the unattenuated G loads.

Another element which is a very important factor in crashworthy design, is floor warpage. Under some crash conditions the floor under the seat is likely to deform. Adequate strength or load limiting features capable of supporting crash loads are of little value if the seat structure cannot conform to floor deformations without failure. In addition to improving the capability of the seats to sustain crash loads on a flat floor or test fixture, it was determined that the ability of the seat to survive floor warpage could be improved. A series of tests conducted by the FAA showed that many current transport seats do not have release mechanisms designed into them to assure that the floor attachments will remain intact if the floor is deformed (reference 9). Some of the seats have rear-leg track fittings attached by a single bolt, which permits rotation about the pitch axis. However, the front-leg fittings are not released in this manner, nor is there any provision for relative motion about the roll axis for either set of fittings. Even without floor deformation, this lack of a roll release has been shown to be a cause of attachment failure in lateral testing.

Furthermore, if a transport seat has too great a torsional rigidity about the pitch axis, the four legs may not remain attached to the floor even if the attachment fittings are released in both the pitch and roll axes. At least one of the fittings (or some portion of the leg structure) will fail if the floor is deformed in a manner which causes one of the fittings to significantly move out of plane with respect to the other three fittings. Some modifications which allow twisting about the pitch axis were considered necessary to be compatible with representative floor warpage conditions. (The design objectives discussed above are consistent with recommendations 3.1.3 and 3.1.5 of ARP 750A, reference 10). Ideally, a seat should be designed with releases in the structure to permit twisting about the pitch axis without failing. A seat incorporating energy absorbers in the rear legs can extend and all four fittings can remain attached if the floor is deformed.

Thus, the design criteria selected for the seat experiments consisted of the tests described in Appendix A, together with the provision that the floor track fittings have a roll release, and that the seat also be able to sustain out-of-plane warpage of the floor. All of the above considerations are directed towards increasing the probability of seat retention during a survivable crash of significant severity.

## CRITERIA

A brief survey of seat design requirements shows that the Code of Federal Regulations references the maximum load factors listed in Part 25.561 as the minimum design criteria for seat strength. These are the minimum ultimate inertial forces a commercial transport seat must be designed to withstand to "give each occupant every reasonable chance of escaping serious injury in a minor crash landing" (reference 1). Based on an average 170-lb. occupant, the forces are given as: 9.0 G forward, 1.5 G sideward; 4.5 G downward, and 2.0 upward. Further performance criteria in Federal Aviation Regulations (FAR) Part 37.136 or TSO-C39a (reference 2), state that seats "manufactured on or after May 1, 1972 must meet the standards set forth in NAS Specification 809, dated January 1, 1956. "Table I of NAS 809 gives ultimate seat loads as: 9.0 G forward, 3.0 G sideward, 6.0 G downward, and 2.0 G upward. However, the TSO also includes an exception that states that the sideward strength need not exceed 1.5 G. The increased downward seat strength is the result of gust-load factors that may exceed specified emergency landing conditions. These criteria have been shown to originate from load factors used for fuselage design (reference 3).

Tests on human subjects during the past 20 years have shown the level of human tolerance to be significantly greater than the ultimate seat loads listed above (references 4 and 5). This, coupled with analyses of survivable aircraft crashes, indicates that the number of fatalities and serious injuries in those accidents may have been reduced by the use of stronger seats and/or seats with energy absorbing capability.

The present standards require that the load factors mentioned in the previous paragraph be applied statically to the seat. Successful resistance of these loads demonstrates that the seat possesses the minimum strength required in the various directions. In the crash environment, loads are applied dynamically and the seat occupant responds accordingly. Because of the dynamic response of the non-rigid system consisting of occupant and seat, peak loads experienced by the occupant and seat can exceed the peak load dynamically imposed on the floor of the aircraft, causing premature failure of the seat, seat-to-floor interface, or the floor surface.

As a result of these considerations, this particular phase of the project was designed to demonstrate the feasibility of improving crash survivability through minor modifications such as load limiting, while not increasing weight or cost significantly.

Recommended seat design and test criteria of 18 G forward, 10 G sideward 10 G downward, and 6 G upward were proposed under this program. Dynamic criteria and corresponding pulse shapes were also defined. (Details concerning the rationale for these criteria are presented in Appendix A). Based on the frequency of occurrence presented in reference 10, meeting these design requirements would provide adequate occupant retention for at least the 50th-percentile survivable crashes.



tests were not as interesting, because little or no increase in downward strength was sought in the redesign of the seats. In some cases, both the forward and lateral test could be conducted with the same seat after some refurbishment.

The flight attendant seat was an exception. It was tested in only the downward direction because the restraint which reacts loads in other directions was attached to the aircraft.

#### DYNAMIC VERIFICATION TESTS.

Dynamic verification tests were also conducted at CAMI. The tests were conducted in the same manner as the initial destructive tests. Again, only the forward test was conducted because of the limited number of test specimens.

The deceleration pulse in the dynamic verification tests was exactly the same as in the destructive dynamic tests even though it did not utilize the full energy-absorbing capability of the modified seats. It did allow a direct comparison between the performance of unmodified and modified seats under identical test conditions. No dynamic tests were conducted on the flight attendant seats.

#### ADDITIONAL SEAT MODIFICATIONS.

After dynamic and static verification tests were conducted with the modified seat designs, additional seats were modified for installation aboard the test aircraft with one exception. Two samples of each modification were fabricated and instrumented prior to shipment to the test site. The installation of the seats in the aircraft is discussed in the "Aircraft Crash Test Setup" section of this report.

## TRACK FITTINGS

Modifying a seat to be stronger or incorporating load-limiting features capable of accommodating crash loads is of little value if the seat structure cannot conform to floor deformations without failure. Dynamic tests of standard seats have demonstrated that those seats do not have the release mechanisms necessary to assure that the floor attachments will remain intact if the floor is deformed. This lack of provision for relative motion about the roll axis has been shown to also be a cause of attachment failure in lateral testing.

### EXISTING FITTINGS.

Of the four track attachments on a transport seat, the two front attachments are generally single studs which have only antirattle devices. They are not released about a pitch or roll axis, and have no shear lock for forward retention. The two rear track fittings are attached to the rear legs by single bolts which permit motion about the pitch axis, but not movement about the roll axis. The rear fittings are stronger in both upward and forward directions due to double studs and a locking mechanism. The antirattle device is either incorporated into the lock or a separate part on the fitting.

Four different rear track fittings were examined and tested to compare their relative strengths and weights:

BROWNLIN FITTING. The fitting illustrated in figure 15 is of the Brownline 21700 Series and is used on the Hardman Model 8727 seat which is discussed in the "Prior Development" section of this report. Two studs with a shear lock located between them, are mounted on the fitting. The lock maintains the longitudinal position of the seat on the track and acts as an antirattle device. It is extended and retracted by a rotating cam mechanism.

ANCRA FITTING. The fitting in figure 16 is manufactured by Ancra Corporation and is used on the Weber seat discussed in the "Prior Development" section. Instead of using separate studs like the Brownline fitting, the necessary features are included in a one-piece forging. The fitting is made of 4140 steel which is heat treated between 180 and 200 ksi. A detented locking plunger slides up and down on the front of the forging and an antirattle mechanism is attached to the rear.

SABRE FITTING. Like the Ancra fitting, the Sabre Industries fitting (P/N 500330) shown in figure 17 is a one-piece fitting, but is cast of 17-4 PH CRES heat treated to 150 ksi. The lock is hinged on the forging and pivots in and out of the track. A screw-operated wedge acts as an antirattle mechanism.

UOP FITTING. The fitting in figure 18 is manufactured by UOP and used on the UOP seat discussed in this report. Two 4130 steel studs are threaded into an aluminum block with a lever-actuated lock in front. The lock is spring loaded, and also acts as an antirattle device.

### TRACK FITTING STRENGTHS AND WEIGHTS.

The Brownline, Ancra and UOP fittings were tested in the vertical, longitudinal, and lateral directions. The Sabre fitting was tested only in the longitudinal direction due to limited availability of test parts.

Testing was performed on a test fixture consisting of a loading frame and hydraulic cylinder. The test fittings were attached to 6-in. sections of Brownline heavy-duty track secured to a 1/2-in. steel plate. This track had the same dimensions as the track in the test aircraft. The plate orientation was rotated as required depending on the direction of the test. A typical test setup is shown in figure 19.

Table 2 shows the load at which ultimate failure occurred and whether it was a result of fitting failure, track failure, or both. Appendix C uses the test results obtained by various fitting manufacturers, and maximum allowable floor track loads from Boeing to develop maximum load capacities which can be anticipated from a double-studded fitting. They are as follows:

Vertical (Z)	8000 lb
Longitudinal (X)	9000 lb
Lateral (Y)	1600 lb

Considering only one test of each type was performed, the vertical and longitudinal loads compare closely with the Simula test results. However, the results show the anticipated lateral loads should be on the order of 5500 lb. As various concepts for track fittings were developed, these maximum load capacities were used as minimum design limits.

TABLE 2. TRACK FITTING TEST RESULTS

Fitting	Weight (oz)	Load at Failure (lb)/Failure Mode*		
		Vertical	Longitudinal	Lateral
BROWNLIN	3.94	6837/F&T	6590/F	4030/F
ANCRA	4.14	7322/T	9979/F&T	5876/T
SABRE		-	6982/F	-
U.O.P.	4.03	7499/F&T	7949/F	4888/F

\*F = Fitting failure, T = Track failure.

#### CONCEPTS FOR NEW FITTINGS.

A number of concepts were developed for a floor track attachment which would release movement about the roll axis due to floor deformation. Swivels and plastic hinges were considered. Priority was given to keeping the axis of rotation of both the added roll release and the existing pitch release as low as possible to minimize moment-caused stresses on the track and studs. It was assumed that the fitting must be compatible with the existing track configuration, and that installation and removal of the seat should not be more difficult than with the existing fittings.

The simplest concept is shown in figure 20. In this concept, the existing Brownline fitting is used with a modified attachment to the seat leg. The additional components form a plastic hinge between the fitting and the seat leg. The primary disadvantage of this concept is the high axis of rotation of the release.

Two other concepts employing plastic hinges are illustrated in figures 21 and 22. In both cases, the plastic hinge is below the axis of the pitch release. The first concept utilizes conventional studs with a shear lock mechanism commonly used by Brownline on single studs, on the rear stud. In the second concept, studs are not used. Rather, the track attachment features are formed as an integral part of the fitting by forging or machining. A special requirement of this concept is that the mechanism which operates the shear lock be flexible enough not to interfere with the operation of the plastic hinge yet still hold the lock securely in the track.

Several concepts were developed which incorporated a mechanical swivel for yaw release. These are illustrated in figures 23 through 25. In the first concept, the studs are screwed into a cylinder which is free to swivel in the housing of the fitting. The second uses a yoke attachment between the stud mount and the seat leg to effect a yaw release. The third concept also employs a yoke, but integral track attachment features are utilized rather than studs. A desirable result of eliminating the studs is that the axes of rotation are lower than if studs are used.

#### FIRST PROTOTYPE FITTING.

The fitting in figure 26 is preferable to the previous concepts discussed above. Two track studs are connected to the clevis with a pin, and this pinned connection provides the required roll release. The release about the pitch axis is provided by the attachment between the clevis and seat. The shear lock is positioned between the studs, and is held down by the clevis. The fitting was fabricated and then tested in the vertical and longitudinal directions. There was no lateral test due to the release feature of the fitting. Table 3 shows the ultimate load capacity for this fitting.

TABLE 3. FIRST PROTOTYPE TRACK FITTING TEST RESULTS

<u>Weight (oz)</u>	<u>Load at Failure (lb)/ Failure Mode*</u>	
	<u>Vertical</u>	<u>Longitudinal</u>
5.25	6922/T	7648/T

\*T = Track Failure.

With this fitting, the seat installation is somewhat unconventional. The entire fitting is not permanently attached to the seat as it is in conventional

designs. Only the clevis remains attached to the seat at all times. The sub-assembly consisting of the two track studs and the lock, all of which is held together by the retainer, is placed in the track first. Then the clevis is positioned over the studs, and locked in place with the pin.

While the unconventional installation may be a disadvantage in some ways, it could be advantageous in others. Present seats must slide forward or aft in the tracks 1/2 in. to be removed. Residue composed of dirt, spilled drinks, and food debris make sliding the seats in the tracks very difficult at times. The first prototype fitting alleviates this problem since the fittings can be removed one at a time after the seat is removed. With conventional fittings, all four must be moved at once.

For the purpose of seat retention in a crash, this design has highly desirable features. The roll axis release is as low as possible, so moments which tend to shear the lips of the track and/or studs will be minimized. The lock is in the optimum position between the two studs, and will not be released due to bending of the track. The lock is also positively held in position. It cannot lift out of the track unless the track or studs fail completely. The design of the lock also provides maximum bearing area in both the fore and aft directions at both the track-lock and lock-stud interface.

While the fitting has the advantage of complete lateral release, multiple parts, unconventional installation, and extra weight led to further development of other fitting concepts.

#### PLASTIC HINGE CONCEPT.

The fitting in figure 27 appears to have a number of highly desirable features. It provides a low roll release using a plastic hinge, has only three parts, and is a relatively conventional design. However, analysis showed that the cross-sectional area of the plastic hinge is too small for the minimum lateral design load. This led to the development of a three-stud configuration. Such a configuration would still yield laterally as a plastic hinge, but ultimate failure should not occur until 5500 lb.

#### SECOND PROTOTYPE FITTING.

The fitting in figure 28 is a triple-studded form of the fitting in figure 27. Three studs in the body of the fitting provide vertical strength, and the leg attachment is a plastic hinge which allows release about the pitch and roll axis. Longitudinal loads are transferred from the leg attachment to the lock, which is also an antirattle device. The optional boss on the fitting is an attachment point for a strap running to the fitting on the other leg in the same track. The strap might be required to keep the legs in position when the seat is removed from the tracks. The fitting can be used in either orientation. Both parts of the fitting are made of 17-4 PH CRES heat treated to 150 ksi. This heat treat retains more than 10 percent elongation, which is required for the design to function yet still provide adequate strength.

Table 4 shows that the fitting surpassed the performance of the first prototype both in strength and weight. Its vertical strength is better than the standard fittings, and its longitudinal strength is higher than the minimum design load. In the lateral test, the fitting began to yield at approximately 800 lb and

TABLE 4. SECOND PROTOTYPE TRACK FITTING TEST RESULTS

<u>Weight (oz)</u>	<u>Load at Failure (lb)/Failure Mode*</u>		
	<u>Vertical</u>	<u>Longitudinal</u>	<u>Lateral</u>
3.13	8493/F	9910/F	4776/F

\*F = Fitting failure.

bent more than 30 degrees before failing. This fitting was used on all the modified seats in the static and dynamic tests, and will be used in the crash test.

A production version of this concept could have even greater strength. For example, the vertical failure has been moved from the tracks to the fitting with the three-stud arrangement. Fitting failure occurs due to tear-out of the lug, which a boss on the leg would prevent. The ultimate limit would be the tensile strength of the hinge area, which is greater than 10,000 lb.

In terms of weight, this fitting is lighter than any other fitting studied during this program. It has virtually no parasitic weight, and represents an advance in both crash protection and weight reduction. Although installed on each leg of the experimental seats, it could be used on only the two rear legs, in place of conventional fittings.

## MODIFICATION CONCEPTS

According to reference 5, none of the accelerations discussed in the "Criteria" section would be expected to cause serious injury or fatality. Therefore, no energy-absorbing devices are required to limit the acceleration on the body. A properly restrained occupant seated in a perfectly rigid seat structure with sufficient strength to sustain such loads would probably not be seriously injured. There is just one problem with the strong, rigid seat approach: weight.

The present day triple-occupant passenger seat weighs just over 50 lb. It is unlikely that a rigid seat of that weight could be designed to withstand the proposed criteria. Likewise, the present floor structure in transport aircraft would probably not be capable of reacting the loads applied by such a seat if it could be built.

Therefore, a more crashworthy transport seat for use in existing aircraft and aircraft which will be produced in the near future requires some energy-absorbing stroke in the forward direction. This happens to be the same conclusion which was reached in the past, as is evidenced by the fact that all energy-absorbing transport seats which were tested or produced in the past had energy-absorbing stroke in the forward direction (discussed in the "Prior Development" section). As shown in Appendix D, approximately 12 in. of stroke is required to accommodate the recommended forward criteria (Appendix A) if the seat is designed to stroke at 9 G in order for the resulting floor reactions to be compatible with the floor strength. Unfortunately, this much space is simply not available. As is illustrated, a 6-in. forward stroke, which was assumed to be more reasonable, can accommodate an input pulse of 18 G and 35 ft/sec but not 18 G and 50 ft/sec as recommended in Appendix A. Previous energy-absorbing seats described in the "Prior Development" section were also designed with a 6-in. forward stroke. However, this was done at a time when the pitch (spacing) of the seats was generally greater than it is now. Present day interior arrangements would be somewhat less conducive to a stroke of 6 in.

Given the limited amount of space available in current transport aircraft, the selection of a maximum forward stroking distance involves some difficult trade-offs. Three adults seated behind a seat which is empty, partially occupied, or occupied by one or more children, could possibly be trapped or at least greatly impeded in their egress. In a crash with inertial loads over 9 G, the seat would stroke forward while the one in front of the three adults may not. Undesirable as this result is, it is less lethal to the overall group of passengers than is a situation where seats break loose. In other words, while a few people may be injured or impeded by the stroking seats, a much larger number will benefit because of their presence. Also, any passengers trapped as discussed above would probably have been much more seriously injured (and perhaps also trapped) if their seat failed completely, which it would do if subjected to an environment which caused an energy-absorbing seat to stroke. Therefore, passengers will have a better chance of surviving the crash providing that a fire does not occur. These are difficult but necessary choices to consider when dealing with the closely spaced seating in transport aircraft.

Stroke in the downward direction could also be beneficial. It could allow the seat to be lighter, and might also provide some protection for elderly passengers who have less tolerance to vertical impact than the general population. It might also prevent or minimize floor failure in some crashes.

However, it must be kept in mind that vertical stroke could be detrimental if it caused the legs of the occupant in the seat behind to become trapped. Also, any intended energy-absorbing stroke (downward, or a combination of downward and forward) could be compromised if the seat pan struck underseat luggage. If blocking the seat in the downward direction prevented stroking in the forward direction, ultimate seat failure or separation of the seat from the track could result. Thus, the advantages of limited downward stroke must be determined by the overall motion of the seat when various loads are applied. Limited downward stroke was assumed to be a desirable, but not essential, feature of any design concept.

The modified seat designs were to have improved floor tiedowns, improved tolerance for floor warpage, lateral bracing, and forward energy absorption. Of all these modifications, forward energy absorption involved the most complex change. Means of providing this feature in the most effective and efficient way were sought first, and other features were incorporated later.

#### ROTATING AND TRANSLATING SEATS.

As a preliminary step toward selecting acceptable seat configurations for the modification procedure, the possible kinematics of a seat with energy-absorbing stroke in the longitudinal direction were evaluated. Basically, the seat could rotate, translate, or perform some combination thereof, to allow the center of mass of the seat/occupant system to travel forward.

Seat configurations which rotate about a fixed axis are illustrated in figure 29, where four possible axes of rotation are indicated. In order to evaluate effectiveness of these concepts, quarter-scale layouts showing the movement of the occupant's center of mass during the energy-absorbing stroke were made. Figure 30 shows the center of mass of a 50th- and 95th-percentile occupant relative to the geometry of a typical transport seat. Figure 31 illustrates the motion of this point as the system rotates about the four indicated axes. The axes at both ends of the front leg result in predominately forward motion, and appear as possible axes for limiting inertial loads in the longitudinal direction. Of these two axes, the one at the bottom of the front leg causes less tipping of the seat pan and is simpler to release on existing transport seats.

The rotating seat offers a very simple and effective means of providing longitudinal stroke. No pivoting fittings would be necessary at any of the leg/seat pan interfaces, and lateral bracing is easily installed between the front legs and the seat pan assembly. There is also minimal chance of malfunction due to the application of asymmetrical loading (unequal occupant weights or partial occupancy). On the negative side, the resulting downward slope of the seat pan could impede egress, and the design may be less stable than others in secondary impacts. The concept can be employed with a single seat pan or with individual seat pans which rotate independently. Examples of both cases are cited in the "Prior Development" section.

Several options for translating seats are illustrated in figure 32. In option A, the seat pan is envisioned as traveling along the top of a pedestal which is fixed to the floor. This design has the unique feature of permitting any desired ratio of forward and vertical load limiting to be incorporated by appropriate selection of the angle of the top of the pedestal. However, the disadvantages are numerous. The bracing needed to support the seat legs independent



of the seat would interfere with feet and luggage, and the framework exposed after stroking would be a lethal hazard. The mechanism required to allow the necessary movement would be complex relative to conventional seat construction, and the associated weight penalties would probably be severe. In addition, the diminishing interface between seat and pedestal would cause the reaction forces between these components to increase as the seat stroked.

Option B allows load limiting in the longitudinal direction only, but is appreciably simpler. It would, however, be difficult to utilize in existing aircraft, since any mechanism permitting the front leg to move forward would have to be above the floor level and would be inconvenient for passengers. A concept for solving this problem is illustrated in figure 33. Here, the rear legs function as in the original concept, but the front legs pivot at both ends rather than translating forward. Although the front of the seat pan travels through an arc in this arrangement, the vertical motion is small. Studies of quarter-scale layouts showed that the amplitude of this arc would be no more than 1/2 in.

The modified translating seat allows the seat pan to remain essentially level, and does not interfere with legs or underseat luggage. Also, the energy absorbers are relatively short and need not be compressive devices. However, a larger vertical load must be supported while the energy absorber functions in the longitudinal direction, and the front leg assemblies must pivot at the seat pan interface. Asymmetrical loading conditions may make it difficult to design a mechanism which will operate reliably.

Option C in figure 32 illustrates a seat which undergoes a curvilinear translation by means of a parallel leg linkage and a compressive energy absorber for a diagonal strut. The motion is predominately forward at first, and then becomes more downward than forward.

The parallel linkage translating seat provides relatively direct load paths between the lap belt tiedown locations and the floor. It also provides some load limiting in the vertical direction. However, the design is somewhat complicated due to the fact that all leg ends must pivot, and the energy absorbers act in compression. Also, if the legs are truly parallel so that the seat pan remains horizontal, the space between the legs and the floor must be reduced, thereby increasing the floor reaction loads. The downward motion may also interfere with legs and luggage.

Any number of seat configurations involving both rotation and translation in their kinematics could be conceived. More complex motions could be achieved with nonparallel linkages and with the use of more than one energy-absorbing device in each leg assembly. In the latter case, the path along which the seat would travel would be dependent upon the loading conditions to which it was subjected.

One possibility is for both the rear legs and the tension diagonals to be tension energy absorbers. The arrangement illustrated in figure 34 was analyzed in detail, and its kinematics were determined for a number of loading conditions. The seat is shown in figure 35 after 6 in. of forward stroke has occurred due to a forward inertial load and an inertial load acting 30 degrees down from horizontal. Proper design of the energy absorbers has produced an interesting feature of this concept: the seat pan remained relatively level

throughout the stroke. This was because the energy absorbers stroked sequentially. First, the rear legs stroked, and the seat pan tipped forward slightly. Then, the diagonals stroked, and the seat pan again approached the horizontal position as the seat stroked further forward.

Further possibilities appear if it is assumed that the seat pan may experience extensive deformation. Conceivably, the rear legs could move forward while the front legs remained fixed and the seat pan telescoped, crushed, or folded between them (figure 36). This concept could actually increase the space available for egress. A Hardman seat was crushed in such a manner, as is discussed in the section on "Prior Development." However, the performance of such a seat would be difficult to predict, and extensive development testing would probably be required.

#### ENERGY-ABSORBING RESTRAINT SYSTEMS.

In addition to the concepts involving energy-absorbing mechanisms within the seat structure, there is another configuration worthy of further study. Such a concept entails designing energy-absorbing load limiters into the restraint system rather than into the seat (see "Prior Development," Hardman Company). Since the weight of the seat itself is only about 10 percent of the weight of the seat-occupant system (based on three 170-lb occupants), this technique is nearly as effective as designing the energy absorption into the seat. Although the occupants are not restrained as securely, this method minimizes the problems associated with unequal occupant weights and partially occupied seats. A concept for a lighter and more efficient lap belt anchorage system than was used on the early model Hardman seats is shown in figure 37.

The energy-absorbing restraint system concept is unaffected by asymmetrical loading conditions, and is, by far, the simplest approach to the problem. The primary disadvantage associated with such a concept is that the occupants are not securely restrained in secondary impacts, and if an attempt were made to incorporate a shoulder belt, there would be a high probability of submarining. (Sliding under the lap belt with probable injury to internal organs, reference 13.) Problems due to the resulting slackness in the system could perhaps be minimized through the use of the concept illustrated in figure 38. Rather than simply allowing the lap belt anchorage to extend as in the past, the lap belt anchorage would be required to travel forward in a guide. The occupant would be restrained against the seat pan even though he moved away from the seat back.

Another concept, simpler but not quite as effective, is illustrated in figure 39. Here, a side strap limits upward motion. A more complete discussion of design considerations for lap belt energy absorbers is included in Appendix F.

#### LOAD PATHS.

The choice of an appropriate energy-absorbing mechanism for modifying a seat is highly dependent upon the design of the seat and the resulting major load paths. For example, the sketch of the bracing members of the UOP seat in figure 40a, can be used as an illustration. Forward load is carried from the lap belt anchorage and rear tube to the diagonal brace (A) placing it in compression, and then to the bottom end of the front leg. From this location it is carried in tension by strap (B) back to the rear track fitting, which has a lock to prevent forward movement. There is also tension in the rear leg from the upward

load on the lap belt anchorage and from the moment created by the forward load component. Little load is carried by the seat pan spreader, and the downward load from the occupant's thighs on the front leg is not large enough to be a problem. This structure is well suited to a rear-leg energy absorber or a compression diagonal energy absorber, but it would not be compatible with a tension diagonal energy absorber or with a crushing seat pan. The latter arrangements would overstress the spreaders and/or front legs.

The Weber and Weberlite seats have different load paths, as is indicated in figure 40b. In these seats, the forward load from the lap belt anchorage is carried through the seat pan spreader (C) as a compressive load to the front tube. The forward load is then transferred to the rear track fitting by tension in the diagonal brace (D). No tension member is required between the bottom ends of the front and rear legs. As in the UOP seat, the rear leg is in tension and the front leg is in compression. This structure can be adapted to most modification concepts except those using a compressive diagonal energy-absorbing brace. Such a modification would be relatively inefficient, since the seat pan spreaders and front legs would be lightly stressed, creating alternate load paths. A discussion of the relative merits of tension and compression braces in a transport seat is included in Appendix F.

#### TORSIONAL RIGIDITY.

If a transport seat has too great a torsional rigidity about the pitch axis, the four legs may not remain attached to the floor even if the attachment fittings are released in both the pitch and roll axis. At least one of the fittings or some portion of the leg structure will fail if the floor is deformed in a manner which causes one of the fittings to move out of plane with respect to the other three. This was, in fact, the case with the Hardman Model 8727 seat. During testing at CAMI, the attachment fittings failed as the seat was subjected to a 10-degree roll of one floor track and a 10-degree pitch of the other floor track. While this test was conducted with standard fittings that do not have a roll release, the primary problem is believed to be torsional rigidity.

Ideally, a seat should be designed with releases in the structure to permit twisting about the pitch axis without the development of destructive stresses. A modification which incorporates energy absorbers in the rear legs provides an alternate solution to the problem. With this feature, one of the rear legs can extend and all four fittings can remain attached if the floor is distorted.

#### LATERAL BRACING.

The most effective way to increase the lateral strength of a transport seat would be to brace the rear legs, since the majority of the load is applied through the restraint system. Some improvement could clearly be gained by putting gussets or small braces on the legs. However, it was desired to increase the strength to 10 G, and bracing adequate for such a load is not compatible

with the requirement that space be preserved for feet and luggage. Therefore, bracing techniques which carried the load to the front legs were sought.

Figure 41a shows a bracing configuration which was considered. The inner braces were to provide lateral stability, while the outer ones were to provide additional lateral stability and also downward support for the ends of the seat pan.

Analysis of this arrangement showed that the seat pan structure is incapable of transferring sufficient lateral load from the rear tube to the forward tube for this arrangement to be effective. Therefore, additional braces, as shown in figure 41b, were necessary. While these were effective, it was found that excessive bending stresses developed in the front tube at the intersection of the two inner front braces. No method of reinforcing this region for 10 G with a reasonable weight penalty was found, so longer braces (illustrated in figure 42a) were used. These braces were attached to the upper and lower ends of the front legs, and the high bending stress in the front tube was avoided.

While the bracing arrangement shown in figure 42a is effective in supporting the seat structure, it was found that the floor tracks were not capable of reacting the loads if weight-efficient tension members were used. Therefore, members capable of supporting compression had to be used so that the lateral load component could be distributed between the two tracks.

An alternate lateral bracing arrangement, shown in figure 42b, was also studied. It was thought that this arrangement might save some weight due to the utilization of more direct load paths from the lap belt anchorages to the floor tracks. However, when analytical models were constructed for a seat modified for a 10-G lateral load using the concepts of figures 42a and 42b, it was found that there was very little actual weight savings. Therefore, the configuration of figure 42a was the preferred choice, since it did not encroach on the foot and luggage space.

#### AFT-FACING SEATS.

It has so far been assumed that the occupant is facing in the forward direction and not rearward. While it is known that human tolerance to inertial loads is greater when applied rearward, it has not been a factor in discussing energy-absorbing concepts since the forward load criteria is within human tolerance, and it has been assumed that both airlines and air passengers would be reluctant to accept aft-facing seats. However, an energy-absorbing aft-facing seat is of interest because the occupant is not thrown forward away from the seat, keeping the location of the c.g. almost unchanged, and thus making its movement more predictable. The load paths also change because the inertial load of the occupant is not applied to the lap belt, but distributed over the seat back. The occupant would also benefit through a greatly reduced chance of flailing injury in a forward impact or an impact with a large forward component. In purely lateral impact, the chance of injury would probably be the same.

Possible energy-absorbing configurations for an aft-facing seat are illustrated in figure 43. Since the leg structure is still basically the same as a forward-facing seat, some of the same arguments can be applied to the feasibility of the concepts. However, as stated, the loads are applied differently and the c.g. is at a different location. The concepts were analyzed using these factors,

and the following discussions deal with their feasibility beyond those arguments used for the forward-facing concepts.

Concepts A, B, E, and F would cause complications in lateral bracing due to the use of rear- (relative to the aircraft, not the occupant) leg energy absorbers. Bracing on the front (relative to the aircraft, not the occupant) legs would be disallowed because it would interfere with leg room. Other disadvantages of concepts A and B are the low loads in the diagonal energy absorbers due to the high tensile loads in the rear legs and the high compressive loads in the front legs. Besides requiring additional forward bracing, concept B causes the c.g. to move upward. This problem also exists in concept E. The high pivot point on a configuration like concept F also causes the back to recline excessively for the required c.g. motion, thus causing possible egress problems for the next row.

The parallel linkage of concept D causes low, nonlinear stroking loads in the energy absorbers, and very large loads in the rear legs. The rearward rotation of the bucket causes the c.g. to move rearward slightly, and offsets some of the benefit derived from the energy absorber. There is also a likelihood of leg entrapment and interference from underseat luggage.

An examination of these concepts shows that in all cases except A, C, and D, a downward load combined with the forward load could inhibit stroking of the energy absorbers. In concept C, the front leg energy absorbers would be more closely in line with the inertial load path and the rear legs would be compatible with lateral bracing, although there could also be some problem with luggage interference due to downward motion of the seat.

Not illustrated is the concept of replacing the seat recline mechanisms with energy absorbers. This would simplify the leg structure by keeping it rigid, and would only allow the seat back to stroke forward. However, analyses show the existing pivot point is too high, and would make the occupant arch upward. The high pivot point also limits the motion of the c.g. The spacing is also too small for the energy absorbers, and reduces the required stroking length. Furthermore, the existing spreaders are not strong enough to anchor the energy absorbers.

These problems originate from the constraints imposed by using an existing seat, and designing around its configuration and inherent weaknesses. Of the concepts discussed, the latter concept appears to be one of the more promising, but should only be approached with the intent of being newly designed. On a new structure, the back pivot point could be relocated to a lower position, which would solve some of the problems associated with a retrofit.

## SEAT MODIFICATIONS

As reported previously, three types of seats were purchased for the passenger seat experiments: the Weber P/N 819493, the Weberlite 4000, and the UOP model 901. This section describes these seats, and the design and test efforts which were conducted to prepare the modifications. It also discusses the modifications to the Trans-Aero flight attendant seat.

### STANDARD WEBER SEAT.

Front and rear views of the seat are shown in figures 44 and 45. This seat was manufactured by the Weber Aircraft Corporation, and was used aboard the Boeing 707, 720, 727, 737, and the Douglas DC-8 (Series 60) aircraft. It is identified as Weber P/N 819493.

### SEAT DESCRIPTION.

Structure. The seat pan assembly is built around aluminum front and rear tubes connected with four spreader tubes. The spreader tubes are connected to the front and rear tubes with forged aluminum fittings. Cantilevered extensions of the fittings, which are attached to the rear tube, support a smaller tube which provides a pivot and anchor point for the seat backs. Perforated aluminum sheets riveted to the three tubes which traverse the width of the seat, support the bottom seat cushions. Figure 46 shows the basic seat structure.

The leg assemblies are fabricated of square 4130 steel tubing, and are heat treated to 125 to 140 ksi. Welded steel fittings on the legs are bolted to the front and rear tubes of the seat pan. The leg assemblies are illustrated in figure 47.

Floor Attachment. The rear legs are attached to the track with a forged fitting manufactured by Ancra Corporation. The forging is made of 4140 steel which is heat treated to 180 to 200 ksi. A detented locking plunger slides up and down on the front of this forging, and an antirattle mechanism is attached to the rear. The fitting is attached to the seat leg with a single bolt, which provides a release about the pitch axis. This fitting is illustrated in figure 48.

The front legs are attached with single studs. The stud is fixed to a steel bracket which is welded into the tubular leg. This stud has no locking mechanism, and is held in the track only as long as the rear fitting and seat structure keep it in the proper longitudinal position.

Restraint. The seat structure includes attachment fittings for standard lap belts. These fittings are mounted on the forgings which connect the rear tube to the spreaders. The lap belt tiedown fittings can be seen in figure 49.

Cushions. Both the back and bottom cushions are fabricated of plastic foam. The bottom cushion has a constant thickness over the entire area, while the back cushion is contoured for comfort.

Accessories. The seat is equipped with features commonly found on transport passenger seats. Food trays are mounted on each of the seat backs and

ENERGY ABSORBERS. The energy absorption mechanism of the modified Weberlite seat is based on the elongation properties of stainless steel tubing. The rear legs and diagonal members were replaced with lengths of this tubing designed to elongate under the loads shown by the finite element model. Component testing (figure 144), showed the maximum elongation to be 42 percent. Both rear legs were designed to attenuate the same load, as were the diagonal energy absorbers. Though not as efficient as the energy absorbers on the other experiments, because of the low initial load, the stainless tension tube offers a very economical energy-absorbing capability. Figure 145 shows that the stainless tubes were placed in housings designed to handle compressive loads during normal operations, and to act in other directions besides forward during crash loads.

RESULTS OF FORWARD STATIC TEST. The applied load in the forward direction caused the seat to begin stroking at 5.0 G and continued to increase as the seat moved forward. The load versus displacement curve, shown with that of the standard seat (figure 146), demonstrates the dependence of the forward load on the geometry of the leg structure and its load attenuating properties. As the rear legs and diagonals began to elongate and their respective angles changed, the load increased in an approximately parabolic manner until, at 9.5 G, the rear window-side leg failed. The seat had stroked forward 5.8 in. when this occurred. Figure 147 is a view of the seat before failure, and figure 148 shows the failed window-side leg, which had elongated 42 percent.

RESULTS OF LATERAL STATIC TEST. A lateral load on the seat caused a combined motion of pitching and yawing (figures 149 and 150). At 6.9 G, the window-side diagonal energy absorber buckled (indicated by the arrow in figure 149) from compressive and bending loads. Conversely, figure 151 shows that the aisle-side diagonal experienced enough tensile force to stroke 1 in. The load versus lateral displacement curve is in figure 152. Further curves and a detailed account of the seat's performance are in reference 46.

RESULTS OF DYNAMIC TEST. The modified seat functioned as planned throughout 95 percent of the dynamic test duration. However, there was an eventual failure of the window-side rear leg and diagonal (figure 153). The rear leg stroked 2.4 in. or 28 percent before failing, and the diagonal stroked 4.5 in. or 30 percent. As demonstrated by the curve in figure 154, one of the two energy absorbers failed 210 msec into the test while the other kept stroking until failure at 240 msec. Since the duration of the 9-G pulse lasted 220 msec, the majority of the energy applied to the seat had already been absorbed when the failures occurred. The seat was still restrained by the aisle-side leg assembly, so the seat remained affixed to the test sled. The window-side leg reaction of the standard seat is included in the figure for comparison.

A failure also occurred when the dummy on the right-hand side pulled the aisle-side lap belt anchor out of its attachment point on the rear tube. Figure 155 is a posttest view with an arrow indicating the anchor, and figure 156 is a closeup of the failure point. The dummy remained in the seat because the failure occurred after the dummy had been almost completely decelerated, and also because the left part of the lap belt was wedged between its abdomen and thigh.

As a result of the CAMI test, several changes were made to the design: the energy absorber end-fitting was modified to reduce the combined bending and tensile stresses in the critical area where the stainless steel tube necks down,

effective, in that the body blocks were still secured by the lap belts and the rear tube, so the test was continued. At 8.8 G, the front tube experienced the same failure, but at a point between the aisle-side leg and its adjacent spreader. Both failures are evident in figure 135. Arrow 1 points to the first failure at 9.1 G, and arrow 2 points to the second at 8.8 G. For further details of the test, see reference 47.

RESULTS OF FORWARD DYNAMIC TEST. Figure 136 shows that the 9-G, 50-ft/sec dynamic test caused the seat to fail completely, and only the redundant restraint straps in the test setup prevented it from leaving the test fixture. A rear view in figure 137 indicates that the front and rear tubes sheared or pulled out of the leg saddles, causing the seat pan structure to become detached from the legs.

A close-up view in figure 138 uses arrows to illustrate failure points: arrow 1 shows the rear tube pulled through the right-hand bolt of the window-side leg fitting, arrow 2 shows a break in the rear tube at the left-hand bolt of the same fitting, arrow 3 shows the same failure as arrow 2 at the aisle-side fitting, and arrow 4 shows the failure of the spreader between the aisle-side and center seats.

#### WEBERLITE MOD SEAT.

MODIFICATION CONCEPT. Initially, thought was given to replacing the tension diagonal with a tensile energy absorber. However, analysis of the structure showed that very high loads would then develop in the rear legs before the seat stroked 6 in. forward. The seat pan would also rock rearward considerably. It became apparent that these problems could be avoided if both the diagonals and the rear legs were capable of an energy-absorbing stroke. The motion of the seat would then be a function of the direction of the applied inertial load due to the two energy absorbers in each leg assembly. A kinematic analysis of the leg structure demonstrated that by replacing the rear legs and diagonals with tensile energy-absorbing members of the proper loads, approximate rectilinear translation of the structure could be achieved. An illustration of the predicted leg motion under a forward load compares it with the actual test result (figure 139). Another benefit of this configuration is the seat's ability to attenuate loads under the two conditions shown in figure 140, either of which could be experienced in a crash. The seat was designed to stroke 6 in. at 9 G so that it could survive an 18-G, 35-ft/sec pulse in the forward direction.

MODIFICATION DETAILS. The Weberlite seat was modified using the design loads of 9 G forward (stroking), 8 G downward (static), and 6 G sideward (static). The basic configuration and design of the standard seat is very similar to the Weber seats discussed in this report, so a similar finite element model was used, with consideration given to members Weber Aircraft had changed or lightened.

The modified seat is shown in figures 141 through 143. Bracing used to strengthen the seats under lateral loads is indicated by the arrows in figure 141, and the "L" arrow in figure 143. The diagonal and rear-leg energy absorbers are shown in figure 143.



center spreaders consist of a tube riveted to front and rear fittings. The front fitting is a forged eye-fitting through which lies the front tube. The rear fitting holds the rear tube and also branches upward to support the seat backs and provide them with a pivot point. These rear fittings also have a brace forged into them to provide an attachment point for seat belt fittings. The two end spreaders are constructed of an oval-shaped tube welded to a "C" bracket, which slips around and bolts to the front tube. The rear of the spreaders is welded to a short cylinder which slips inside the rear tube, and is bolted into place through the walls of the tube. The two outside seat belt fittings are anchored with nut plates at the juncture of the cylinders and the rear tube.

The seat pans consist of flexible, plasticized fabric stretched between the front and rear tubes. The pans are attached by stretcher bars which run through hems in the fabric and bolt to each tube. Figure 130 shows the seat pans and the basic seat structure.

The leg structure consists of front and rear legs of square steel tubing connected by a diagonal brace of the same material. Welded to the top of each leg is a "C" shaped bracket which straddles and bolts to either the front or the rear tube. A view of the leg structure is in figure 131.

Floor Attachment. The rear legs are attached to the track with a forged fitting manufactured by Ancra Corporation. The forging is made of 4140 steel which is heat treated to 180 to 200 ksi. A detented locking plunger slides up and down on the front of this forging, and an antirattle mechanism is attached to the rear. The fitting is attached to the seat leg with a single bolt, which provides a release about the pitch axis. This fitting is shown in figure 132.

The front legs are attached with single studs. The stud is affixed to a steel bracket which is welded into the tubular leg. The stud has no locking mechanism, and is held in the track only as long as the rear fitting and seat structure keep it in the proper longitudinal position. The stud is illustrated in figure 133.

Restraint. The seat structure has attachment fittings for standard lap belts. The fittings are connected to the two middle rear spreader forgings and the two outside nut plates.

Cushions. Seat backs and bottoms are cushioned with contoured foam padding attached to the structure with Velcro strips.

Accessories. Each seat has a food tray mounted on its back, and the seats have an adjustable reclining mechanism. The seat backs also have a shear clip, which allows them to rotate forward if struck from behind with a force above a predetermined level.

Seat Weight. The measured weight of the complete seat assembly including lap belts and cushions but less upholstery, is 55.2 lb.

RESULTS OF FORWARD STATIC TEST. A forward static test on the seat showed that its ultimate strength is 9.1 G. Failure occurred when the front tube sheared between the window-side leg and the adjacent spreader, allowing the window-side seat to pitch forward as shown in figure 134. Occupant retention was still

47.5 lb, respectively. If these loads had occurred under static conditions, the energy absorbers would have stroked. The reason for this anomaly was not known at the writing of this report, but further component testing of the energy absorbers will be performed to determine its solution.

Despite the nonoperation of the energy absorbers, the seat passed the test with only minor bending of the front and rear tubes. This fact might lend itself to the misconception that since the seat survived the test without energy absorption, it is therefore strong enough for the design criteria. It must be noted that the 9-G, 50-ft/sec pulse this seat was tested at is less severe than the recommended 18-G, 35-ft/sec design pulse, and was used only because it was an established baseline by which other transport seats had been tested. Simple releases and load-spreading techniques which contributed to the seat's survival can, of course, be adapted to any transport seat without energy absorption, and achieve the same results at 9 G. Such a seat would not have the survival capacity necessary for 18 G, and is not recommended. However, as evidenced by the test results in this report, it would be superior to many seats in the "as is" condition.

WEIGHT DISCUSSION. A breakdown of the weight increases caused by modification of the seat are shown in table 8. A 5.3-percent increase of the original weight increased the seat's forward strength to handle a 9-G, 50-ft/sec dynamic load without failing. A 1.4-percent lateral strength weight increase enabled the seat to survive an 8.9-G lateral load before failing, 197 percent higher than the minimum design load of 3.0 G.

TABLE 8. BREAKDOWN OF WEIGHT INCREASES FOR THE  
UOP MOD II SEAT

Standard Seat Weight	<u>Forward Strength Weight Increase</u>		<u>Lateral Strength Weight Increase</u>		Modified Seat Weight
	<u>lb</u>	<u>Percent Original Weight</u>	<u>lb</u>	<u>Percent Original Weight</u>	
62.2 lb	3.3	5.3	0.9	1.4	66.4 lb

#### STANDARD WEBERLITE SEAT.

Front and rear views of the seat are shown in figures 128 and 129. This seat is manufactured by Weber Aircraft Corporation, a division of Walter Kidde and Company, Inc., and is designed for use aboard the Boeing 727, 747, 757, and 767 aircraft. The seat is identified as model number 829633-401.

#### SEAT DESCRIPTION.

Structure. The seat pan structure consists of front and rear aluminum tubes which run the entire width of the seat assembly and are connected by tubular spreaders placed between each seating position and on each end. The two

seats. Only minor changes were made to account for the release of certain members and moving attachment points. The energy absorbers were sized by the same method of modeling "before" stroking and "after" stroking configurations. The straps used for lateral strength, and the reinforcing insert tubes to prevent twisting, are the same for both seats.

The final configuration is shown in figures 116 through 119. Figure 118 shows that the front legs have been extended as in the first modification, but are fixed at the top and strengthened with doublers.

ENERGY ABSORBERS. A sketch of the energy absorber used on the UOP MOD II seat is shown in figure 120. This energy absorber uses two means of attenuating loads: inverting an aluminum tube, and pulling a die through an aluminum tube.

The energy absorbers for the modification were first approached on the basis of using tandem inversion tubes like the Weber MOD II. However, differences in leg geometry because of the seat's reduced pitch, made the load in the rear window-side leg of the UOP seat 30 percent higher than the Weber seat, and the front-to-rear leg spacing 3 in. shorter. If a tandem inversion tube arrangement had been developed for the higher load, there would not be enough space to achieve the necessary stroking distance. Developmental work on pulling a die through a tube showed that it could attenuate the load, but could not provide support under reverse loading conditions. However, the work did demonstrate that the attenuated loads were predictable with a high degree of accuracy, and that the walls of the tubes could be tapered to provide varying load attenuating capabilities. This led to the hybrid design of using an inversion tube to provide a fixed limit load, and a die through a tapered tube to provide the balance of the varying load (figure 121).

RESULTS OF STATIC TEST. At 9.2 G, the seat began stroking forward. The applied load was increased as the seat kept stroking until, at 10.9 G, the energy absorbers reached the end of their stroke and the test was stopped. The two energy absorbers stroked, for the most part, in unison, and displaced 4.6 in. on the window side, and 4.8 in. on the aisle side. Figures 122 and 123 show posttest views of the seat.

Figure 124 demonstrates the difference between the standard and modified UOP seats by comparing the two seat displacements under the applied static test load. Both seats experienced 0.8 in. of deformation before one seat failed and the other began attenuating the load, stroking another 5.0 in. Since the load attenuation is to occur through 6 in. of displacement, the energy absorbers used in the test aircraft were modified to provide the additional inch of stroke.

RESULTS OF LATERAL TEST. The modified seat was tested laterally (figure 125) and failed at 8.9 G when the front window-side track fitting failed. A top view of the leg and fitting is in figure 126, and the load versus displacement curve is in figure 127. A further description of the seat's performance is in reference 44.

RESULTS OF DYNAMIC TEST. The releases designed into the energy absorbers and track fittings enabled the seat to conform to the deformation of the floor tracks during the test. However, the 9-G deceleration of the test failed to produce any stroking of the energy absorbers. Results from the test showed that the window- and aisle-side energy absorbers experienced a force of 6900 lb and

the releases provided by the bending of the track fittings and the single-bolt attachments (figures 112 and 113). The only significant deformation of the seat structure was the bending of the rear tube on the window side about the rear-leg fitting.

The window- and aisle-side energy absorbers stroked 3.3 and 2.4 in., respectively. This represents 55 and 40 percent of their capacity.

An obvious difference between the standard and modified seats is demonstrated by the plot of the window-side leg force resultants (figure 114). The standard leg pulled out of the track at 4800 lb, leading to ultimate seat failure. The force on the modified leg went to 6400 lb and continued to 7200 lb as the energy absorbers stroked during the 9-G deceleration.

WEIGHT DISCUSSION. Table 7 shows the breakdown of weight increases caused by the modification to the standard UOP seat. An increase of 3.7 percent of the original weight enabled the seat to experience a 9-G, 50-ft/sec dynamic load without failing, while using only 50 percent of its energy-absorbing capacity.

TABLE 7. BREAKDOWN OF WEIGHT INCREASES FOR THE UOP MOD I SEAT

Standard Seat Weight	Forward Strength Weight Increase		Lateral Strength Weight Increase		Modified Seat Weight
	lb	Percent Original Weight	lb	Percent Original Weight	
62.2 lb	2.3	3.7	0.9	1.4	65.4 lb

#### UOP MOD II SEAT.

MODIFICATION CONCEPT. As stated earlier, one of the configurations considered for modifying the UOP seat was a rear-leg energy-absorbing concept. This concept was already used in MOD II of the Weber seat. However, the Weber MOD II seat used two rear-leg energy absorbers, both designed with the same limit load. This design proved to work well, but testing showed the energy absorbers to stroke unequally, causing the seat to pitch forward more on the window side, due to the asymmetric loading of the rear legs. This is not an entirely undesirable condition, for it lends itself to egress toward the aisle. However, it results in severe deformation of (and therefore high stresses in) many of the structural components. It was therefore decided to design rear-leg energy absorbers for the UOP seat that limit their respective loads according to the finite element model. This would demonstrate the performance of a seat which pitched forward with limited yawing. The design would also necessitate the development of a means of energy absorption other than the inversion tube type, due to the higher rear-leg loads and limited space. Figure 115 illustrates the seat kinematics using a rear-leg energy absorber.

MODIFICATION DETAILS. The similarities in leg structure between the UOP MOD II and the UOP MOD I seat allowed the same finite element model to be used on both

In the design of the UOP MOD I seat, another choice was made. The energy absorbers were designed to be unequal so that the seat could stroke forward with limited rotation about the yaw axis. This would minimize damage to the structure and/or minimize the expense and weight of fittings required to permit such rotation without structural failure. This consideration seemed especially important in a device which used compression rather than tension devices to minimize stability problems. The preceding discussion assumes there are three occupants of approximately equal weight, and is less valid if there is partial occupancy. However, seat stroke will then usually be less in either case.

The use of unequal energy absorber loads is a departure from the philosophy used in the design of MOD II of the Weber seat. In the latter case, the energy absorbers had equal load capability and were sized for the window-side leg assembly load. The aisle-side leg assembly was therefore overdesigned relative to the window side; the window-side leg would therefore stroke first. However, the track is capable of supporting the same load on either side, so the Weber redesign represents the greatest seat retention capability consistent with the airframe strength. It also represents maximum energy absorption capability. It was also assumed that restraining the motion of the aisle end of the seat as much as possible might aid egress. However, that approach also introduces considerable twisting of the structure about the yaw axis. It was thought best to avoid this as much as possible in the UOP MOD.

RESULTS OF FORWARD STATIC TEST. The modified seat was tested in the forward direction. At 7.6 G the seat began stroking forward and exhibited little rotation about the yaw axis (figure 105). The applied load was increased until, at 10.1 G, the fitting on the rear window-side leg failed at the weld and the test was stopped. Figure 106 shows the fitting, and figure 107 shows a similar failure occurring to the fitting on the aisle-side leg. Figure 108 shows a posttest view of the stroked window-side energy absorber and the pitching forward of the front leg caused by the failed fitting. Figure 109 is a view of the stroked aisle-side energy absorber.

In order to compare the performance of the modified seat versus the standard seat, the average displacement of both seats was plotted against the applied static test load (figure 110). As the figure indicates, both seats deflected about 1 in. before reaching the ultimate load. The standard seat then failed, but the energy absorbers on the modified seat stroked, displacing the seat another 3.8 in. until failure occurred. The window-side energy absorber stroked 3.5 in., and the aisle-side energy absorber stroked 2.9 in.

The rear-leg fittings were reinforced before the design was dynamically tested. Based on analysis of the structure and reinforcement, the successful functioning of the seat through 3.8 in. of stroke, and because test samples and time were limited, the static test was not repeated prior to the dynamic test.

RESULTS OF LATERAL STATIC TEST. The lateral bracing of the UOP MOD I seat is identical to the UOP MOD II seat, which is discussed in the next section. Since the MOD II seat exhibited an ultimate lateral strength of 8.9 G, it was not necessary to validate the ultimate lateral strength of the MOD I seat.

RESULTS OF DYNAMIC TEST. As is evidenced by the posttest view in figure 111, the seat did not experience any failures in the dynamic test. The floor deformation prior to the test did not affect the performance of the seat, due to

MODIFICATION DETAILS. A finite element model was made of the UOP seat and changed to account for the release of the front and rear legs, and to provide for possible attachment points of the energy absorbers. Weak points shown by the model were reinforced. The energy absorbers were also sized using data from the model. However, the design requirement that the seat stroke under a constant forward load, and the changing geometry of the leg structure during the seat's forward motion, necessitated modeling the seat in "before" stroking and "after" stroking conditions to determine the load attenuation requirements of the energy absorbers. To obtain an efficient design, the energy absorbers would need to limit the load so the seat stroked at a constant 9 G throughout its 6 in. of travel.

The seat was also modeled under a 6-G lateral loading condition. The 6-G criterion was selected since it was felt that 10 G might entail an unacceptable weight penalty for such a light structure. It was also felt that it would be useful to demonstrate the impact of simply doubling the lateral strength. The impact of a 10-G reinforcement had already been explored with the Weber seat.

The final modification is shown in figures 100 through 103. Arrows marked "L" indicate the straps used to transfer lateral loads from the front window-side leg to the aisle-side track fitting, and from the rear tube to the front tube. Arrows marked "R" point to where the front and rear legs are released to pivot forward. Reinforcing tubes were inserted in the front and rear tubes at the intersections of the front and rear legs to prevent twisting of the aisle- and window-side seats about the yaw axis. The energy absorbers are labeled "E."

Initially, tests were done to determine if the front tube could simply be allowed to bend locally to permit it and the front legs to rotate relative to the spreaders. If so, a simple retrofit kit could have been developed for this seat. It would have involved replacing the rear-leg/diagonal brace assembly by removing just a few bolts. However, while the seat could deform through the desired distance in these areas without ultimate failure, the load required to do so made an efficient energy-absorbing design impossible. Therefore, the full releases in the legs were installed.

ENERGY ABSORBERS. The energy absorbers used on the UOP MOD I are shown in figure 104. Both employ the load attenuation method of inverting an aluminum tube. Due to the asymmetry of the seat, the window-side energy absorber is required to stroke at twice the load of the aisle-side energy absorber if both ends of the seat are to stroke at 9 G, and thus uses two inversion tubes. The kinematics of the leg structure also require the loads on the energy absorbers to decrease as they stroke if the seat is to move at a constant 9-G load. For example, the window-side energy absorber needs to begin stroking at 3300 lb and decrease to 1600 lb by the end of its stroke. Varying the load is possible by tapering the walls of the inversion tubes. However, the strength of the tube material did not allow for this large variation, so complete compensation was not possible. The energy absorber begins stroking at 2800 lb and ends at 2000 lb, thus causing the seat to begin stroking at a load below 9 G and increasing above that by the end of its 6-in. displacement.

Analysis showed that bending moments would adversely affect the performance of the energy absorbers, so released fittings were built into both ends of the energy absorbers, and one fitting used a threaded connection to provide a torsional release.

Floor Attachment. The rear legs are attached to the floor track by a fitting consisting of two studs and a lever-operated plunger. The plunger moves in and out of the track and is in the front of the fitting. The fitting is attached to the leg by a single bolt and is shown in figure 91.

The front legs are attached to the track by a single stud which is incorporated in an antirattle mechanism shown in figure 92. The stud is bolted to a yoke, which is attached to both the front leg and diagonal tube by a single bolt. An aluminum strap connects the front stud and rear fitting in order to transfer the loads from the tubular diagonal brace to the plunger.

Restraint. The seat structure includes attachment fittings for standard lap belts. These fittings are bolted to the forged aluminum supports and are indicated by arrow 1 in figure 89.

Cushions. Both the back and bottom cushions are fabricated of plastic foam. The back cushion is contoured for comfort while the bottom cushion is flat on top but curved on the bottom to conform to the perforated aluminum seat pan.

Accessories. Each seat has a food tray mounted on its back, and the seat backs have an adjustable reclining mechanism. The two middle armrests can pivot up flush with the seat backs.

Seat Weight. The measured weight of the complete seat assembly is 62.2 lb.

RESULTS OF FORWARD STATIC TEST. The seat was tested in the forward direction by the method described earlier. At 10.0 G, the rivets and bolts connecting the rear window-side leg to the rear tube failed (figure 93). This freed the rear tube, which moved forward and bent around the strap attaching the rear tube to the aisle-side rear leg, as is shown in figure 94. Since complete failure had occurred, the test was terminated. Further details of the test are described in reference 42.

RESULTS OF FORWARD DYNAMIC TEST. Figure 95 shows that the seat failed by separating from the track on the window side, then failing the front and rear tubes on the aisle side. A closeup of the window-side legs in figure 96 shows that the front track-fitting stud is missing, and the rear track-fitting studs have been sheared through the track. A view of the aisle-side legs in figure 97 indicates that the front tube failed in shear and bending at the front leg bolt hole, and the rear-leg strap tore through the rear tube. The seat failure was such that both occupants and seat frame became detached from the test fixture, and ended up as illustrated in figure 98.

#### UOP MOD I SEAT.

MODIFICATION CONCEPT. The configuration of the UOP seat leg structure lent itself especially well to two possible modification configurations. The first was a rear-leg energy absorber, and the second was a compressive energy absorber replacing the diagonal brace. The latter configuration was chosen for the first modification. A sketch of the seat kinematics using the compressive energy absorber is shown in figure 99. In order for the seat to undergo the approximate curvilinear translation the sketch depicts, the front and rear legs needed to be released to act as a linkage.

WEIGHT DISCUSSION. Weight added to the seat from the modification is grouped in table 6 according to its contribution to lateral or forward strength. An increase in weight of 2.0 percent added energy absorption to the seat, allowing it to sustain, with only one-half of its energy-absorbing capacity, a 9-G, 50-ft/sec dynamic test that resulted in the complete destruction of the standard seat. A weight addition of 2.1 percent increased the seat's lateral strength to 10.4 G, 247 percent higher than the 3.0 G minimum design load.

TABLE 6. BREAKDOWN OF WEIGHT INCREASES FOR THE  
WEBER MOD II SEAT

Standard Seat weight	<u>Forward Strength Weight Increase</u>		<u>Lateral Strength Weight Increase</u>		Modified Seat Weight
	<u>lb</u>	<u>Percent Original Weight</u>	<u>lb</u>	<u>Percent Original Weight</u>	
82.0 lb	1.6	2.0	1.7	2.1	85.3 lb

#### STANDARD UOP SEAT.

Front and rear views of the seat are shown in figures 87 and 88. This seat is manufactured by the Aerospace Division of the Universal Oil Products Company and is designed for use aboard the Boeing 707, 727, 737, and 757 aircraft. It is identified as model number 901-02A-3.

#### SEAT DESCRIPTION.

Structure. The seat pan assembly is built around aluminum front and rear tubes which are connected by four forged aluminum supports. The front of each support rests on top of the front tube and is attached by two bolts running through the support and the tube. The rear of each support has a semicircular cut-out that slips over the rear tube and attaches with one bolt. Three of the supports have cantilevered rear extensions which provide a pivot and anchor point for the armrests and seat backs. The seat cushions rest on perforated aluminum sheets which are riveted to the front tube in front, and wrapped around a small aluminum tube which slips in between the cantilevered extensions in the rear. Figure 89 shows the basic seat structure.

The leg assembly consists of front and rear legs of formed stainless steel sheet, which are connected diagonally by a square aluminum tube. The front legs cradle and bolt to the front tube, while the rear legs are held to the rear tube by steel straps which are wrapped around the tube and bolted to the legs. Each rear leg is connected to the diagonal tube by a steel fitting which is riveted to the leg and the tube, and is also bolted to the steel strap. The leg assembly is shown in figure 90.



simply develop a larger inversion tube, with a thicker wall and a larger diameter. However, this led to a design that was too bulky for its application. A simpler and far more satisfactory solution was to use two inversion tubes in tandem, thereby doubling the required stroking force. The remainder of the load increase was achieved by inverting relatively thick-walled tubing. A drawing of the energy absorber is shown in figure 77. In the Weber seat application, the energy absorbers stroked at equal loads in order to provide maximum retention to the tracks. This caused the window end of the seat to stroke first, and stroke further, since more load is applied at this location due to the asymmetry of the seat.

RESULTS OF FORWARD STATIC TEST. When loaded in the forward direction as described earlier, the seat began stroking at 10.2 G. The window-side energy absorber stroked about 1 in. before the aisle-side absorber began stroking. As the seat moved forward, the applied load dropped until, at 9.5 G, the top inversion tube on the window-side energy absorber separated from the rivets joining it to the housing. By the time it separated, the tube had exceeded its designed stroking distance. Therefore, the test was completely successful. However, a doubler was added to the energy absorber design to increase the ultimate load following complete stroke. A posttest view of the seat is in figure 78, and figure 79 shows the location where the inversion tube separated from its housing.

The significant difference between the standard and modified seats is demonstrated by the load/displacement curves in figure 80. Further curves, and a detailed performance description of the seat, are in reference 41.

RESULTS OF LATERAL STATIC TEST. The lateral load applied by the body blocks on the seat caused it to fail at 10.4 G. The failure occurred when the bolt at the bottom of the front window-side leg pulled through the track fitting. Figure 81 is an overall posttest view, and figure 82 is a view of the track fitting failure. A production design of this fitting would include a boss which would prevent the shear failure. However, the structure did meet the design criteria with the unmodified fitting. The load versus lateral displacement curve is in figure 83.

RESULTS OF DYNAMIC TEST. The floor deformation prior to the dynamic test did not affect the performance of the seat, due to the releases provided by the bending of the track fittings and the upper fittings of the energy absorbers.

The posttest view in figure 84 shows that the dummies were retained in their seat positions, and a rear view in figure 85 indicates that the window-side energy absorber stroked but the aisle-side energy absorber did not. Test data show that the window-side energy absorber experienced an average force of 5370 lb which caused it to stroke 3.0 in. The aisle-side energy absorber was subjected to only 3900 lb, which is less than the static design stroking load of 4700 lb. (Dynamic stroking loads are higher than static stroking loads.)

The window-side rear-leg force reactions of the standard and modified seats (figure 86), demonstrate the difference between the two seats. The leg on the standard seat detached from the track fitting at 5900 lb, whereas the energy-absorbing leg limited the load to 5370 lb for 110 msec. Furthermore, as mentioned previously, only one-half of the energy-absorbing capacity was utilized.

WEIGHT DISCUSSION. Table 5 gives a breakdown of the weight additions made to the seat with regard to their contribution to forward or lateral strength. An increase in weight of 10.4 percent added energy absorption to the seat and increased its ultimate strength from 11.2 G to 16.0 G, a 43 percent increase in forward strength. A weight addition of 2.1 percent enabled the seat to fail laterally at 7.8 G, 160 percent higher than the minimum design load of 3.0 G. As mentioned previously, the prototype energy absorbers were quite heavy. Much lighter devices capable of performing the same energy-absorbing function could be developed.

TABLE 5. BREAKDOWN OF WEIGHT INCREASES FOR THE  
WEBER MOD I SEAT

Standard Seat Weight	<u>Forward Strength</u> <u>Weight Increase</u>		<u>Lateral Strength</u> <u>Weight Increase</u>		Modified Seat Weight
	<u>lb</u>	<u>Percent</u> <u>Original</u> <u>Weight</u>	<u>lb</u>	<u>Percent</u> <u>Original</u> <u>Weight</u>	
82.0 lb	8.5	10.4	1.7	2.1	92.2 lb

#### WEBER MOD II SEAT.

MODIFICATION CONCEPT. As discussed earlier, the second concept for modification of the Weber seat was a rear-leg, energy-absorbing seat. This concept, as shown in figure 72, uses tensile energy absorbers to replace the standard seat rear legs, and allows the seat to pivot forward about the track fitting attachments on the front legs.

MODIFICATION DETAILS. The Weber MOD II seat was designed to fully comply with the selected criteria: it can sustain a peak load of 18 G with a 35-ft/sec velocity change, and can support static loads of 10 G downward, and 10 G laterally. A finite element model similar to the one employed for the first modification was used, except changes were made to accommodate the rear-leg energy absorber and associated releases, and the increased lateral strength. A detailed account of the design process is in reference 39.

The modified seat is shown in figures 73 through 76. Arrows in figure 75 indicate diagonal braces and straps used to reinforce the seat under lateral loads. Figure 76 shows the energy absorbers and modified seat pan.

ENERGY ABSORBERS. The energy absorbers on the Weber MOD II seat use the method of inverting an aluminum tube to limit the tensile load in the rear legs. Besides having a high specific energy absorption, the inversion tube is unaffected by friction, and provides good resistance against rebound loads. The inversion tube has proven to be an effective means of attenuating loads in other applications such as crashworthy helicopter seats, but its use on the Weber seat required further development due to the leg loads being several times the load for which previous inversion tubes had been designed. One solution was to

arrows pointing to diagonal members reinforcing the seat under lateral loads. Figure 59 shows the energy absorbers and modified seat pans.

ENERGY ABSORBERS. The energy absorbers on the Weber MOD I feature a wire-bending mechanism consisting of a housing, trolley, and two wires. The housing is a square tube which contains and constrains the trolley as it is pulled forward by the lap belt through a slot which runs the length of the housing. The trolley limits the forward component of the lap belt load by deforming two pieces of music wire through three sets of double rollers. The number of rollers, their diameter and spacing, and the wire diameter and material, determine the force required to pull the trolley. Component testing to determine the specifics of these parameters for the seat modification is described in Appendix H. Figure 60 shows the components in the lap belt energy absorber. A unique feature of the design is that the same rollers serve to limit the friction caused by the large upward load component.

RESULTS OF FORWARD STATIC TEST. The modified seat was tested in the forward direction as described earlier. As the applied load was increased, all three body blocks rotated forward about the lap belts. At 9.0 G, the window body block began stroking forward until it arrived at the position shown in figure 61. The test was continued by removing the body block and hooking the hydraulic cylinder to the window lap belt. The center body block began stroking at 12.1 G as shown in figure 62. After it stroked, the body block was removed, the cylinder was connected directly to the lap belt, and the test was repeated as before. At 12.2 G, the aisle-side body block began stroking as shown in figure 63. Finally, all the lap belts were attached to the hydraulic cylinders and the seat was tested to destruction at 16.0 G. Figure 64 demonstrates the behavior of the three seat positions during the applied loads, and compares them to the average (average displacement of the three-seat position) performance of the standard Weber seat. The large displacements (beyond the 6-in. design stroke) of the modified seat positions are due to rotation of the body blocks before stroking, and further rotation after they stroked forward and the thighs cleared the seat cushion. Much of the drop-off in the load was caused by the body block acting as a lever against the front tube, and would not occur with inertial loads acting on a restrained body.

RESULTS OF LATERAL STATIC TEST. A lateral load was applied to the body blocks (figure 65) until the seat failed. This occurred at 7.8 G, when the front window-side leg pulled through the bolt attaching it to the track fitting. Figure 66 shows this failure, and figure 67 is the loading curve during the test. Further details of the seat's performance are in reference 40.

RESULTS OF DYNAMIC TEST. The floor deformation and test pulse caused bending of the rear window-side track fitting and the rear tube of the seat (figure 68). No other damage occurred on the seat structure. The dummies were held by the lap belt energy absorbers (figure 69), which stroked only a short distance, as shown in figure 70.

The reactions of the window-side legs of the Weber standard and MOD I seats from the dynamic pulse are both illustrated in figure 71. The curves are similar until the standard seat fails at 5900 lb. The load on the modified seat leg goes up to 7000 lb until the energy absorbers start stroking and attenuate the load for 60 msec.

the backs have an adjustable reclining mechanism. Provisions also allow the seat back to rotate forward if struck from behind in a crash.

Seat Weight. The measured weight of the complete seat assembly is 82 lb.

RESULTS OF FORWARD STATIC TEST. The seat was tested in the forward direction by the method described earlier. At a load of 11.2 G, the rear tube ruptured at the rear-leg fitting (figure 50), and complete failure occurred. Other damage was exhibited by the buckled spreader tubes (figure 51), and the bending of the front tube (figure 52). Further details of the test are described in reference 37.

RESULTS OF FORWARD DYNAMIC TEST. Figure 53 shows the final position of the seat after being tested at 9 G with a 50-ft/sec velocity change. Note that the seat separated completely from the leg structure, and only the redundant tiedown straps (part of the test setup) kept it from leaving the test fixture. Failure points are labeled in figure 54. Arrow 1 indicates the window-side leg detached from the rear track fitting, arrow 2 indicates failure of the front and rear tube fittings on the window-side leg, and arrow 3 indicates a similar situation which occurred on the aisle-side leg.

#### WEBER MOD I SEAT.

MODIFICATION CONCEPT. Four modification concepts were originally considered for the Weber seat, including the energy-absorbing restraint system shown in figure 55. Based on preliminary studies (reference 38), the energy-absorbing restraint system was selected as the preferred configuration. A rear-leg energy-absorbing concept was the runner-up, and was the subject of a second modification.

MODIFICATION DETAILS. As discussed in the "Criteria" section, the objective of the experiment was to modify the seats to withstand an 18-G, 50-ft/sec pulse. For reasons discussed further in Appendix A, the 50 ft/sec had to be reduced to 35 ft/sec. The downward and lateral strength objectives, both 10 G (static) were still assumed to apply. In the design of the modification, it was not found to be feasible to design the lap belt energy absorbers for a 10-G lateral load in a retrofit. Therefore, the criterion was reduced to 7 G for the Weber MOD I seat, and the lateral bracing was lightened accordingly to accurately demonstrate the effect of a 7-G lateral criterion. It was assumed that the lateral load could be applied in the aisle direction, since the seat could lean against the wall if loaded towards the window. This assumption was applicable to all seat modifications. Weak points shown by the finite element model were reinforced. The front and rear tubes were released in torsion by removing fasteners which attached these tubes to the spreaders. Other parts were added to keep the spreaders from moving along the length of the tubes. The legs were also attached with released fittings. Since the seat had failed at 10.4 G in a downward static test, no modifications were required to increase the downward strength. Further considerations and a detailed account of the modification analysis can be found in reference 39.

The final modification is shown in figures 56 through 59. The arrow in figure 56 indicates straps used to carry a forward load from the top of the front legs to the rear track fittings. There are also compression braces (the rationale for the redundant bracing is discussed in Appendix F). Figures 57 and 58 have

the stroking load on the window-side energy absorber was increased to reduce twisting of the seat structure and to reduce the amount of elongation, and the lap belt anchorage was reinforced. These improvements have been implemented on the seats installed on the crash test aircraft.

WEIGHT DISCUSSION. A breakdown of weight increases to the standard seat regarding forward or lateral strength additions, is shown in table 9. An increase in weight of 1.6 percent added energy absorption to the seat and increased its ultimate static strength by 4.4 percent. It also enabled the seat to withstand a 9-G, 50-ft/sec dynamic test without complete separation from the floor. The changes to further improve forward performance involved negligible weight increases. A weight addition of 3.3 percent increased the seat's lateral strength to 6.9 G, 130 percent higher than the 3.0 G minimum design load.

TABLE 9. BREAKDOWN OF WEIGHT INCREASES FOR THE  
WEBERLITE MOD SEAT

Standard Seat Weight	<u>Forward Strength</u> <u>Weight Increase</u>		<u>Lateral Strength</u> <u>Weight Increase</u>		Modified Seat Weight
	<u>lb</u>	<u>Percent</u> <u>Original</u> <u>Weight</u>	<u>lb</u>	<u>Percent</u> <u>Original</u> <u>Weight</u>	
55.2 lb	0.9	1.6	1.8	3.3	57.9 lb

#### WEBER AFT-FACING MOD SEAT

The modification chosen for the aft-facing seat concept was based on the arguments presented in the "Modification Concepts" section. The seat that pivoted about the bottom of the rear leg (relative to the aircraft) and used a front leg (relative to the aircraft) energy absorber appeared the most promising. Such a concept places the line of motion of the c.g. and the energy absorber approximately in line with probable inertial load paths (assuming a partial downward load), is easily compatible with lateral bracing, and allows easy egress. A compressive energy absorber is required, but this disadvantage can be overcome with the development of a suitable design. A sketch of the concept is in figure 157.

MODIFICATION DETAILS. Since the aft-facing modification was developed around the Weber seat, lateral bracing methods similar to those of the Weber modifications were used to strengthen the seat to 10 G laterally. As previously mentioned, the unmodified Weber seat had met the 10-G downward criteria, so no reinforcement was required in that direction. The compressive energy absorbers on the front legs were sized according to loads given by the finite element model in the "before" stroking and "after" stroking conditions, in order to achieve an average load curve of 9 G, and to minimize twisting of the seat structure during stroking.

It was assumed that the entire inertial load of the occupant would be distributed over the seat back. This led to the design of the seat back in figure 158, and the addition of bracing members, as indicated by the arrows, to transfer loads from the seat back to other parts of the seat structure. This bracing arrangement eliminated the adjustability of the back, and the hydraulic devices were removed. Obviously, the use of this rear-facing concept in commercial transports would require development of an adjustment mechanism capable of supporting the loads reached by the seat back. Other views of the seat are in figures 159 through 162.

ENERGY ABSORBERS. The compressive energy absorbers use the method of inverting an aluminum tube, as is shown in figure 163. The load they were designed to attenuate is based on the mean load derived from modeling the seat in the unstroked and stroked configurations. If the energy absorbers were designed to begin stroking at 9 G, and their limit load did not vary, the kinematics of the seat would require the applied load to increase to 12 G to make the energy absorbers complete their stroke. Therefore, a mean value was used so the stroking load of the seat would begin at 7.5 G and end at 10.5 G, resulting in an average load of 9 G. A plastic hinge was designed into the upper fitting of the energy absorbers to limit the bending moments due to structural deformation. The release at the bottom is provided by the Simula track fitting.

RESULTS OF FORWARD STATIC TEST. To apply the loads on the seat backs during the forward static test, the body blocks in figure 164 were used (dimensions are defined in reference 47). At 7.4 G the seat began stroking forward, not showing any twist due to the simultaneous stroking of the energy absorbers. The applied load was increased until, at 9.2 G, the yokes connecting the body blocks to the hydraulic cylinders interfered with the movement of the seat backs (figure 165). Figure 166 shows that the seat stroked 3.9 in., and measurements showed the window- and aisle-side energy absorbers stroked 2.5 and 2.6 in. respectively. Since the energy absorbers were designed to stroke 4 in., it can be concluded that if they had been allowed to stroke fully, the seat would have moved approximately 6.0 in. as planned.

A problem occurred which did not influence the results of the test: the window-side energy absorber pushed into the front tube (figure 167). This caused the diagonal brace to begin peeling open the tube bracket (figure 168). The portion of the tube that collapsed was reinforced on the seat used for the dynamic test.

Because the seat performed satisfactorily through the majority of its potential stroke, and because test samples were limited, the forward static test was not repeated prior to the dynamic test.

RESULTS OF LATERAL STATIC TEST. A lateral test was performed on the seat, as is illustrated in figure 169. The first failure occurred at 3.7 G, when the bolt connecting the rear window-side leg to the rear tube fitting pulled through the leg, as is indicated by arrow 1 in figure 170. Since ultimate failure of the complete structure had not occurred, the test was continued until, at 9.1 G, the bolt connecting the rear tube aisle-side fitting to the diagonal pulled through the diagonal, as is indicated by arrow 2. The loading curve during the test is shown in figure 171. A further description of the seat's performance is in reference 48.

RESULTS OF DYNAMIC TEST. The pretest track-rolling on the window legs applied a moment to the energy absorber that was not released by the track fitting as planned. Instead, the energy absorber deflected to accommodate the deformation. Apparently, this caused misalignment of the parts connecting the two tandem inversion tubes and subsequent failure of the energy absorber during the dynamic test. Two views of the window-side energy absorber are in figure 172. The aisle-side energy absorber failed while stroking, allowing the full reaction load to push it through the front tube (figure 173). Since both energy absorbers failed, the seat fell forward and struck the test fixture, causing the bolt indicated in figure 174 to shear. This occurred on the window-side back. Both outer tension straps pulled out of their attachment points. This is illustrated in figure 175, which shows the aisle-side strap.

Appropriate corrective action for this failure would be to further release the fitting at the lower end of the energy absorber so that a moment large enough to interfere with the performance of the energy absorber would not be transferred. However, the track fitting selected for these tests would not perform as intended under other loading conditions if the moment required to deform it were decreased appreciably. Therefore, a different fitting should be used with the compression inversion tubes. A design with a complete release similar to the first prototype fitting would solve the problem. Since the test seats were already installed on the test aircraft when this test was run, no design changes were made. Based on the performance of the seat in the static test, it is expected that the seat will perform as intended if the floor warpage is less severe than in the dynamic test.

This aft-facing seat design concept could also employ a compressive energy absorber with a higher moment capability. The crushing graphite tube would be a logical candidate, but a design should be developed to sustain rebound loads as well.

Although floor warpage was a variable not included in the static test, the difference in performance of the seat between the static and dynamic tests is an indication of the importance dynamic tests should have in certifying passenger seats.

WEIGHT DISCUSSION. The seat weighs 80 lb, 2 lb less than the standard Weber seat. However, this is not indicative of the effect the modification had on the seat's weight, due to the difference in seat backs. The standard Weber seat is an older one with more cushion material and a fold-down feature in the middle seat back. The modified seat has a redesigned seat back and uses the cushion material from a Weberlite seat. Without their seat backs, the standard and modified seats weigh 56.5 and 60.1 lb, respectively. This means that 3.6 lb were added to the basic seat pan and leg structure for the modification. A survey of the seat back weights without food trays on the other seats in this report shows that those on the Weberlite weigh 13.1 lb, the UOP 13.4 lb, the Weber 18.1 lb, and the Weber aft-facing MOD 19.9 lb.

The breakdown in table 10 shows that almost twice as much weight addition was needed in the Weber aft-facing MOD seat backs than the addition needed in the seat pan structure. The lateral bracing added 4.1 percent to the weight and increased the seat's strength to 9.2 G, 200 percent higher than the minimum design load of 3.0 G.

TABLE 10. BREAKDOWN OF WEIGHT INCREASES FOR  
THE WEBER AFT-FACING MOD SEAT

	<u>Forward Strength</u> <u>Weight Increase</u>		<u>Lateral Strength</u> <u>Weight Increase</u>		<u>Total</u> <u>(lb)</u>
	<u>lb</u>	<u>Percent</u>	<u>lb</u>	<u>Percent</u>	
Seat pan structure	1.3	2.3	2.3	4.1	3.6
Seat backs	6.8*	52	-	-	6.8

\*Compared to Weberlite.

Development of a production configuration could of course decrease these weights. The numbers shown in table 10 should be interpreted as upper limits, and not actual values for the specified seat performance.

#### STANDARD TRANS-AERO FLIGHT ATTENDANT SEAT.

Front and side views of the seat are in figures 176 and 177. This seat is manufactured by Trans-Aero Industries, and is identified as model number 90835-6.

#### SEAT DESCRIPTION.

Structure. The flight attendant seat structure is made up of a foam core seat pan installed on rails for folded storage when not in use. The seat pan itself consists of a sheet metal face over the foam core. A spar traverses the seat pan about 1 in. forward of the pivot arm attach points. A steel frame is attached to the spar and around the periphery of the topfac (figure 178). The bottom and sides of the seat pan are covered by a decorative, thermoplastic sheet with a recessed handle. At each rear corner of the seat pan is a roller on a bracket that attaches to the rear and sides of the seat pan frame (figure 179).

These rollers travel inside a vertical extruded track on either side of the seat pan. A pivot arm is attached to the seat pan on the sides just behind the seat pan spar, and to the side rail above the stopping point of the roller. The pivot arm is spring-loaded to fold the seat against the wall when it is not held down.

The upper pivot arm attachment is made with a NAS 517-6-7 countersunk screw through the pivot arm, a NAS 77A8-12P shoulder bushing, and an angle bracket fastened to the rear flange of the rail extrusion.

Wall Attachment. The seat is designed to be wall mounted with a separate seat back cushion and restraint system attached directly to the aircraft wall. The side rails are connected to the wall with bolts through six holes in each rear flange: four near the top and two near the bottom. These holes are 0.25 in. in diameter.



This seat was designed to meet the requirements of the Boeing Commercial Airplane Company Specification Control Drawing 10-61365, which specifies that the reaction at any attachment point shall not exceed 500 lb in any direction when subjected to a down load of 6.5 G.

Restraint. The restraint system used with this seat (a one-piece belt with three attachment points), is attached directly to the wall and has no bearing on the strength of the seat itself. Therefore, no restraint system was considered in the static test.

Cushions. The seat back and bottom cushions are fabricated of plastic foam and cloth covers with Velcro closures. The seat back is attached to the wall with Velcro strips. Since this cushion has no relevance to the downward loading test, it was not utilized in the static test.

The seat bottom cushion is in two pieces, and fastened to the seat pan with Velcro strips. These cushions are about 2 in. thick and consist of two flat layers of foam, with the lower layer being denser than the upper.

Seat Weight. The weight of the seat assembly is shown as 13 lb on the nameplate, which is in accordance with the measured weight of the structure minus cushions. The weight of the complete assembly is 20 lb.

RESULTS OF DOWNWARD STATIC TEST. The body blocks used in this test were designed and fabricated by Simula Inc. The seat bottom contact area was patterned after actual occupant loading of a seat during a high G downward load, which provides more realistic loading conditions on the seat pan than would the flat bottoms of the conventional body blocks per NAS 809. A steel channel framework was used to pull the body blocks down through the occupant's center of gravity, and the framework was free to pivot at each of the four corners to maintain equal loads on each body block. Views of the test setup are in figures 180 and 181.

At a load of 7.5 G, the seat failed at the pivot bolt attachment on the left-side rail bracket. The 1/8-in.-thick bracket failed in shear tearout at the pivot arm bolt and bushing (figure 182). This failure left no rigid attachment for the left side of the seat pan, and the test was stopped. A loading curve of the left seat pan is in figure 183. Further details of this test are described in reference 49.

#### MODIFIED TRANS-AERO FLIGHT ATTENDANT SEAT.

The FAA made four seats available for the flight attendant seat modification experiment. Three were 90835-6 seats, and one was a 90835-4 seat. Since two 90835-6 seats were needed for the test aircraft, the 90835-4 seat was used for the modification prototype. The model 90835-4 seat used for the modified version of the flight attendant seat differs from the model 90835-6 seat of the static test only in the depth of the right-hand side rail. The depth of the aluminum extrusion on the model 90835-4 seat is 2 in. on the right rail versus 3 in. on the left rail. On the model 90835-6 seat, the depth is 3 in. on both rails. The difference is due to a 1-in. offset in the surface of the aircraft wall to which the model 90835-4 seat mounts.

The 2-in. side rail has the same location of the seat pan roller track and the same location of the pivot arm attachment to the pivot arm bracket relative to a flat wall baseline. This bracket is the only other part to differ between the two seats. Dimensional differences of the brackets and side rails are noted in figure 184.

MODIFICATION CONCEPT. The only design criterion of interest to this seat structure is the downward design load of 10-G.

No energy-absorbing stroke to limit the loads on the aircraft structure was incorporated, since the occupant's restraint system is attached to the wall of the aircraft and would not provide proper retention of the occupant should the seat pan be displaced. Relocating the restraint attachments to the seat structure was deemed impractical because of the FAA shoulder restraint requirement for crewmembers and the possible seat-to-wall attachment overloads with the forward design load requirement. On the forward-facing seats, an energy-absorbing forward stroke of the seat to reduce the fastener loads would encroach into emergency exit areas, and is unacceptable.

The flight attendant seat was therefore modified as a stationary structure by strengthening those parts which would increase its load capacity to 10 G.

#### MODIFICATION DETAILS.

Pivot Arm Bracket. The standard flight attendant seat experienced gross failure of the pivot arm bracket when the pivot bolt tore out of the bracket. The bracket height was increased to provide a greater cross-sectional area to resist the tear out of the pivot bolt (figure 185). The 2.475 and 1.475 in. dimensions in figure 184 were increased to 2.635 and 1.635 in. respectively, giving a 120 percent increase in the local edge distance of the pivot bolt. A weight increase of .09 oz per bracket was added to the seat.

Pivot Arm Assembly. To withstand the moments imposed by a 10-G downward load, the pivot arm assembly was strengthened at the arm-to-seat pivot pin joint. The pin picks up two attachment points to the seat pan spar, and by its rigid connection to the pivot arm, allows the seat pan to rotate to its storage position. The standard seat utilized a single-sided weld or silver-solder joint where the pin fit into a hole through the pivot arm. The increased moments required a stronger joint, which is illustrated in figure 186. A headed pivot pin was inserted into the pivot arm and welded on both sides. The modified pin and weld added .77 oz per assembly to the seat weight. The two parts are shown in figure 187.

Seat Pan Roller Bracket. The standard seat exhibited a forward pitching of the seat pan as the load was applied, resulting from deformation of the roller brackets located at the rear corners of the seat pan. The roller shaft support had bent downward and forward on the roller end, allowing the rear of the seat pan to move upward and aftward, causing the pitch change. At the time of the ultimate seat failure, welds along the lateral gusset had cracked.

A new roller bracket (figure 188) was designed to eliminate this deformation. The modified roller bracket contains an extended tube to prevent the roller shaft from bending the bracket. The lateral gusset was heightened to meet this extended tube and provide vertical and horizontal stabilization of the seat

pan roller. An extended roller shaft was included to complete the modification (figure 189). The strengthened roller bracket and shaft added this roller stabilization with only a .55 oz per bracket weight increase.

RESULTS OF DOWNWARD STATIC TEST. As the test proceeded, very little forward pitching of the seat pan was noticed in comparison to the standard seat tested previously. At 9.9 G, the right pivot arm failed in tension and bending through its minimum cross section (figure 190). This allowed the right side of the seat pan to move downward until the right-side roller jammed in its track. A loading curve of the right seat pan is in figure 191. Reference 50 contains further information concerning the modification and test results.

WEIGHT DISCUSSION. A weight addition of 2.8 oz, or 1.3 percent of the original weight, increased the seat's ultimate downward strength from 7.5 G to 9.9 G, a 32 percent increase.

Strengthening the right pivot arm that failed would increase the ultimate load of the seat, but a limiting factor may be the adjacent aircraft structure. Further development would be necessary to determine the maximum loads allowed by the structure.

## AIRCRAFT TEST SETUP

### FLOOR PLAN.

All of the experimental seats were placed aboard the test aircraft at the NASA Dryden Flight Research Facility at Edwards, California. The seats were placed as shown in figure 192. The seats were modified in pairs: there is one left and one right of each seat, except for the aft-facing Weber seat. There are also pairs of most of the standard seats. As illustrated, the seats were placed with most of the seat pairs separated, one forward and one aft. This was done since it was believed that the crash environment would probably vary along the longitudinal axis of the aircraft. Thus, separating pairs of identical seats provided the opportunity to obtain data for two different impact conditions for the seat.

The seats were spaced in an attempt to minimize interaction between experiments. While there is obvious interaction between seat/occupant systems in a real crash due to the close spacing, it was felt that little could be learned in these tests if close spacing was used, due to the fact that the seat designs are all different. If load was transferred from one seat to another due to extensive dummy/seat contact, there would be no way of determining how the seat would have performed had the load not been transferred. (A closely spaced test with identical seats would of course be meaningful; the load transferred to the seat ahead could be presumed to be offset by load applied to the seat by the occupants behind it). To limit interaction between seat experiments, the spacing was arranged to prevent or at least limit head and torso impact of the dummies into the next seat. It was not possible to space the seats to prevent arm and leg impact.

It is also desirable to limit seat experiment interaction because computer simulations with program SOM-TA are planned for the postcrash analysis. The response of the structure itself will be of interest. Dummy impact on the rear of a seat would provide input to the accelerometers which would not be simulated in the analysis and which would interfere with correlations.

### ANTHROPOMORPHIC DUMMIES

Eleven instrumented 50th-percentile anthropomorphic dummies are being used in these experiments. Nine of these dummies are Part 572 dummies from Humanoid Systems Inc. The other two are Sierra dummies. They are dressed in tight-fitting thermal underwear to obtain a realistic coefficient of friction between the dummy and the seat upholstery. The joints of the dummy are adjusted so that the limbs will just barely move under the influence of gravity. They are positioned in the seats shown by table 11 to have instrumented dummies. There is one instrumented dummy in each of 10 passenger seats, and in each case the dummy is in the center position, except the Hardman dual seat, where the dummy is in the aisle position. One instrumented dummy is in the pilot seat. More dummies could not be used because of a limitation on the total number of data channels.

The remainder of the seats are occupied by uninstrumented Model 500H dummies manufactured by Med-d-Trane. They are not anthropomorphic dummies, but they

TABLE 11. LOCATIONS AND QUANTITIES OF SEAT AND DUMMY ACCELEROMETERS

Item	Description	Head	Thorax	Pelvis	Seat	Belt*	Shoulder Harness	Floor
d	Pilot	0	0	3	3	2	2	3
S	Trans-Aero Flight Attendant, aft-facing	0	0	0	0	0	0	0
A	Weberlite Standard	0	0	3	4	2	0	3**
E	Weberlite MOD I	0	0	3	4	2	0	2**
G	Weber MOD I	0	0	0	3	0	0	1
C	Weber Standard	0	0	0	3	0	0	1
B	UOP Standard	2	3	3	4	2	0	2**
H	UOP MOD II	2	2	3	4	2	0	3**
F	UOP MOD I	0	0	0	3	0	0	1
I	Weber MOD II	0	0	0	3	0	0	1
D	Hardman aft-facing Standard	2	2	3	4	2	0	3
D	Hardman aft-facing Standard	0	0	0	3	0	0	1
P	Weber Standard with Simula Inc. Fittings	0	0	0	0	0	0	0
K	Weber aft-facing MOD	0	0	0	0	0	0	0
C	Weber Standard	0	0	3	4	2	0	3**
G	Weber MOD I	0	0	3	4	2	0	2**
E	Weberlite MOD I	0	0	0	3	0	0	1
A	Weberlite Standard	0	0	0	3	0	0	1
H	UOP MOD II	0	0	0	3	0	0	1
B	UOP Standard	0	0	0	3	0	0	1
I	Weber MOD II	0	0	3	4	2	0	2**
F	UOP MOD I	0	0	3	4	2	0	3**
J	UOP Composite Standard	0	0	0	0	0	0	0
T	Trans-Aero Flight Attendant, forward- facing (MOD)	0	0	3	3	2	2	3

\*Belt tensiometer transducers.

\*\*Common with structural measurements.

Note: Seats are listed in body station sequence.

do have the proper mass and physical dimensions, and should apply the proper inertial loads to the seats with one exception: seat P contains an infant dummy.

Paper targets are positioned on the head, shoulder, and knees of all the dummies so that it will be easier to evaluate motion observed with the available camera coverage.

All dummies are secured in their respective seats with new lap belts. The belts are Model No. 449470 from American Safety Equipment Corporation. The belts will be pulled as tightly as possible by hand prior to the test.

#### INSTRUMENTATION.

The experimental seats and dummies are instrumented with accelerometers and lap belt tensiometers. The accelerometers are Endevco Model 7264-200 and the tensiometers are LeBow Model 3419. To obtain various data requirements with limited data channels, the instruments are distributed unequally. The location of instruments in the most completely instrumented seats is shown in figure 193.

#### ACCELEROMETERS.

Each of the eleven anthropomorphic dummies is instrumented with accelerometers, but some have more than others. All have pelvis accelerometers, but the other accelerometers are installed only in selected locations. Table 11 shows which dummies have accelerometers in the head, thorax, and/or pelvis.

All seats have accelerometers mounted on the rear-facing seat pan tube. Some have two mounts, with a triaxial arrangement on one mount but only a longitudinal accelerometer on the other. The second longitudinal accelerometer is placed on the seat because of the asymmetry of the seat structure. The aisle side of the seats will, in most cases, experience higher decelerations than the window side because the window side is subjected to a greater inertial load and thus will experience more deformation. The triax is placed on the aisle side because more output could be expected (important if the crash pulse is not very severe) and because this seat accelerometer is in line with the floor accelerometers and should give the best correlation of input versus output for the structure. The seat accelerometers were mounted near the intersection of the rear leg and the rear tube to attempt to measure a representative acceleration of the structure independent of the free vibration response of any of the components.

The floor accelerometers are mounted on the floor track or on the beam directly between the floor tracks (beam and track are one extrusion). Where there is no lateral accelerometer under the seat, the acceleration from the opposite side of the aircraft will be assumed to apply. This assumption appears reasonable since the floor should be very rigid in the lateral direction.

#### LAP BELT TENSIONIOMETERS

The lap belt tensiometers are mounted on the belts restraining the dummies; their locations are indicated in table 11. The tensiometers being used are known to produce erroneous readings under certain conditions where a load is

applied to the base of the device as tension is applied to the belt on which it is installed. In the intended application, the thigh and/or pelvis of the dummy will apply a load to the base of the tensiometer. Therefore, guide blocks (figure 194) were installed to suspend the tensiometers on the belts and prevent them from experiencing loads other than tension.

#### SECONDARY RESTRAINT.

If any of the experimental seats, or more likely, any of the standard seats, should fail, it would apply load to the seat ahead of it which could cause it to fail also. It is possible that a sequence of such failures could occur, and that data from seats which would not have failed by themselves would be lost. Therefore, a secondary restraint system was designed and installed to keep a seat in position even if it failed.

The components of the secondary restraint system consist of polyester slings and expanding-tube energy absorbers. The slings were cinched about the waist of the dummies, and connected to the energy absorbers, which were in turn connected to floor track fittings. The attachment to the dummies is illustrated in figure 195. The energy absorbers were designed to stroke at a load of 6000 lb for a distance of 6 in. One energy absorber in the unstroked and stroked position is illustrated in figure 196. This system uses two energy absorbers per seat, and would therefore decelerate a typical experimental seat at 20 G were the seat to fail. The secondary restraint system is installed with 6 in of slack, so that it will not interfere with the energy-absorbing function of the seat. The system is tied to the dummies, because this appeared to be the most reliable means of restraining the seat should it fail. The installation shown in figure 195 is typical of the restraint system used on the various seat configuration.

#### FLIGHT ATTENDANT SEATS INSTALLATION.

The seats to be installed were Trans Aero Flight Attendant seats part number 90835. These modern seats are used in current production aircraft. They were installed in typical locations for this type aircraft. One seat was located in the forward end of the fuselage, by the door and was aft facing and mounted on the bulkhead at station 302. The other seat was located in the aft end of the fuselage and was forward facing and mounted on the bulkhead at body station 1380 (figure 192). There had been no seats mounted on these bulkheads before so there were no attaching points or hard points that would line up with the seat attachment points. Therefore considerable engineering work had to be expended to make detail drawings of the existing bulkheads and then later in the engineering office to proceed to design an interfacing framework through which the seat structure was mated to the existing bulkhead. The other alternative would have been to redesign the bulkhead itself which would have been too expensive and not as reliable. Considerable stress analysis work was also expended to ensure that the seat would take the loads that the bulkhead was designed for.

The aft facing seat was not instrumented, however, the forward facing seat contains a dummy and is instrumented according to table 11.

## DISCUSSION

At the time this report was written, the experimental seats had been placed aboard the test aircraft, but the crash test had not been conducted. Therefore, the determination of conclusions for the overall project is premature. However, certain observations and determinations concerning the crashworthiness of existing transport seats and the potential for improvement have become apparent during the development of the experimental seats.

First, the briefest examination of the accident data and literature relating to transport seats, reveals that the crashworthiness of transport seats is a controversial topic. Whereas manufacturers and operators once frequently developed and deployed crashworthy features that exceeded the minimum design standards, in more recent years, opposition to a higher level of protection has appeared because of present economic considerations. The following quotation from reference 53 demonstrates one such position:

Increased seat densities have lead to an interesting change of policy on seat strength. Manufacturers at one time designed for crash conditions, assuming a controlled deflection under G. But airlines now require no distortion up to the point of actual failure, since even quite small deflections can so reduce clearances between adjacent seats that injury might result.

While it is true that the pitch of the seats is reduced, some of that reduction is due to a change in seat dimensions, and does not necessarily reduce the space between the occupant and the next seat. A portion of the pitch reduction does reduce the space available to the occupant, and increases the chances that an occupant could be injured and/or trapped if his seat strokes and the one in front of it does not. However, occupancy rates are also higher, so there is a much better chance that the seat ahead will also stroke, in which case the pitch of the seats is not as significant a factor. A seat failure is more likely to trap and/or injure the occupant, than is the controlled stroking of an energy-absorbing seat. Energy-absorbing seats can be designed to deform only at loads equal to or above the present ultimate failure loads, and not under any conditions less severe than those which would cause ultimate failure of a non-energy-absorbing seat. The energy-absorbing seat would not conceivably be a cause of injury, but it would have the potential for preventing injury in certain crashes. The increased seating density does not therefore provide a reason to eliminate crash survival considerations.

Frequently, the argument is advanced that as aircraft have become larger, the criteria for seats have become less critical because the larger structures will experience a less severe acceleration at the floor due to increased energy absorption below the floor. While the presumed effect of scale may be largely true, the assumption that aircraft have continually gotten larger is questionable. Table 12, compiled from reference 52, clearly show that many modern jets other than the jumbo jets (747, DC 10, and L1011) are no larger than those of 20 years ago. If energy-absorbing transport seats were appropriate for the 707 and the 727, they should be appropriate for a 737 and a DC9, which are smaller aircraft. They should also be appropriate for a 757 and a 767, which are of similar size. Construction techniques have not changed in a way which would support such a change in philosophy.



TABLE 12. RELATIVE TRANSPORT SIZES

	Passengers (a)	Cabin Length/ Width (max.) (ft)	Maximum Passengers	Maximum Gross T.O. Weight (lb)
	143	111.5/11.6	219	333,600
7-200	980	92.6/11.6	145	209,500
7-200	187	68.5/11.5	130	126,100
7-200	1,429	187/20	442	805,000
	NA	NA	223	240,000
7-200	1,696	111.3/15.5	289	310,000
7-200 Super 20	965	101/10	172	147,000
7-200 Series 30	NA	136/18.8	380	572,000
7-200	2,320	136/19	400	477,000
7-200	NA	128.5/17.6	320	363,760

\*Not available

Attempts at using the crash investigation data to determine realistic criteria for transport seats have only been partially successful, since the primary objective during investigation has been to determine probable cause and not the effect seats had on occupant survivability. As shown by references cited in this report, opposing positions regarding the subject have employed the crash data for support. It is admittedly a difficult task to extract design criteria from crash investigation data; however, it is believed that the widely divergent conclusions with respect to transport seats are, at least in part, the result of different initial assumptions. These assumptions primarily involve the selection of those accidents which should be considered survivable, and the extent of injury which may be related to the seat structure.

One extreme view of survivability requires that the occupied volume remain intact in the vicinity of the occupant. Emphasis is on the individual occupant's environment. On an aircraft as large as a transport, this is not survivable for some occupants and nonsurvivable for others. Very often, it is survivable for the majority of passengers, and nonsurvivable for only a few. This is because transports frequently fracture at one or two stations while the resulting sections remain relatively intact. In these cases, only the passengers in the vicinity of the fracture are endangered, while those in the intact sections remain in a survivable environment with regard to living space. Others assume that for a crash to be considered survivable, the overall aircraft fuselage, or total occupied volume, must remain intact. No consideration is given to the concept of partial survivability, a condition existing for

a majority of the passengers. It is then assumed that seat failures occurring in crashes with separation of the fuselage are acceptable because the crash is nonsurvivable; an assumption obviously invalid if a majority of the passengers are considered. These two approaches result in widely different conclusions concerning appropriate seat criteria.

In addition to different assumptions concerning the preservation of occupied volume in a survivable crash, there are different assumptions made concerning tolerable acceleration levels. Some reports claim that since spinal injuries occur in some crashes, seats are already too strong in the vertical direction and stronger seats will lead to more injuries. Careful consideration of conclusions that have been based on the observed spinal injuries reveals several possible misinterpretations. First, it cannot be assumed that spinal injuries result exclusively from vertical accelerations transmitted through the seat structure. If seats fail, the secondary impacts occurring when the seat and occupants strike the floor can result in far higher accelerations than would be experienced if the seat remained intact. Therefore, seat failure can be a cause of spinal injury. Spinal injury may also occur when the occupant jack-knifes over the lap belt due to the forward inertial loads. This injury-causing mechanism is documented in reference 36, and shows that spinal injury can occur even without any vertical acceleration. It is also possible that reverse flexure of the spine can be a cause of fracture. This type of injury could occur from the upper torso striking the back of the next row of seats while the forward inertial loads imposed on the lower abdominal region drives it forward. Very detailed autopsy reports would be required to attempt to identify the exact cause of fracture.

Another problem with the conclusions concerning spinal injury is that available human tolerance data indicate that the body can withstand higher vertical loads than would be imposed by seats designed to existing seat standards. Although human tolerance limits continue to be a subject of research, and obviously vary with age and other factors, there is every reason to believe that the mean value is well over 6 G. Volunteers consistently have permitted themselves to be exposed to downward loading considerably exceeding 6 G, with an upper voluntary limit of 15 G.

It is, therefore, not reasonable to assume that the observed spinal injuries are due to vertical acceleration transmitted through the existing seat structure, nor is it reasonable to assume that increased vertical seat strength will increase the frequency of spinal injury.

The present discussion presents only a few highlights of the circumstances surrounding the interest in increased crash survivability for transport seats. Because of the limited interest expressed by the airline industry, this experiment was designed to demonstrate changes to transport seats which could be made without a prohibitive impact on operations. Therefore, as discussed in the report, intermediate design criteria were selected.

When comparing the selected design criteria with published human tolerance data, and with a belt-only restraint, it was concluded that no energy absorber was necessary to limit the acceleration acting on the occupants to less than was experienced by the aircraft floor (this itself is, of course, limited

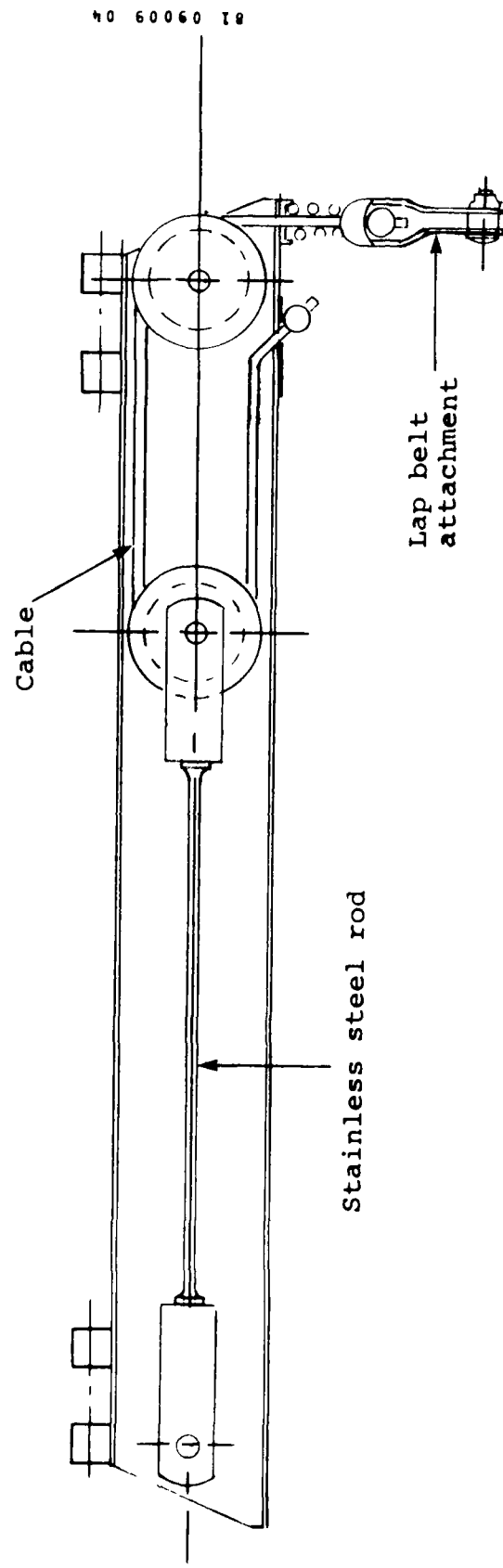
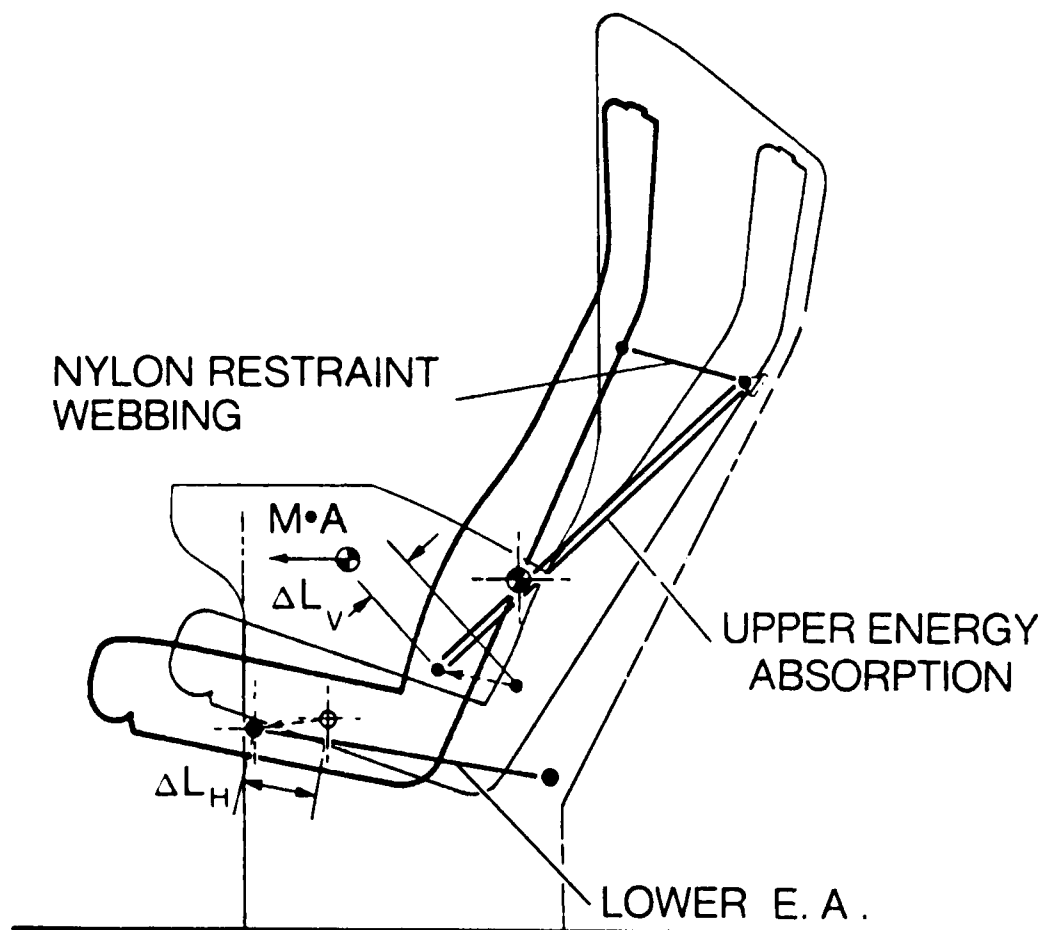


Figure 4. Hardman lap belt energy absorber.



01 09009 03

Figure 3. Energy-absorbing arrangement in NASA seat.

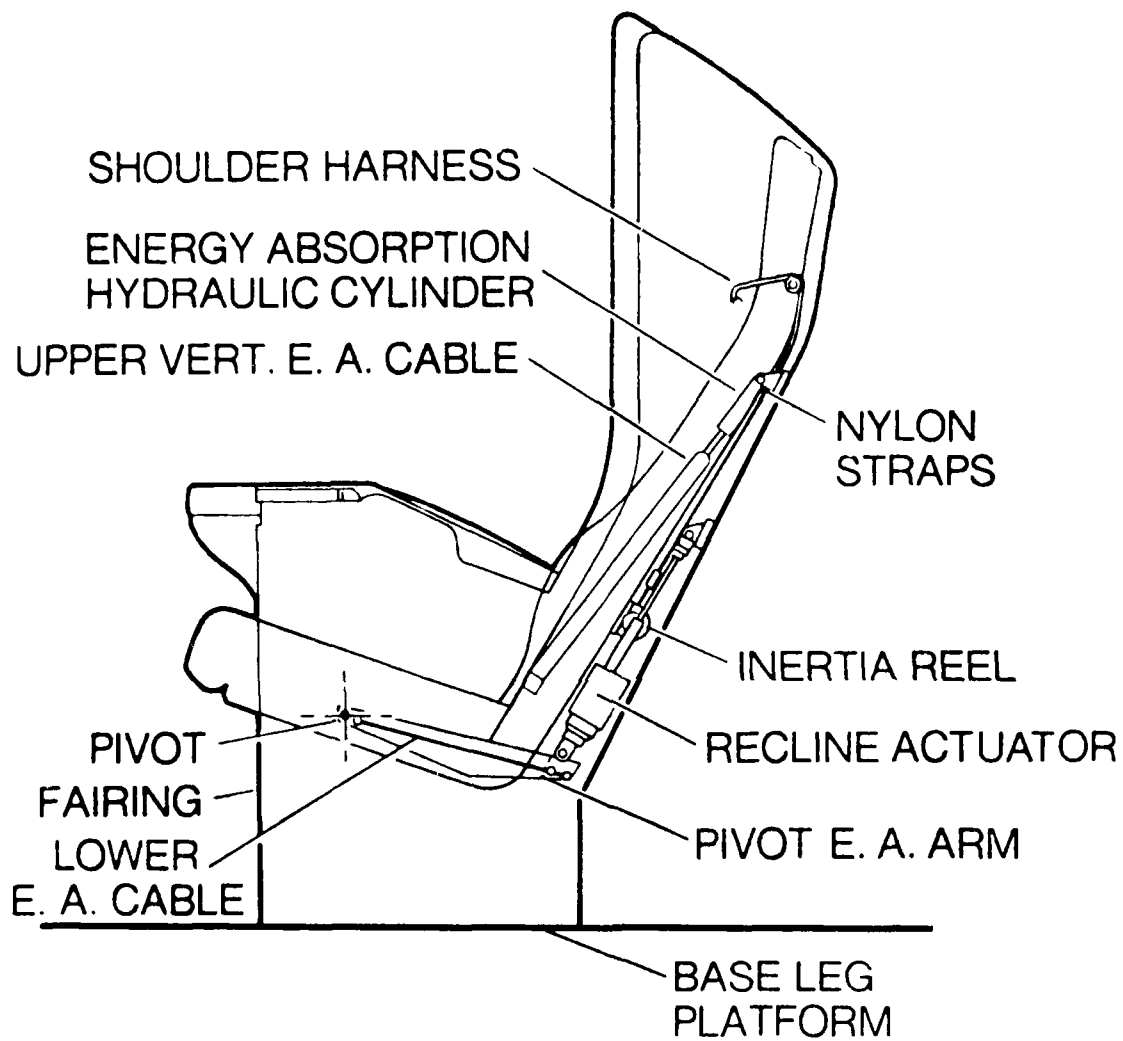
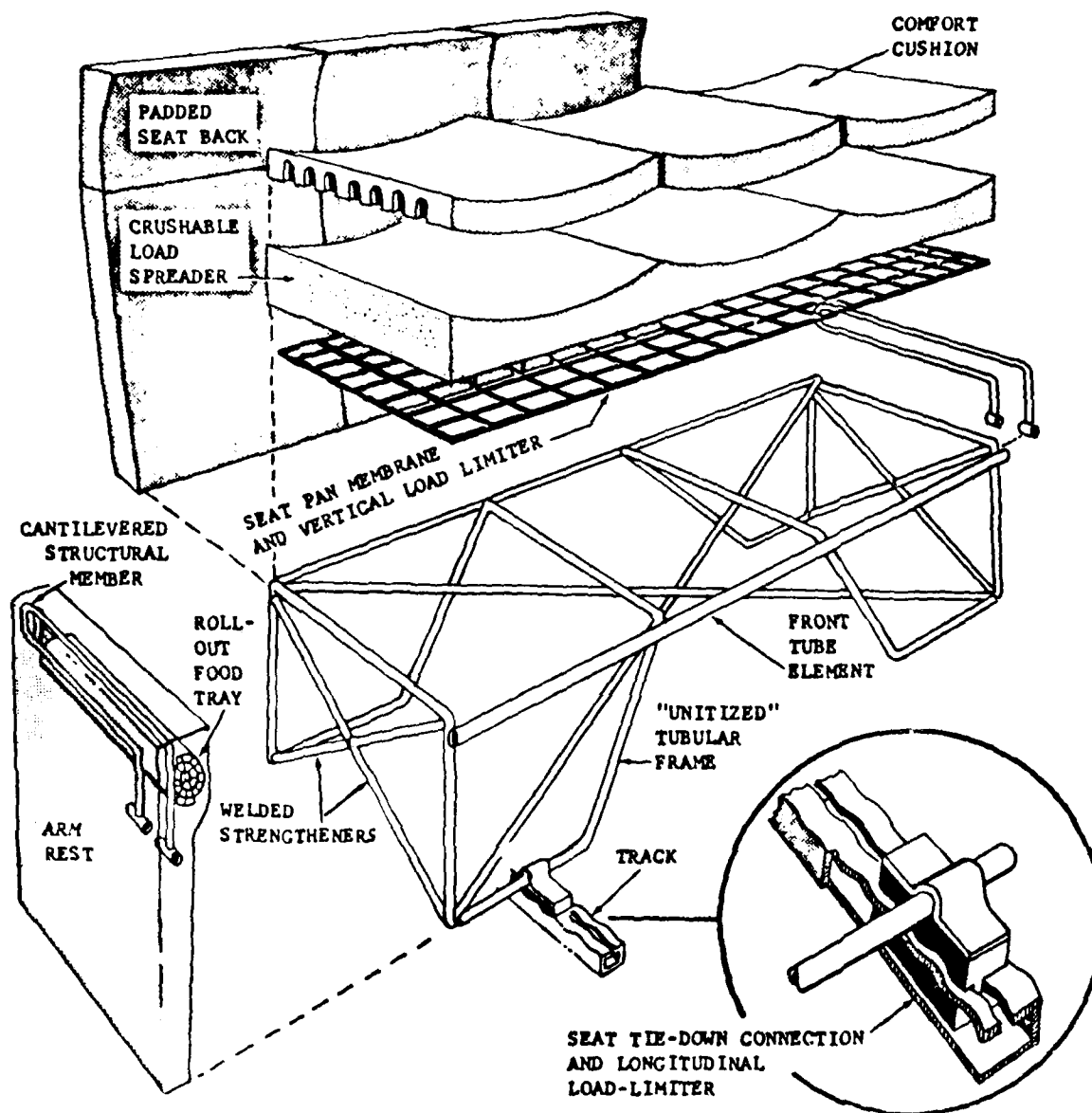


Figure 2. NASA single-occupant seat design.



81 09009 01

Figure 1. Floor track load-limiting device from Arizona State University design study.

50. Eisentraut, D. K., and Bradney, C., STATIC TEST REPORT FOR THE MODIFIED TRANS-AERO INDUSTRIES MODEL 90835-4 WALL-MOUNTED DOUBLE CABIN ATTENDANT SEAT, Report No. TI-83425, Simula Inc., Tempe, Arizona, December 20, 1983.
51. Goold, I., SEATS: THE PASSENGER/AIRLINE INTERFACE, Flight International, September 15, 1979, pp. 892-894.
52. Taylor, J. W., ed., JANE'S ALL THE WORLD'S AIRCRAFT 1980-1981, Jane's Publishing Co., London, England, 1982.
53. Laananen, D. H., Coltman, J. W., and Bolukbasi, A. O., COMPUTER SIMULATION OF AN AIRCRAFT SEAT AND OCCUPANT IN A CRASH ENVIRONMENT, Volume II - PROGRAM SOM-LA USER MANUAL, Report No. TR 81415, Simula Inc., Tempe, Arizona, September, 1982; Report No. DOT/FAA/CT-82/33-II, Federal Aviation Administration, Atlantic City Airport, New Jersey.
54. Laananen, D. H., and Bolukbasi, A. O., COMPUTER SIMULATION OF AN AIRCRAFT SEAT AND OCCUPANT IN A CRASH ENVIRONMENT, Volume I - TECHNICAL REPORT, Report No. TR-82401, Simula Inc., Tempe, Arizona, March 1982; Federal Aviation Administration, Atlantic City Airport, New Jersey.

36. Snyder, R. G., et al., SEAT BELT INJURY IN IMPACT, Report Number AM-69-5, Federal Aviation Administration, Washington, D.C., December 1969.
37. Zimmermann, R. E., and Bradney, C., STATIC TEST REPORT FOR THE WEBER P/N 819493 TRIPLE-PASSENGER TRANSPORT SEAT, Report No. TR-81424, Simula Inc., Tempe, Arizona, January 28, 1982.
38. Zimmermann, R. E., PRELIMINARY STUDY AND SELECTION OF DESIGN CONCEPTS FOR THE SEAT AND RESTRAINT SYSTEM EXPERIMENTS FOR THE BOEING 720 CRASH TEST, Report No. TI-81413, Simula Inc., Tempe, Arizona, August 12, 1981.
39. Zimmermann, R. E., and Bolukbasi, A. O., CONCEPTUAL DESIGN STUDIES FOR THE SEAT AND RESTRAINT SYSTEM EXPERIMENTS FOR THE BOEING 720 CRASH TEST, Report No. TR-81425, Simula Inc., Tempe, Arizona, February 18, 1982.
40. Bradney, C., and Shane, S. J., STATIC TEST REPORT FOR THE WEBER MOD I THREE-PASSENGER TRANSPORT SEAT, Report No. TI-84410, Simula Inc., Tempe, Arizona, May 17, 1984.
41. Bradney, C., and Shane, S. J., STATIC TEST REPORT FOR THE WEBER MOD II THREE-PASSENGER TRANSPORT SEAT, Report No. TI-84411, Simula Inc., Tempe, Arizona, June 1984.
42. Bradney, C., and Cannon, M. R., STATIC TEST REPORT FOR THE UOP 901-02A-3 THREE-PASSENGER TRANSPORT SEAT, Report No. TI-83413, Simula Inc., Tempe, Arizona, August 10, 1983.
43. Bradney, C., and Cannon, M. R., STATIC TEST REPORT FOR THE UOP MOD I THREE-PASSENGER TRANSPORT SEAT, Report No. TI-84412, Simula Inc., Tempe, Arizona, April 6, 1984.
44. Bradney, C., and Cannon, M. R., STATIC TEST REPORT FOR THE UOP MOD II THREE-PASSENGER TRANSPORT SEAT, Report No. TI-84413, Simula Inc., Tempe, Arizona, April 18, 1984.
45. Bradney, C., and Eisentraut, D. K., STATIC TEST REPORT FOR THE WEBERLITE THREE-PASSENGER TRANSPORT SEAT, Report No. TI-84409, Simula Inc., Tempe, Arizona, March 26, 1984.
46. Bradney, C., and Cannon, M. R., STATIC TEST REPORT FOR THE WEBERLITE MOD THREE-PASSENGER TRANSPORT SEAT, Report No. TI-84414, Simula Inc., Tempe, Arizona, May 14, 1984.
47. Bradney C., SIMULA-DEVELOPED 95TH-PERCENTILE BODY BLOCK, Report No. TI-84408, Simula Inc., Tempe, Arizona, March 8, 1984.
48. Bradney, C., and Cannon, M. R., STATIC TEST REPORT FOR WEBER AFT-FACING MOD TRIPLE-OCCUPANT TRANSPORT SEAT, Report No. TI-84415, Simula Inc., Tempe, Arizona, June 1984.
49. Eisentraut, D. K., STATIC TEST REPORT FOR THE TRANS-AERO INDUSTRIES MODEL 90835-6 WALL-MOUNTED DOUBLE CABIN ATTENDANT SEAT, Report No. TI-83408, Simula Inc., Tempe, Arizona, June 23, 1983.



23. Federal Aviation Administration Hearing Synopsis No. 9660, In the Matter of: Transport Category Airplanes, Seat and Seat Restraint Strength, Washington, D.C., June 3-5, 1980, and September 10, 1980.
24. Voyls, D. W., DYNAMIC TEST CRITERIA FOR AIRCRAFT SEATS, Federal Aviation Administration, National Aviation Facilities Experimental Center; Final Report NA-69-5 (DS-69-10), Aircraft Development Service, October 1969, AD 696963.
25. Langner, F. C., CONDUCT STUDY, DESIGN, DEVELOP AND FURNISH PROTOTYPES OF ENERGY ABSORPTION SYSTEMS FOR AIRCRAFT SEATS, Aerotec Industries, Inc.; Navy Bureau of Aeronautics, March 30, 1960, AD 272672.
26. SPECIAL EDITION, ENERGY ABSORPTION, The Project Engineer, A Thermix Corporation publication, Volume 17, No. 4, April 1958, pp. 1-12 (included in Reference 9 as pages 650-659).
27. Haley, J. L., Jr., Turnbow, J. W., and Klemme, R. E., EVALUATION OF 1000-4000 POUND LOAD-LIMITING DEVICES FOR USE IN AIRCRAFT SEATS AND CARGO RESTRAINT SYSTEMS, Dynamic Science, Division of Marshall Industries; (AvSER) Memorandum Report M69-2, U.S. Army Aviation Materiel Laboratories, February 1969.
28. AEROTHERM SEAT BROCHURES FOR ZEPHYR II, DC-8 SEAT, and SPACESAVER, AOT 502, 503, and 504, Aerotherm Division, Aerotec Industries, Inc., Bantam, Connecticut.
29. Babcock, F. A., PASSENGER SAFETY, Aerotec Industries Review, Volume II, Number 3, Winter 1961-62, Aerotec Industries, Inc., South Norwalk, Connecticut.
30. Cress, G., DOUBLE AND TRIPLE COACH SEAT STATIC AND DYNAMIC TESTS WEBER PART NOS. 804001-602, 804003-604, 804003-605, Weber Aircraft Corporation; Engineering Report TR-218, Trans World Airlines Inc., April 3, 1962.
31. Carmody, J. K., DYNAMIC TESTING OF THE ASD TYPE Ib and TYPE IIb AFT FACING PASSENGER SEATS WEBER P/N 804392 DOUBLE (TYPE Ib) WEBER P/N 804391 TRIPLE (TYPE IIb), Weber Aircraft Corporation; United States Air Force Aeronautical Systems Division, Wright-Patterson Air Force Base, Ohio, January 1962.
32. Snyder, R. G., ADVANCED TECHNIQUES IN CRASH IMPACT PROTECTION AND EMERGENCY EGRESS FOR AIR TRANSPORT AIRCRAFT, Advisory Group for Aerospace Research and Development, AGARDOGRAPH 221, 1975.
33. IMPACT PROTECTIVE DESIGN OF OCCUPANT ENVIRONMENT TRANSPORT AIRCRAFT, SAE ARP 767A, Society of Automotive Engineers, Inc., Warrendale, Pennsylvania, January 1978.
34. Horsfall, J., CABIN DESIGN FOR SURVIVAL, Department of Geodes and Geophysics, Cambridge University; Flight International, June 29, 1980, pp. 1493-1494.
35. Swearingen, J. J., et al., KINEMATIC BEHAVIOR OF THE HUMAN BODY DURING DECELERATION, Civil Aeromedical Research Institute, Federal Aviation Agency, Oklahoma City, Oklahoma; Aerospace Medicine, February 1962, pp. 188-197.

11. Desjardins, S. P., and Laananen, D. H., AIRCRAFT CRASH SURVIVAL DESIGN GUIDE, Volume IV - AIRCRAFT SEATS, RESTRAINTS, LITTERS, AND PADDING, Simula Inc. Tempe, Arizona; USARTL Technical Report 79-22D, Applied Technology Laboratory, U.S. Army Research and Technology Laboratories (AVRADCOM), Fort Eustis, Virginia, June 1980.
12. COMPARISON OF SEAT/DUMMY LOADS WITH AND WITHOUT LOAD-LIMITING DEVICES IN A STANDARD AIRLINE TRIPLE SEAT, Dynamic Science, Division of Marshall Industries; Aviation Safety Engineering Research (AvSER) Memorandum Report 68-10, National Aeronautics and Space Administration, October 1968.
13. Collins, J. A., et al., CRASHWORTHINESS STUDY FOR PASSENGER SEAT DESIGN, ASU Engineering Report No. 66-51, Arizona State University; Aviation Safety Engineering and Research, Division of Flight Safety Foundation Inc., Phoenix, Arizona, July 1966.
14. SEAT COMPONENT TESTING, Memorandum Report 66-2, Aviation Safety Engineering Research (AvSER), Division of Flight Safety Foundation, Inc., Phoenix, Arizona.
15. Weinberg, L. W. T., STATIC AND DYNAMIC TEST OF TECO FIRST CLASS PASSENGER SEAT, Memorandum Report 66-3, Aviation Safety Engineering Research (AvSER), Division of Flight Safety Foundation, Inc., Phoenix, Arizona.
16. Weinberg, L. W. T., DYNAMIC TEST OF A TRIPLE PASSENGER TRANSPORT SEAT, Memorandum Report 66-4, Aviation Safety Engineering Research (AvSER), Division of Flight Safety Foundation, Inc., Phoenix, Arizona, February 10, 1966.
17. Weinberg, L. W. T., A SIMULATED SEAT LEG ENERGY ABSORPTION TEST, Memorandum Report 66-5, Aviation Safety Engineering Research (AvSER), Division of Flight Safety Foundation, Inc., Phoenix, Arizona, February 2, 1966.
18. DYNAMIC TESTS OF A HARDMAN MODEL 8027 TRIPLE PASSENGER SEAT - TESTS MTT-16 AND MTT-17, Aviation Safety Engineering Research (AvSER), Division of Flight Safety Foundation, Inc., Phoenix, Arizona, April 1967.
19. Kubokawa, C. C., THE NASA AMES INTEGRAL AIRCRAFT PASSENGER SEAT CONCEPT - A HUMAN ENGINEERING APPROACH, Ames Research Center, NASA, Moffett Field, California, 1974.
20. Pinkel, I. I., and Rosenberg, E. G., SEAT DESIGN FOR CRASHWORTHINESS, NACA TN 3777, Report 1332, NASA Advisory Committee for Aeronautics, Cleveland, Ohio, 1956.
21. Parks, D. L., and Twigg, D. W., ATTENDANT RESTRAINT SYSTEM TECHNICAL EVALUATION AND GUIDELINES, The Boeing Company, Boeing Document D6-44779TN-0, June 1978.
22. Domzalski, L., CRASHWORTHY MILITARY PASSENGER SEAT DEVELOPMENT, Aircraft and Crew Technology Directorate, Naval Air Development Center, Warminster, Pennsylvania.

## REFERENCES

1. CODE OF FEDERAL REGULATIONS, Title 14: Aeronautics and Space, Parts 1 to 59, National Archives and Records Service, U.S. Government Printing Office, Washington, D.C., January 1983.
2. FEDERAL AVIATION REGULATIONS TECHNICAL STANDARD ORDER AUTHORIZATIONS, Part 37, Department of Transportation, Federal Aviation Administration, Washington, D.C., May 1974.
3. CRASH SURVIVAL DESIGN GUIDE, Dynamic Science, Division of Marshall Industries; USAAMRDL Technical Report 70-22, Eustis Directorate, U.S. Army Air Mobility Research and Development Laboratory, Fort Eustis, Virginia, 1970.
4. Ryan, J. J., HUMAN CRASH DECELERATION TESTS ON SEAT-BELTS, Aerospace Medicine, February 1962, pp. 167-174.
5. Laananen, D. H., WHOLE-BODY HUMAN TOLERANCE TO IMPACT WITH LAP BELT-ONLY RESTRAINT, Report Number TI-83405, Simula Inc., Tempe, Arizona; Department of Transportation, Federal Aviation Administration Technical Center, Atlantic City, New Jersey, May 1983.
6. Widmayer, E., and Brende, O. B., COMMERCIAL JET TRANSPORT CRASHWORTHINESS, NASA CR-165849 (DOT-FAA-CT-82-86), Nasa Langley Research Center, Hampton, Virginia, March 1982.
7. Wittlin, G., Gamon, M., and Skycoff, D., TRANSPORT AIRCRAFT CRASH DYNAMICS, NASA CR-16851 (DOT-FAA-CT-82-69), NASA Langley Research Center, Hampton, Virginia, March 1982.
8. CRASH SURVIVAL DESIGN GUIDE, Dynamic Science, Division of Marshall Industries; USAAMRDL Technical Report 71-22, Fort Eustis Directorate, U.S. Army Air Mobility Research and Development Laboratory, Fort Eustis, Virginia, October 1971.
9. Chandler, R. F., and Gowdy, R. V., LOADS MEASURED DURING PASSENGER SEAT TESTS, Memorandum Report AAC-119-81-8, Protection and Survival Laboratory, Civil Aeromedical Institute, Mike Monroney Aeronautical Center, Federal Aviation Administration, Oklahoma City, Oklahoma.
10. PASSENGER SEAT DESIGN COMMERCIAL TRANSPORT AIRCRAFT, SAE ARP 750A, Society of Automotive Engineers, Inc., New York, New York, January 1974.

Some upgrading of the seat criteria could result in improved seat performance and it is expected that manufacturers would have little difficulty meeting these criteria. As evidenced in the "Prior Development" section, most manufacturers voluntarily upgraded seat design criteria 20 years ago, with no significant problems.

The transport aircraft full-scale Controlled Impact Demonstration will provide further data if the impact is severe enough to initiate failure of standard seats. If the anticipated crash environment in the aircraft is not severe enough to obtain the desired data, higher impact conditions could be simulated through further laboratory testing after the seats are removed from the aircraft. These data, coupled with follow-on computer modeling with Program SOM-TA, and cost benefit studies, should provide more useful data in the development of improved seat design criteria. (Program SOM-TA will be a triple-occupant variation of Program SOM-LA, which is described in references 53 and 54. SOM-TA was not used in the design of the seat modifications because it was still under development at the time this report was prepared).

Conclusions concerning the modified seats are as follows:

1. There are simple and highly effective ways for improving the attachment of the seats to existing floor tracks. As demonstrated in this report, it is possible to achieve greatly improved seat retention and weight savings at the same time.
2. With the operationally reasonable amount of forward stroke (6 in.) selected, and the existing presumed floor strength of 9 G, the recommended 18-G peak, 50-ft/sec pulse cannot be survived. However, it can probably be if the velocity change is reduced to 35 ft/sec.
3. The construction of most conventional seat pan structures lends itself to simple reduction of torsional rigidity so that relative track pitch will not destroy the structure. Usually the changes involve removal of material with an appropriate weight reduction.
4. Lateral bracing to meet the 10-G criterion is not easy if foot/leg and luggage space under the seat must be maintained, but it is achievable. Distribution of loads to both floor tracks, and compression, as well as tensile braces, are required with resulting weight increases. Upgrading the lateral strength from 3 to 6 G is not difficult, and involves much less of a weight increase.
5. Simple load-spreading techniques in leg attachment fitting design can greatly increase the ultimate failure loads of the seat pan structure frame tubes.
6. The 9-G, 50-ft/sec test pulse which destroys standard seats uses only about one half the energy-absorbing capability of most of the modified seats.
7. The results of the static and dynamic testing of the modified seats demonstrated that static tests alone are not sufficient evidence to certify dynamic performance. The large dynamic overshoot effects resulting from the lap-belt-only restraint of three occupants creates an especially severe design condition which necessitates dynamic testing.
8. Considerable improvements in crash survivability in the forward direction can be made with very little additional weight.
9. Much of the added weight needed to improve crashworthiness could be recovered from other parts of the seat. Even the lightweight seats feature opportunities for compensating weight reduction. For example, about 2 lb could be removed from the seat cushion while still maintaining the same comfort level.

Thus, the development of the experimental modified seats has already answered many of the questions associated with the program objectives. While the design criteria selected for the experiments may result in some weight increases, it is apparent that great improvements in the structural integrity of transport seats can be made with little or no weight increase. A modest upgrading of performance criteria coupled with dynamic test requirements could provide considerable improvement in crash protection.

## CONCLUSIONS

At the time of this writing, the project has progressed through the static and dynamic testing of seats in the standard and modified conditions. Based on these tests alone, certain observations and conclusions have been made concerning the structural integrity of standard seats and the feasibility of modifying the seats for improved crash survivability. In the case of the standard seats, the conclusions are further supported by CAMI tests of other seats as discussed in this report.

Conclusions concerning standard seats are as follows:

1. Existing seats have little tolerance for floor warpage. Relative track roll can cause failures because the fittings have no release, and relative track pitch can cause failures because the torsional rigidity of the seat pan structure is too great.
2. Existing seats experience little energy-absorbing deformation prior to ultimate failure. Ultimate failure frequently occurs in fasteners or fittings which do not allow major structural members to deform significantly.
3. While still meeting minimum FAA requirements, the new lightweight seats are not as strong as older seats. Obviously, weight savings have been achieved through the reduction of design margins. This trend demonstrates manufacturer resistance to voluntarily upgrade seat designs beyond the FAR specified minimums. The competitive marketplace forces each manufacturer to reduce the margins as much as possible to achieve the weight savings the operators are seeking. The same philosophy applies to crashworthy features not involving weight increases. The manufacturers cannot recover the added development cost if their competitors are not required to meet the same upgraded performance standards. The test results on the flight attendant seat are an example showing that development stops when the minimum FAR requirements are met, even though a few more ounces of material (properly placed) would greatly increase the strength of the structure.
4. While existing seats survive the specified 9-G forward static test, they fail catastrophically if subjected to a 9-G dynamic test pulse (with floor warpage).
5. In the downward direction, existing seats are somewhat stronger than required. Apparently this is because other loading conditions determine the design of the structure.
6. In the lateral direction, existing seats are entirely unbraced and just meet the 3-G requirement.
7. Older seats constructed of sheet metal perform better both statically and dynamically than newer tubular seats.

However, there was also appreciable unused stroke capacity evident in most of the tests. Testing must still be accomplished to verify that the seats will withstand the 18-G, 35-ft/sec design pulse. However, the tests performed thus far indicate that the seats will sustain the design pulse.

The design of the modifications was supported by the best available static analysis methods and by static testing. Yet several of the modifications did not function as desired in the dynamic tests. The aft-facing seat modification failed when the energy absorbers did not function as intended, the UOP MOD with energy-absorbing rear legs sustained the test pulse but failed to stroke, and the Weberlite MOD seat experienced ultimate failure of an energy-absorbing component near the end of the test pulse. Although the addition of simulated floor warpage in the dynamic tests may have contributed to the malfunctions, it is obvious that it is impossible to reliably design for dynamic applications with static analysis and tests. The static tests do provide useful information for validating the analysis and verifying the strength of the structure. A seat which failed the static test would probably not pass the dynamic test. However, passing the static test does not completely insure passing the dynamic test because of load redistribution, strain rate effects, dynamic responses, friction, binding, and perhaps other effects too difficult to predict accurately. While the dynamic testing is necessary, it need not entail an overly complex or costly design/test iteration process. The problems encountered in the discussed tests could probably all be resolved with one or two iterations. The probability of first-time success will also be enhanced by dynamic analysis of transport seats. This capability will be available shortly in the form of program SOM-TA. Dynamic testing would probably increase development cost, but not to any considerable amount relative to the benefit it would produce.

by the energy absorbed in the crushing of the lower fuselage). Therefore, a high-strength, rigid structure would serve to protect the occupant. However, the aircraft floor and tracks cannot react the forces associated with an 18-G forward load. Therefore, to avoid requiring structural reinforcement of the floors, the seat structure must have energy-absorbing capability in the forward direction. This conclusion was applied to each of the experimental seats.

The seat experiments developed for the Crash Impact Demonstration were all based on an ideal stroking load of 9 G, a load that would be compatible with existing aircraft floor and track strength. However, the work done in this study has shown that attachments to the existing tracks can easily be designed which would permit a much higher stroking load. If it could be shown that the ultimate strength of the floor structure is capable of supporting greater loads acting simultaneously at most seat positions, or if the floor can be modified to do so, then the energy-absorbing seat system could be made appreciably more efficient. Either the seat could stroke a shorter distance at a higher load, and still be capable of surviving the same design pulse, or it could stroke the same distance but absorb more energy, and therefore be able to survive a more severe crash pulse.

The tests described in this report were limited to forward, lateral, and downward directions, with the lateral tests deleted on the standard seats, and the downward tests deleted on the modified seats. The reasons for the deletions were explained in the text. However, even testing in each individual direction is inadequate to support the rigorous development of the structure designed for enhanced crash survival. Worst case loads should also be imposed in a manner which simultaneously combines components in all three directions on various seat occupancies. These tests are recommended to assure that: the structure can withstand the resulting stress distributions, any energy-absorbing devices will function without binding, and releases designed into the system will function as intended. The recommended certification requirements of Appendix A include dynamic testing with combined loading.

It should be remembered that the weight increments presented in this report apply to experimental hardware only. The test hardware was prototype hardware modified in appropriate ways. The same changes could probably be made in production configurations with less weight and in some cases, the production weight could even be greatly reduced. For example, lap belt energy-absorbing devices could be made extremely light in production, perhaps by using the method of tearing composite material. The devices used in the test are functionally equivalent, but too heavy for application into operational aircraft. Likewise, the aft-facing seat, made out of a forward-facing seat, does not accurately reflect the weight of a seat initially designed as an aft-facing energy-absorbing configuration. Also, the aft-facing seat has no luggage restraint. In the event of a crash, a piece of luggage placed under the seat in front (relative to the passenger, not the aircraft) of a passenger, would become a projectile finding its way back toward the owner. Some sort of retainer would be needed so the passenger could stow his baggage beneath his own seat.

Since the test pulse, chosen for comparison to other data as discussed, had only a 9-G amplitude, it could be presumed that the seats should not stroke at all. In fact, there was considerable stroke experienced during dynamic testing due to the dynamic overshoot resulting from the lap-belt-only restraint systems.



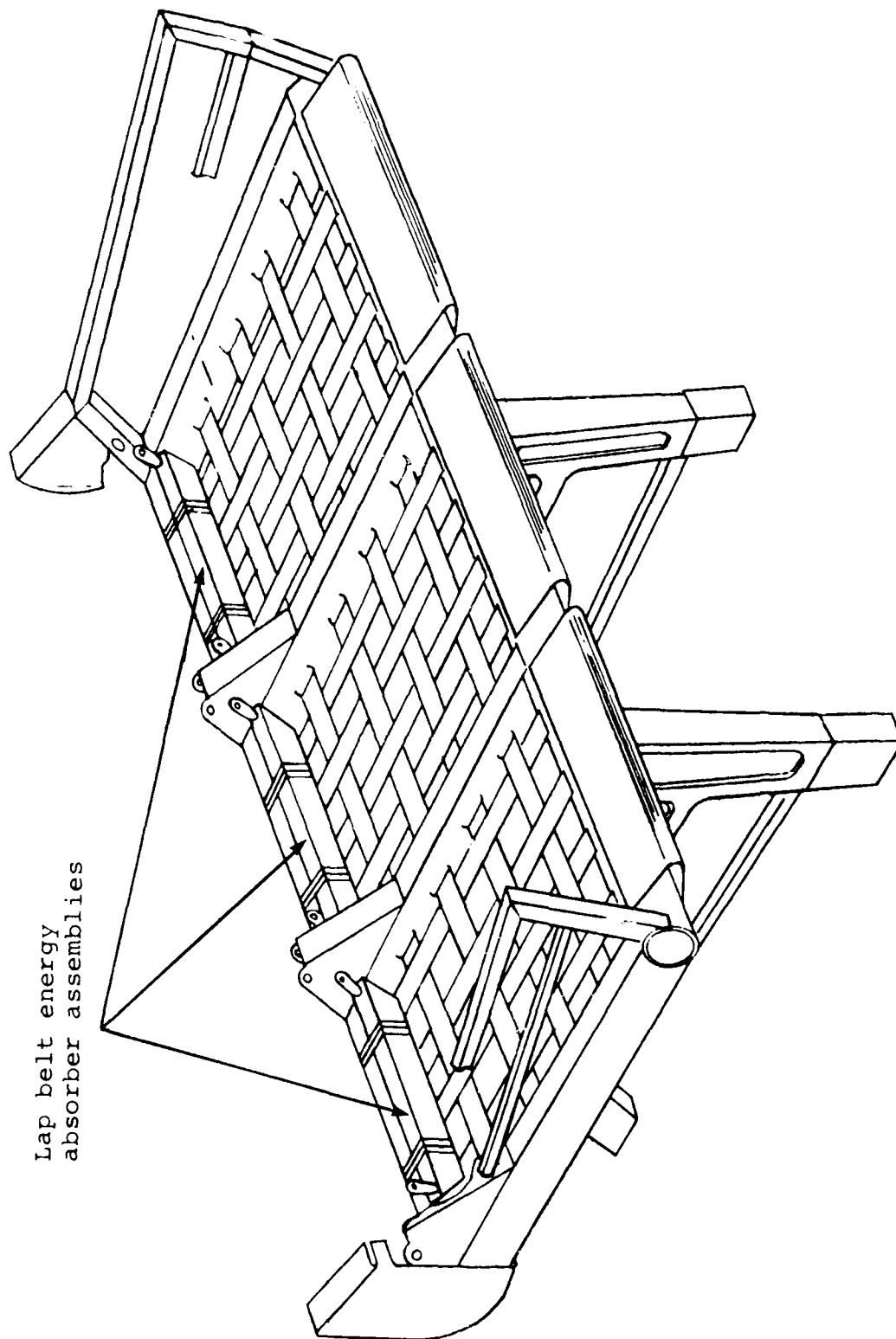
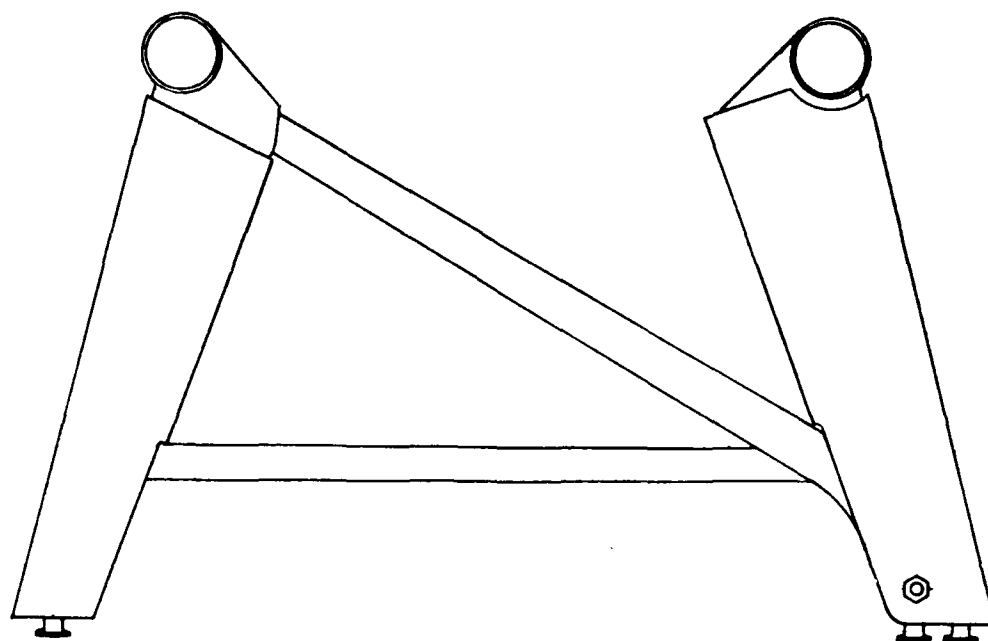
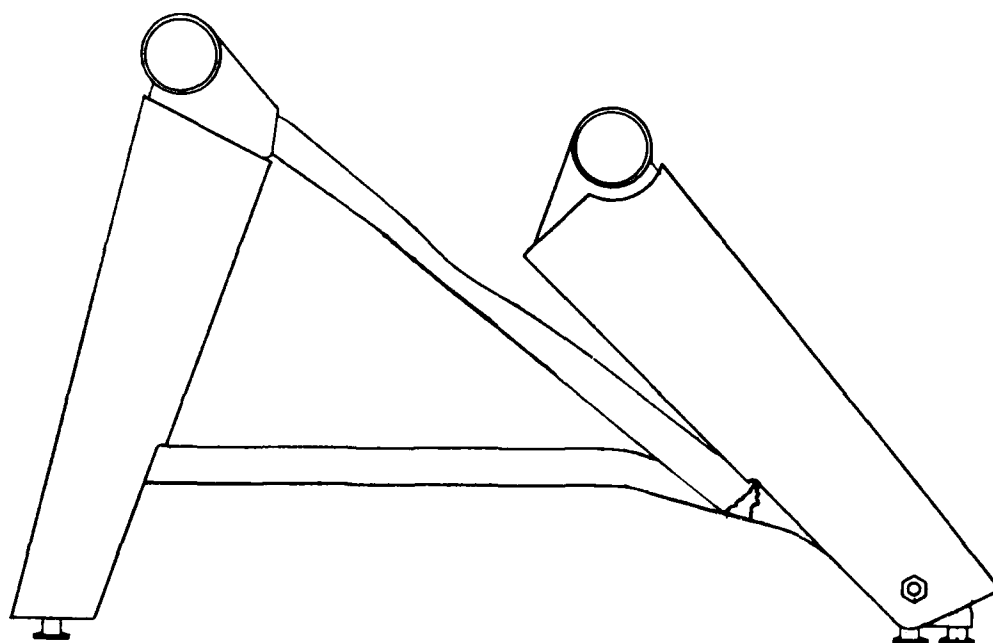


Figure 5. Installation of Hardman lap belt energy absorber.



Pretest

← FORWARD



Posttest

Figure 6. Leg deformation of Hardman seat (Forward Static Test).

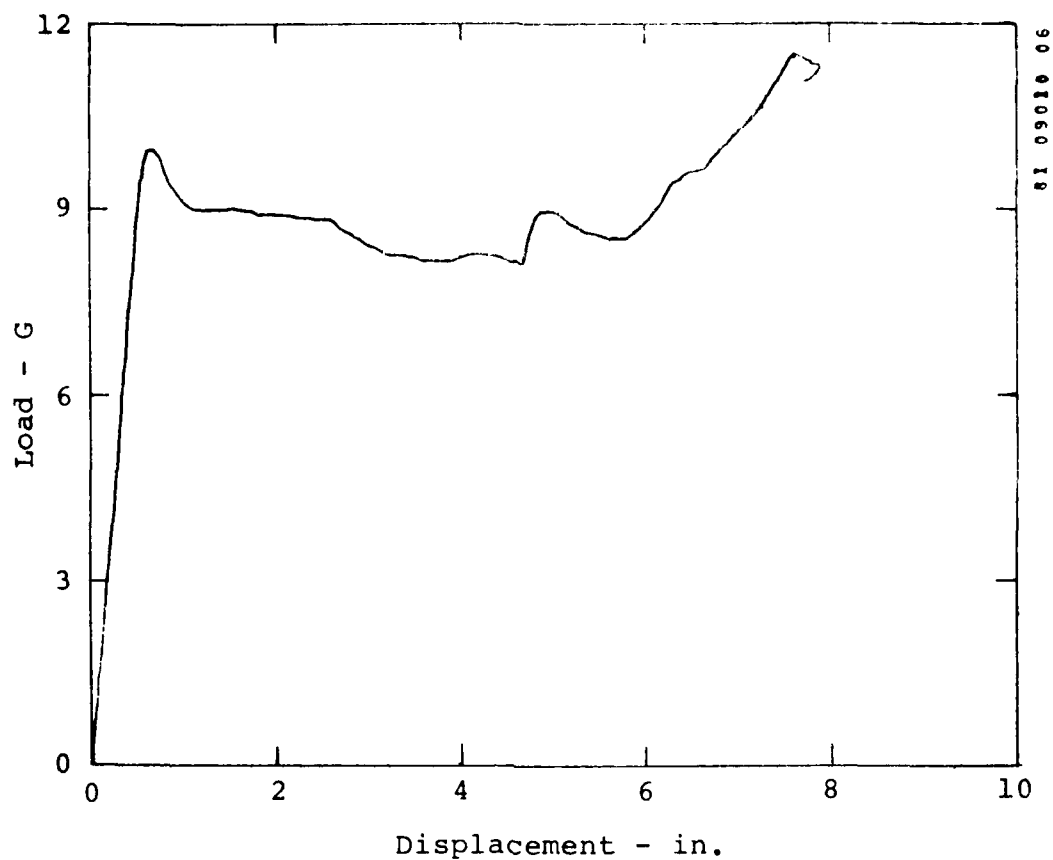


Figure 7. Load versus longitudinal displacement for window position of Hardman 8727 seat tested to failure (Forward Static Test).

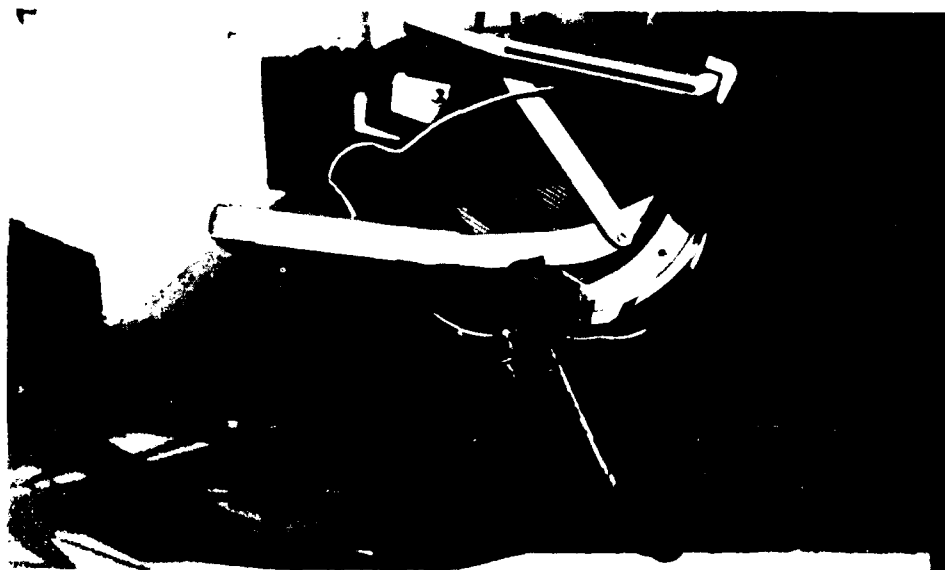


Figure 8. Aerotherm Model 723 seat - side view.



Figure 9. Aerotherm Model 723 seat - rear view.

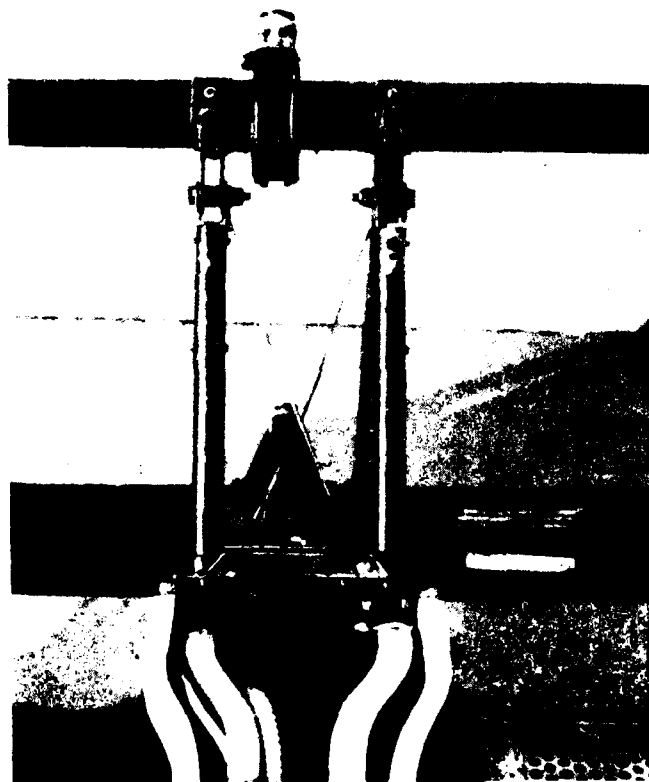
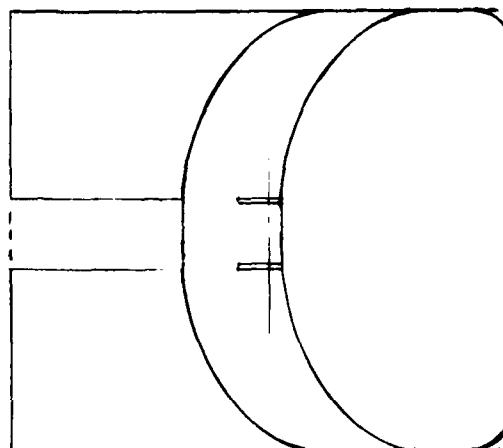


Figure 10. Energy absorbers on Aerotherm Model 723 seat - rear view.

NOTE: Dashed lines show  
configuration per  
NAS 809.



61 09010 34

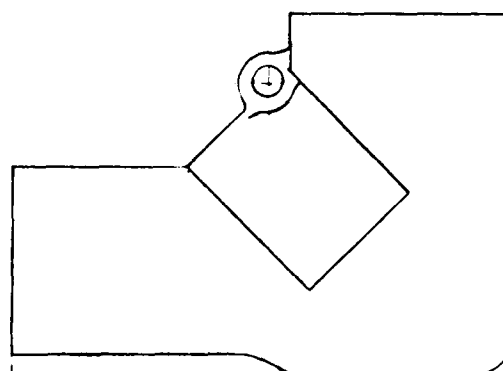
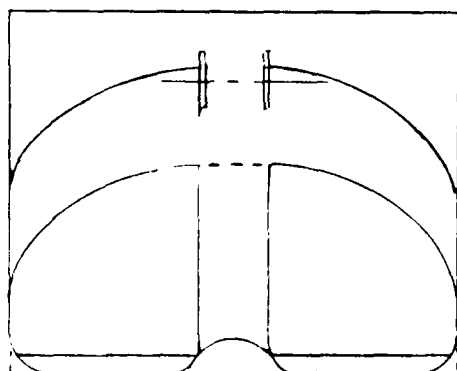


Figure 11. Body block used in static tests.

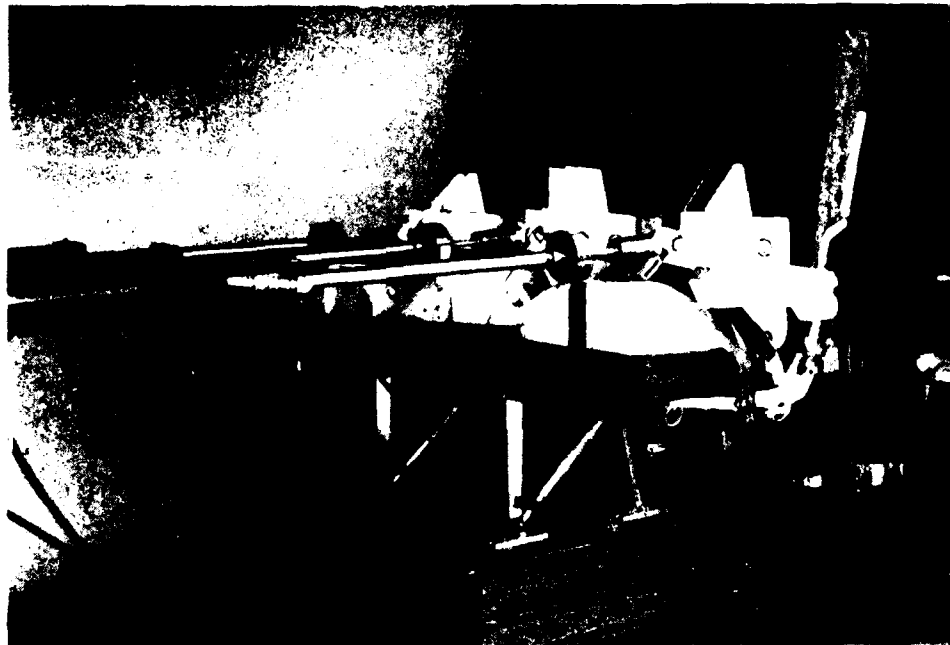


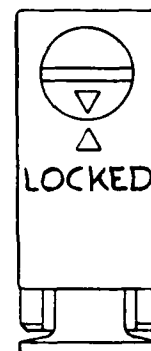
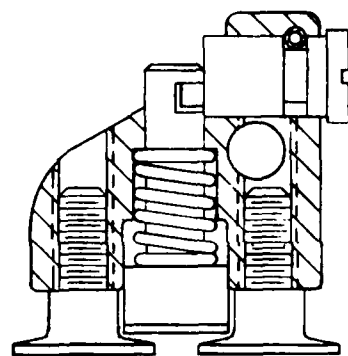
Figure 12. Forward static test arrangement.



Figure 13. Downward static test arrangement.

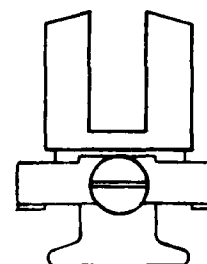
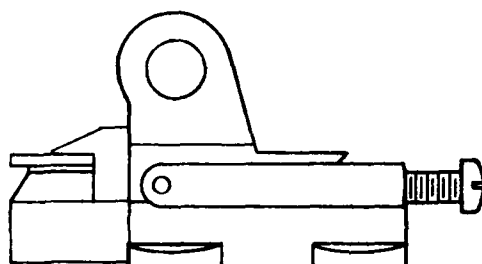


Figure 14. Lateral static test arrangement.



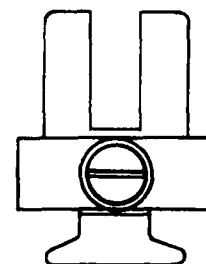
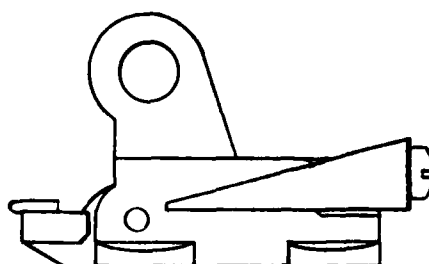
81 09009 11

Figure 15. Brownline track fitting.



84 02002 09

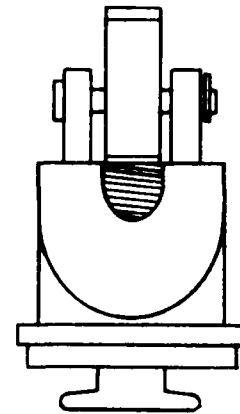
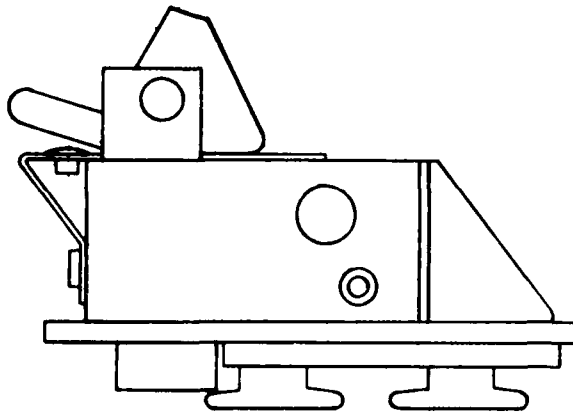
Figure 16. Ancra track fitting.



84 02002 08

Figure 17. Sabre track fitting.



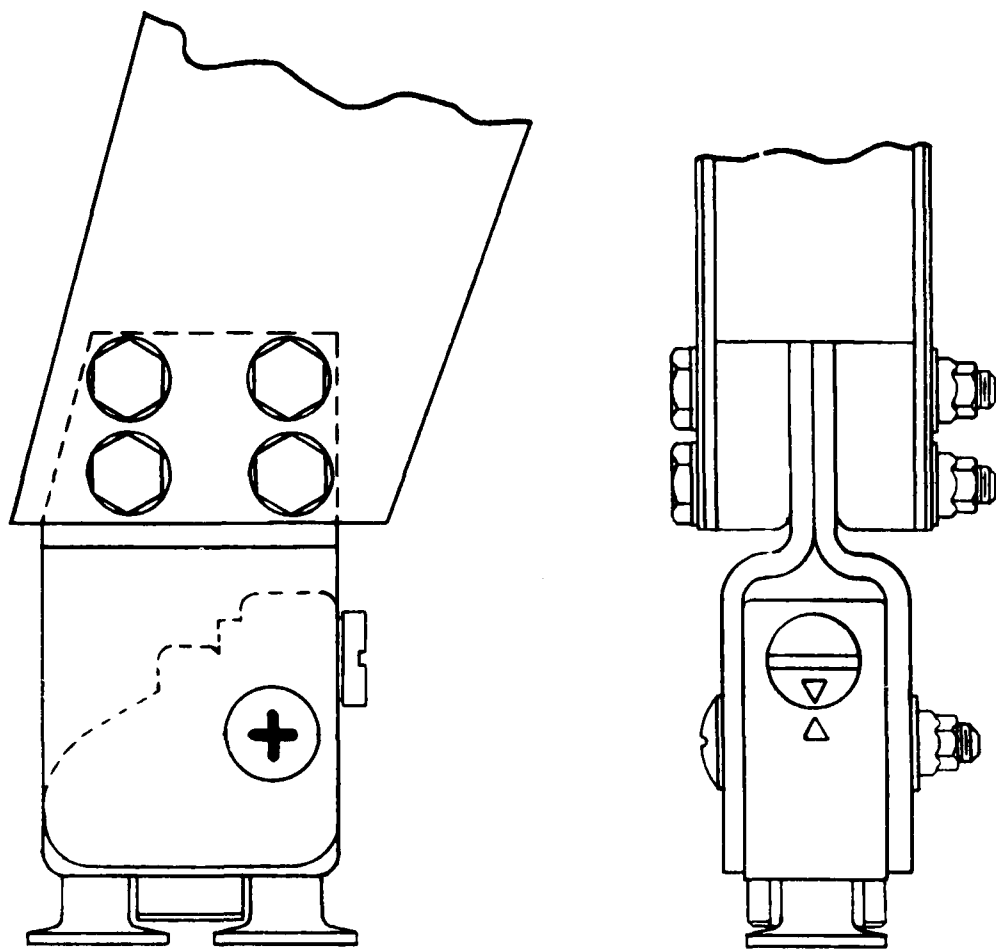


84 02002 10

Figure 18. UOP track fitting.



Figure 19. Track fitting test fixture.



81 09009 12

Figure 20. Plastic hinge adapted to Brownline track fitting.

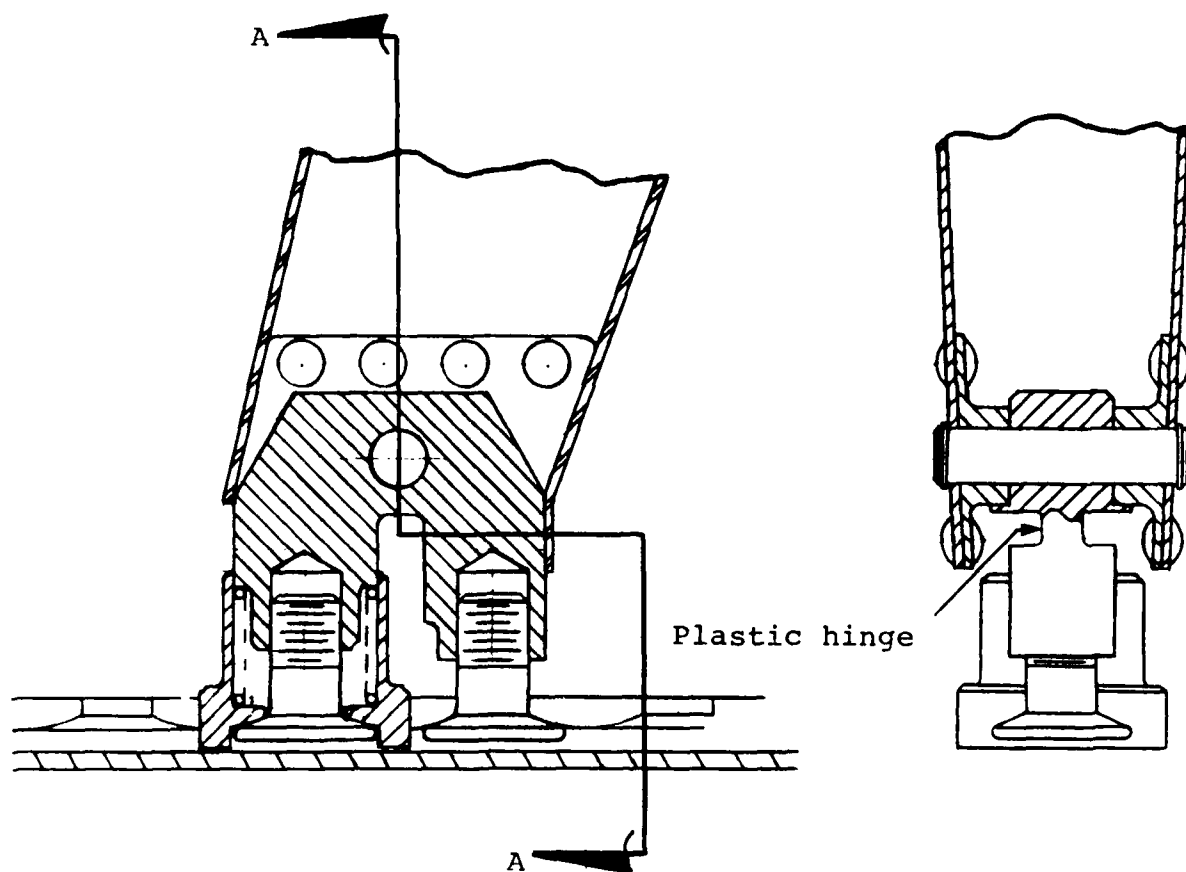
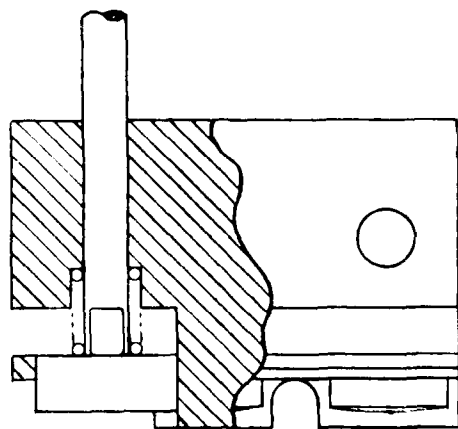
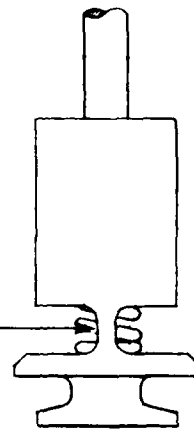


Figure 21. Track fitting concept with plastic hinge.



Plastic hinge



81 09009 14

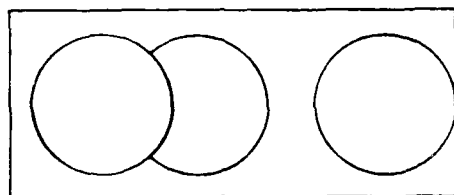


Figure 22. Track fitting concept with plastic hinge at track level.

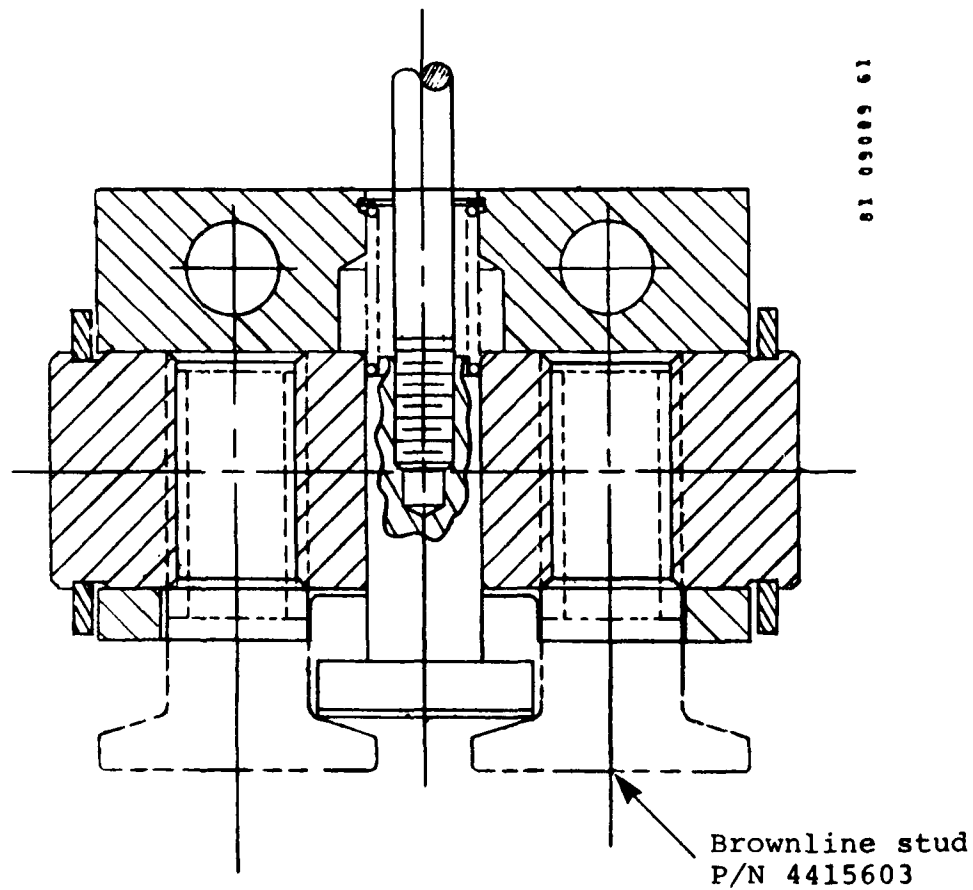
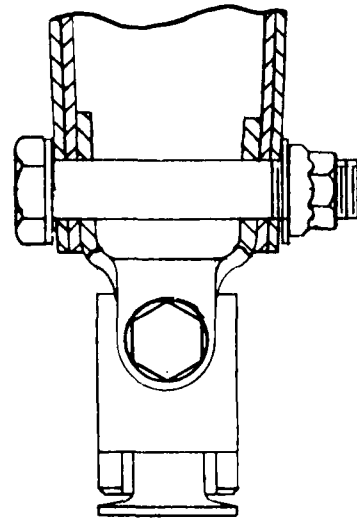
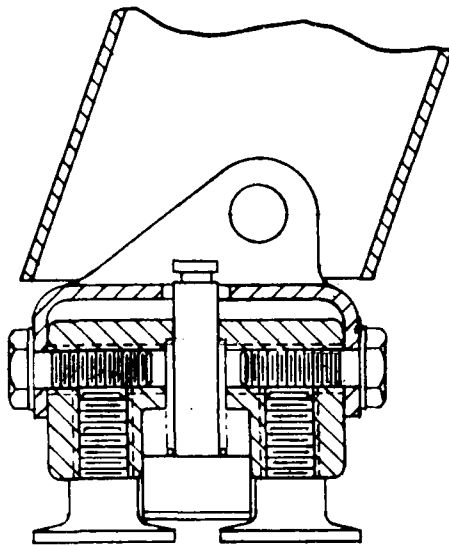
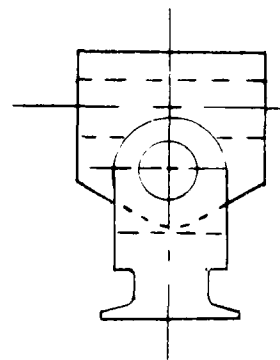
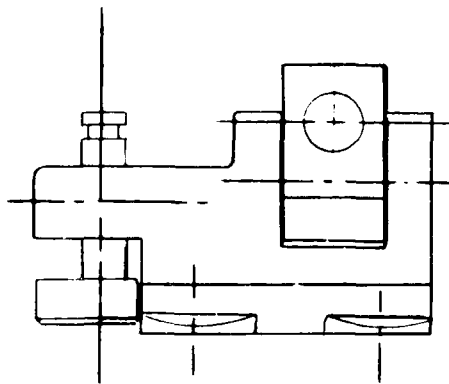


Figure 23. Track fitting concept with pitch and roll axis release.



81 09009 15

Figure 24. Track fitting concept with pitch and roll axis release.



81 09009 16

Figure 25. Track fitting concept with pitch and roll axis release.

AD-A155 824

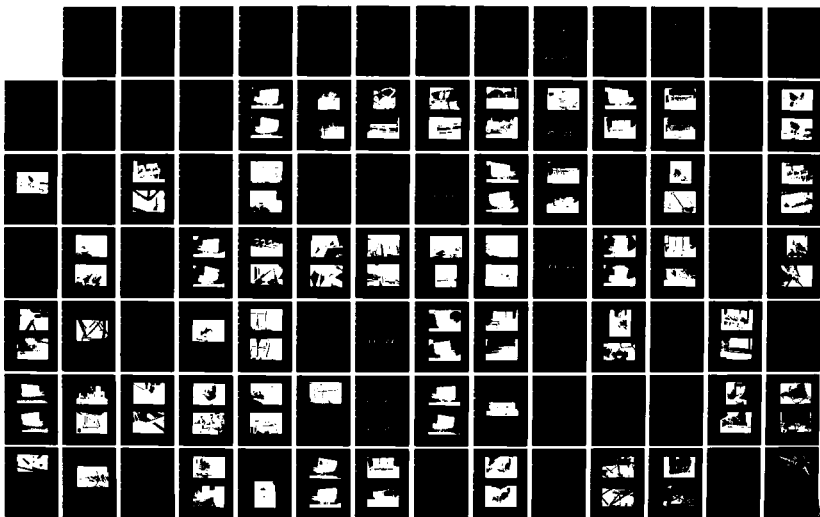
SEAT EXPERIMENTS FOR THE FULL-SCALE TRANSPORT AIRCRAFT  
CONTROLLED IMPACT. (U) RMS TECHNOLOGIES INC TREVOSE PA  
M R CANNON ET AL. MAR 85 DOT/FAR/CT-84/18  
DTFA83-81-C-00048

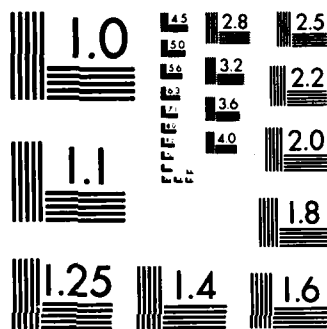
2/3

UNCLASSIFIED

F/G 1/3

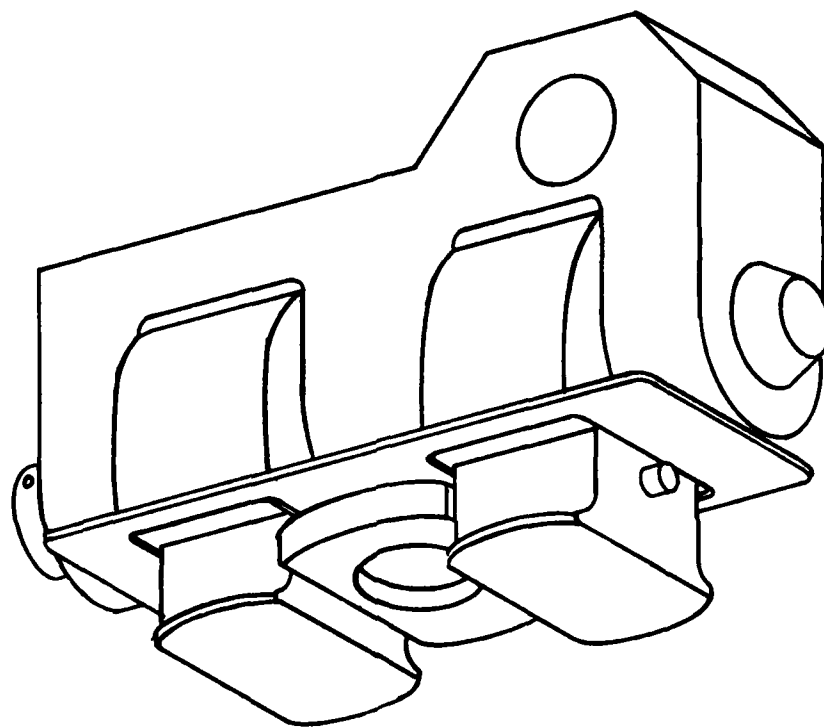
NL





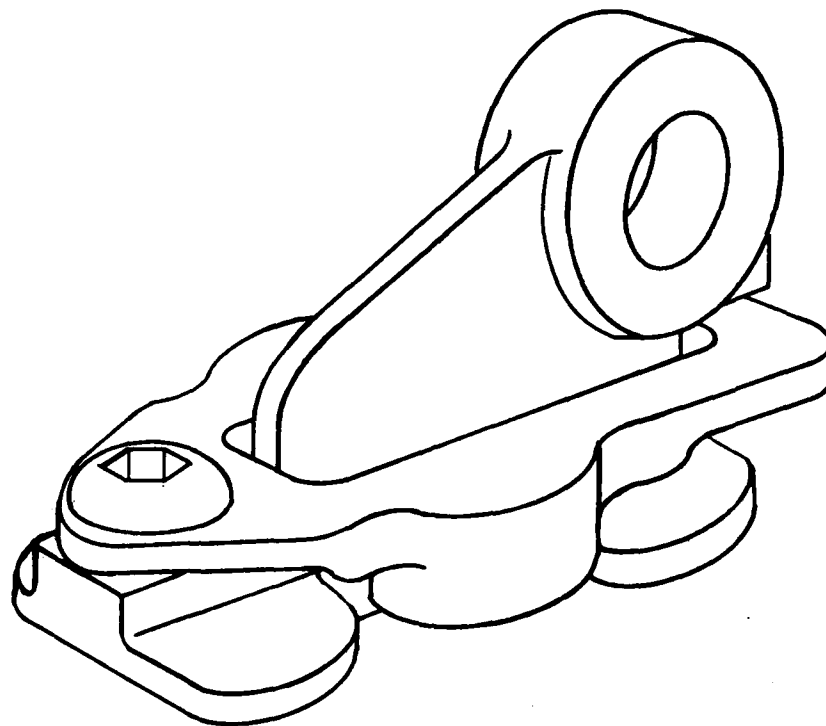
MICROCOPY RESOLUTION TEST CHART  
NATIONAL BUREAU OF STANDARDS-1963-A





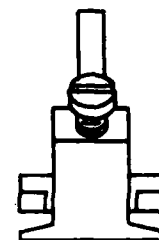
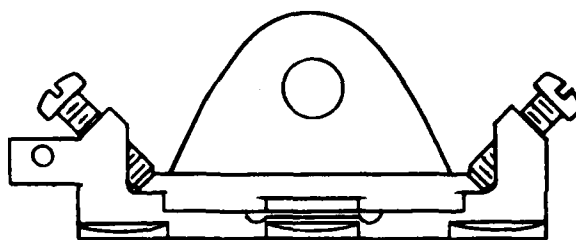
84 02002 11

Figure 26. First prototype track fitting.



84 02002 59

Figure 27. Concept of second prototype track fitting.



84 02002 12

Figure 28. Second prototype track fitting.

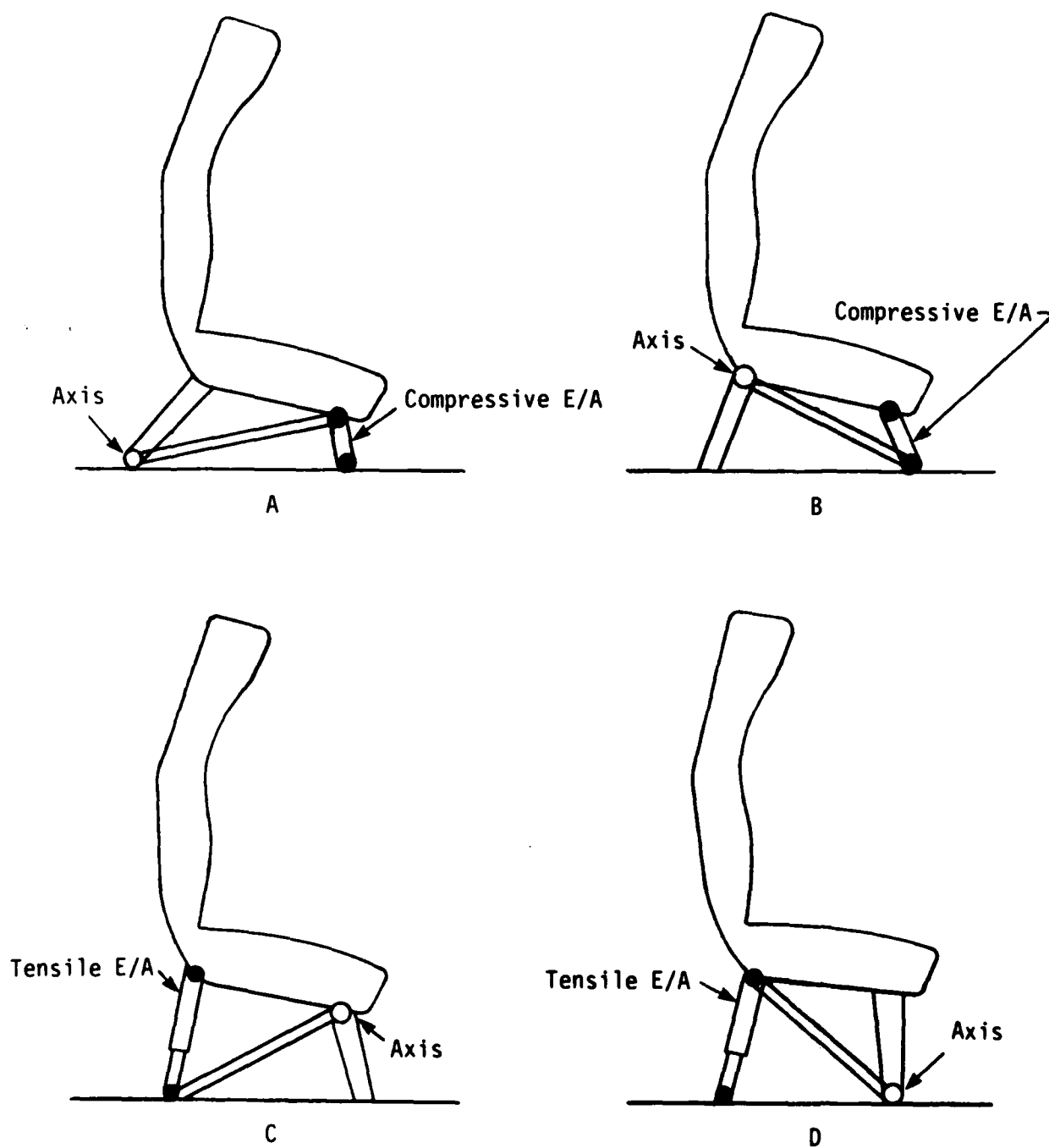


Figure 29. Rotating seats.

1 = Upright  
2 = Doubled over lap belt

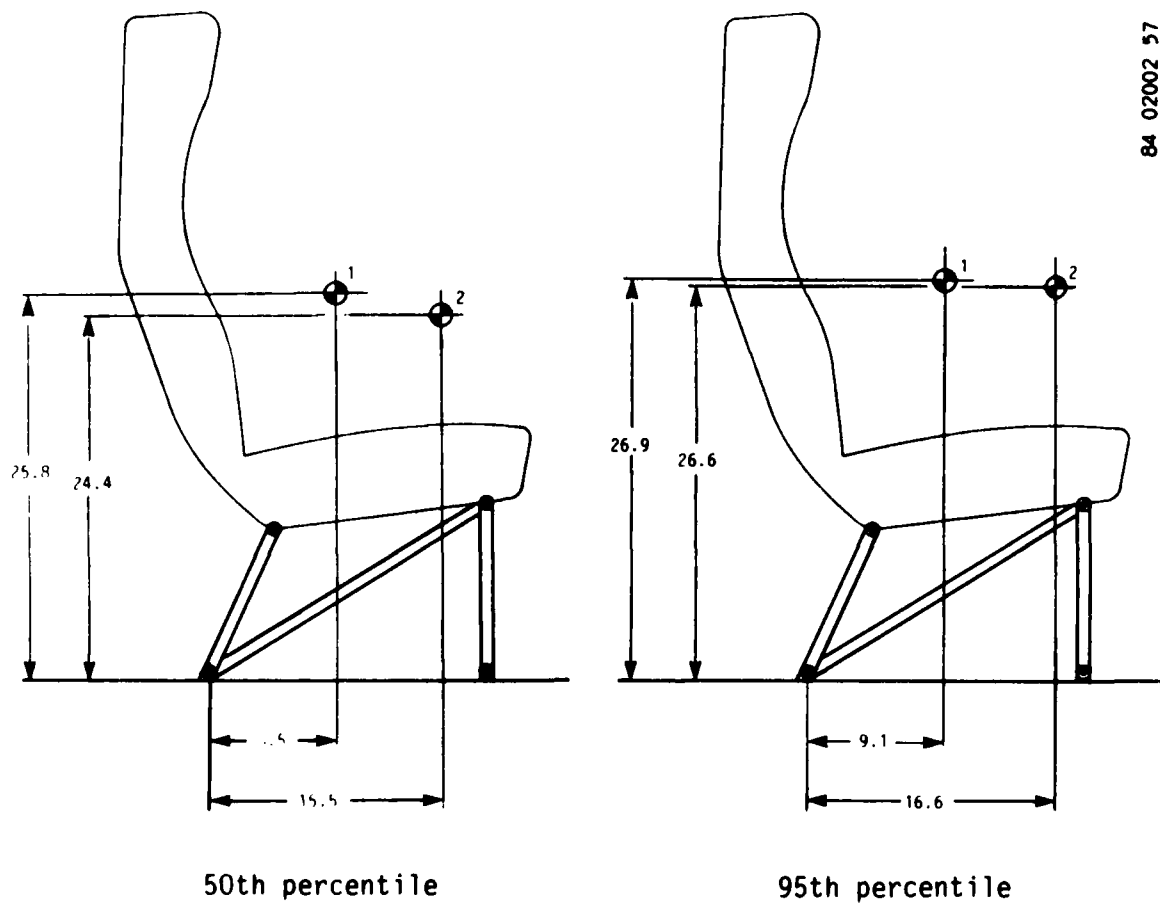
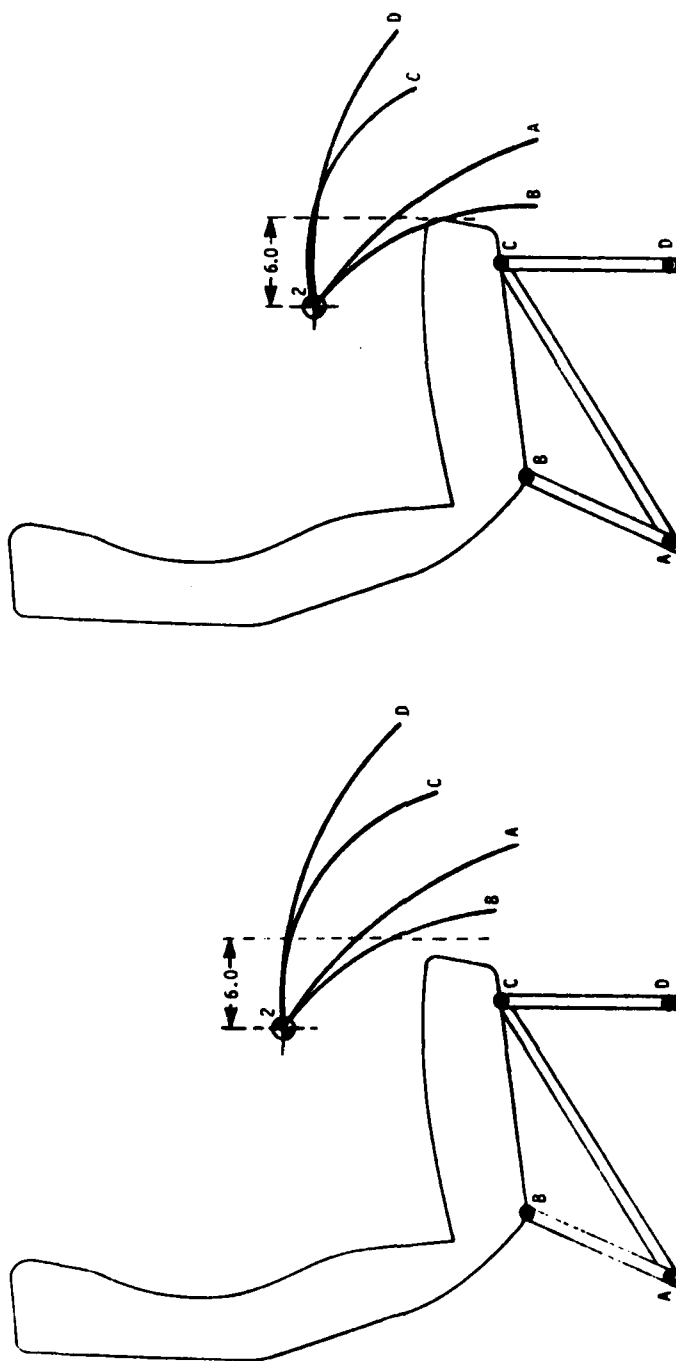


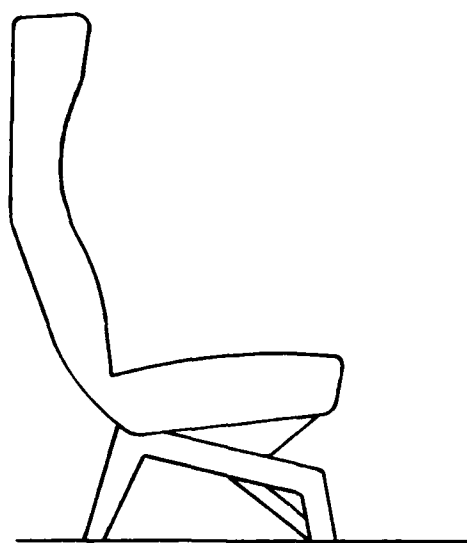
Figure 30. Locations of occupant c.g.



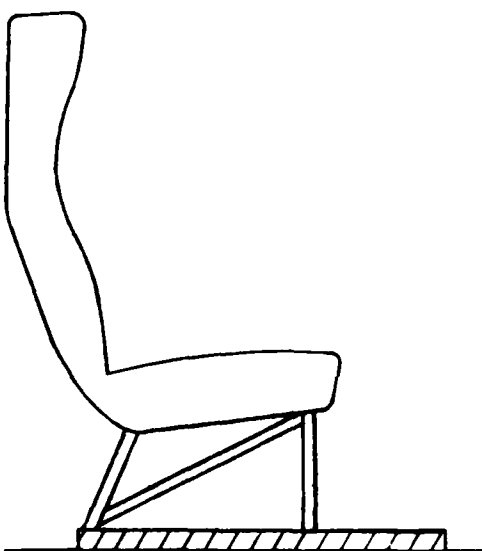
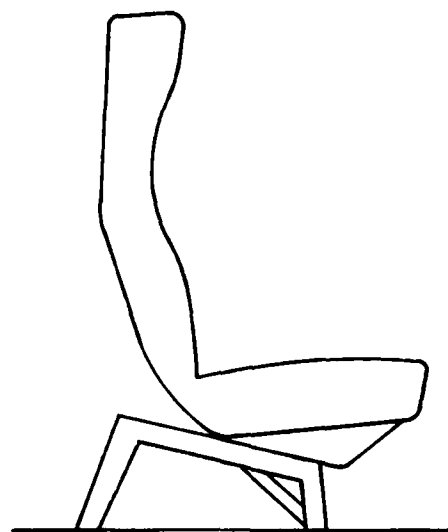
50th percentile

95th percentile

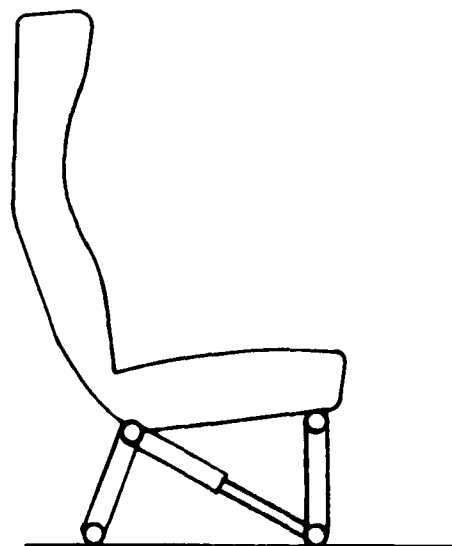
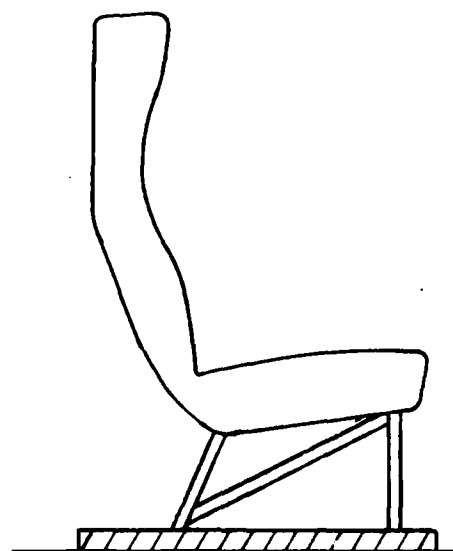
Figure 31. Motion of c.g. for four axes of rotation of doubled-over occupant.



A



B



C

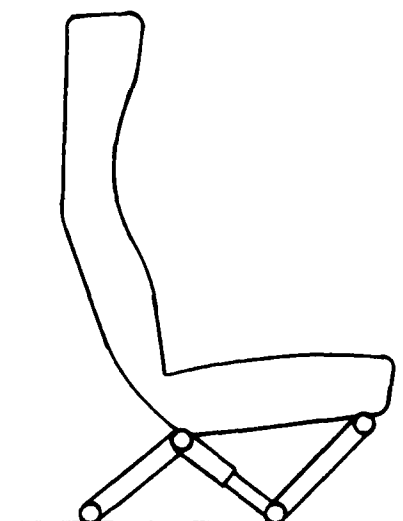


Figure 32. Translating seats.

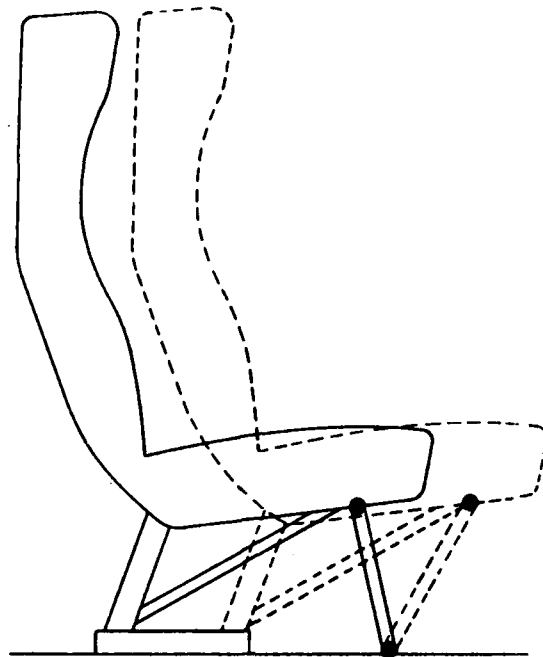


Figure 33. Modified translating seat.

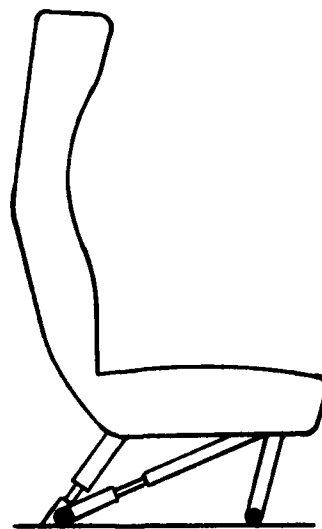
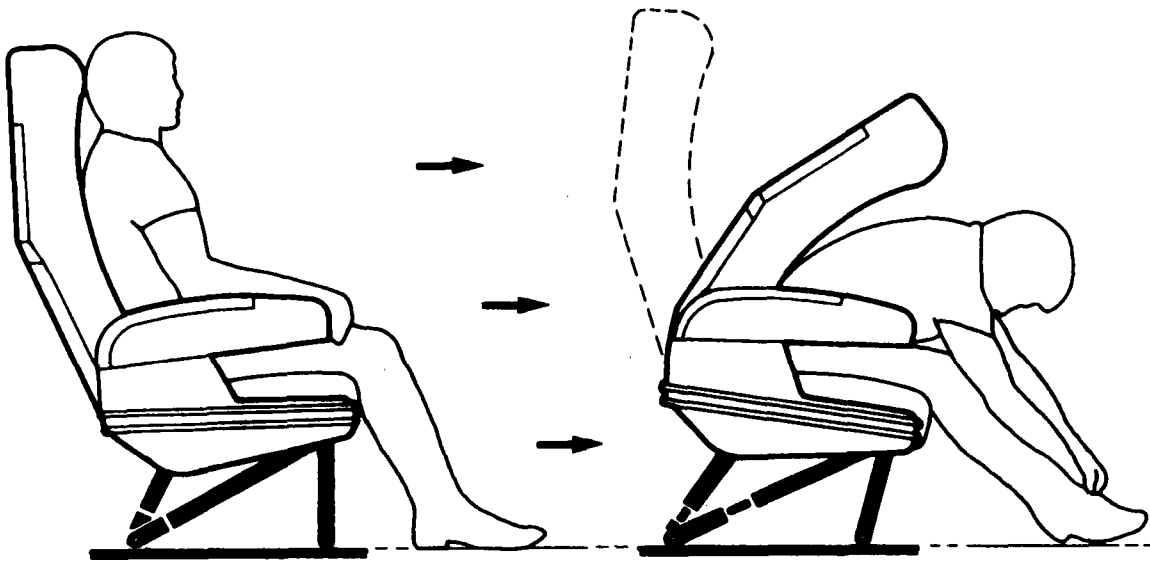
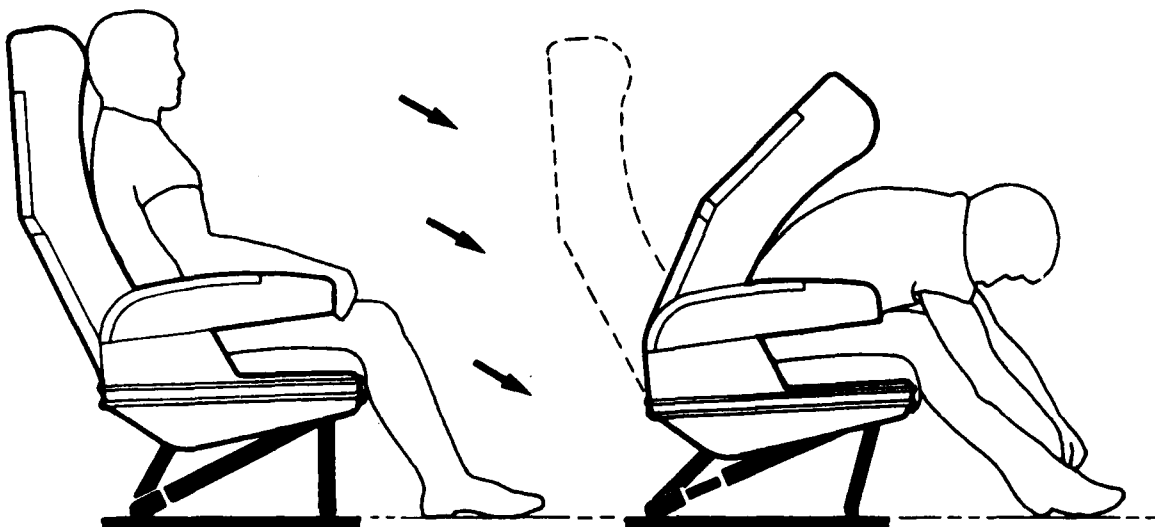


Figure 34. Seat concept with motion dependent upon load direction.



Condition 1: forward inertial load



Condition 2: inertial load pitched downward 30°

Figure 35. Seat concept using rear leg and diagonal energy absorbers.



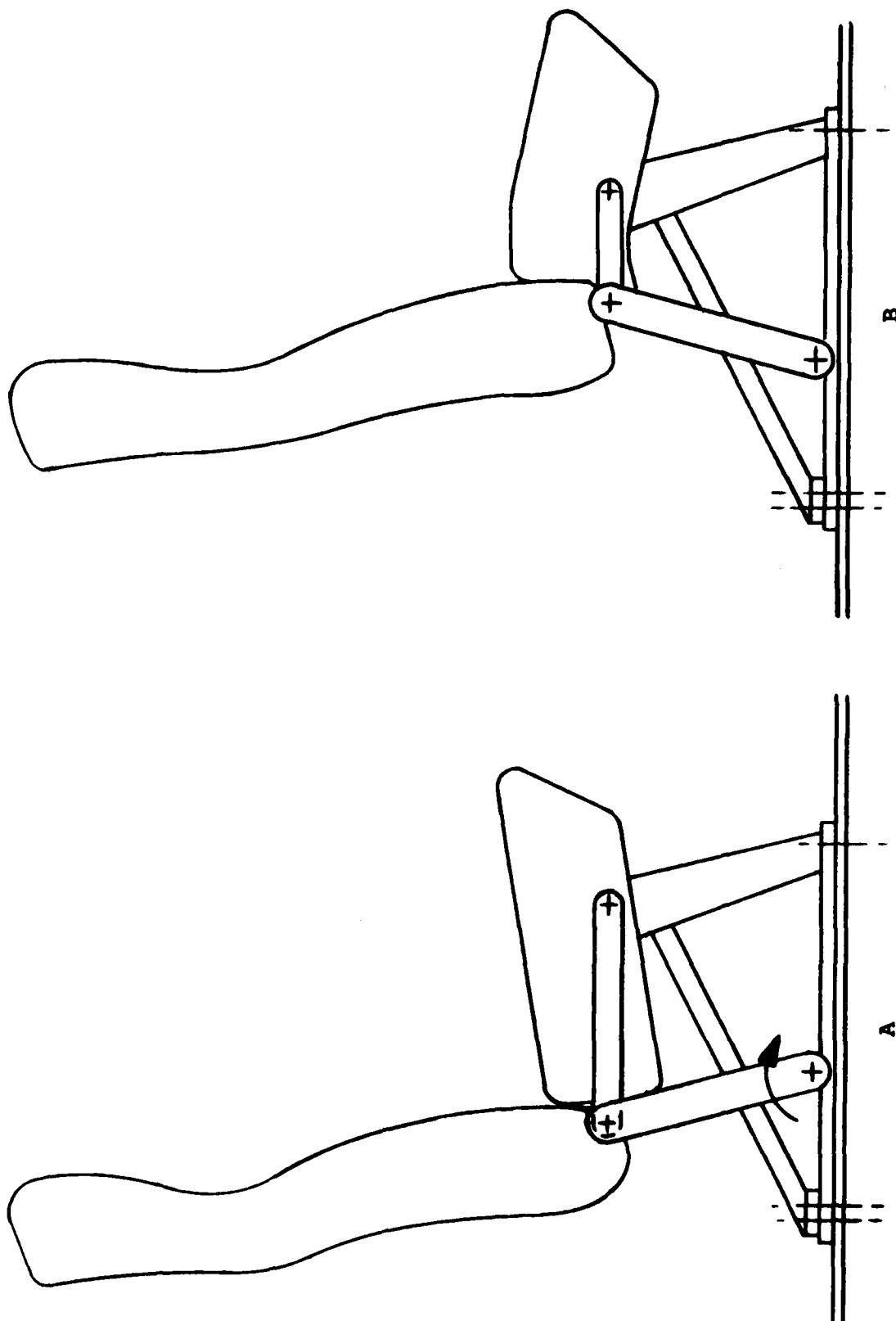


Figure 36. Telescoping seat pan arrangement.



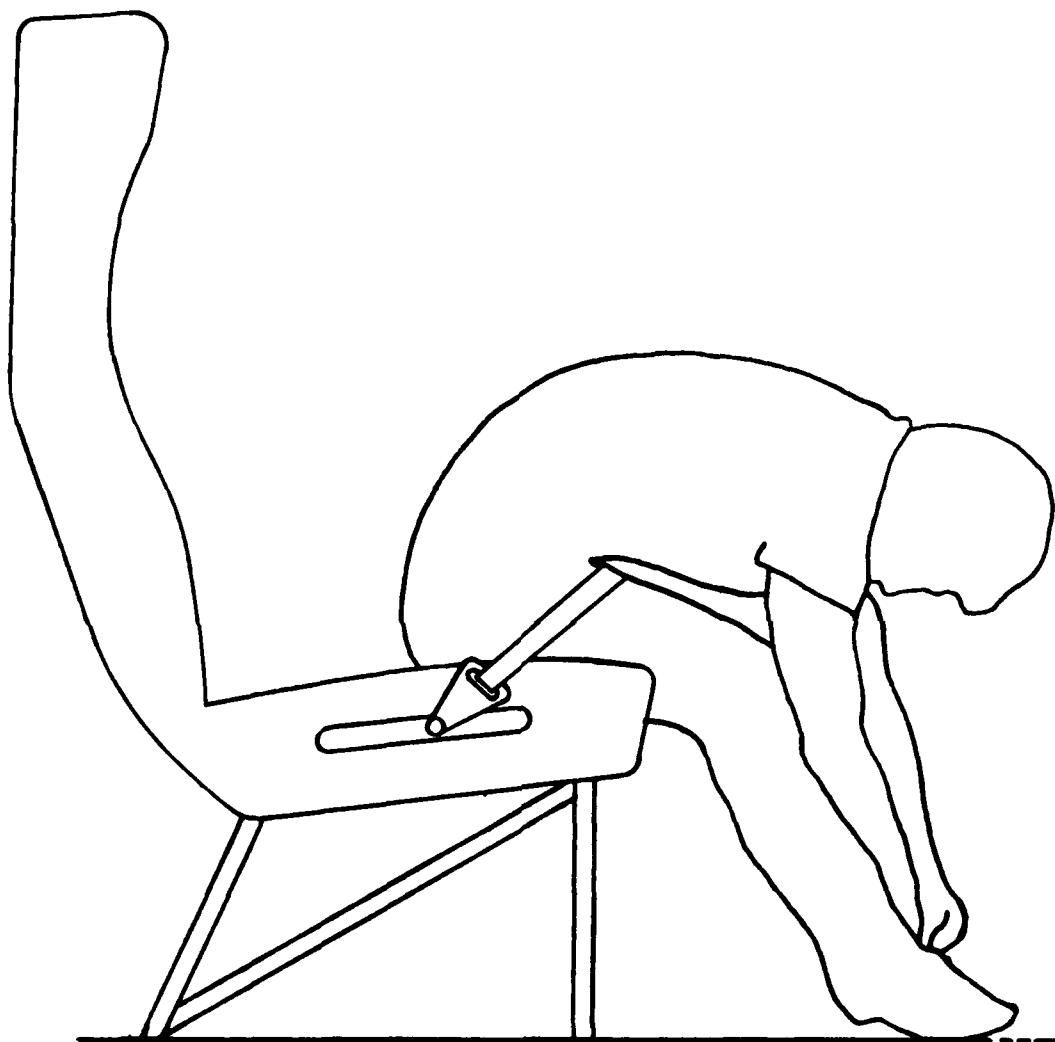


Figure 38. Guided lap belt energy absorber.

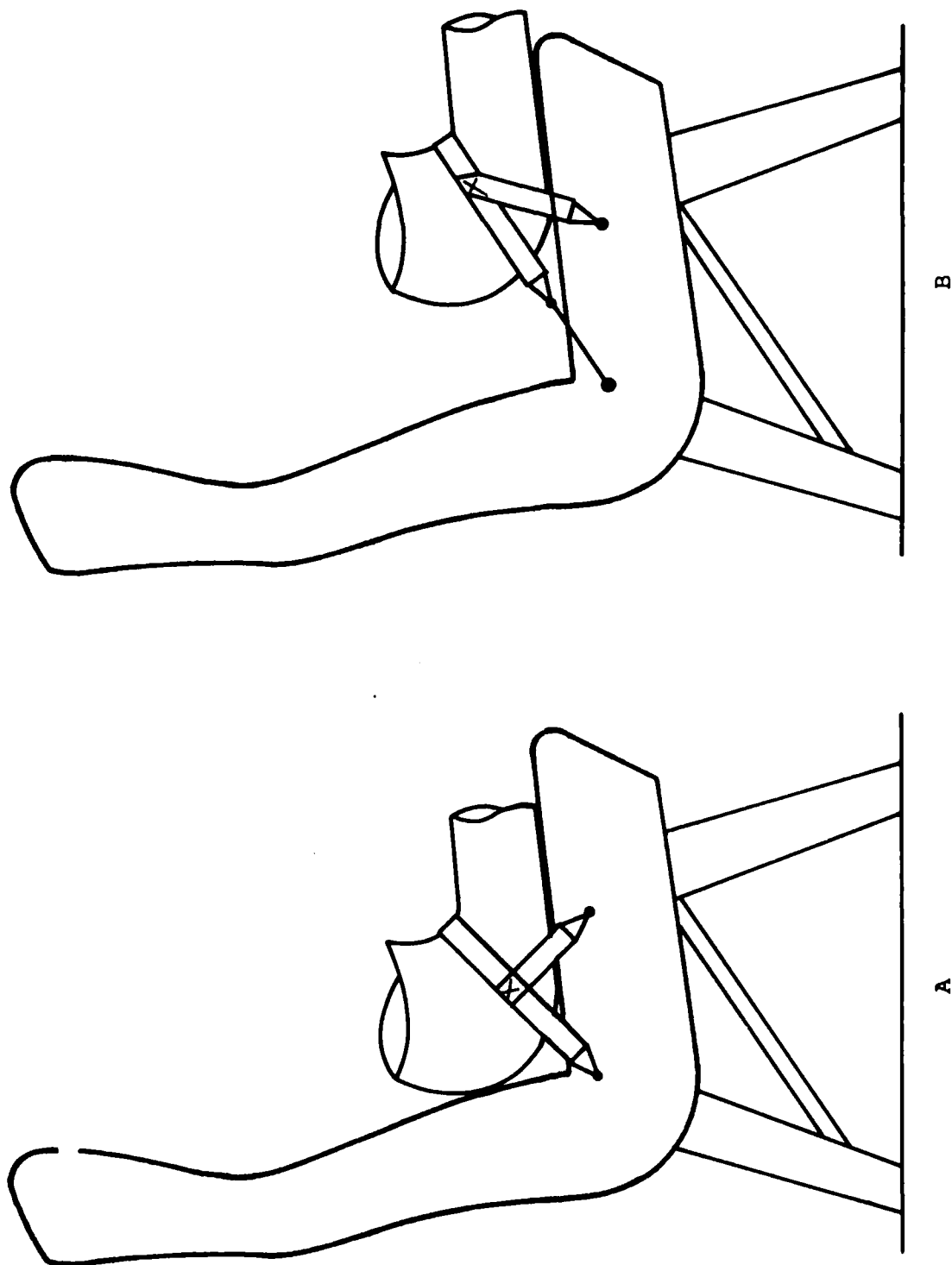


Figure 39. Lap belt energy absorber with side strap.

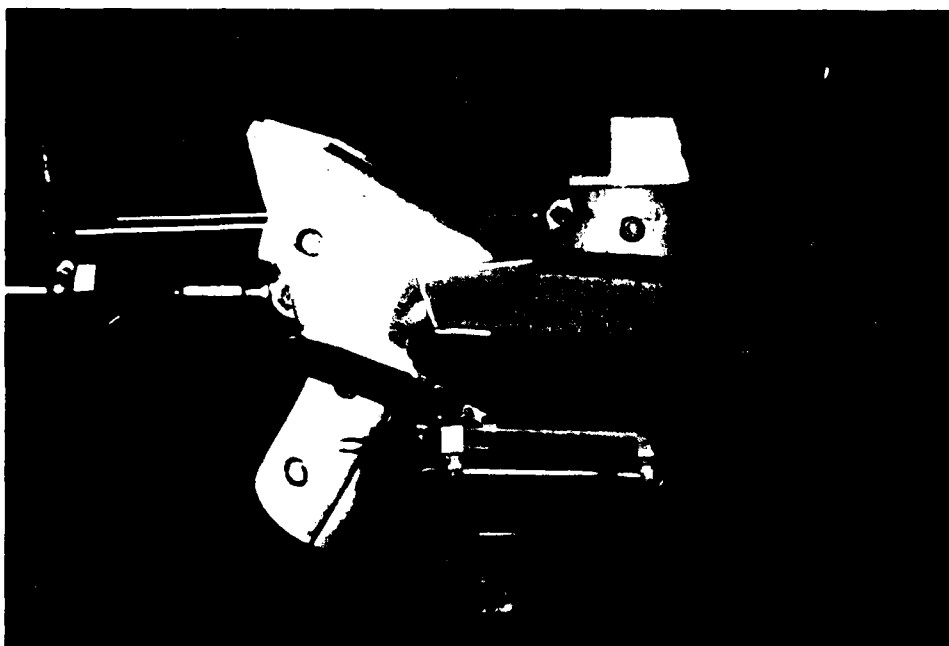


Figure 61. Weber MOD I seat window-side block after stroking.

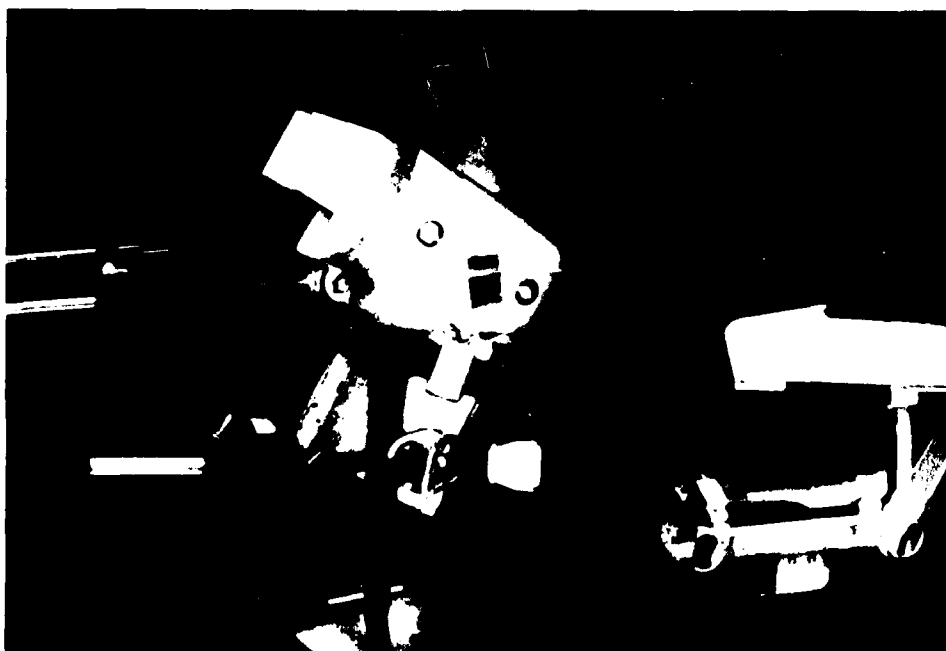


Figure 62. Weber MOD I seat center body block after stroking.

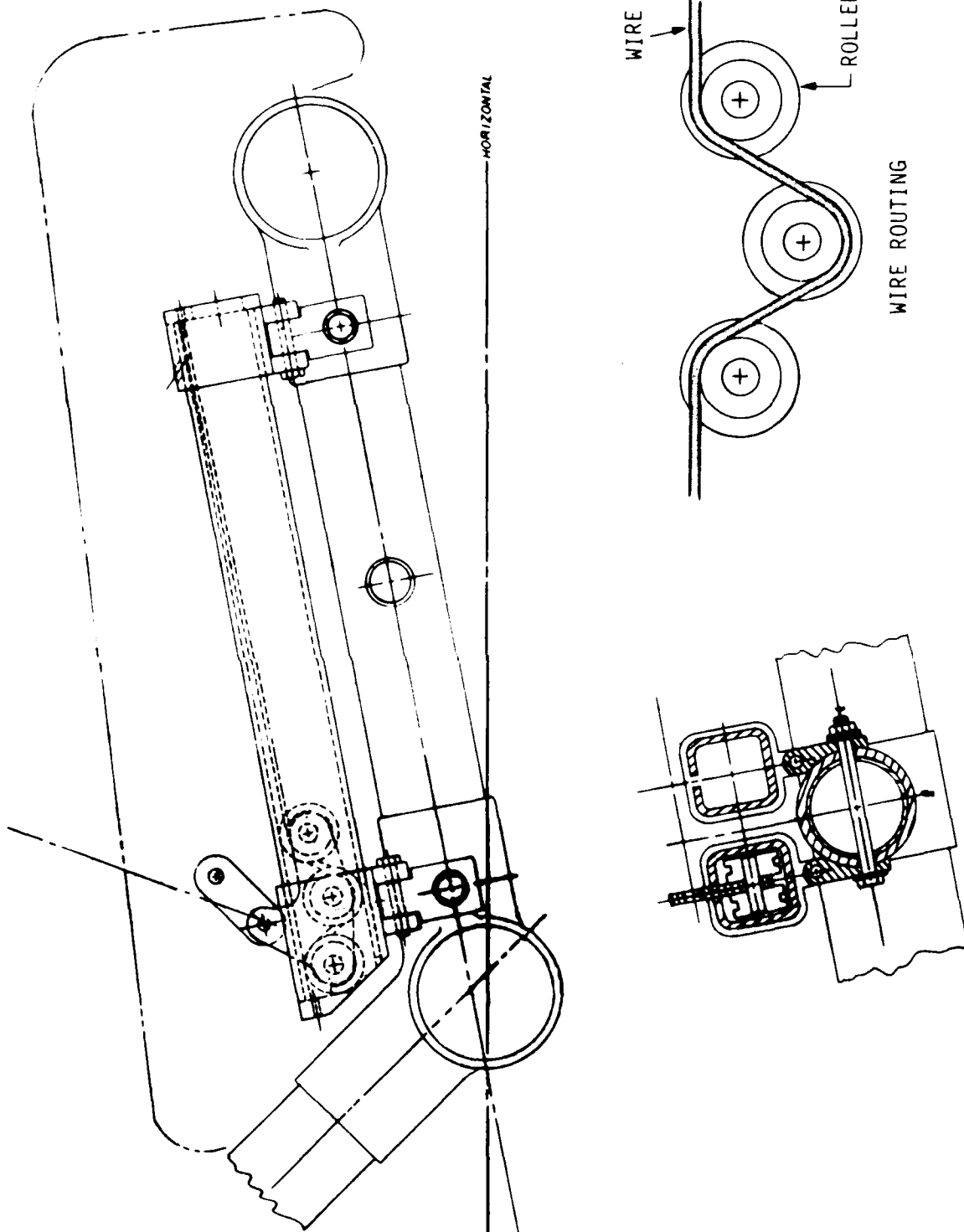


Figure 60. Weber MOD I seat lap belt energy absorber.



Figure 58. Weber MOD I seat - bottom view.



Figure 59. Weber MOD I seat - top view.

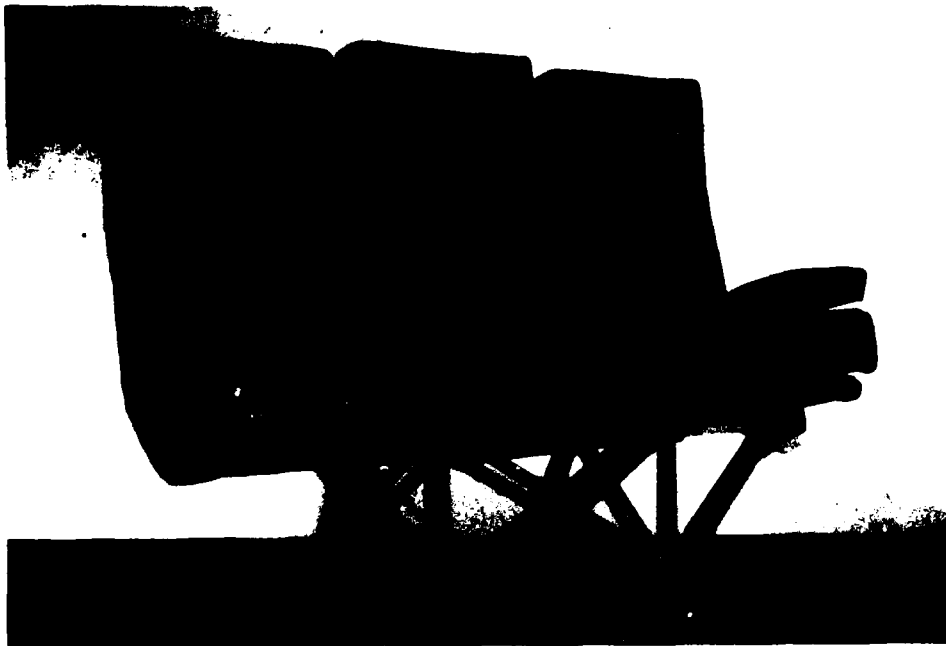


Figure 56. Weber MOD I seat - front view.

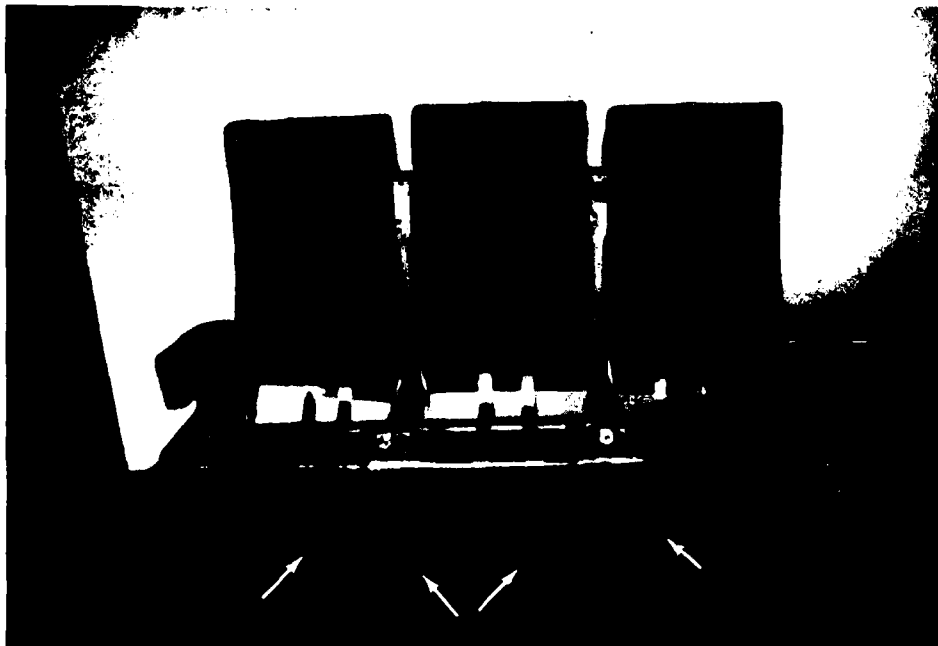


Figure 57. Weber MOD I seat front leg structure and energy absorbers.



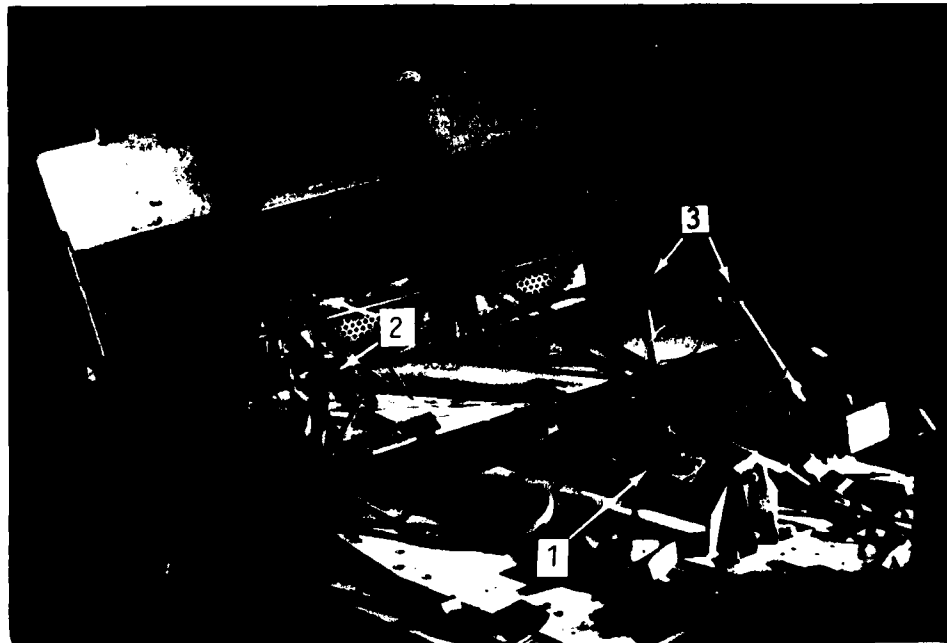


Figure 54. Failure points on standard Weber seat (Dynamic Test).

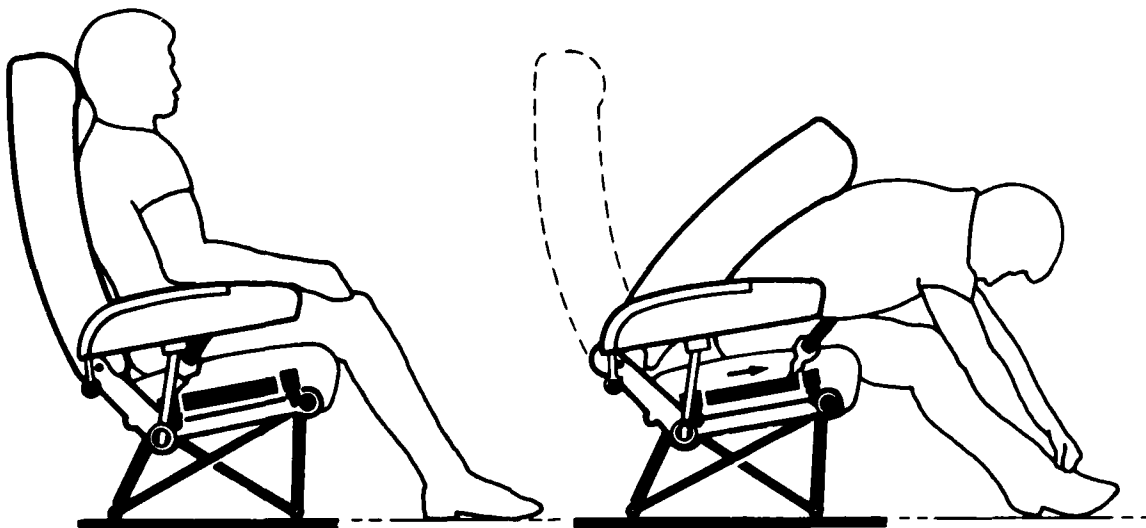


Figure 55. Weber MOD I seat before and after stroking.

84 01004 35



Figure 52. Posttest bent front tube of standard Weber seat (Forward Static Test).

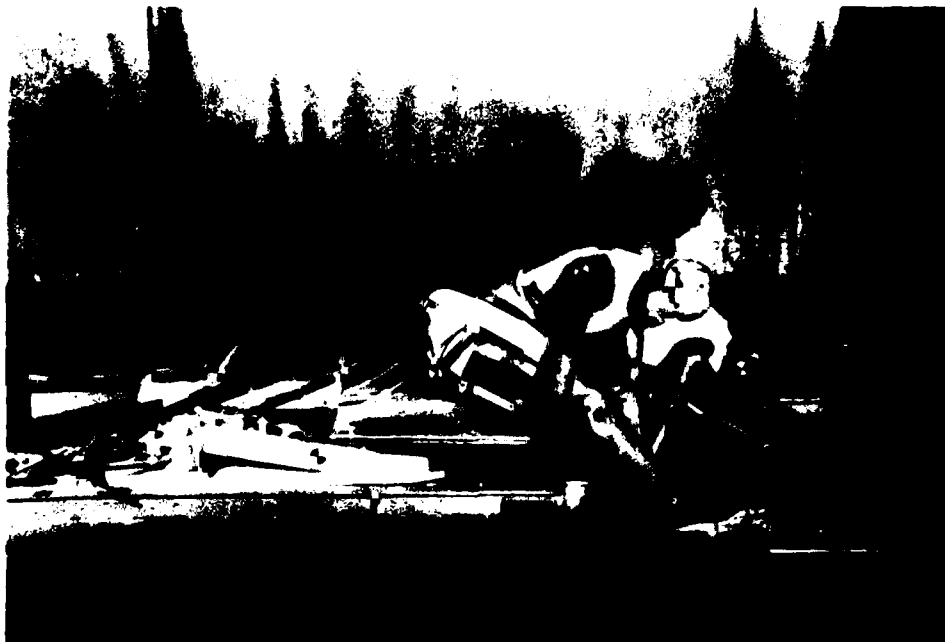


Figure 53. Posttest standard Weber seat (Dynamic Test).



Figure 50. Posttest ruptured rear tube of standard Weber seat (Forward Static Test).



Figure 51. Posttest buckled spreader tube of standard Weber seat (Forward Static Test).

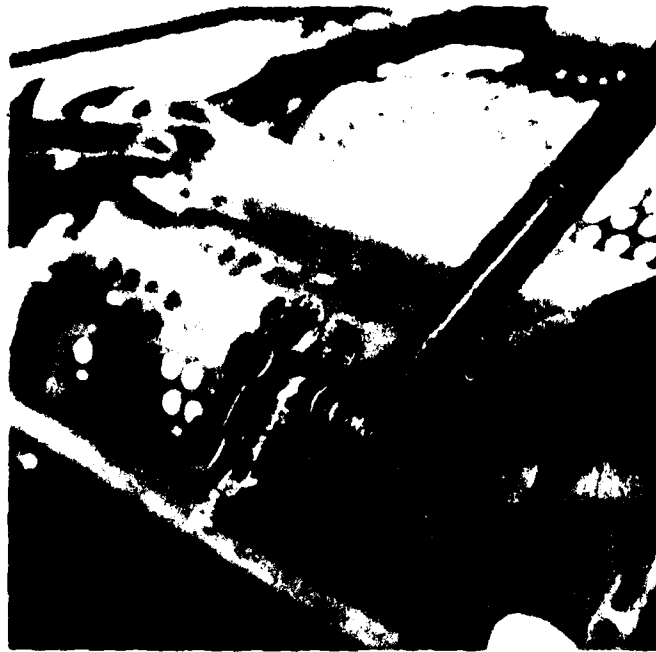


Figure 48. Rear track fitting of standard Weber seat.

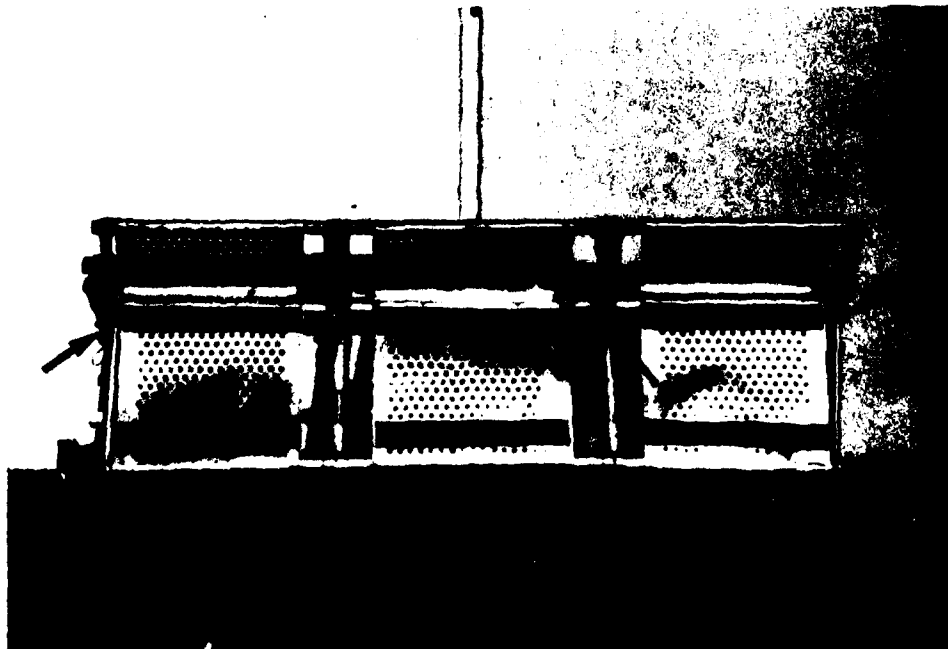


Figure 49. Standard Weber seat pan showing lap belt tiedown fittings - top view.

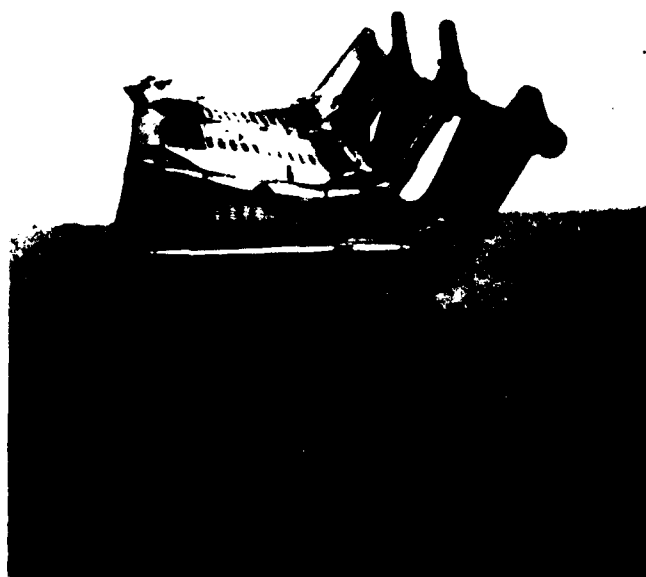


Figure 46. Seat pan and leg assembly of standard Weber seat.

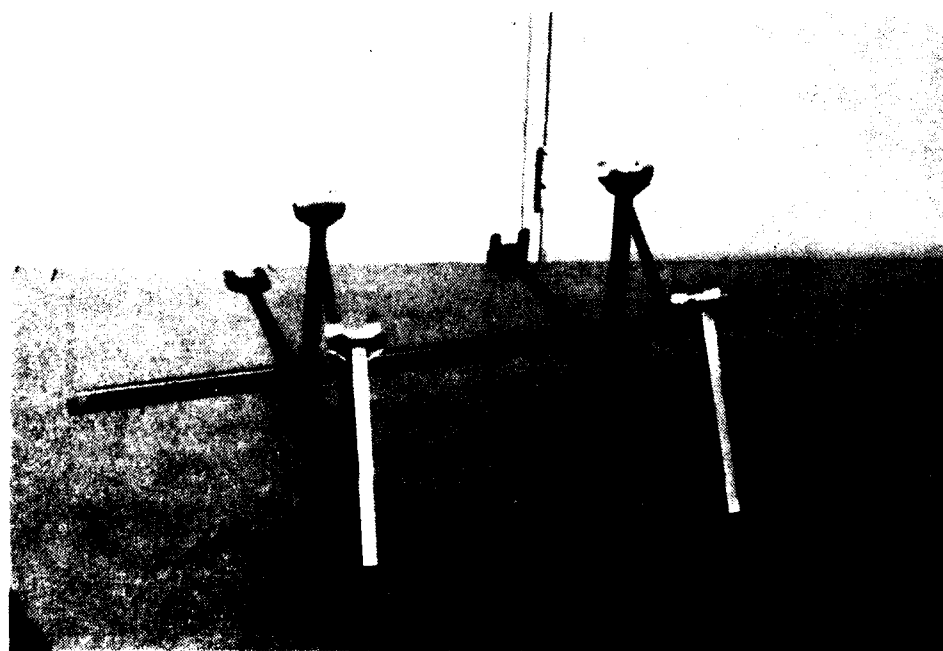


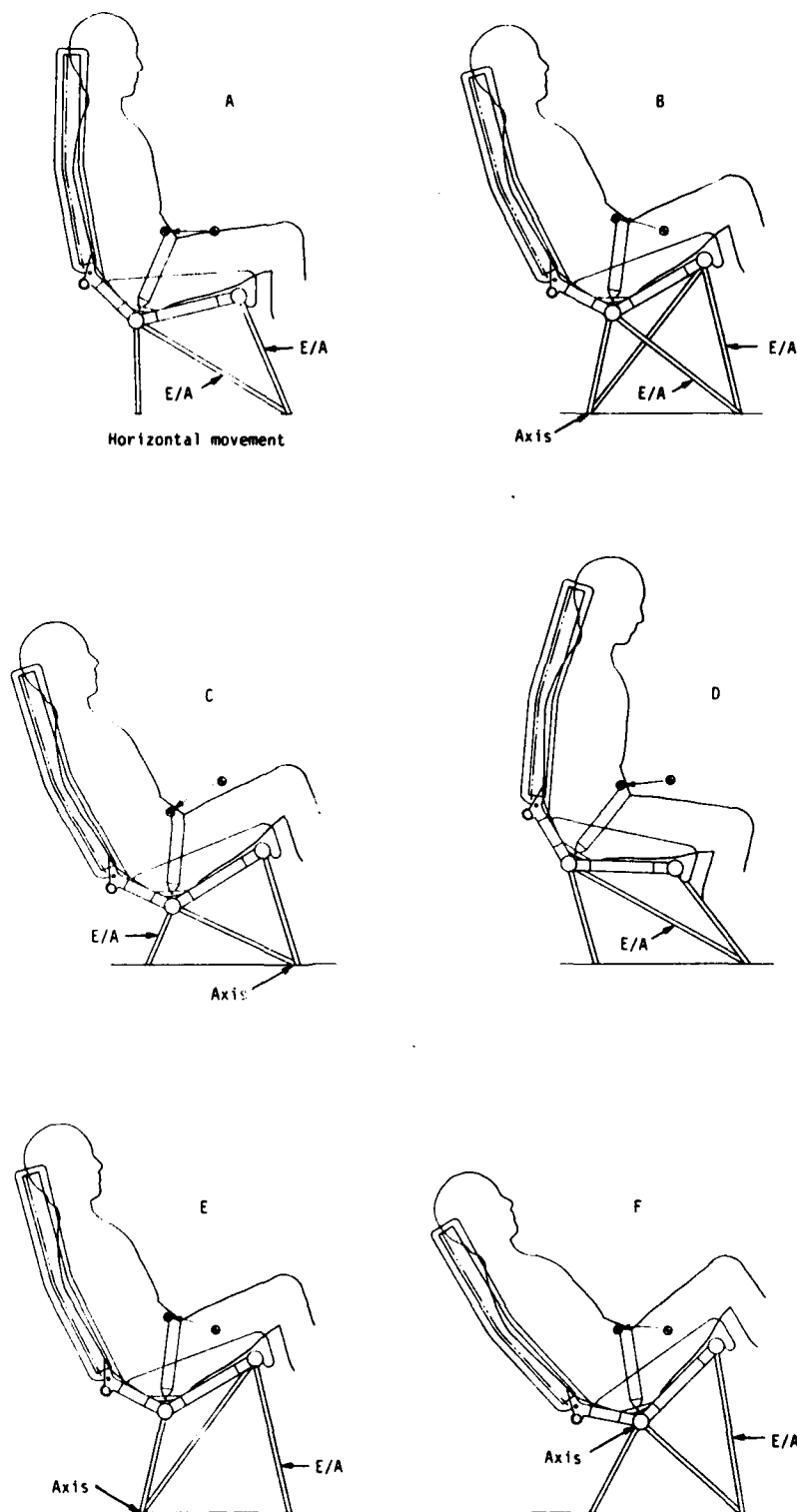
Figure 47. Leg assembly of standard Weber seat.



Figure 44. Standard Weber seat - front view.

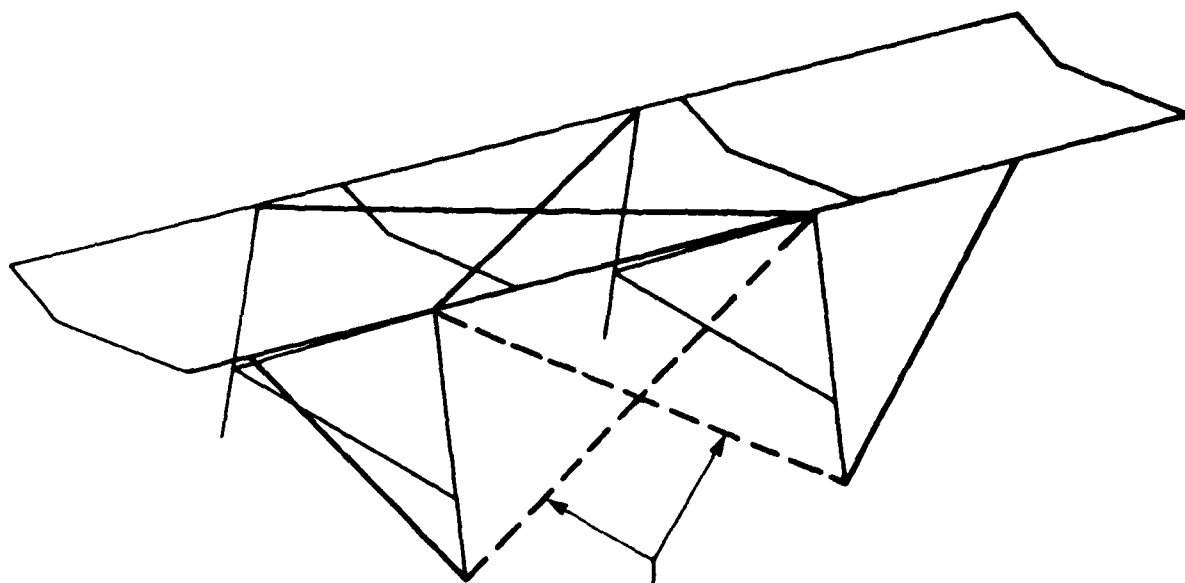


Figure 45. Standard Weber seat - rear view.



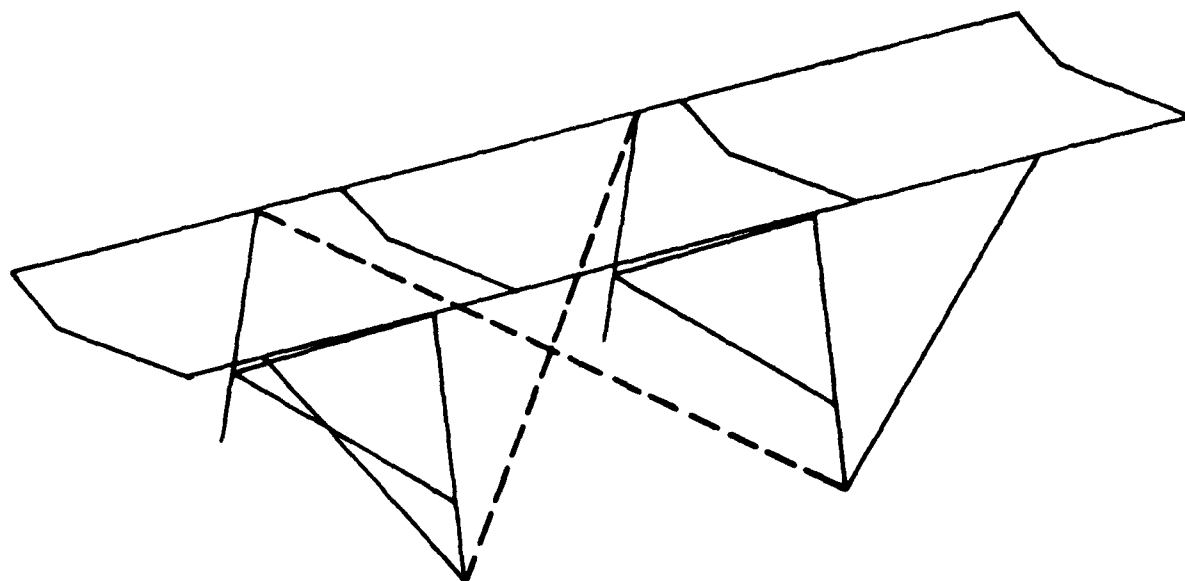
84 02002 66

Figure 43. Aft-facing seat concepts shown in stroked position.



Straps crossing at front legs

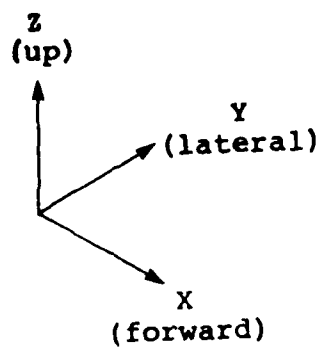
a. Diagonal straps used between front legs.



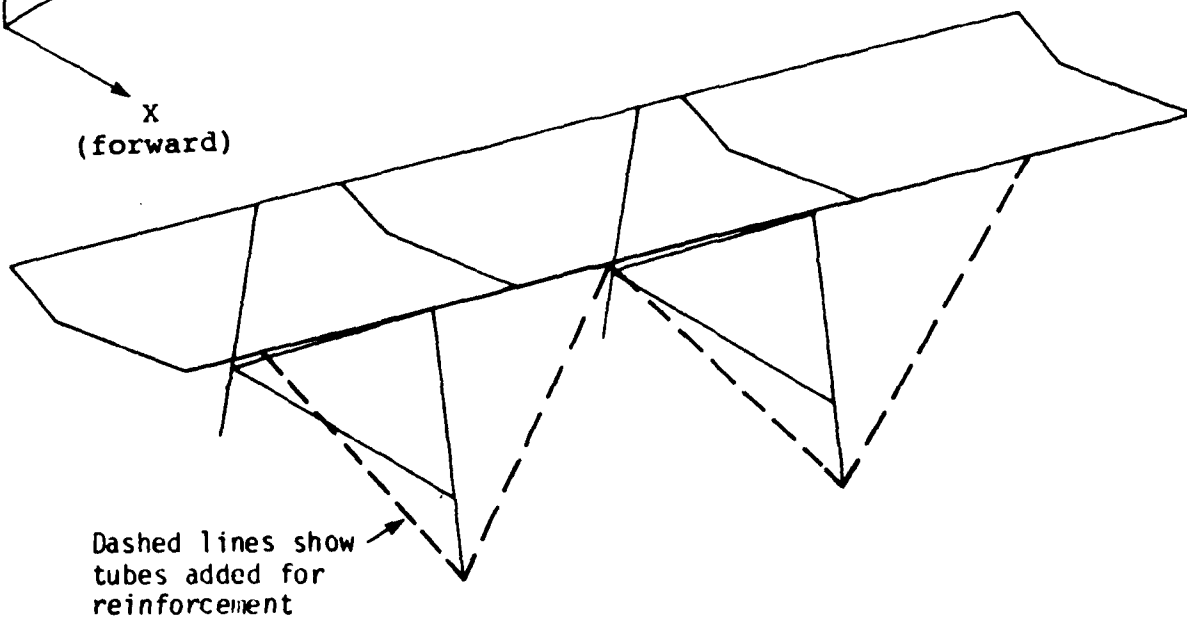
b. Diagonals between tops of rear legs and front track fittings.

Figure 42. Alternate lateral bracing configurations.

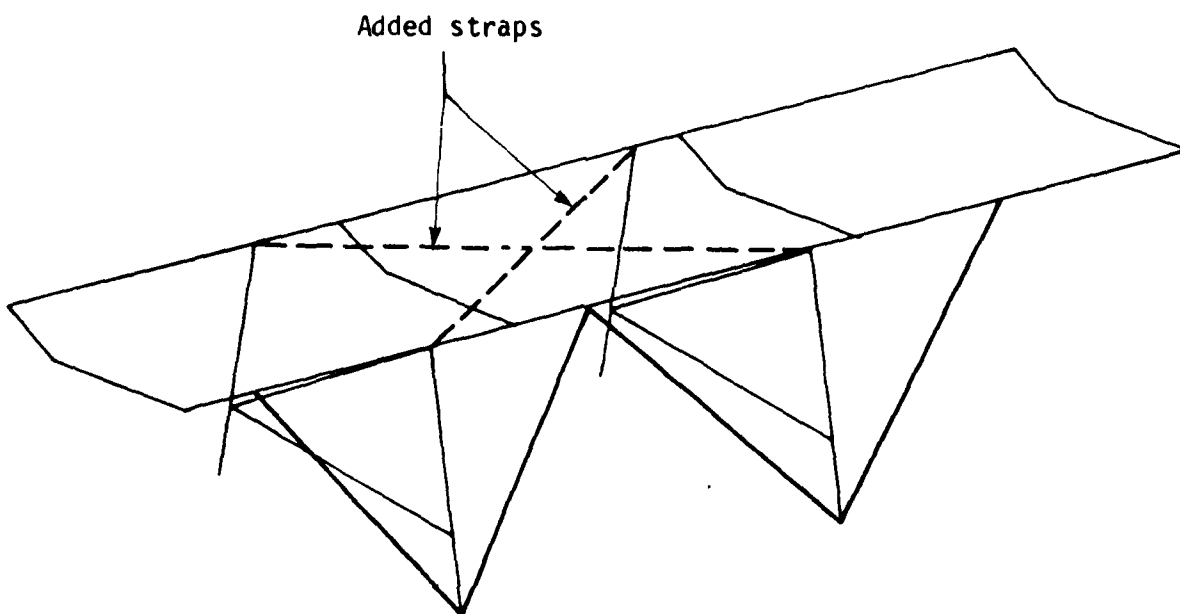




84 02002 77

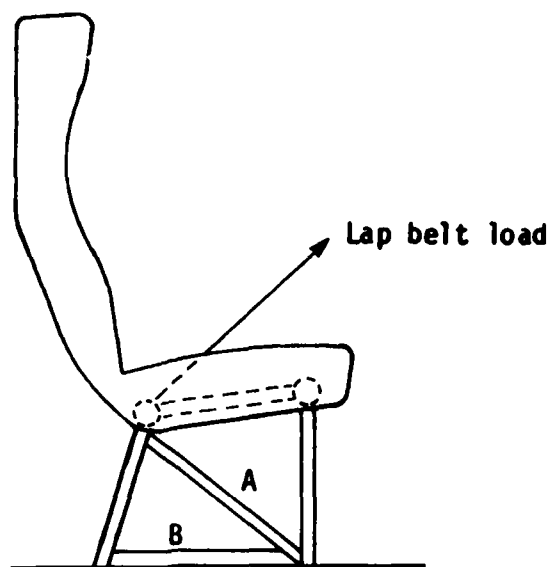


a. Front legs braced with additional tubes.

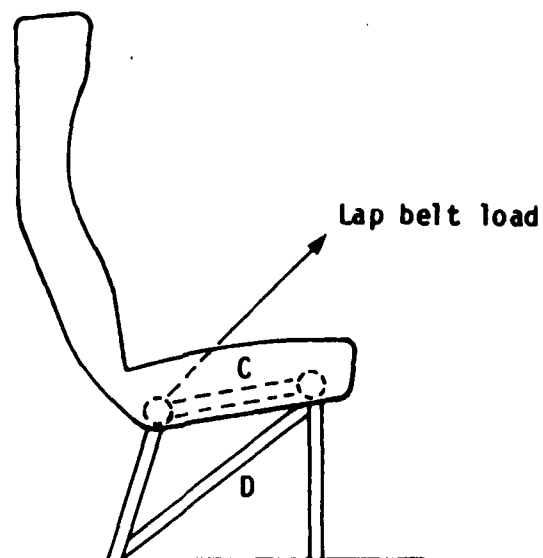


b. Straps added between tops of legs.

Figure 41. Lateral bracing concepts.



a. UOP



b. Weber and Weberlite

Figure 40. Bracing members of the UOP, Weber, and Weberlite seats.



Figure 63. Weber MOD I seat aisle-side body block after stroking.

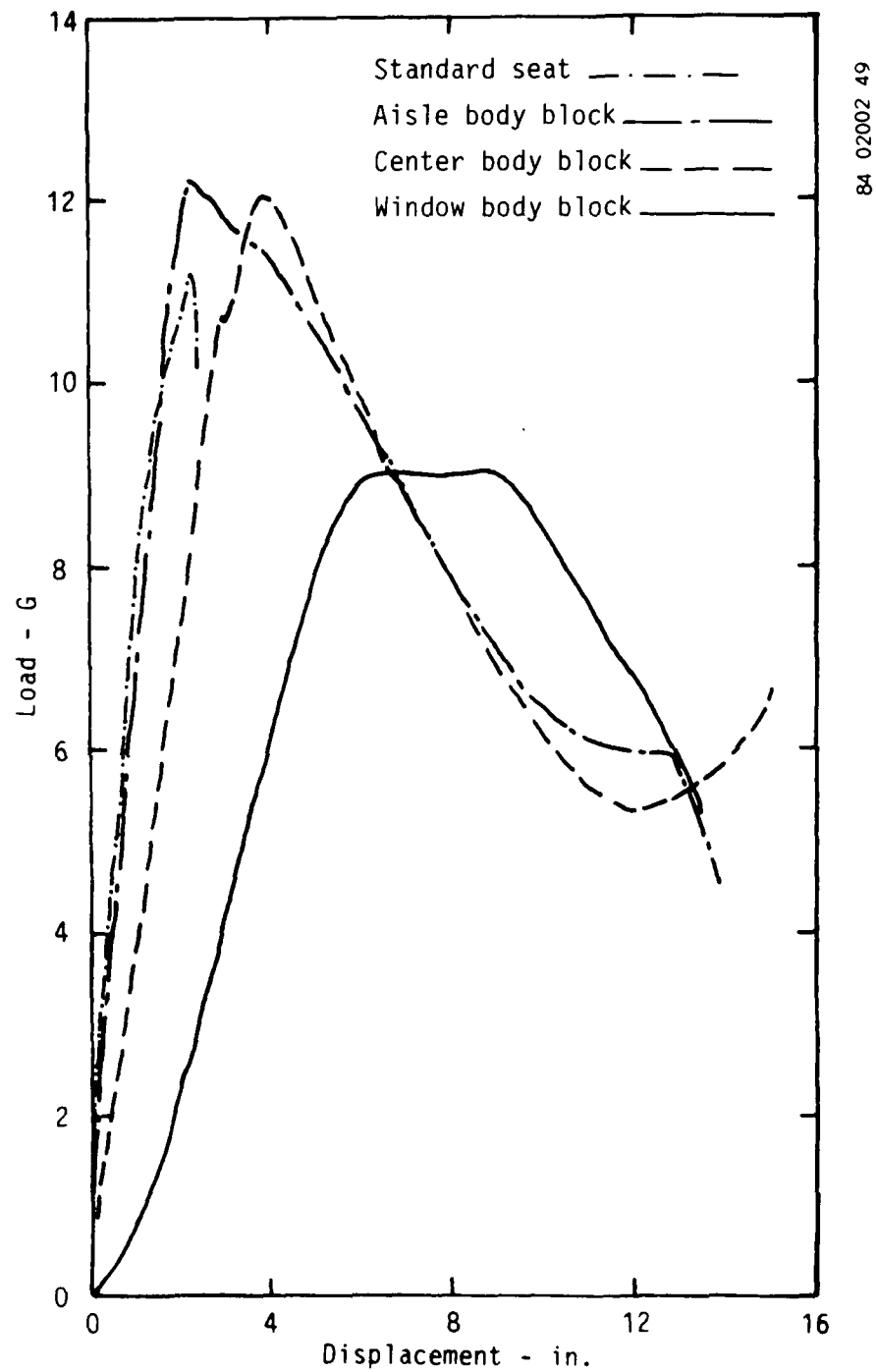


Figure 64. Load versus forward displacement of standard seat and body blocks of Weber MOD I seat.



Figure 65. Posttest Weber MOD I seat (Lateral Test).

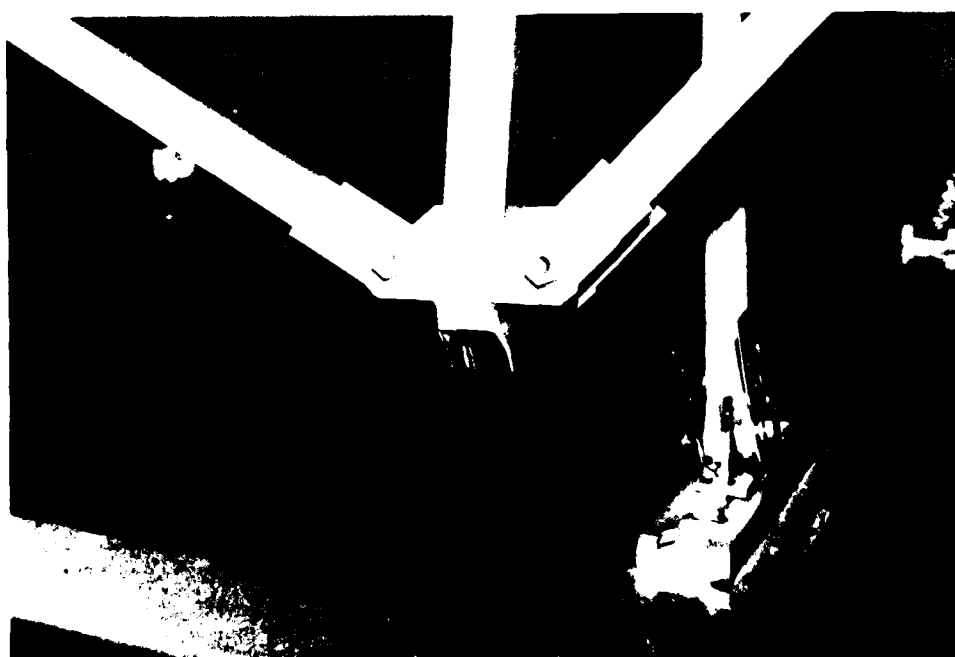
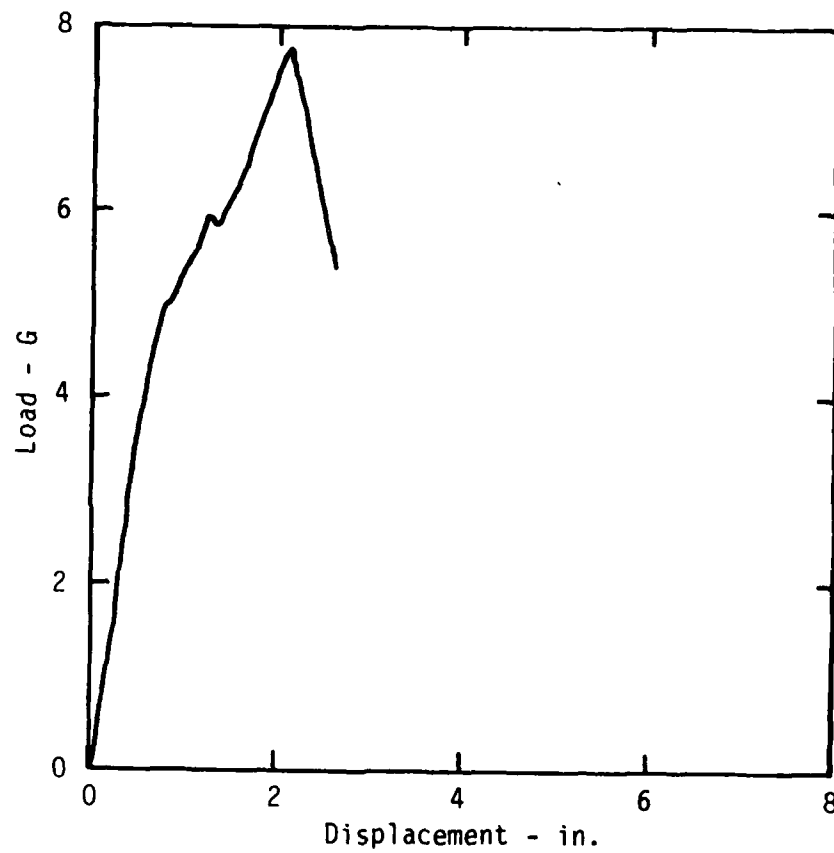


Figure 66. Failure point on Weber MOD I seat (Lateral Test).



84 02002 27

Figure 67. Load versus lateral displacement of Weber MOD I seat.




Figure 68. Posttest rear window-side leg and rear tube of Weber MOD I seat (Dynamic Test).



Figure 69. Posttest dummy positions of Weber MOD I seat (Dynamic Test).

POSITION	E/A STROKE (IN.)
WINDOW SEAT	.75
	1.50
CENTER SEAT	1.00
	2.25
AISLE SEAT	.88
	.25

  
 FORWARD

84 02002 74

Figure 70. Stroking distances of individual lap belt energy absorbers on Weber MOD I seat (Dynamic Test).



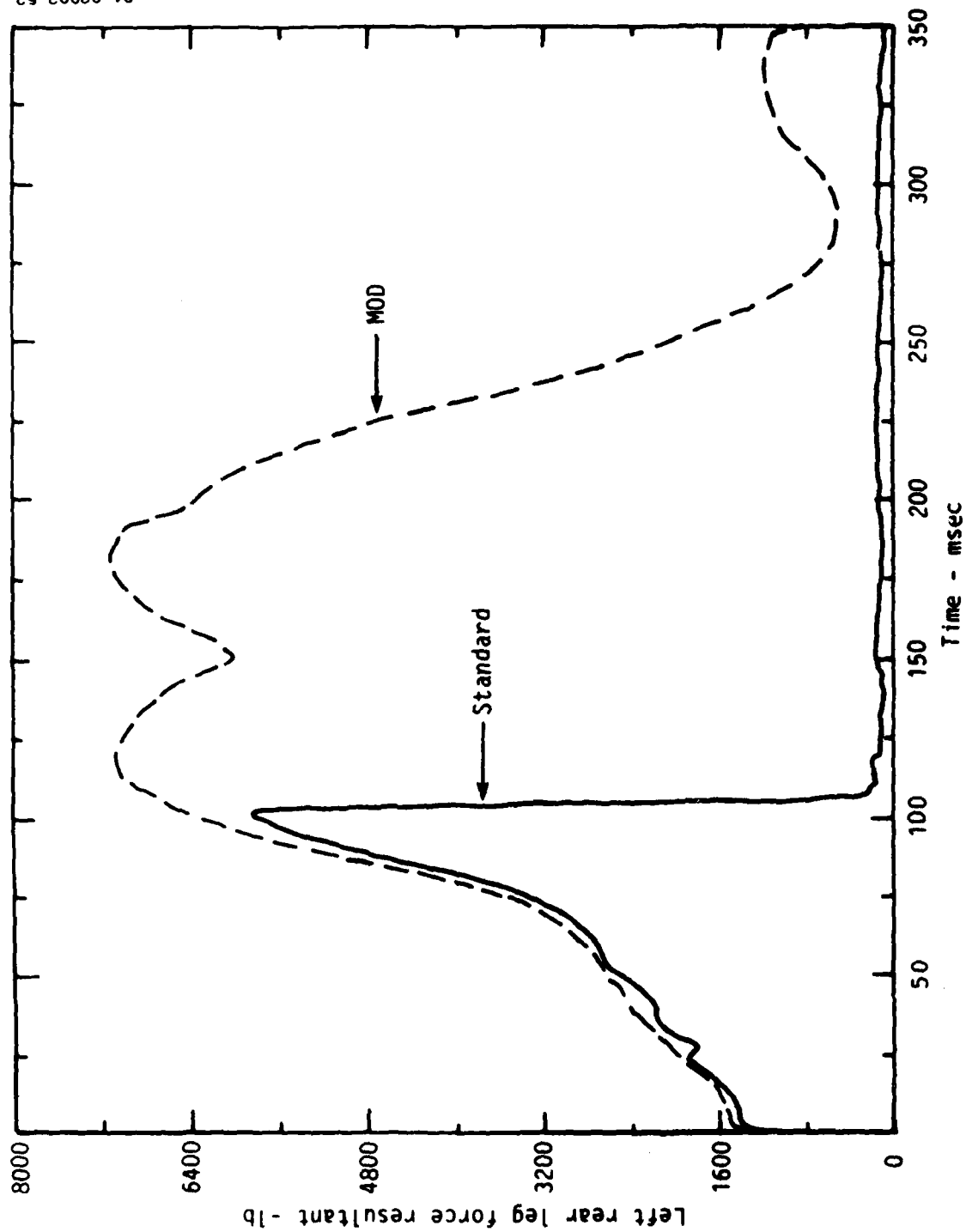
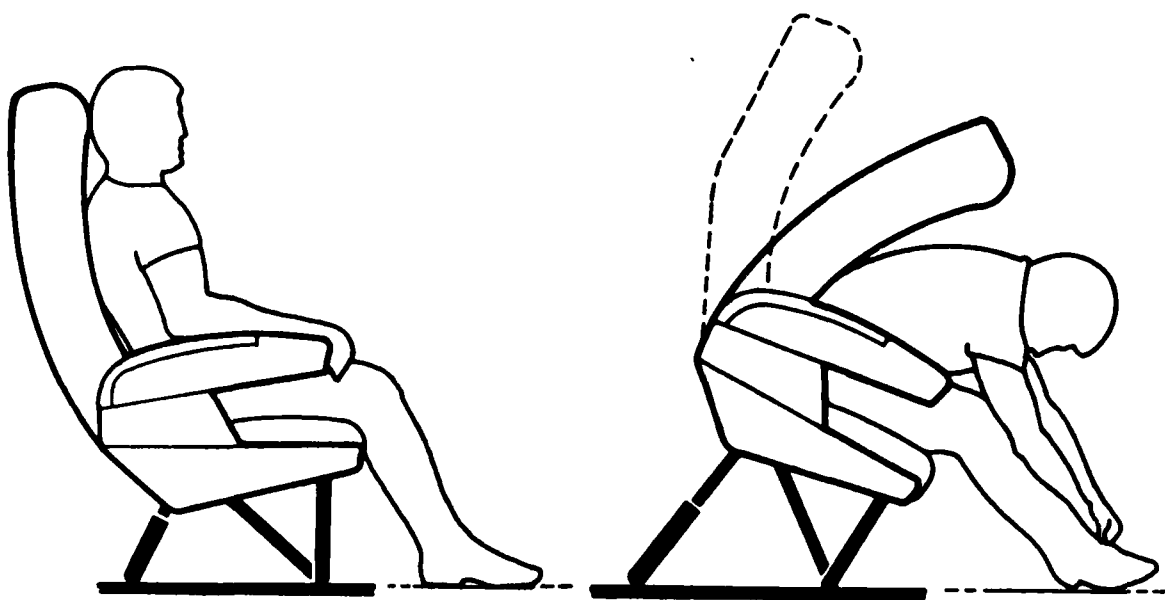


Figure 71. Rear window-side leg force resultants of standard and Weber MOD I seats.



84 01004 34

Figure 72. Weber MOD II seat before and after stroking.

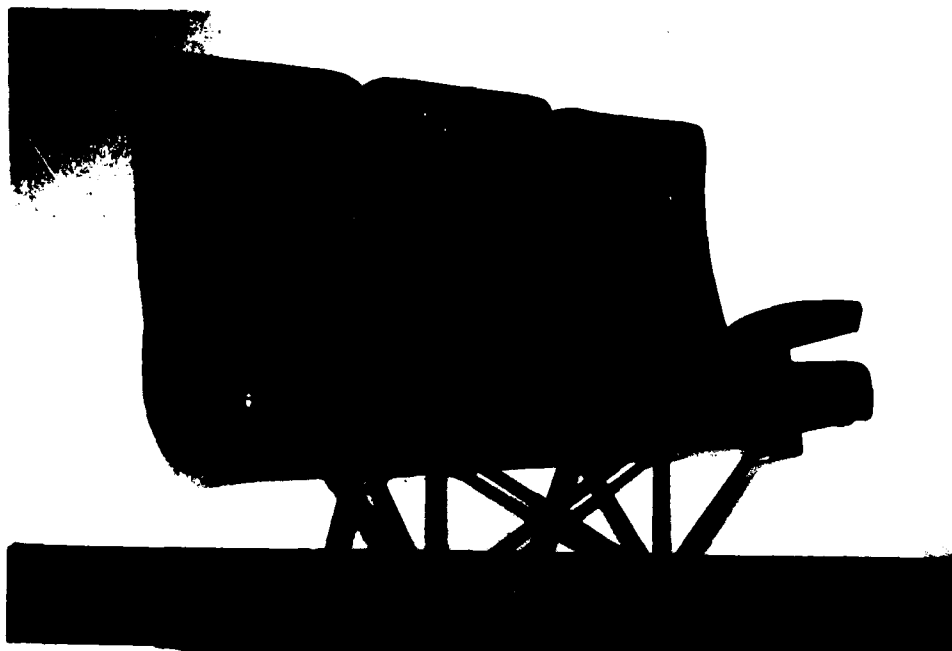


Figure 73. Weber MOD II seat - front view.



Figure 74. Weber MOD II seat - rear view.



Figure 75. Weber MOD II seat lateral bracing - bottom view.



Figure 76. Weber MOD II seat energy absorbers and modified seat pans.

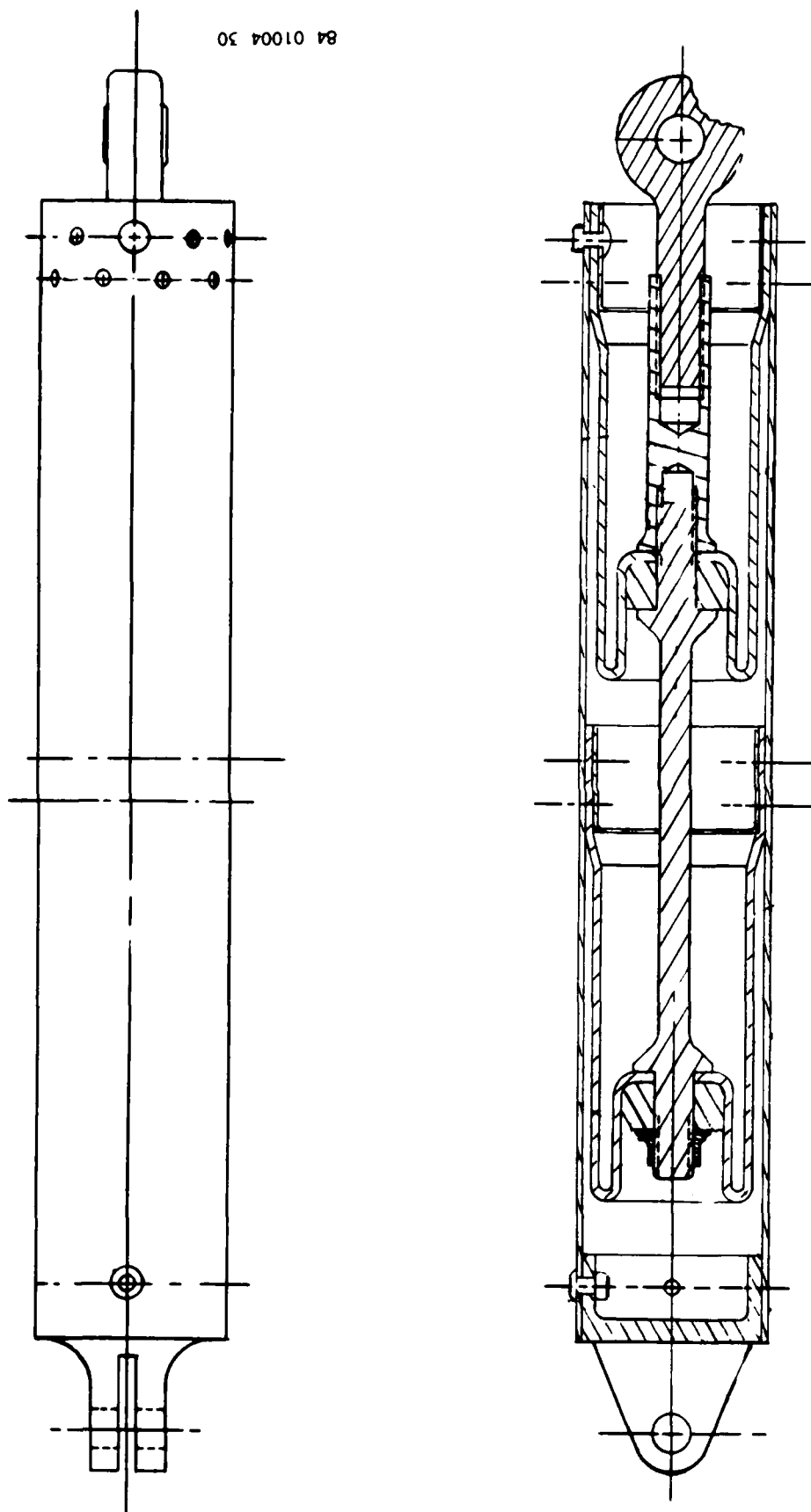


Figure 77. Weber MOD II seat energy absorber.



Figure 78. Posttest Weber MOD II seat (Forward Static Test).



Figure 79. Location of energy absorber failure on the Weber MOD II seat (Forward Static Test).

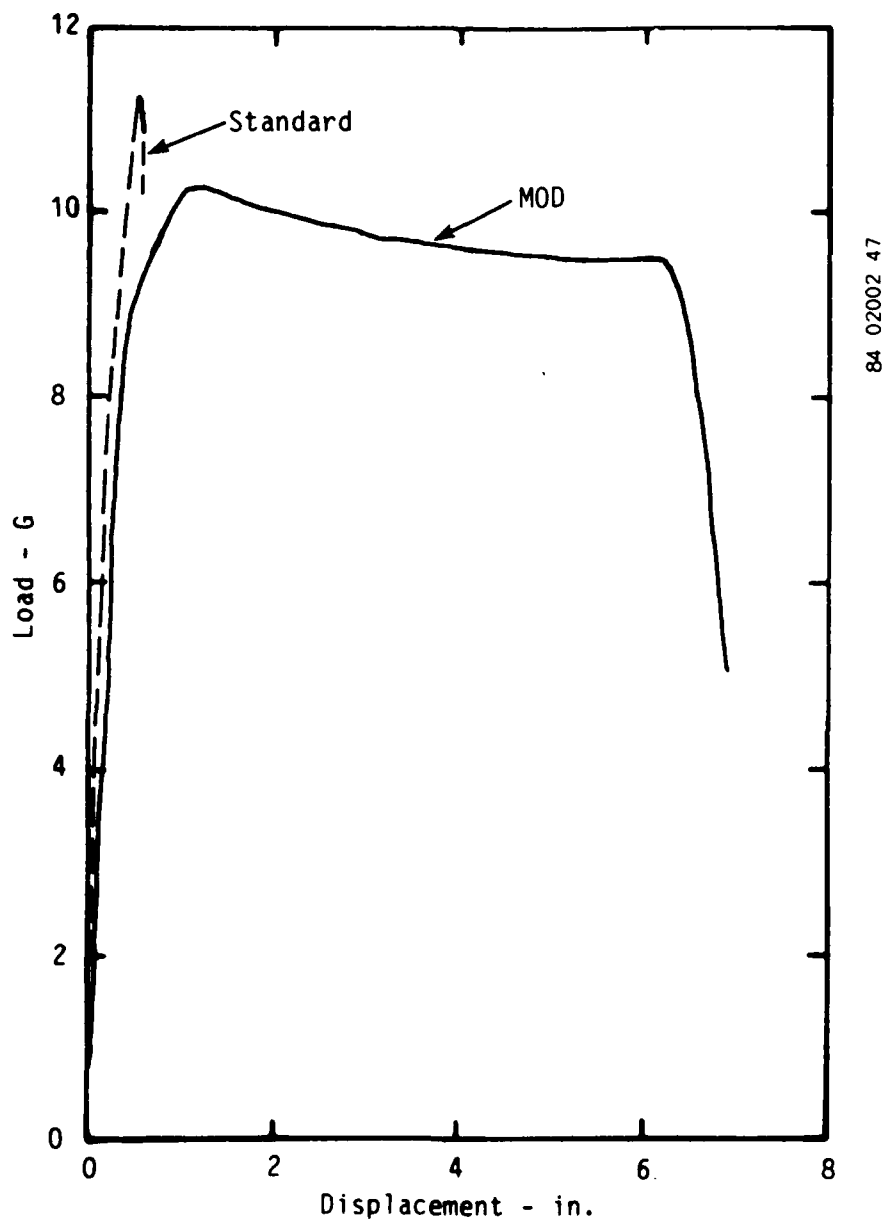


Figure 80. Load versus forward displacement of standard and Weber MOD II seats.



Figure 81. Posttest Weber MOD II seat (Lateral Test).



Figure 82. Failure point on the Weber MOD II seat (Lateral Test).





Figure 105. Posttest UOP MOD I seat (Forward Static Test).



Figure 106. Posttest failed window-side fitting on UOP MOD I seat (Forward Static Test).

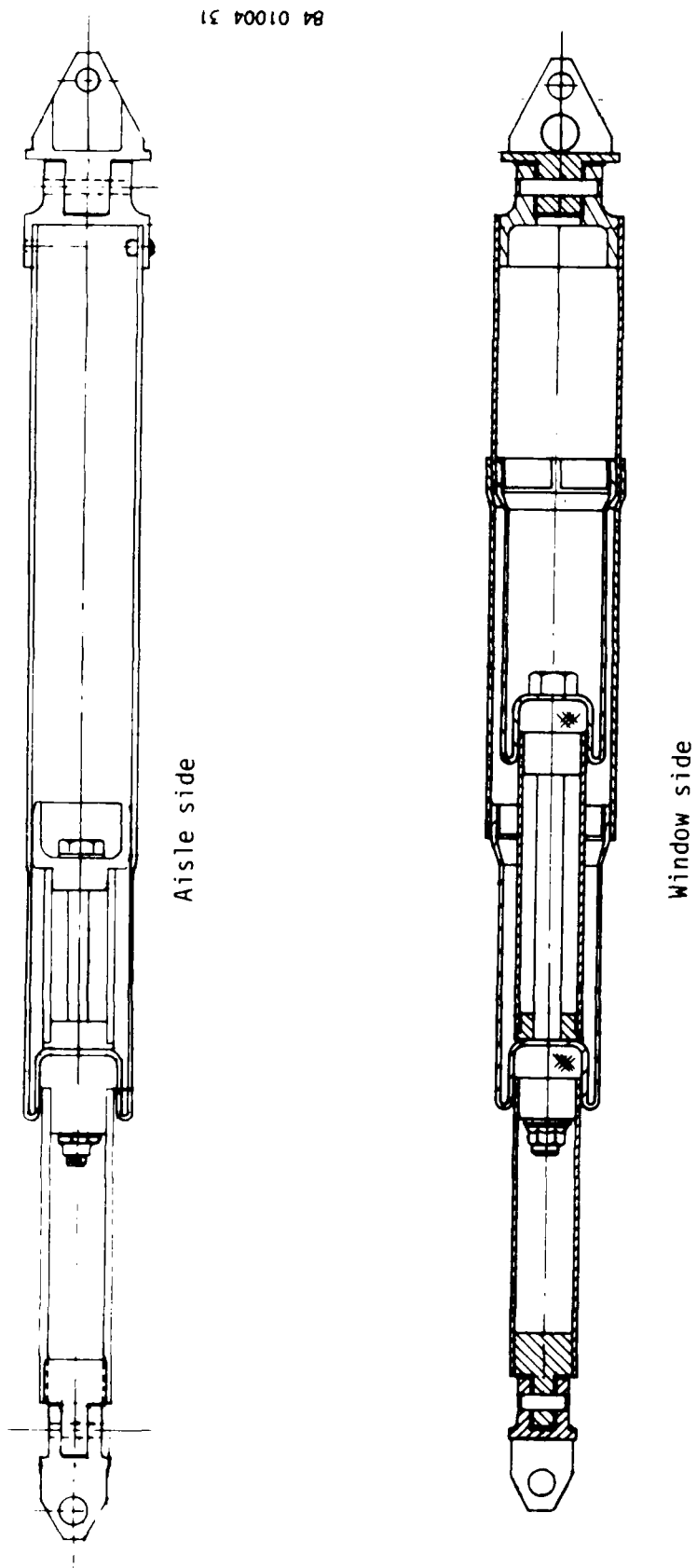


Figure 104. UOP MOD I energy absorbers.

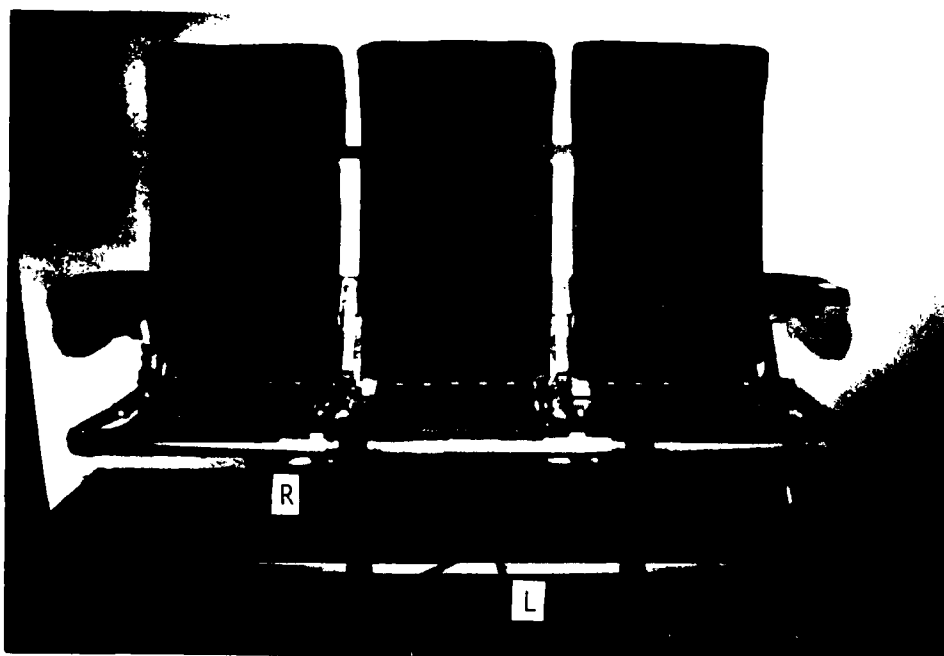


Figure 102. Seat pan and leg structure of UOP MOD I seat.

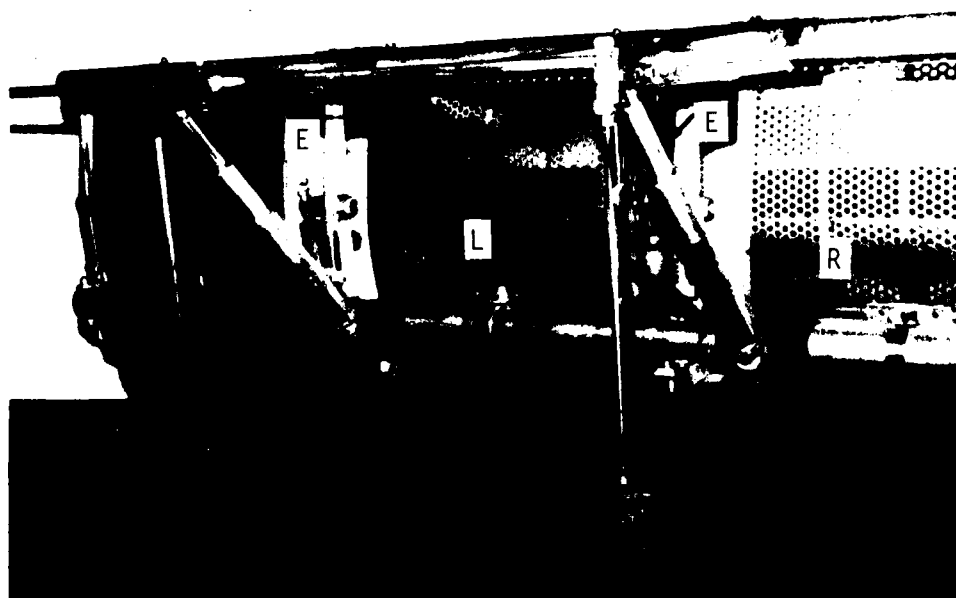


Figure 103. Leg structure and energy absorbers of UOP MOD I seat.



Figure 100. UOP MOD I seat - front view.



Figure 101. UOP MOD I seat - rear view.

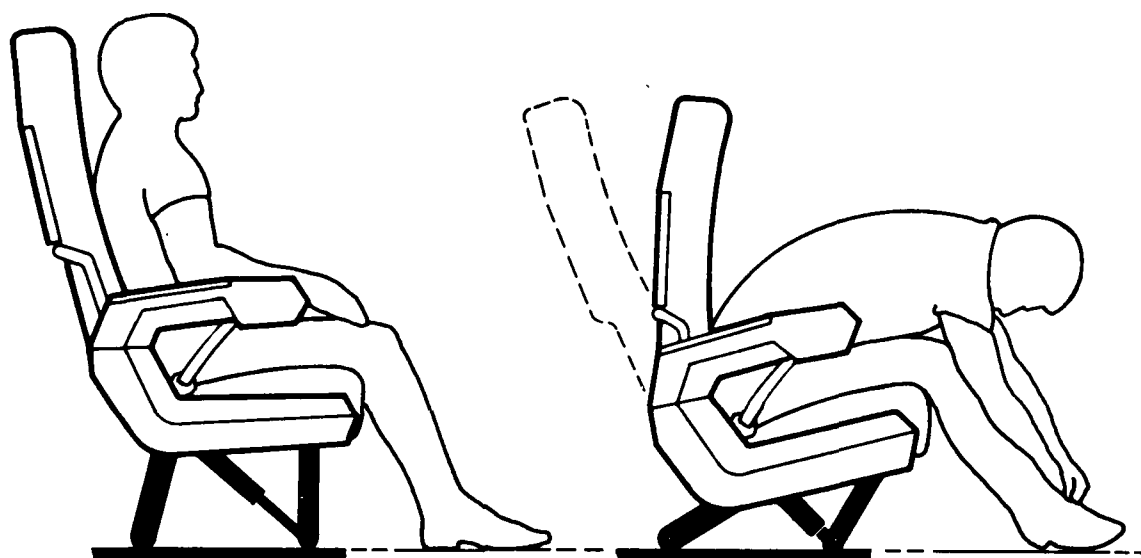


Figure 99. UOP MOD I seat before and after stroking.



Figure 97. Failures on aisle-side legs of standard UOP seat (Dynamic Test).



Figure 98. Posttest standard UOP seat (Dynamic Test).

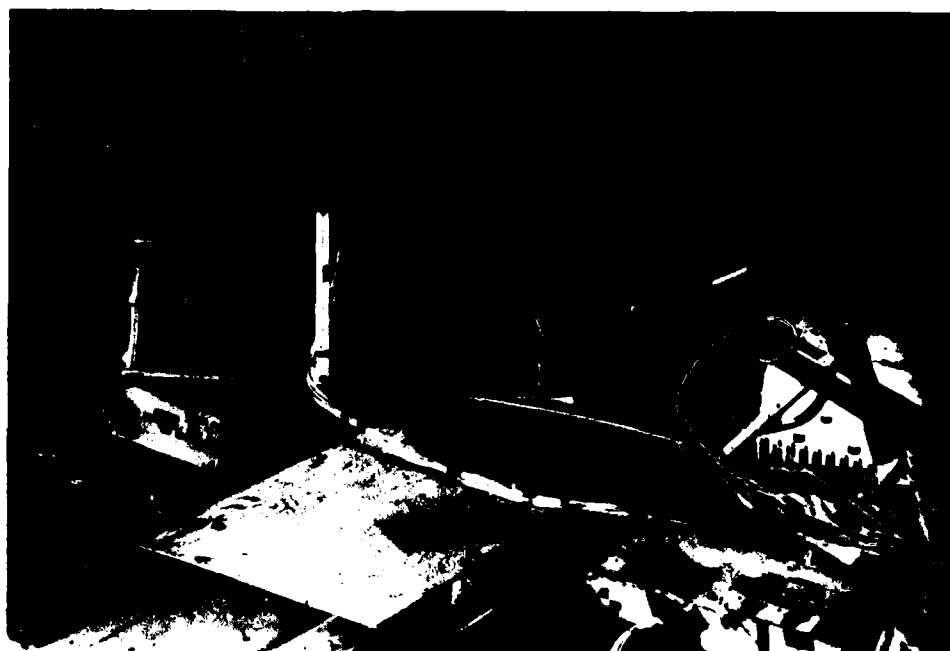


Figure 95. Posttest leg failures on standard UOP seat (Dynamic Test).



Figure 96. Failed window-side leg track fittings of standard UOP seat (Dynamic Test).



Figure 93. Posttest failed leg fitting on standard UOP seat (Forward Static Test).



Figure 94. Posttest bent rear tube of standard UOP seat (Forward Static Test).





Figure 91. Rear track fitting of standard UOP seat.



Figure 92. Anti-rattle mechanism on front leg of UOP seat.



Figure 89. Seat pan and leg assembly of UOP seat.

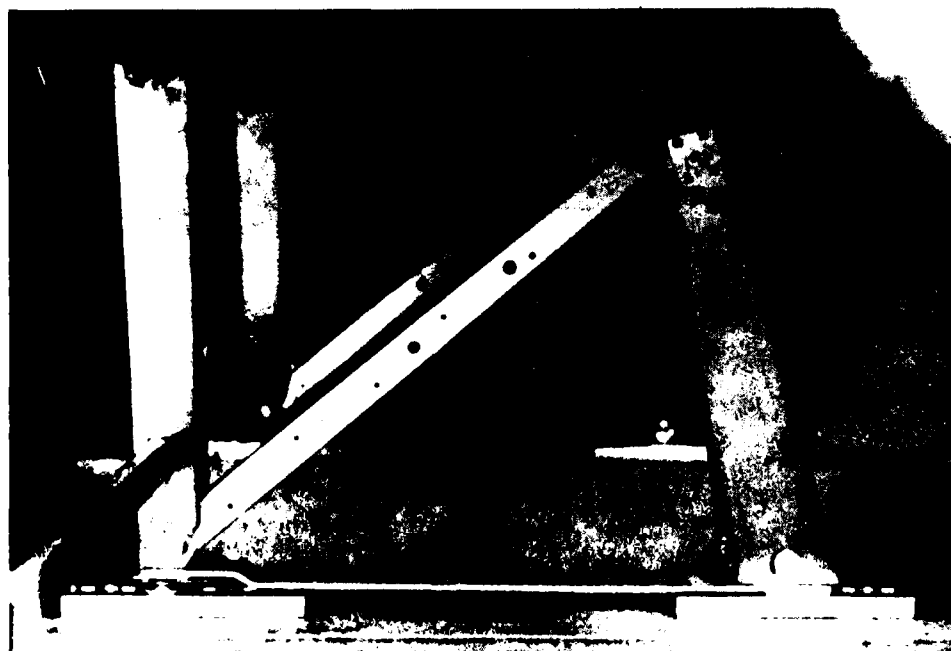


Figure 90. Leg assembly of standard UOP seat.



Figure 87. Standard UOP seat - front view.

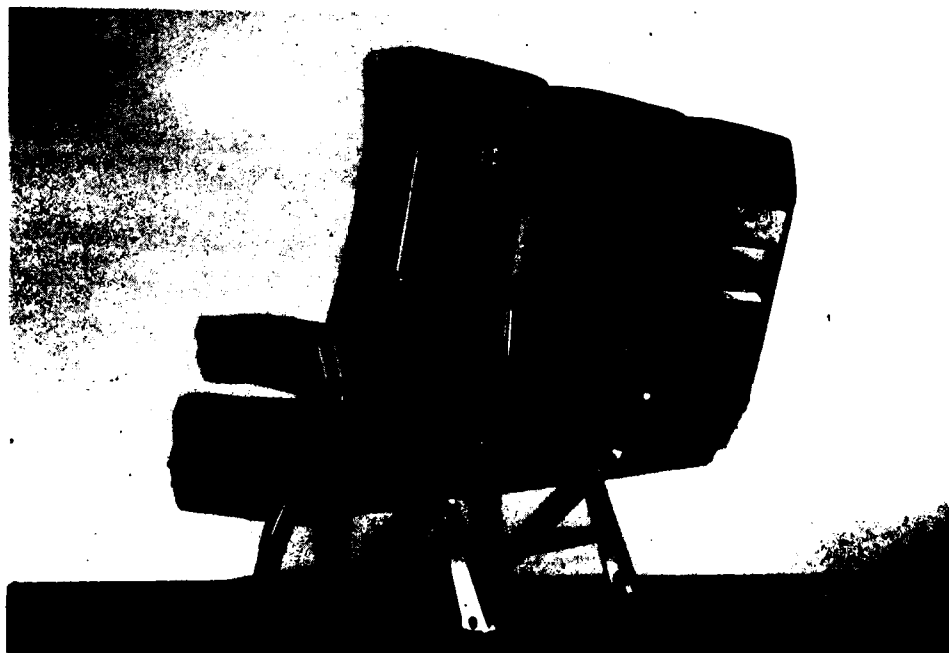


Figure 88. Standard UOP seat - rear view.

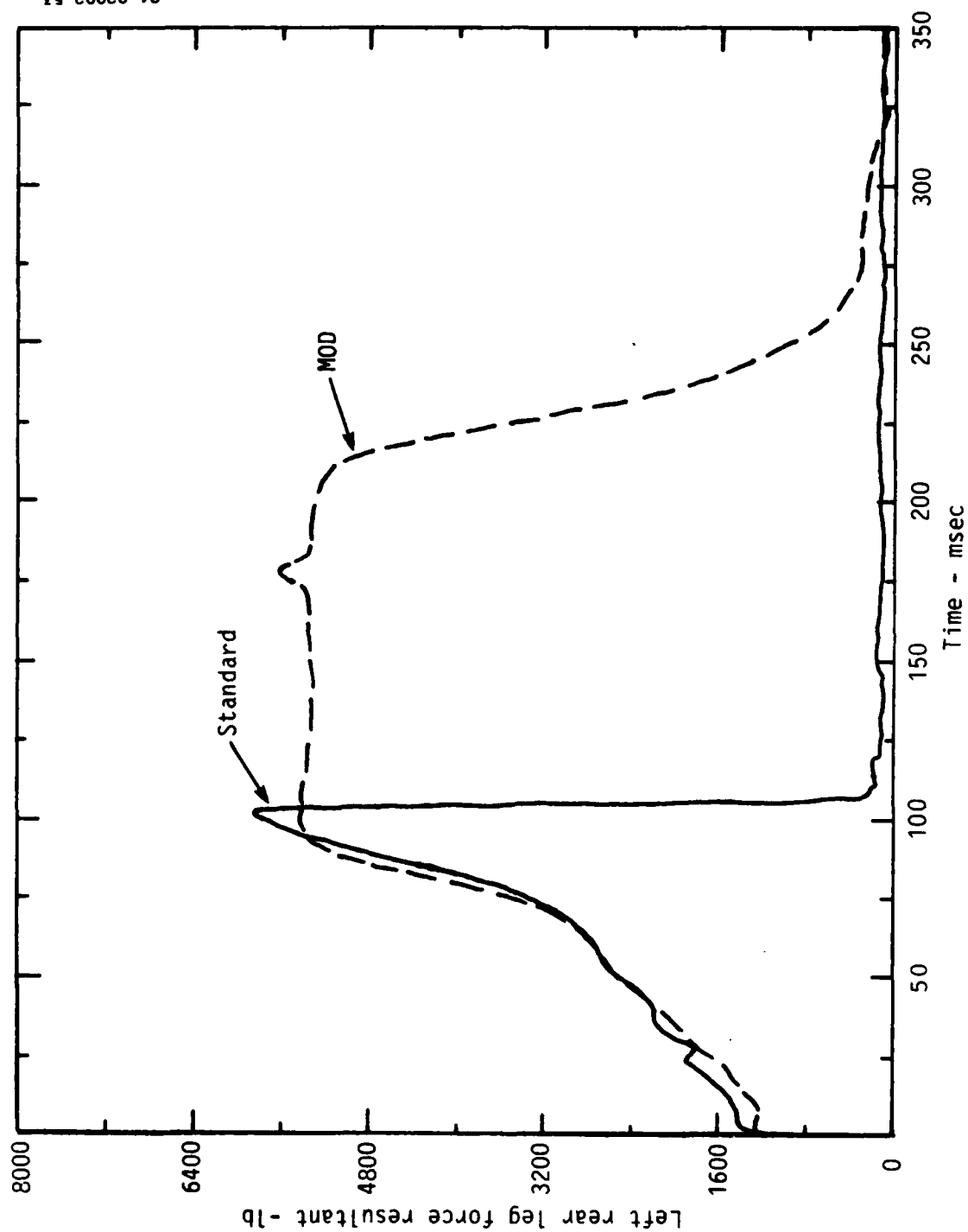


Figure 86. Rear window-side leg force resultants of standard and Weber MOD II seats.



Figure 84. Posttest Weber MOD II seat (Dynamic Test).

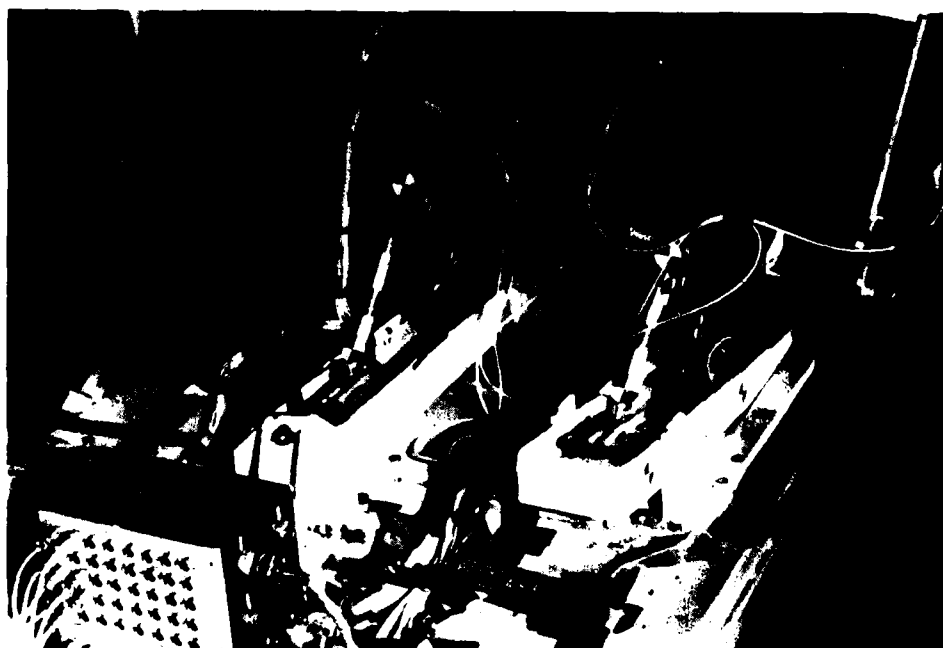


Figure 85. Posttest rear leg energy absorbers of the Weber MOD II seat (Dynamic Test).

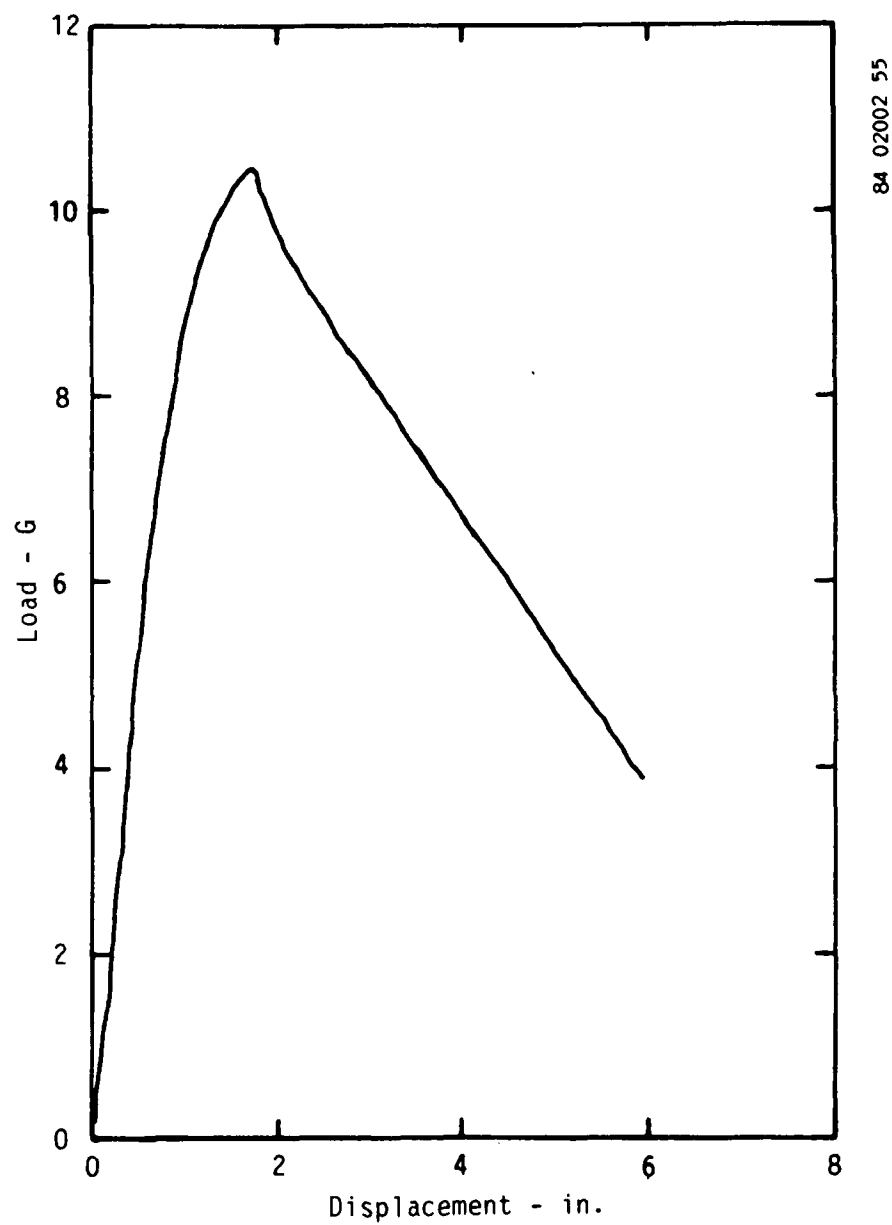


Figure 83. Load versus lateral displacement of Weber MOD II seat.

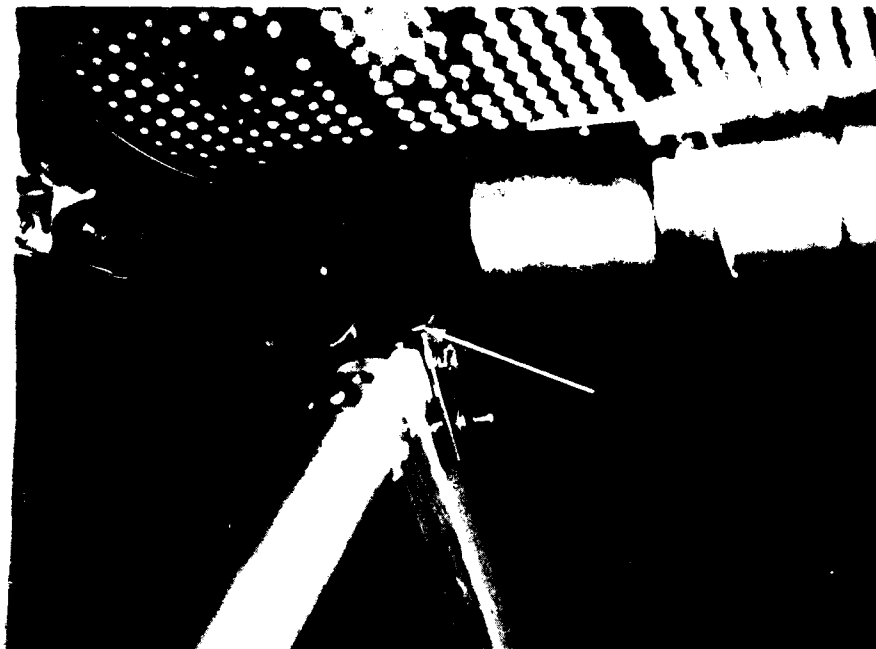


Figure 107. Posttest aisle-side rear leg fitting of UOP MOD I seat (Forward Static Test).

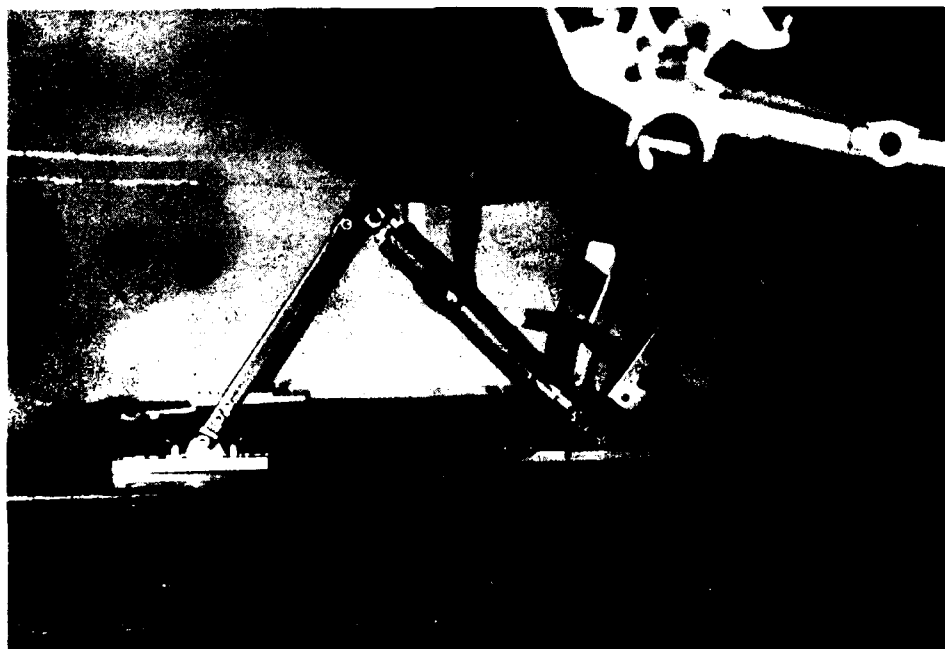


Figure 108. Posttest window-side energy absorber of UOP MOD I seat (Forward Static Test).

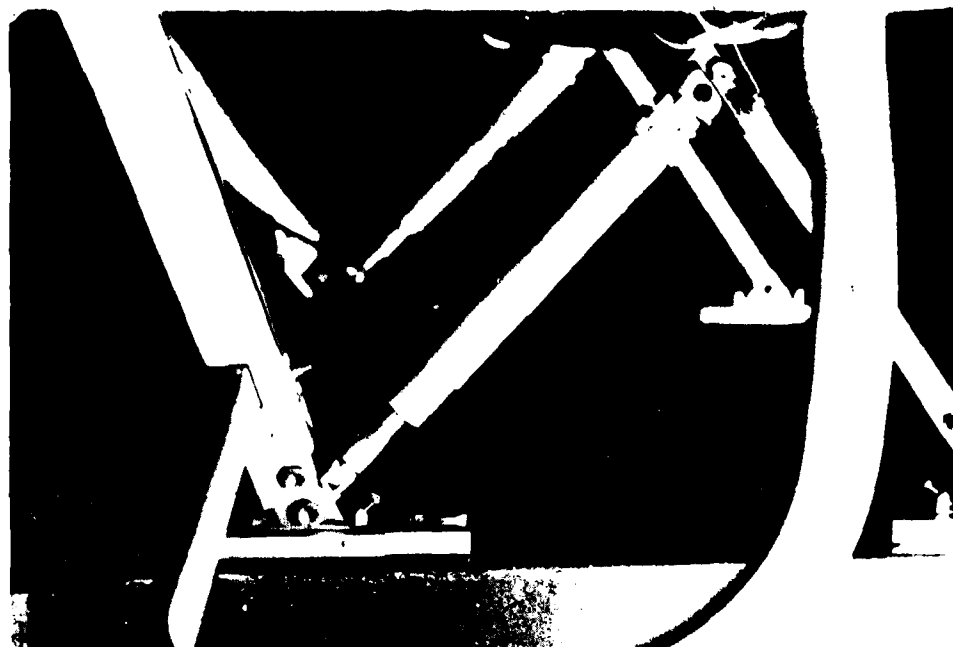
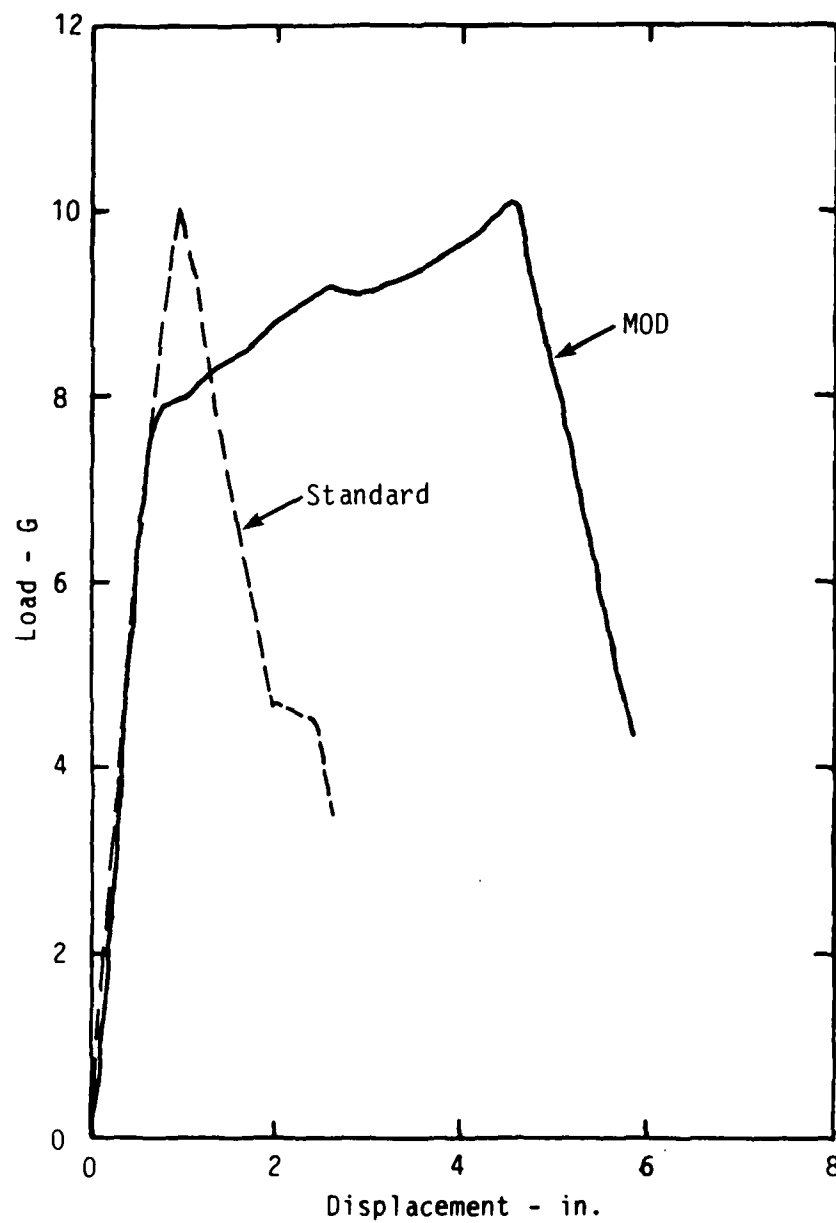


Figure 109. Posttest aisle-side energy absorber on UOP MOD I seat (Forward Static Test).





84 02002 34

Figure 110. Load versus forward displacement of standard and UOP MOD I seats.

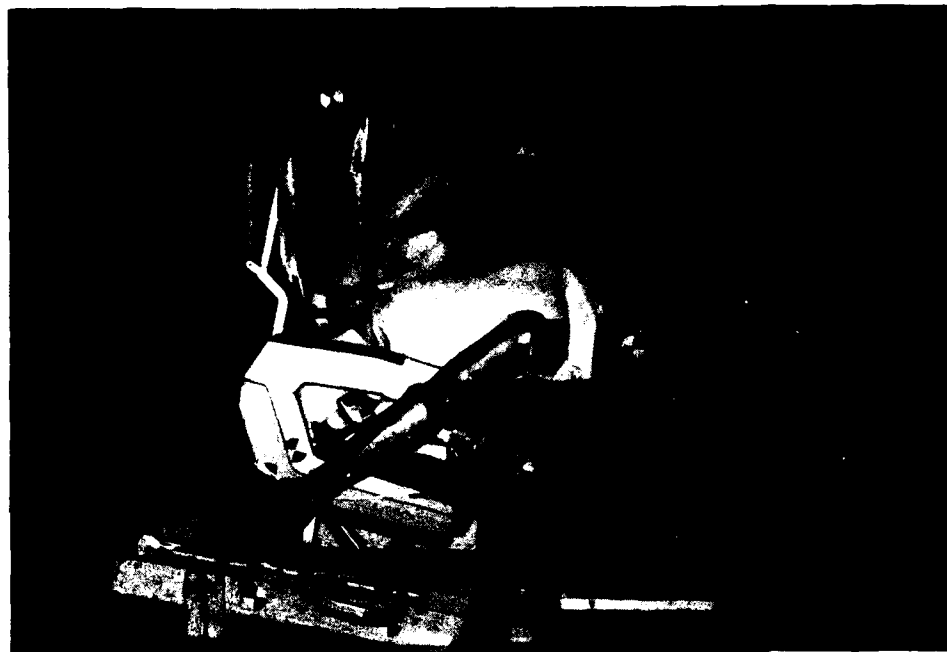


Figure 111. Posttest UOP MOD I seat (Dynamic Test).

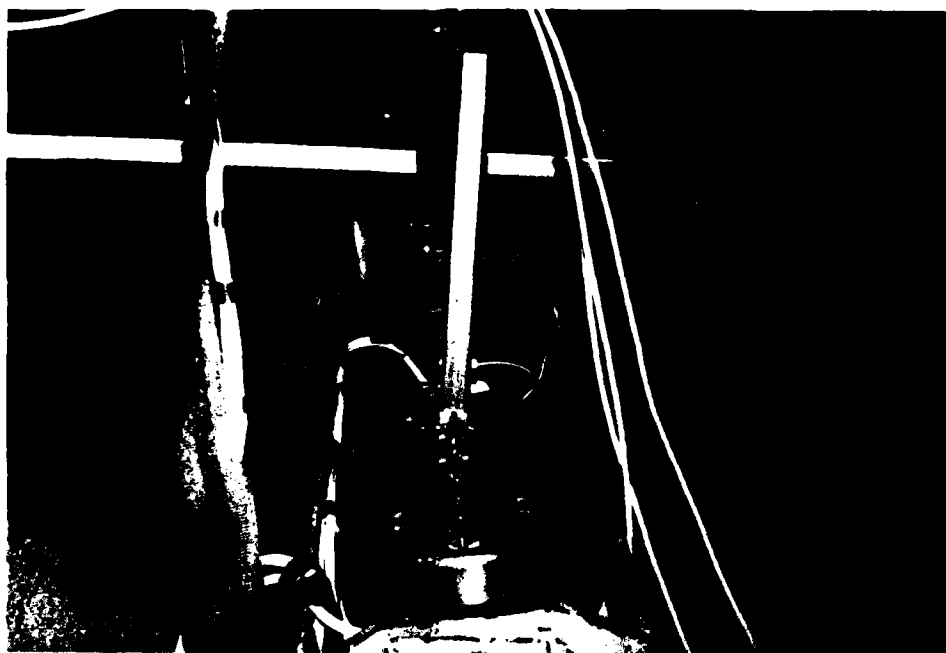


Figure 112. Pretest window-side rear leg of UOP MOD I seat after 10-degree track roll (Dynamic Test).



Figure 113. Pretest aisle-side rear leg of UOP MOD I seat after 10-degree track pitch (Dynamic Test).

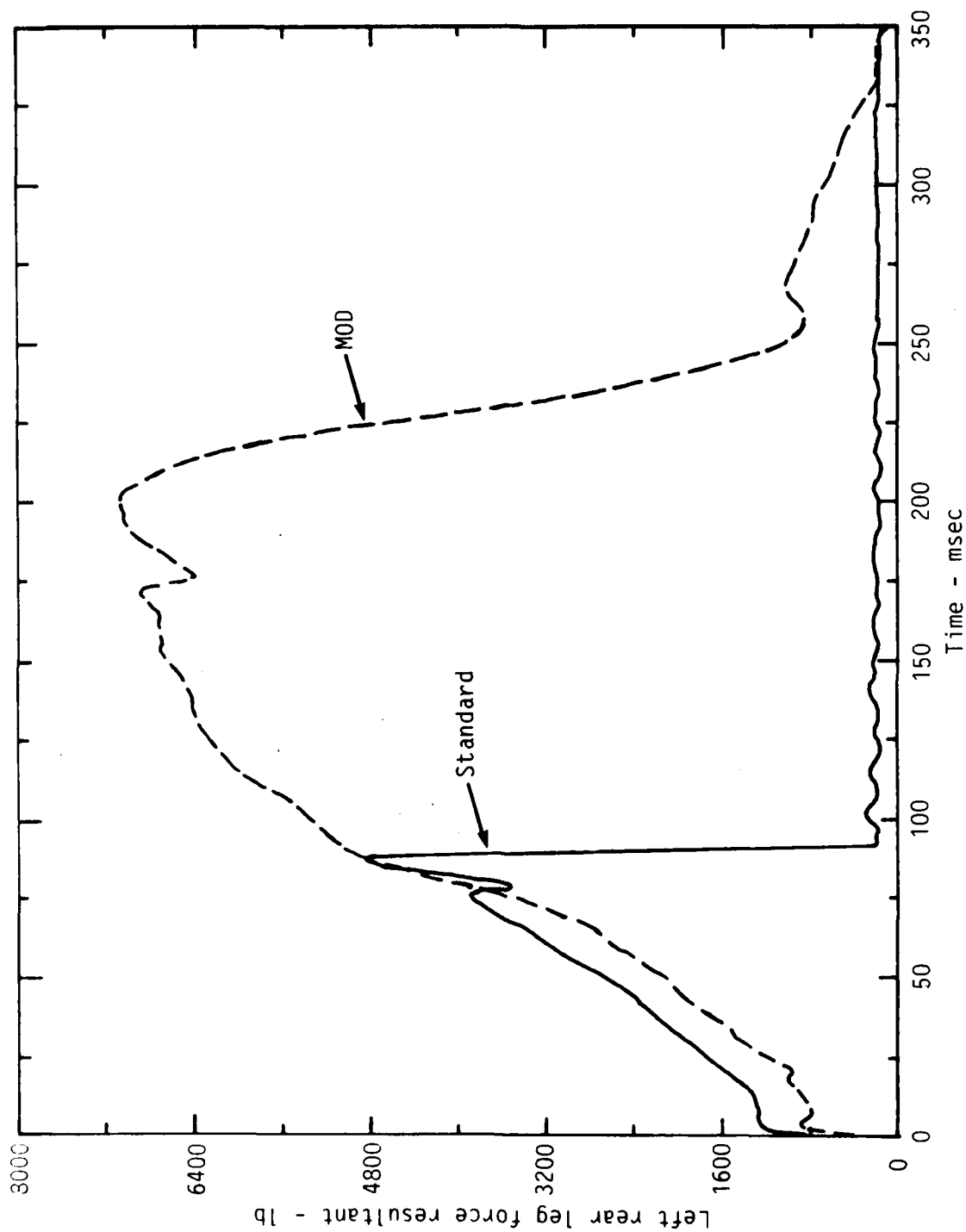


Figure 114. Rear window-side leg force resultants of standard and UOP MOD I seats.

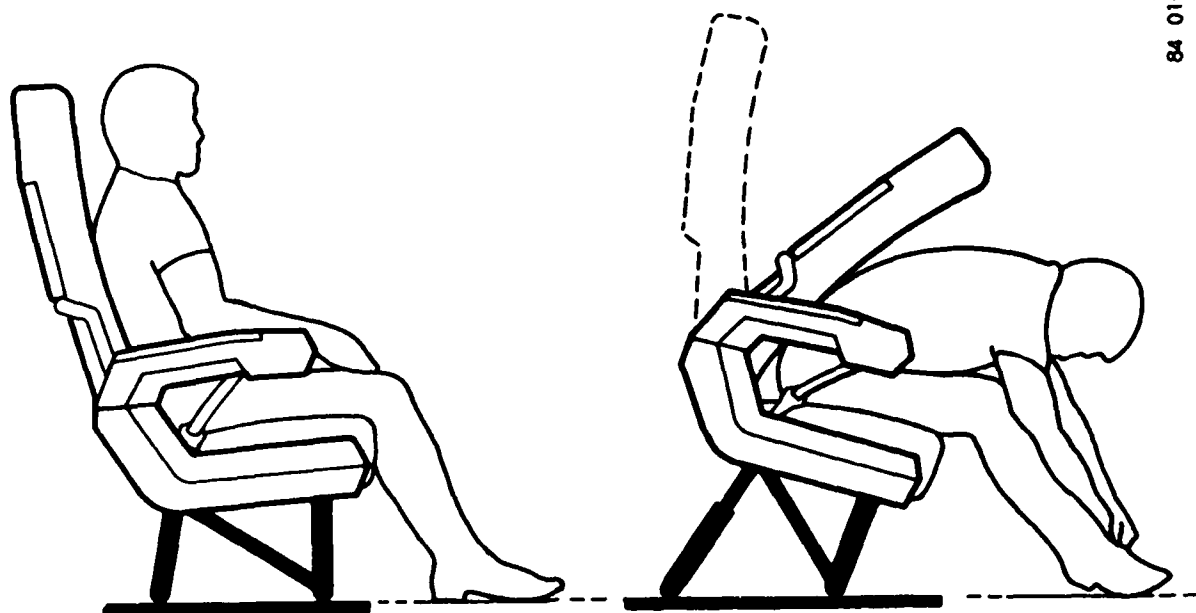


Figure 115. UOP MOD II seat before and after stroking.



Figure 116. UOP MOD II seat - front view.

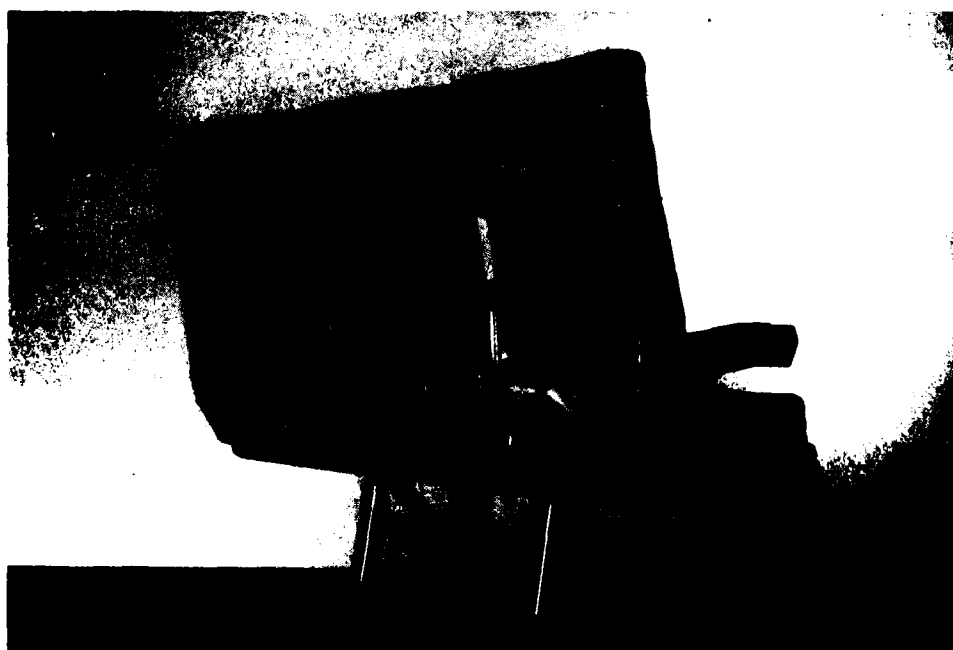


Figure 117. UOP MOD II seat - rear view.

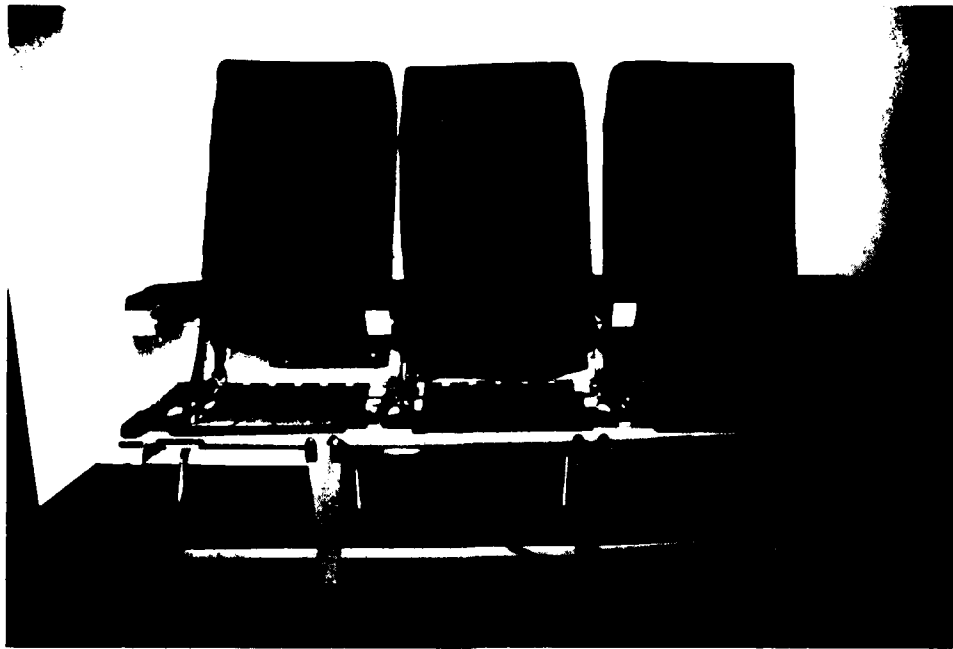
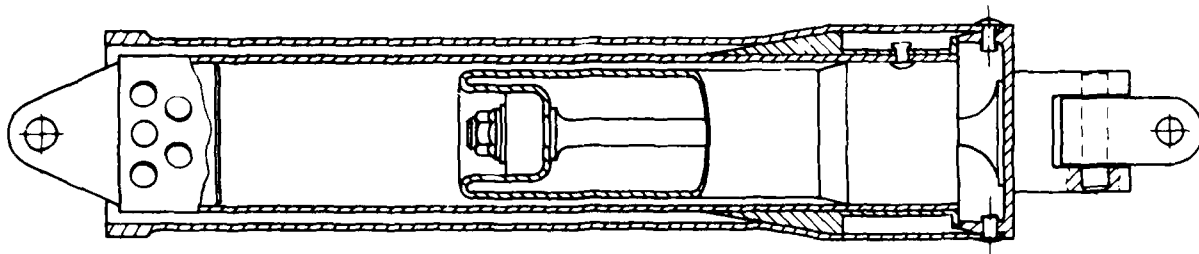


Figure 118. Seat pan and leg structure of UOP MOD II seat.

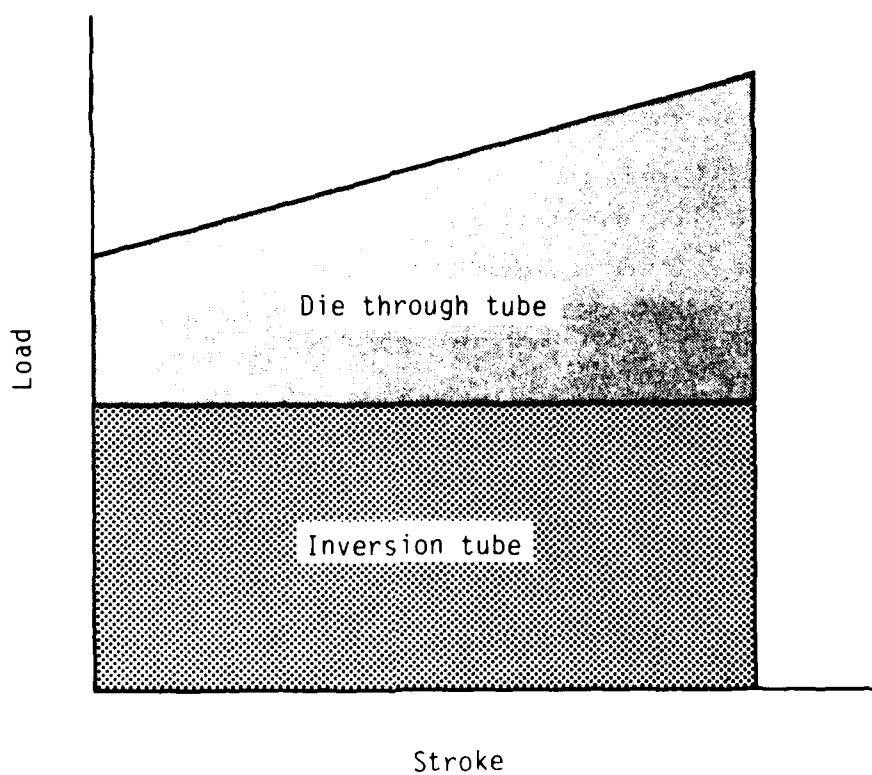


Figure 119. Leg structure and energy absorbers of UOP MOD II seat.



84 04010 02

Figure 120. UOP MOD II seat energy absorber.



84 02002 65

Figure 121. Characteristic load versus stroke curve for hybrid energy absorber.



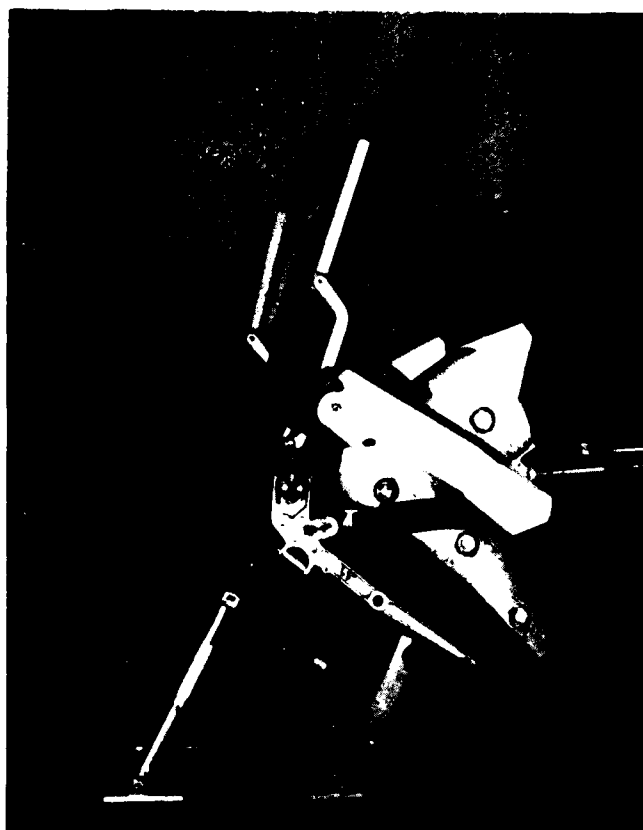
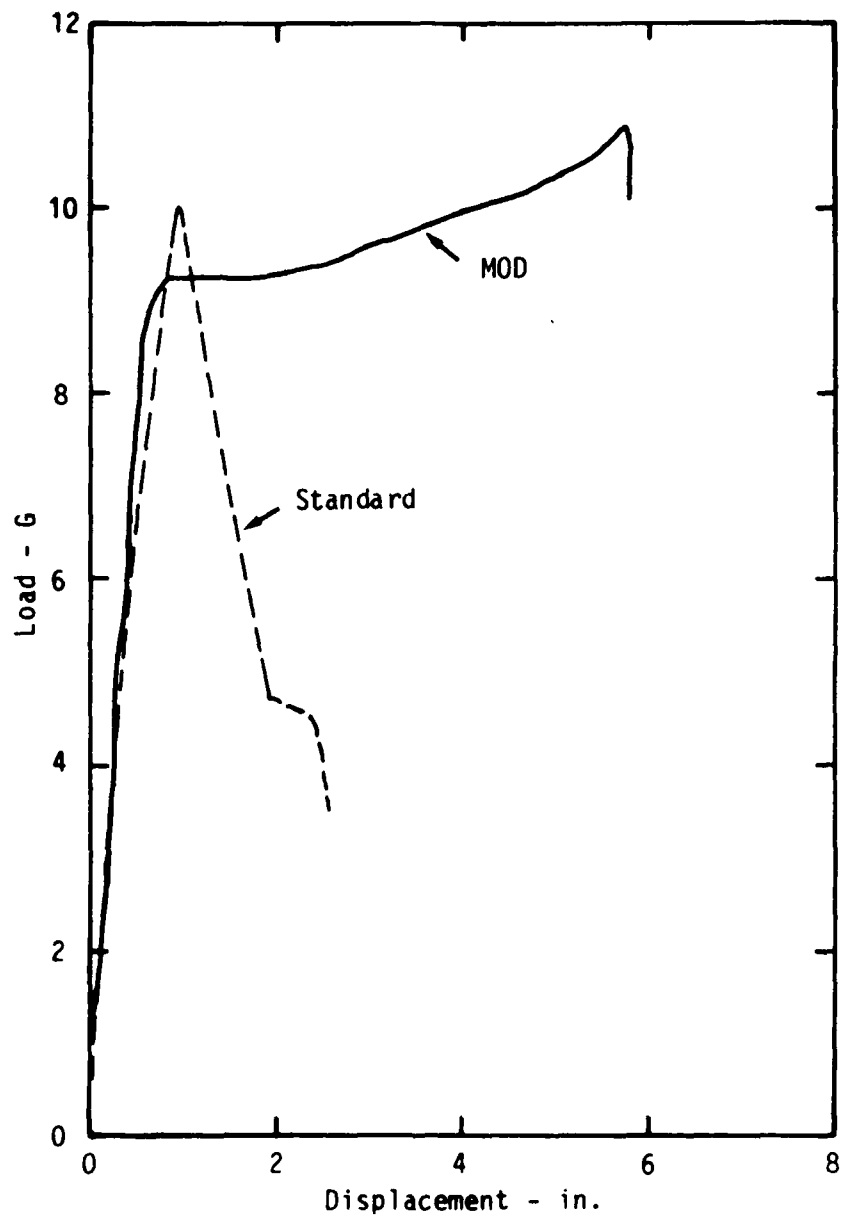


Figure 122. Posttest UOP MOD II seat (Forward Static Test).



Figure 123. Posttest stroked rear leg energy absorbers of UOP MOD II seat (Forward Static Test).



84 02002 35

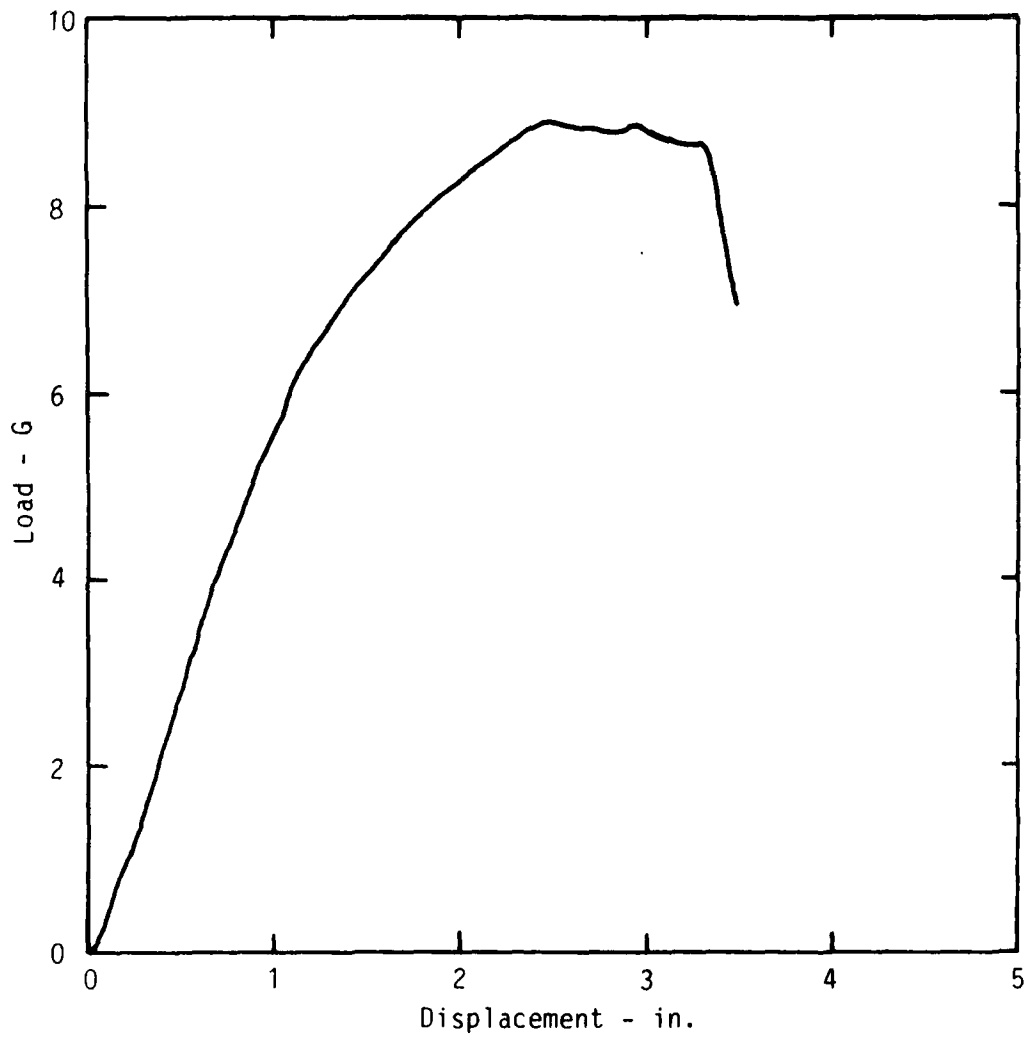
Figure 124. Load versus forward displacement of standard and UOP MOD II seats.



Figure 125. Posttest UOP MOD II seat (Lateral Test).



Figure 126. Posttest top view of front window-side leg and failed track fitting of UOP MOD II seat (Lateral Test).



84 02002 33

Figure 127. Load versus lateral displacement of UOP MOD II seat.

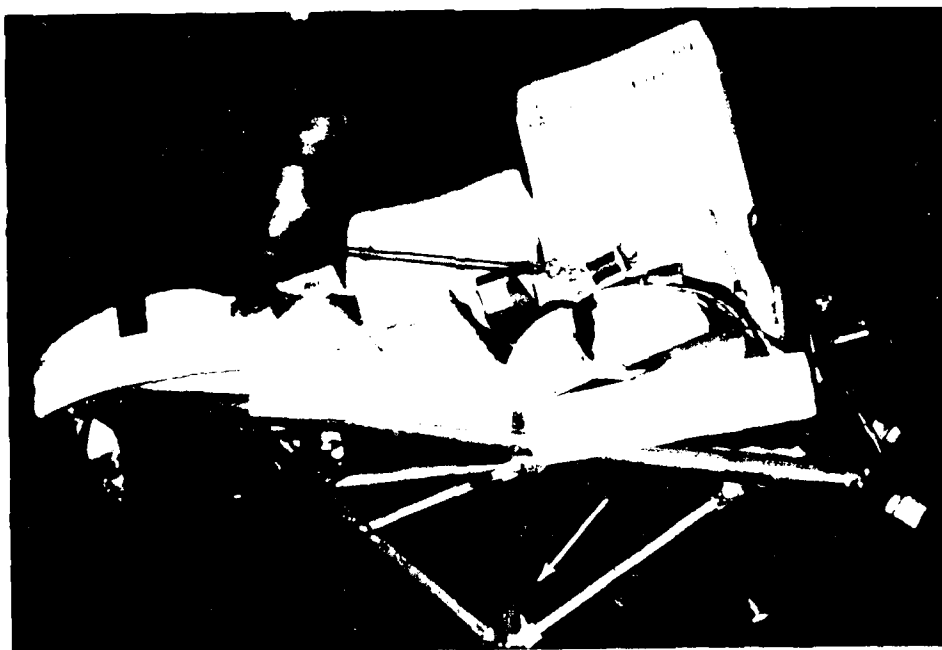


Figure 149. Posttest front view of Weberlite MOD seat (Lateral Test).



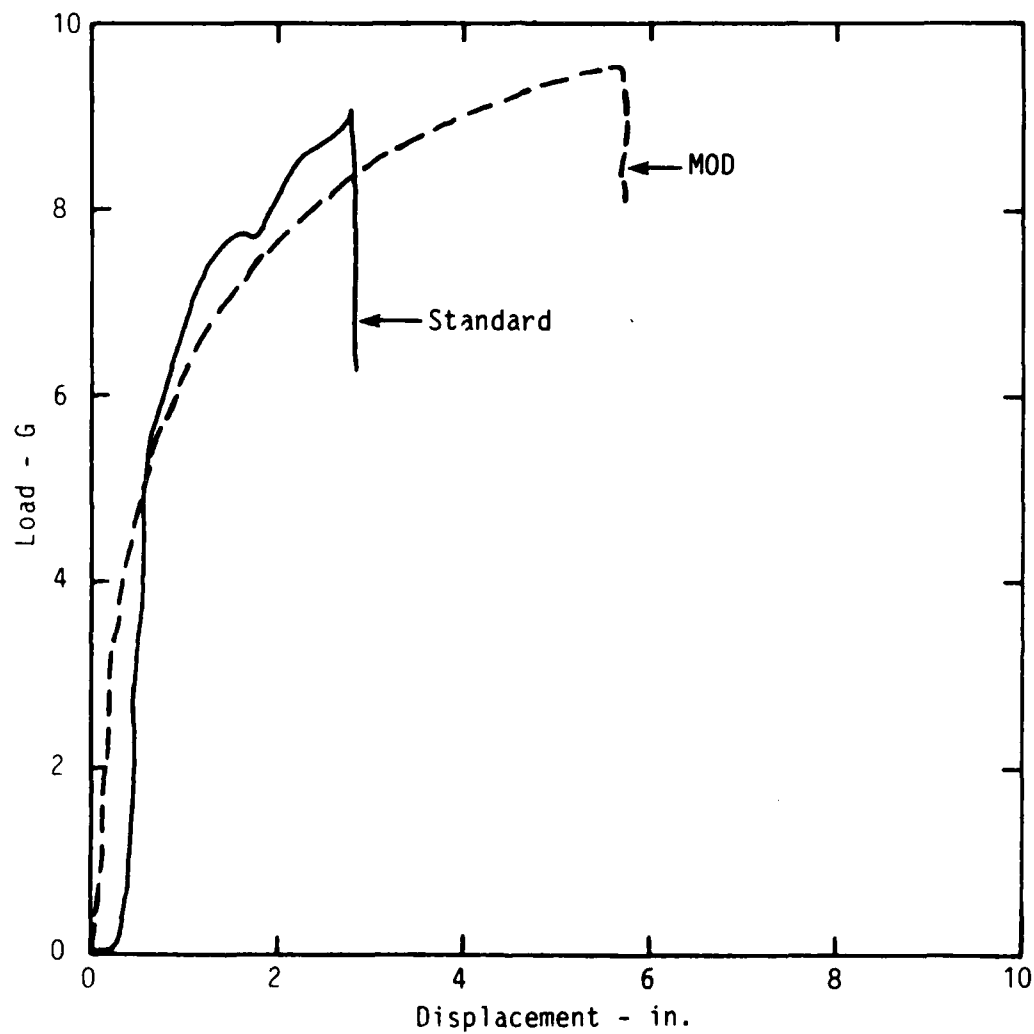
Figure 150. Posttest rear view of Weberlite MOD seat (Lateral Test).



Figure 147. Posttest Weberlite MOD seat (Forward Static Test).

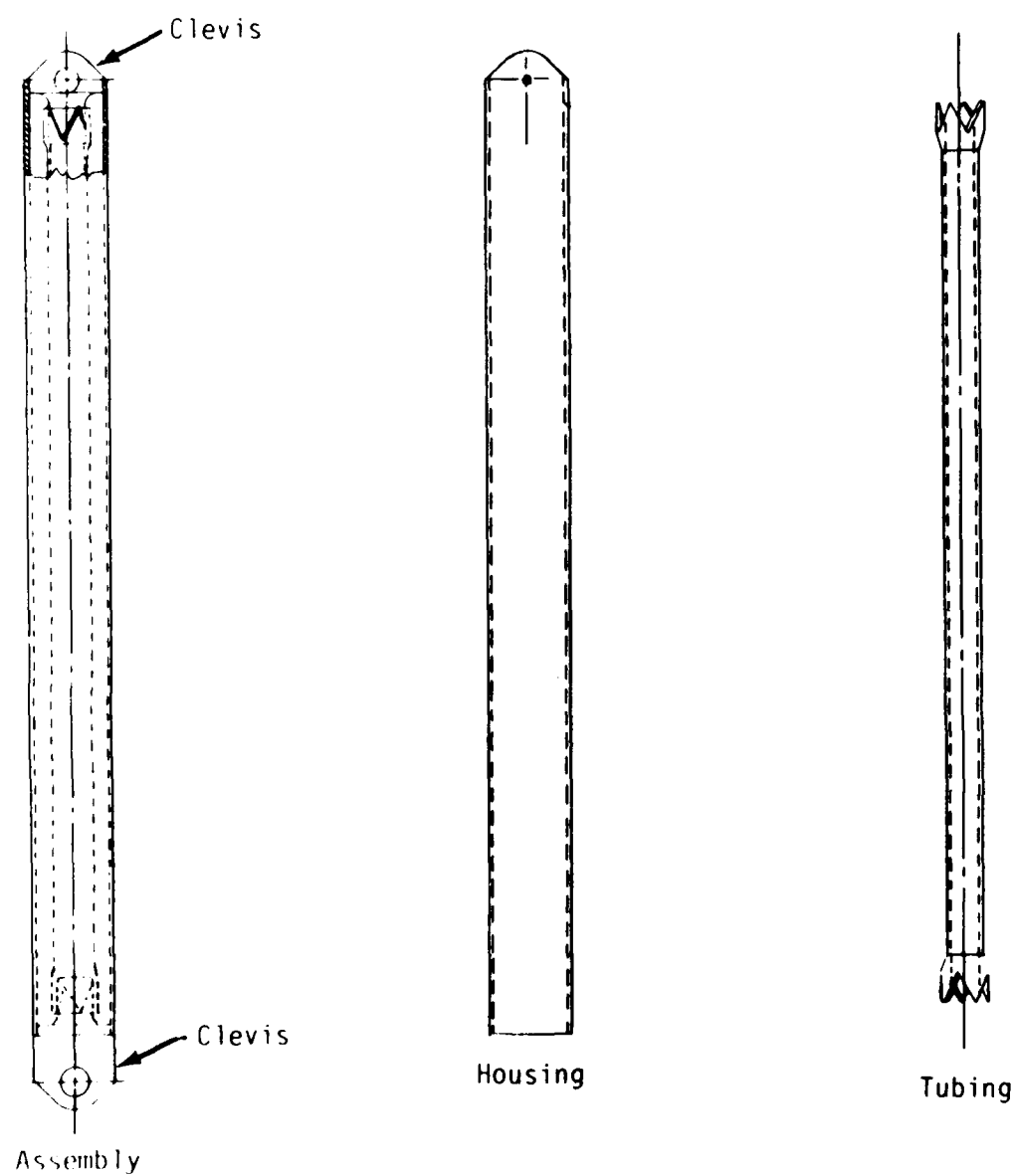


Figure 148. Posttest failed window-side leg energy absorber of Weberlite MOD seat (Forward Static Test).



84 02002 23

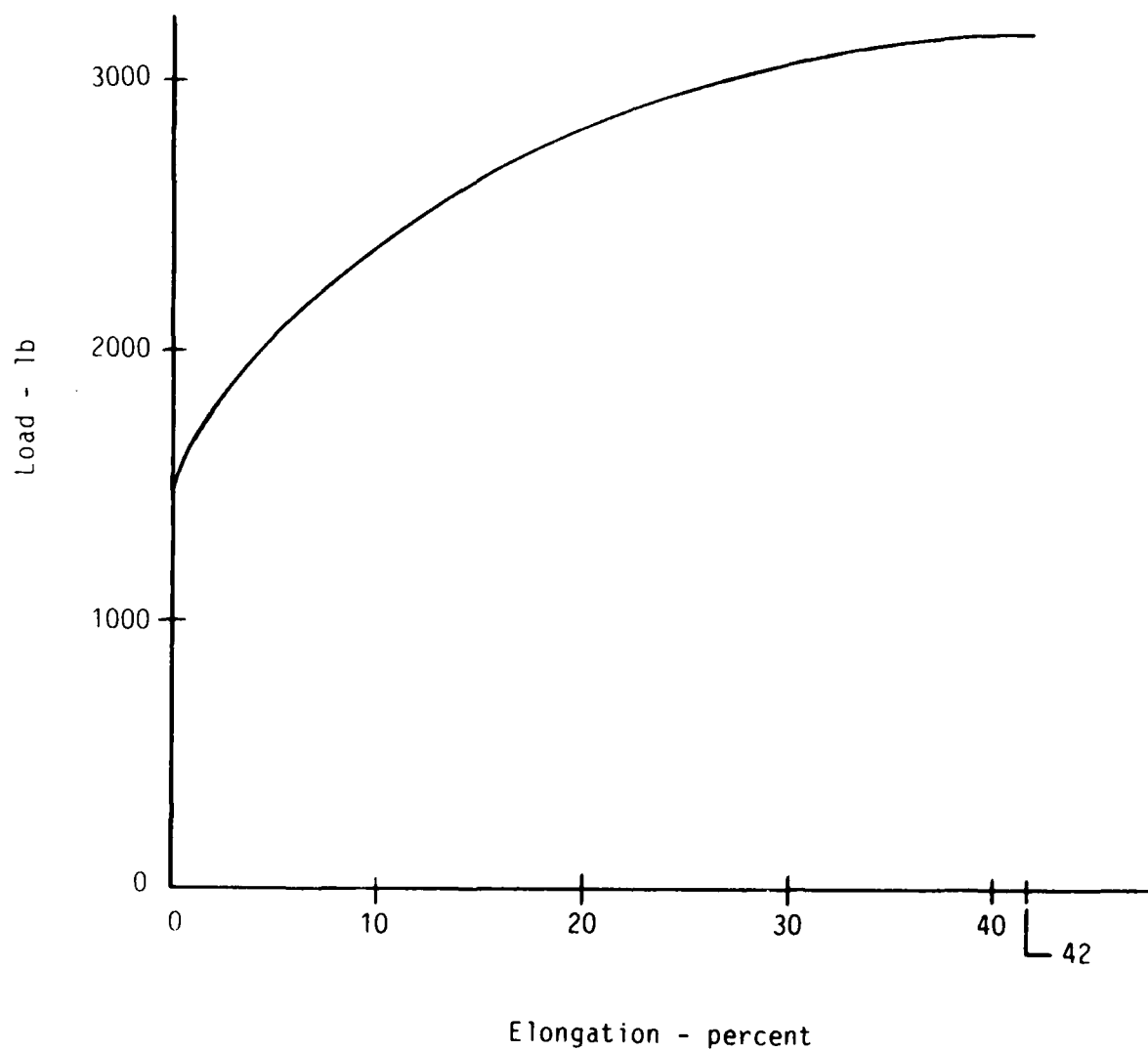
Figure 146. Load versus forward displacement of standard and Weberlite MOD seats.



84 02002 68

Figure 145. Weberlite MOD seat energy absorber.





84 02002 62

Figure 144. Typical loading curve for stainless steel tubing used in energy absorbers.

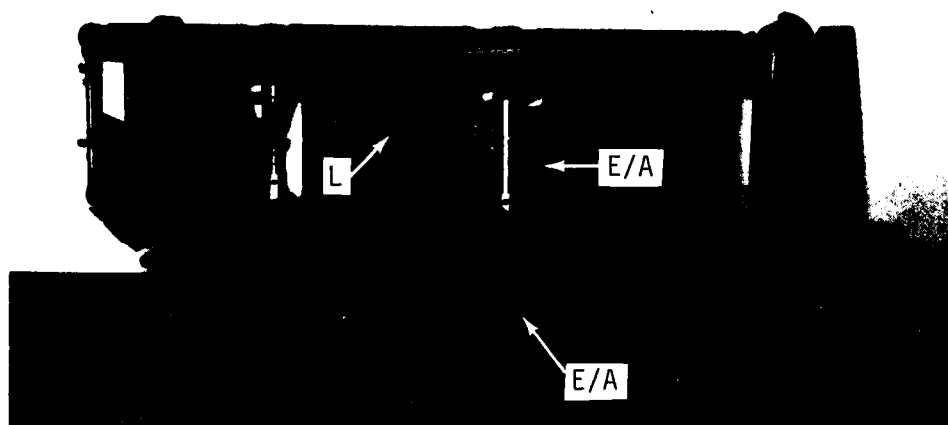


Figure 143. Weberlite MOD seat - bottom view.



Figure 141. Weberlite MOD seat - front view.

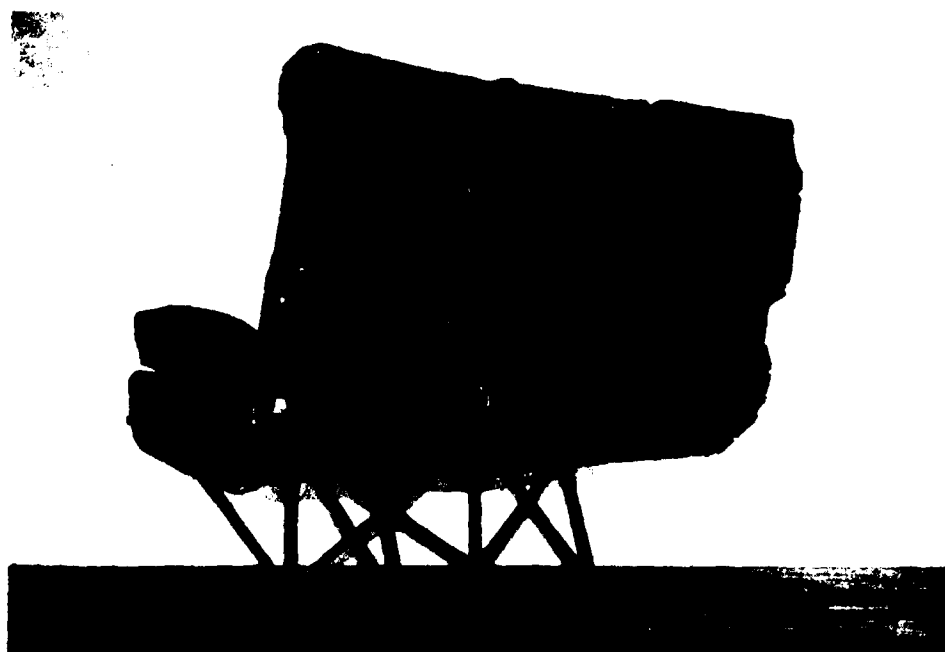
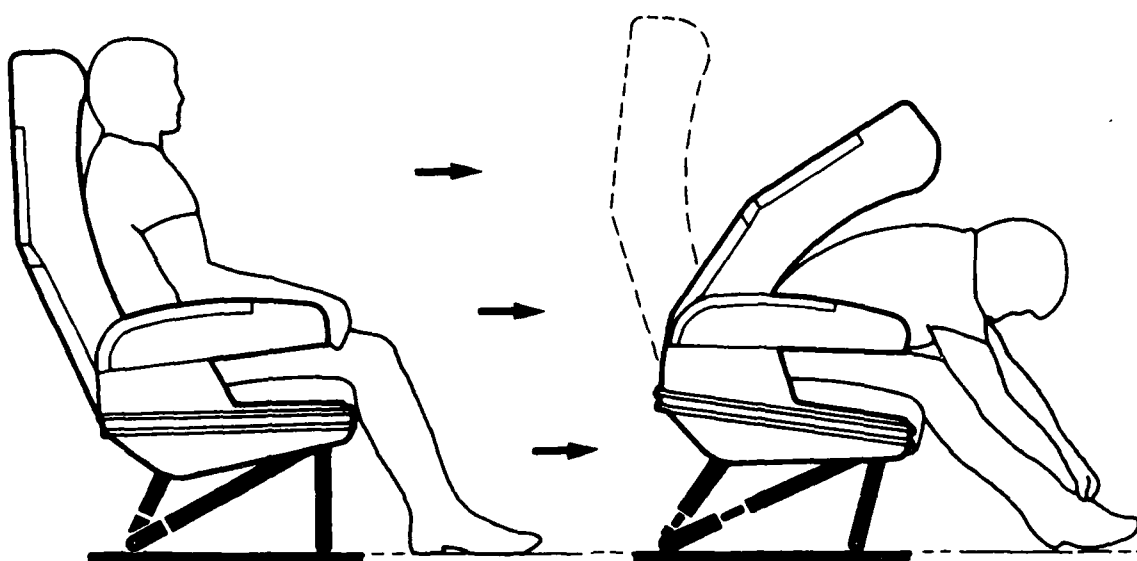
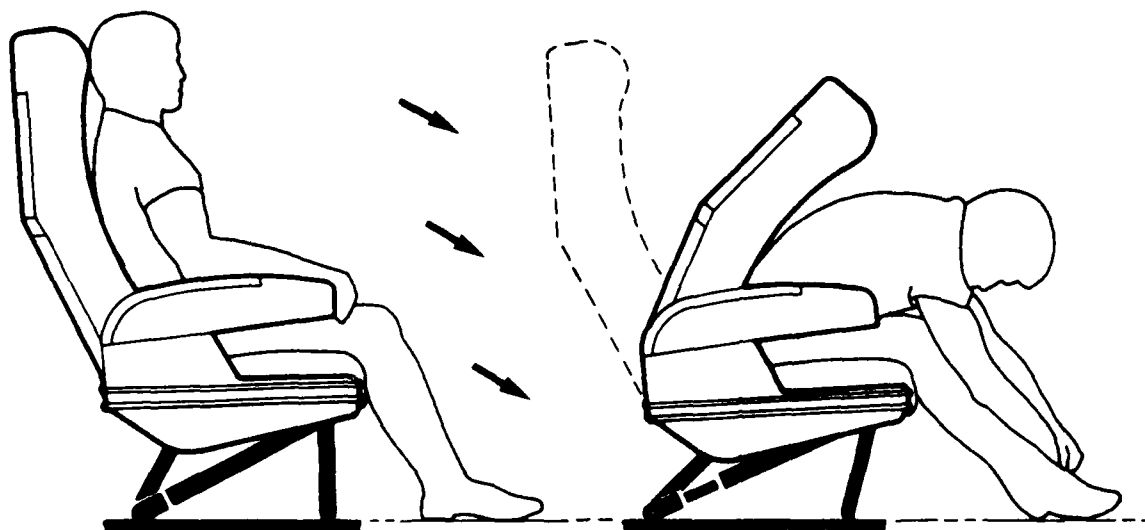


Figure 142. Weberlite MOD seat - rear view.



Condition 1: forward inertial load



Condition 2: inertial load pitched downward 30°

Figure 140. Energy-absorbing motion of the Weberlite MOD seat under two loading conditions.



Figure 138. Failure points of standard Weberlite seat (Dynamic Test).

--- Predicted motion  
 — Actual test motion

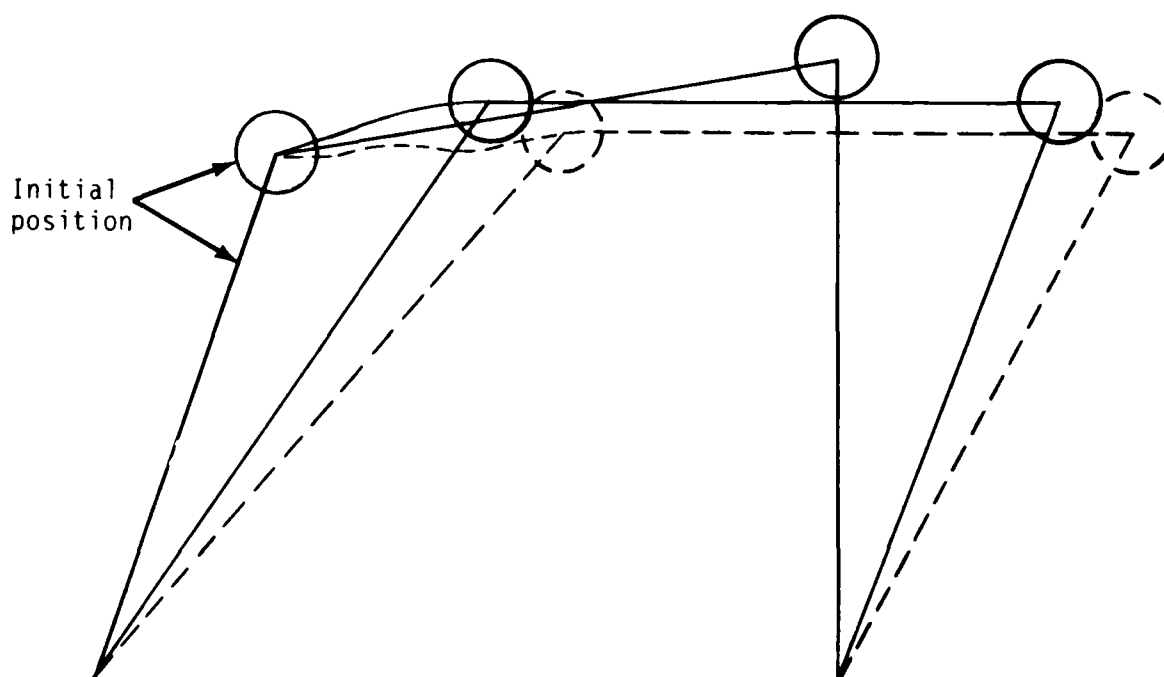


Figure 139. Leg structure kinematics of Weberlite MOD seat.

84 02002 61



Figure 136. Posttest standard Weberlite seat (Dynamic Test).

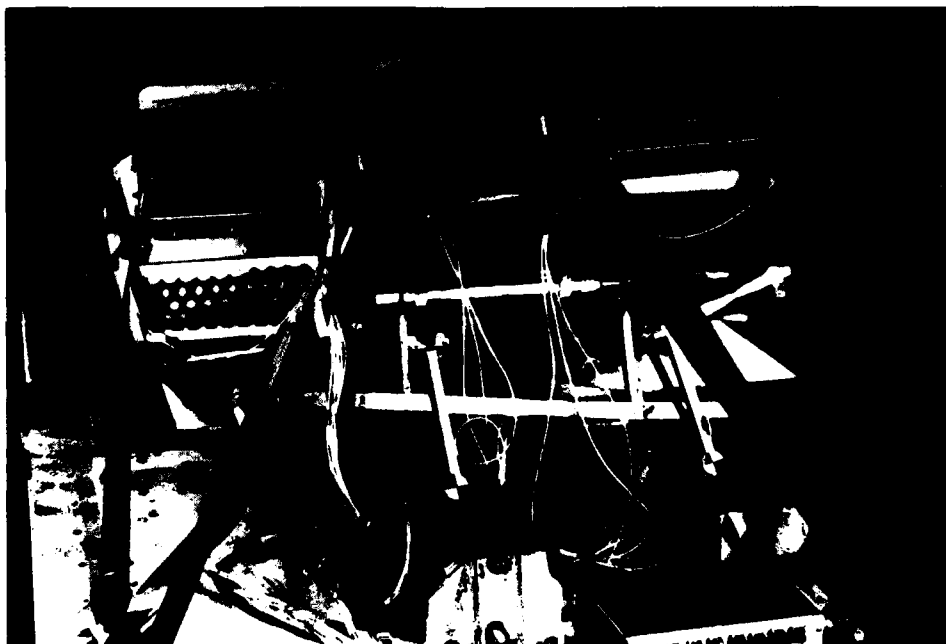


Figure 137. Posttest rear view of standard Weberlite seat (Dynamic Test).



Figure 134. Posttest standard Weberlite seat (Forward Static Test).



Figure 135. Failure points of standard Weberlite seat (Forward Static Test).



Figure 132. Standard Weberlite seat rear track fitting.



Figure 133. Standard Weberlite seat front track fitting.





Figure 130. Standard Weberlite seat structure.

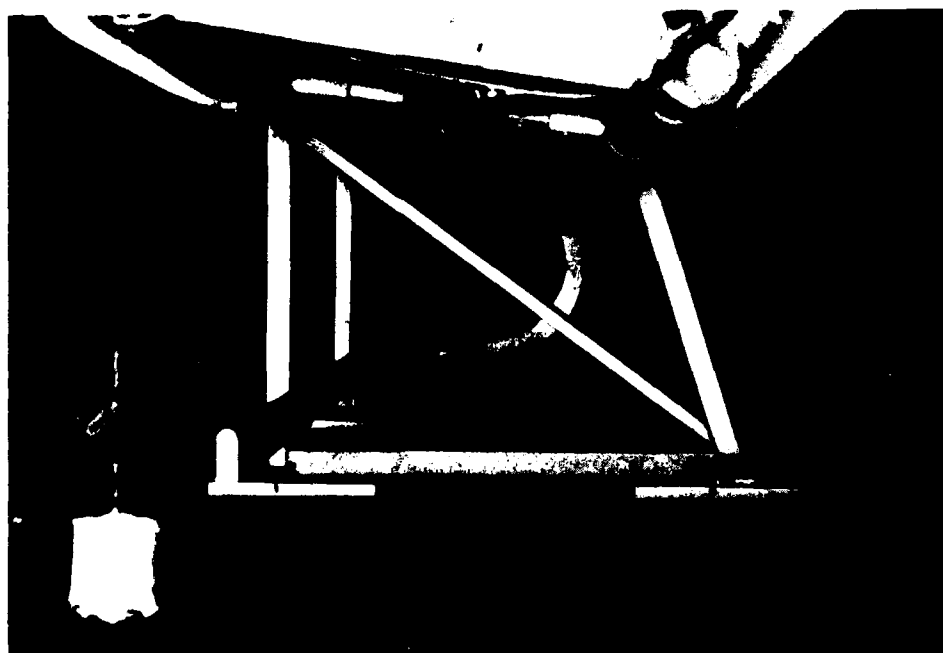


Figure 131. Standard Weberlite seat leg structure.

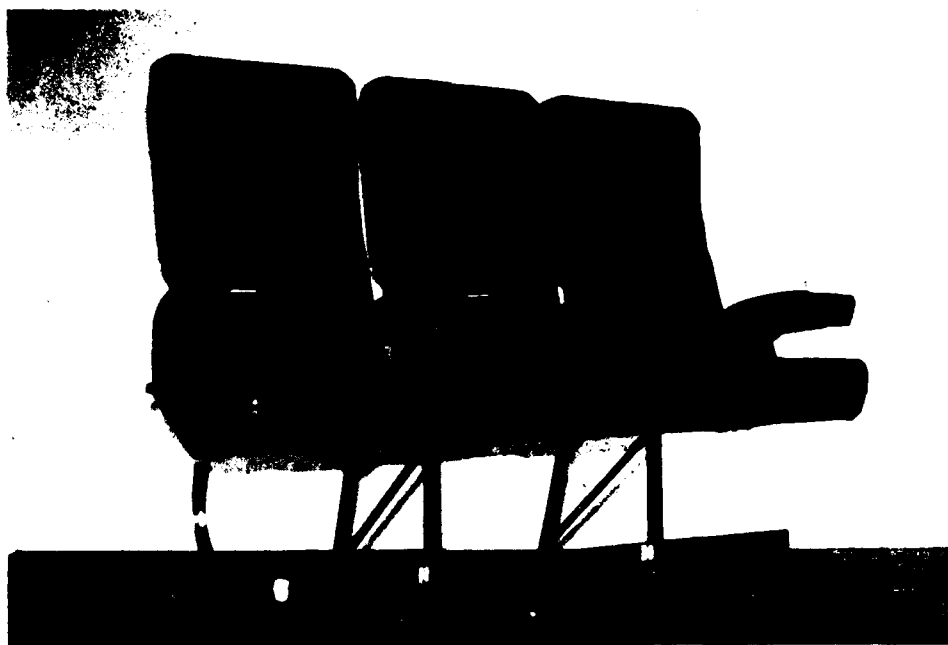


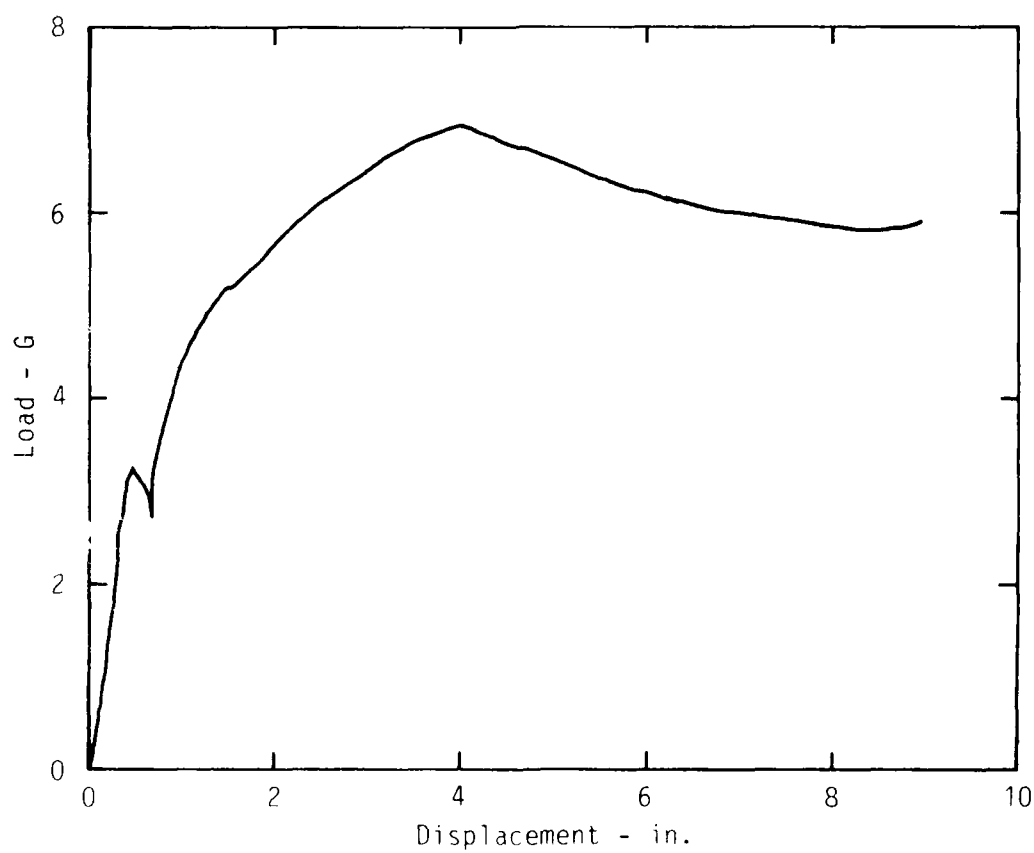
Figure 128. Standard Weberlite seat - front view.



Figure 129. Standard Weberlite seat - rear view.



Figure 151. Stroked aisle-side diagonal of Weberlite MOD seat (Lateral Test).



84 02002 24

Figure 152. Load versus lateral displacement of Weberlite MOD seat.



Figure 153. Posttest failed rear leg and diagonal energy absorber of Weberlite MOD seat (Dynamic Test).

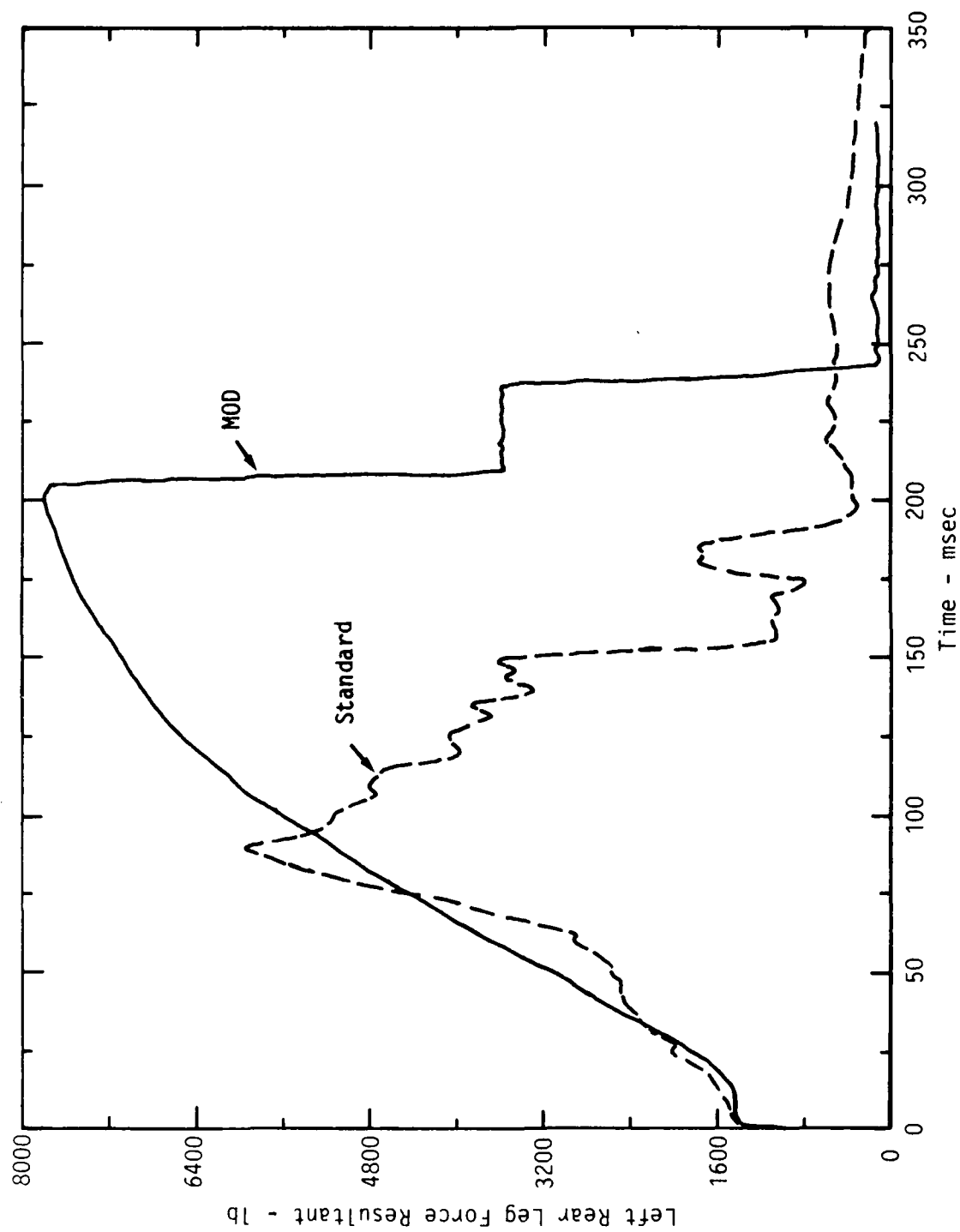


Figure 154. Rear window-side leg force resultants of standard and Weberlite MOD seats.

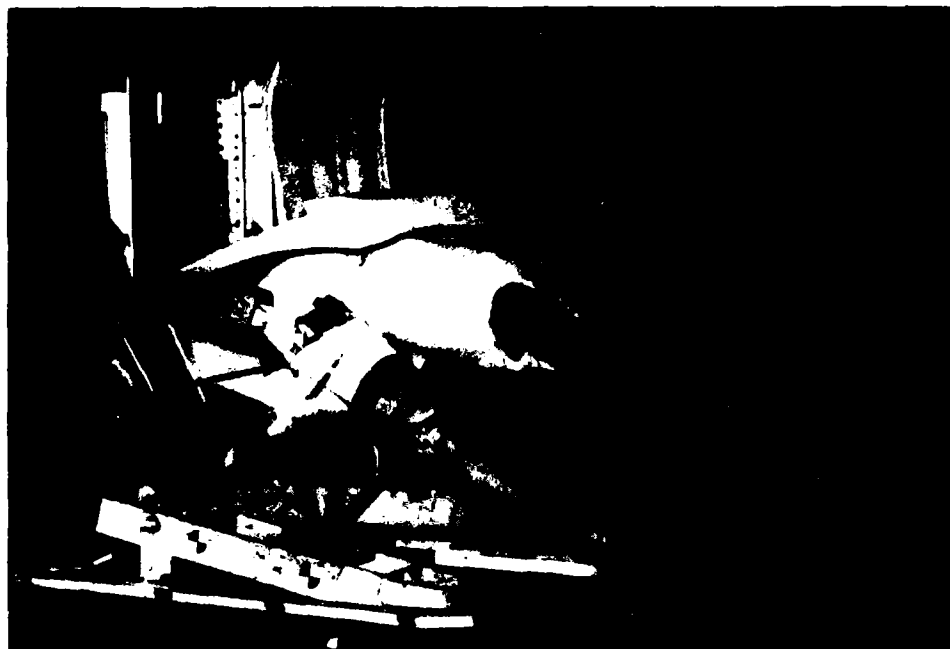
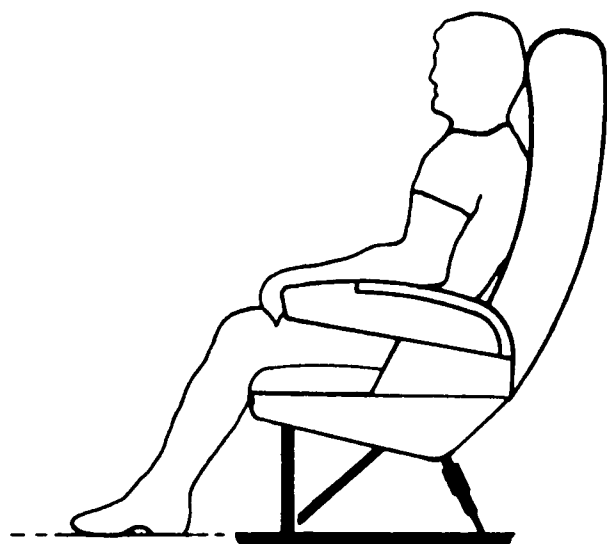


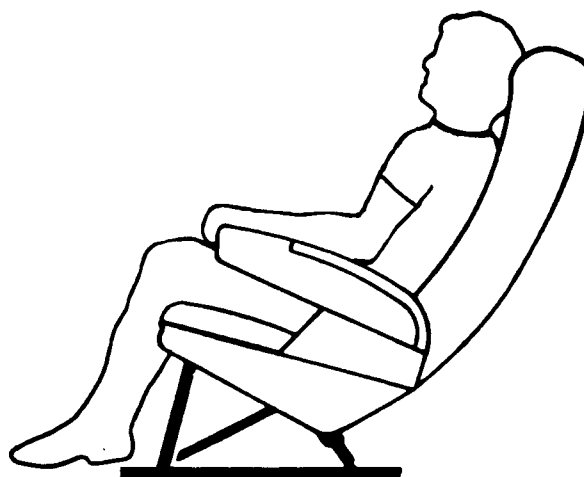
Figure 155. Posttest Weberlite MOD seat showing lap belt anchorage failure (Dynamic Test).



Figure 156. Lap belt anchorage failure point and anchor (inset) of Weberlite MOD seat (Dynamic Test).



Before



After

84 01004 37

Figure 157. Weber aft-facing concept before and after stroking.

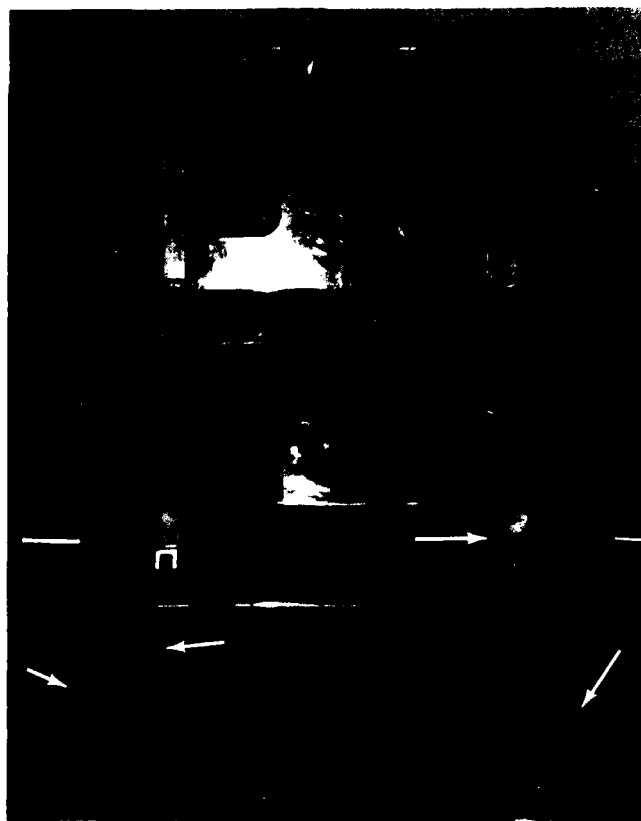


Figure 158. Weber aft-facing MOD seat back and bracing members.

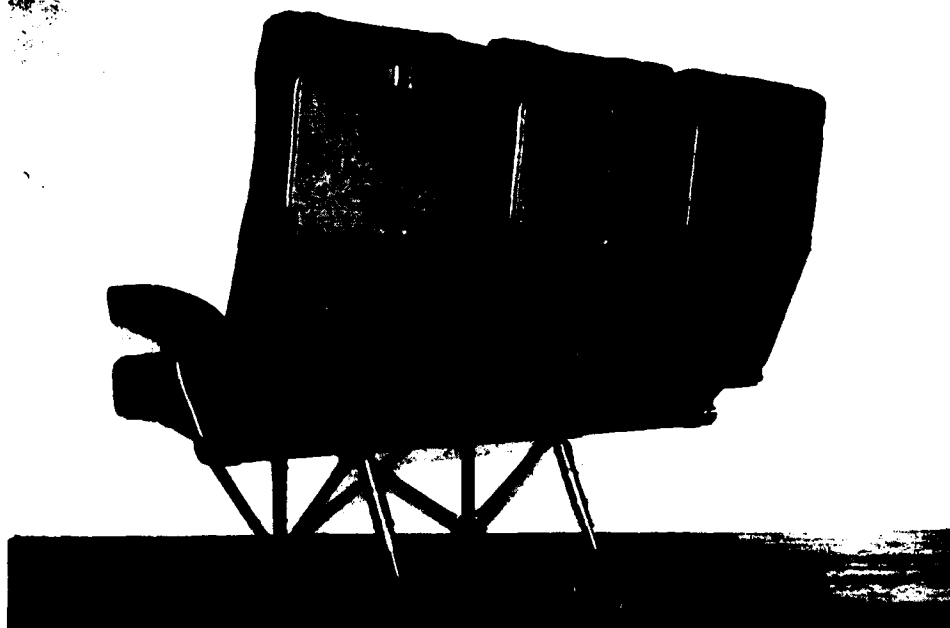


Figure 159. Weber aft-facing MOD seat - front view.

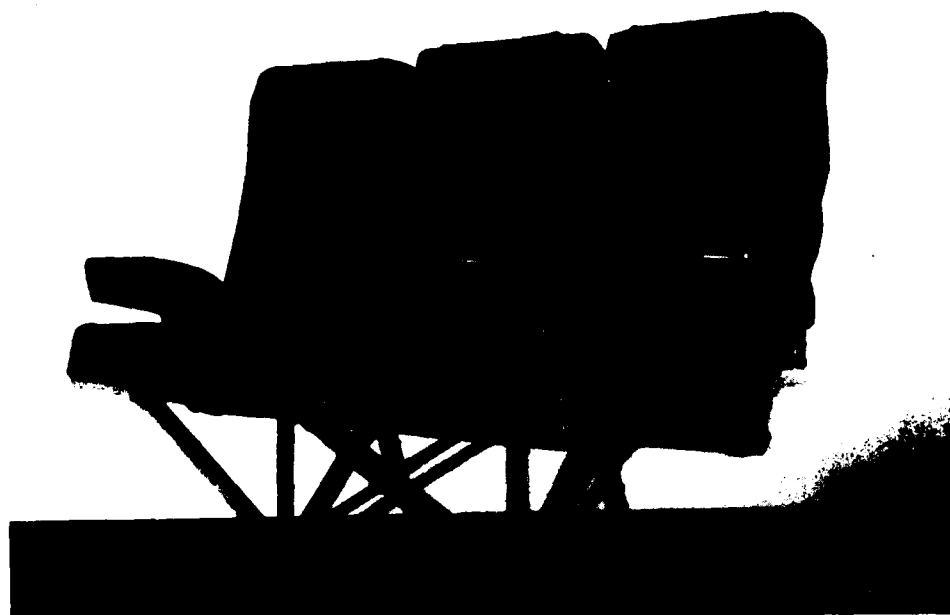


Figure 160. Weber aft-facing MOD seat - rear view.





Figure 161. Weber aft-facing MOD seat structure.



Figure 162. Weber aft-facing MOD seat - bottom view.

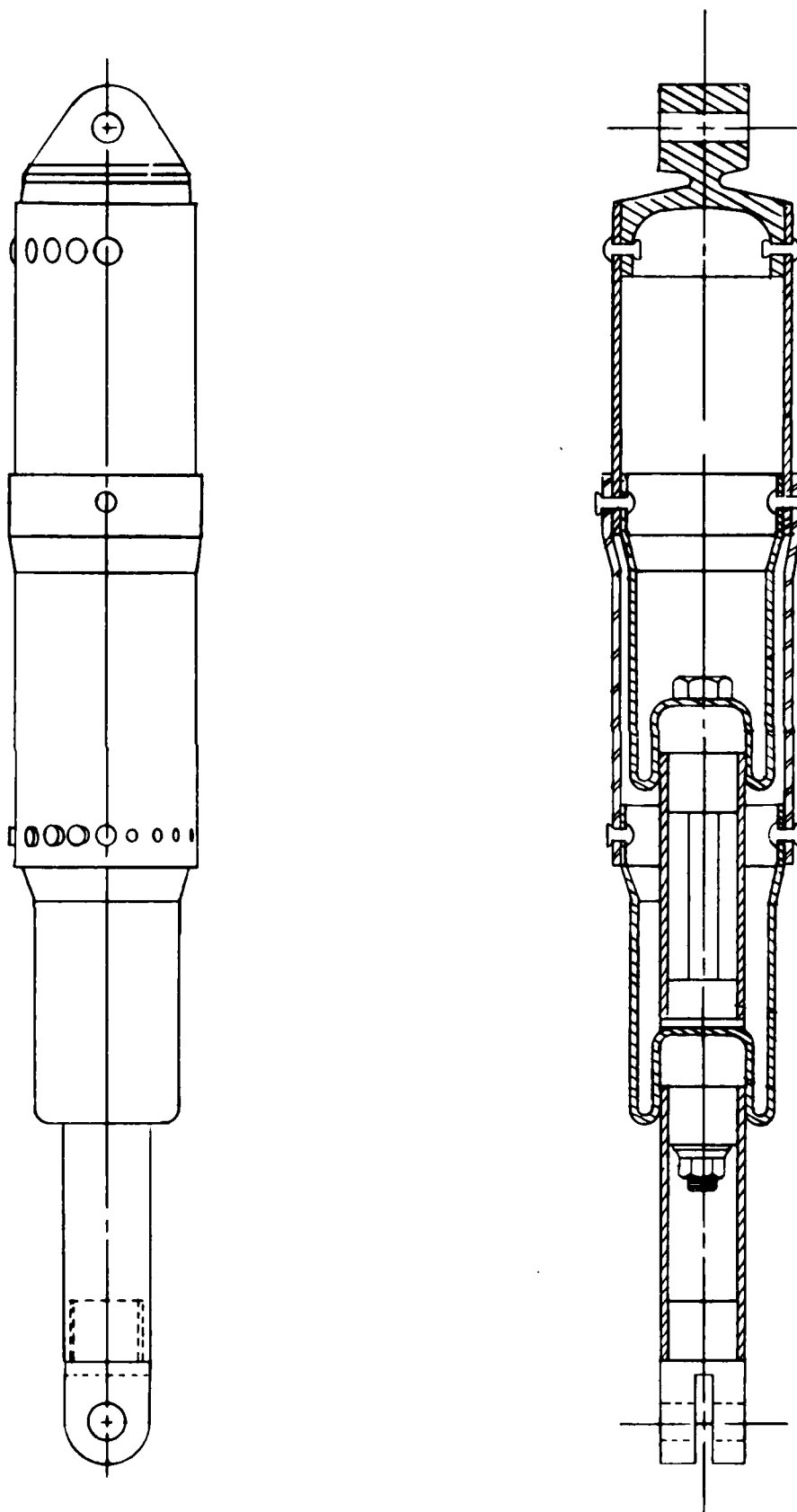


Figure 163. Weber aft-facing MOD seat energy absorber.



Figure 164. Arrangement of Weber aft-facing MOD seat (Forward Static Test).

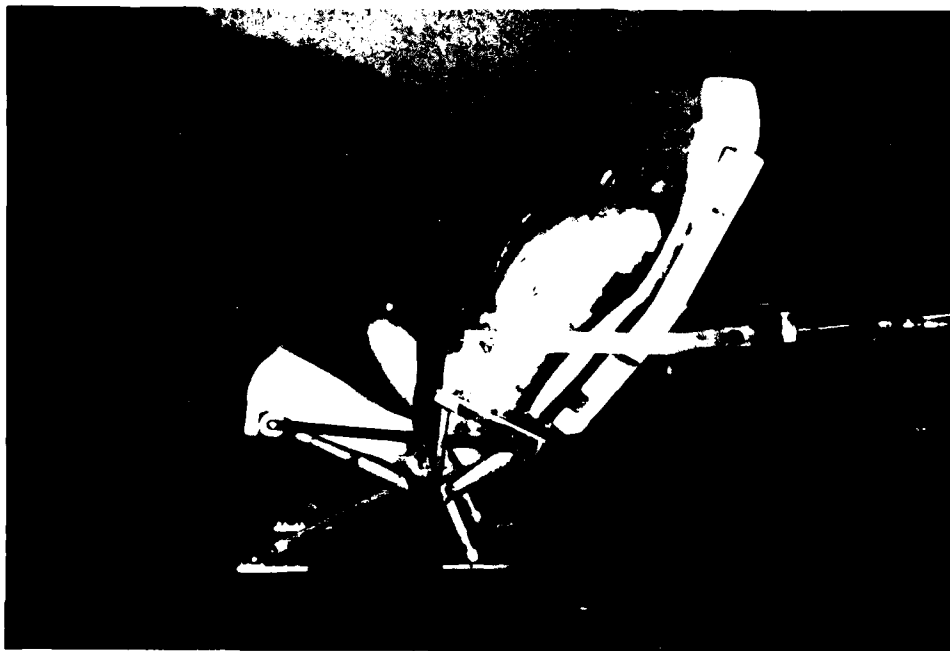
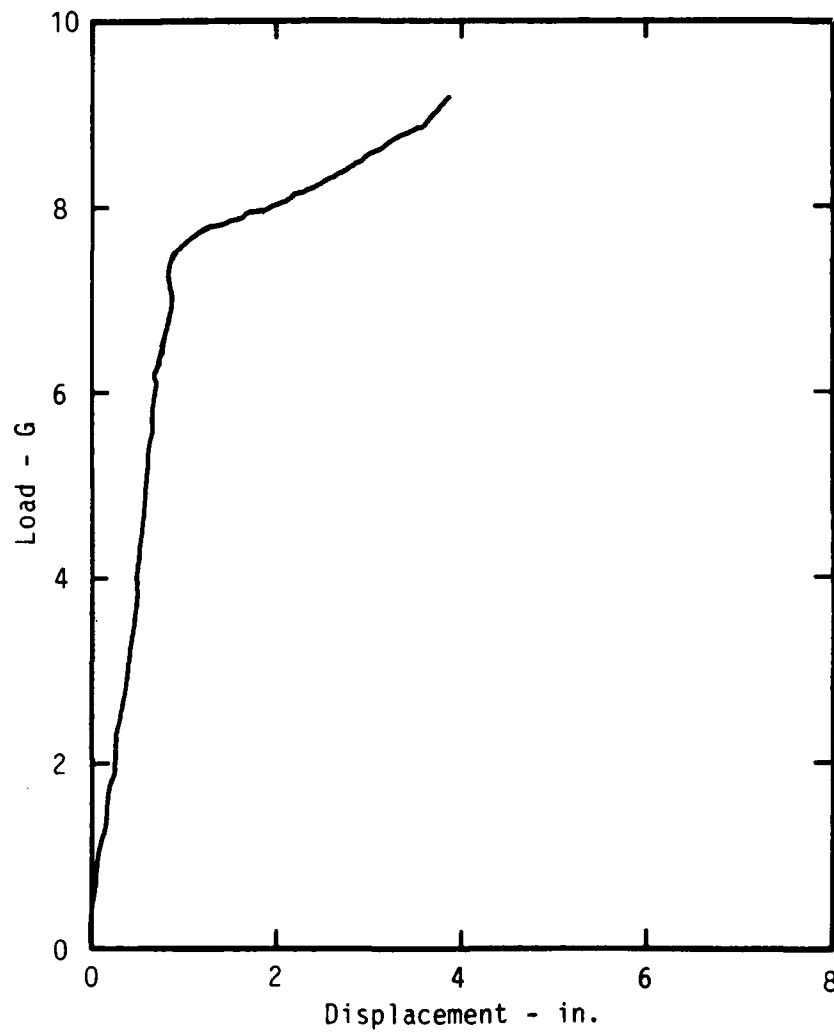


Figure 165. Posttest Weber aft-facing MOD seat (Forward Static Test).



84 02002 13

Figure 166. Load versus forward displacement of Weber aft-facing MOD seat.

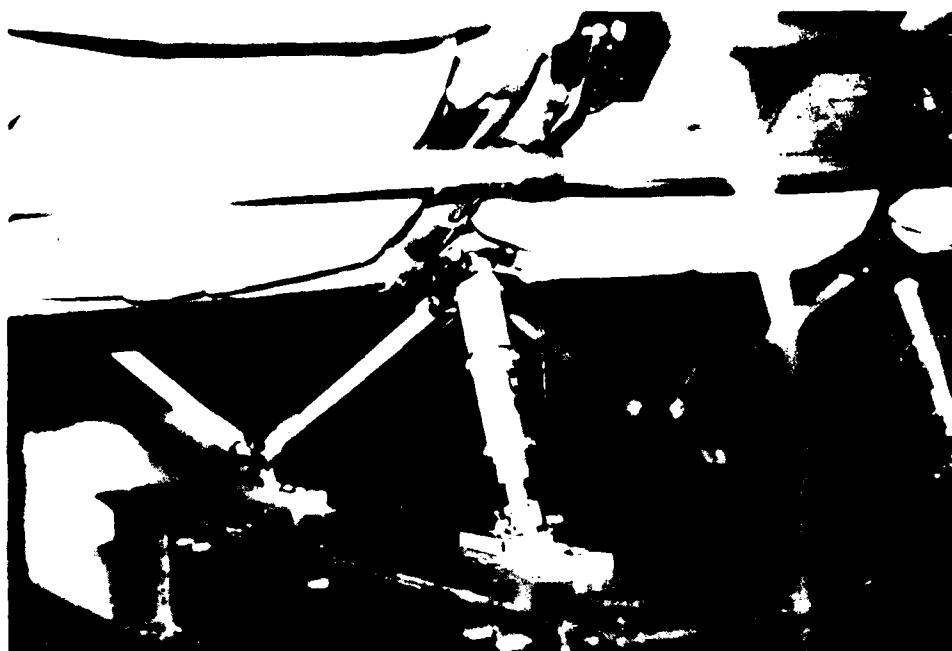


Figure 167. Posttest damage to front tube of Weber aft-facing MOD seat (Forward Static Test).

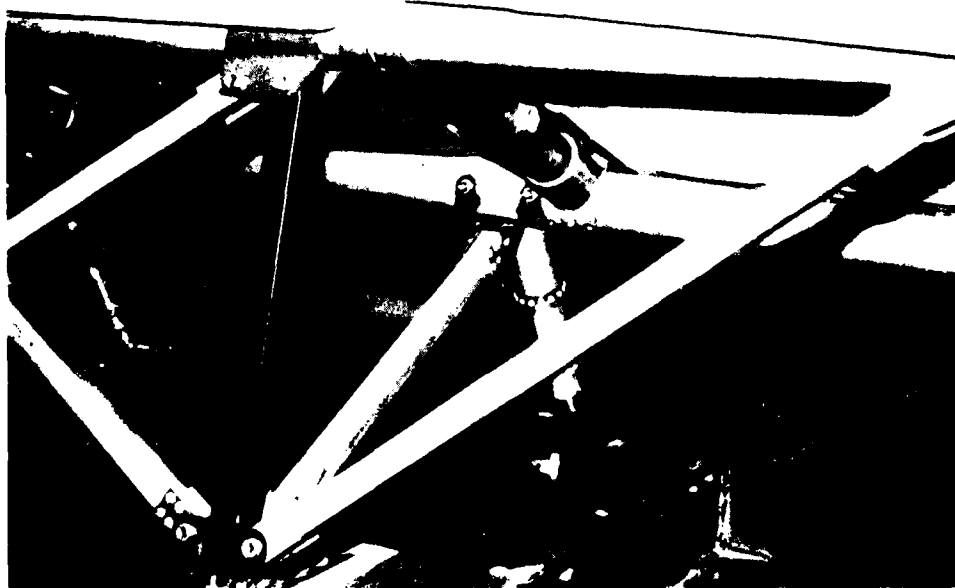


Figure 168. Posttest damage to front tube bracket of Weber aft-facing MOD seat (Forward Static Test).

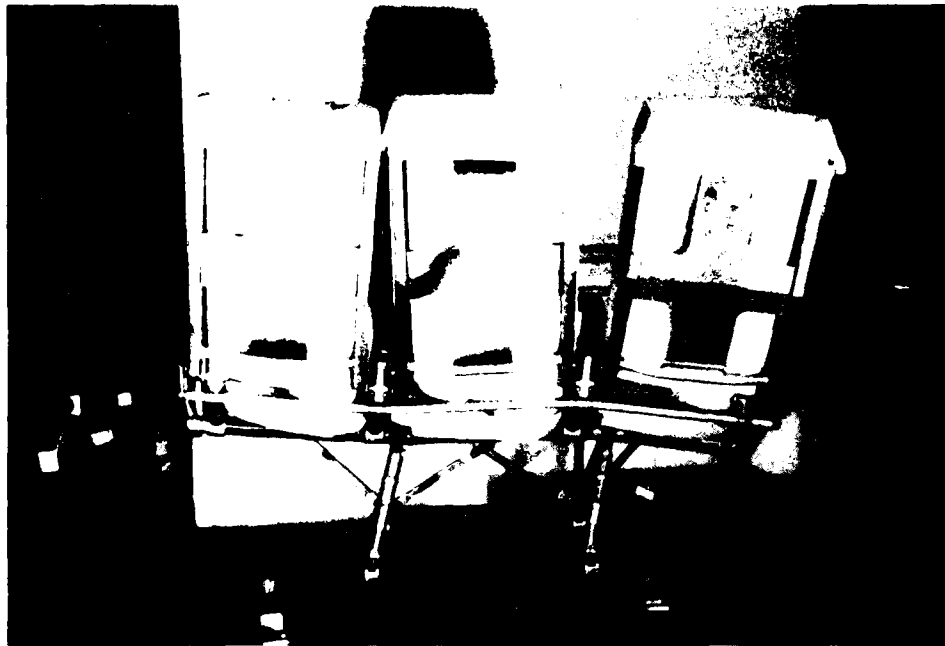


Figure 169. Posttest Weber aft-facing MOD seat (Lateral Test).

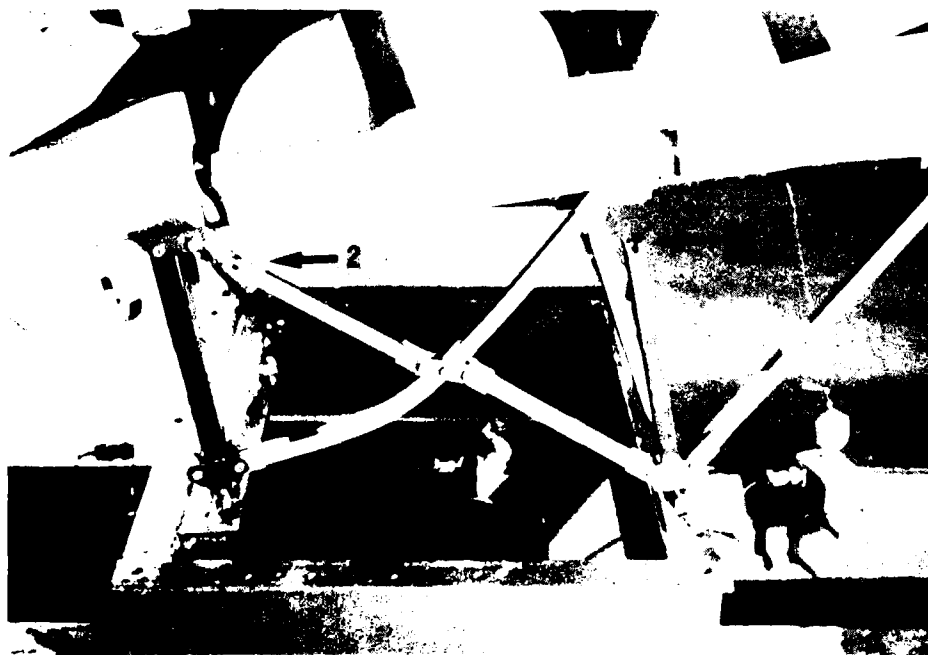
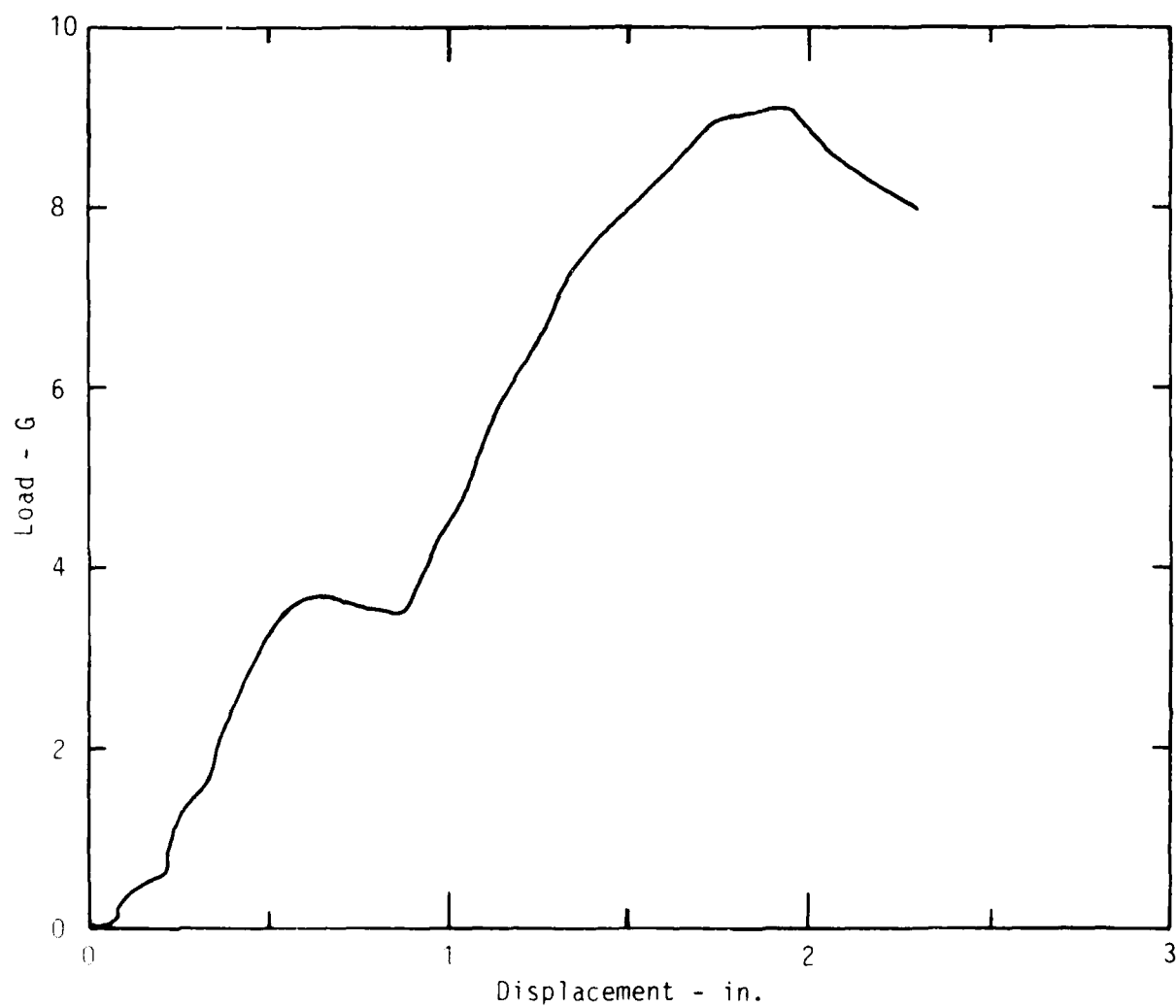
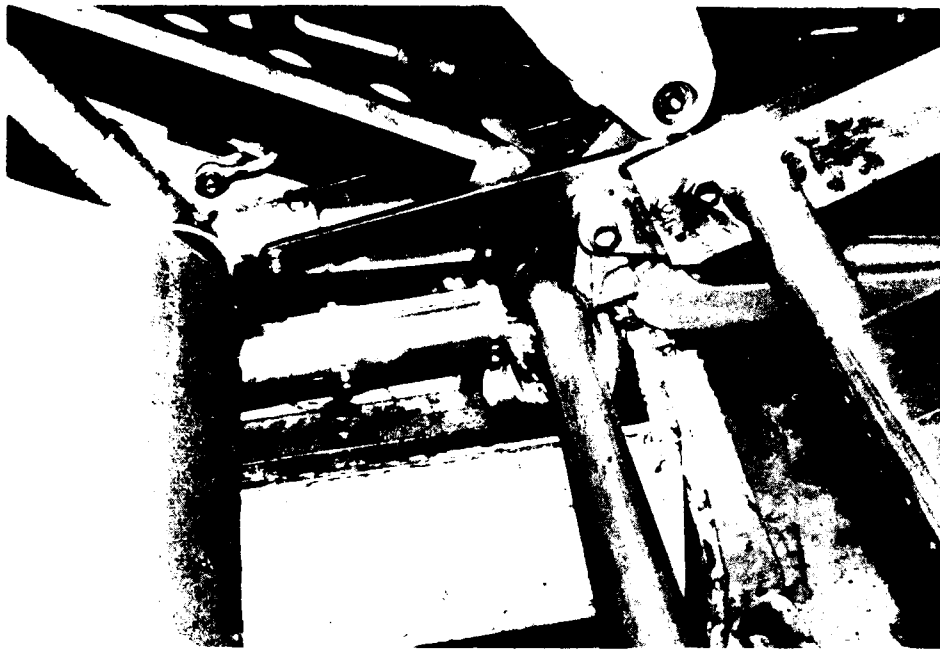


Figure 170. Failure points of Weber aft-facing MOD seat (Lateral Test).

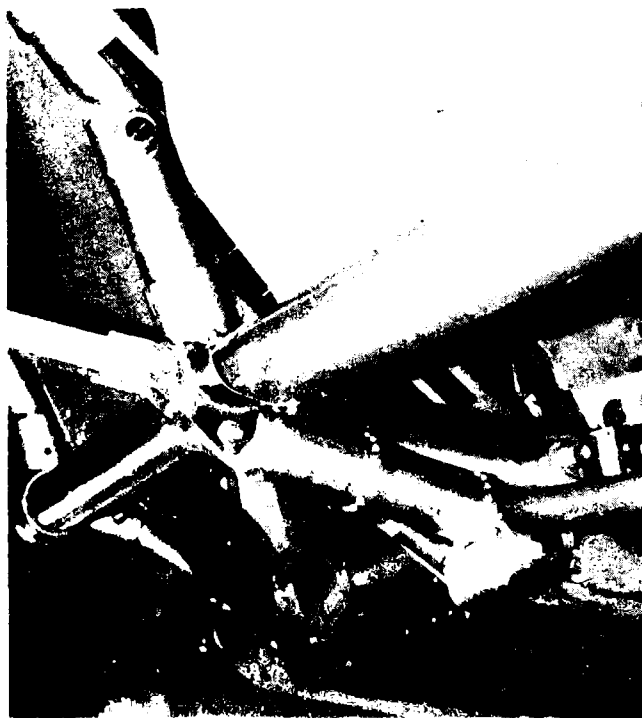


84 02002 16

Figure 171. Load versus lateral displacement of Weber aft-facing MOD seat.



Side



Bottom

Figure 172. Side and bottom view of lower side energy absorber  
to vehicle structure and M-100000 dynamic test rig.



AD-A155 024

SEAT EXPERIMENTS FOR THE FULL-SCALE TRANSPORT AIRCRAFT  
CONTROLLED IMPACT. (U) RMS TECHNOLOGIES INC TREVOSE PA  
M R CANNON ET AL. MAR 85 DOT/FAA/CT-84/10

3/3

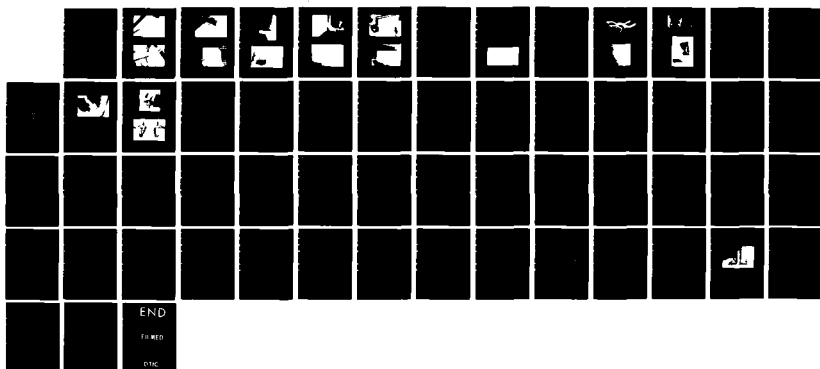
CONTROLLED IMPACT. (U) RWS TECHNOLOGIES I  
M R CANNON ET AL. MAR 85 DOT/FAR/CT-84/10

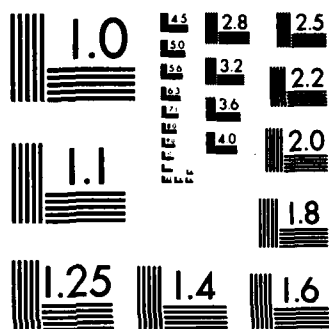
UNCLASSIFIED

DTFA03-81-C-00040

F/G 1/3

NL





MICROCOPY RESOLUTION TEST CHART  
NATIONAL BUREAU OF STANDARDS-1963-A



Figure 173. Posttest aisle-side energy absorber of Weber aft-facing MOD seat (Dynamic Test).

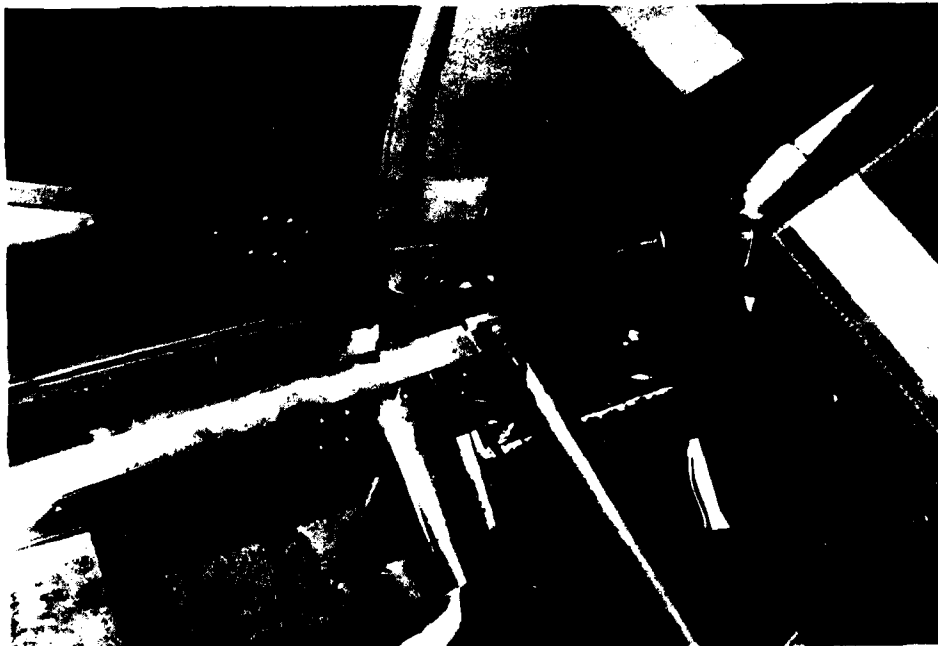


Figure 174. Posttest sheared bolt on window seat back of Weber aft-facing MOD seat (Dynamic test).



Figure 175. Attachment point of aisle-side strap to rear tube of Weber aft-facing MOD seat.

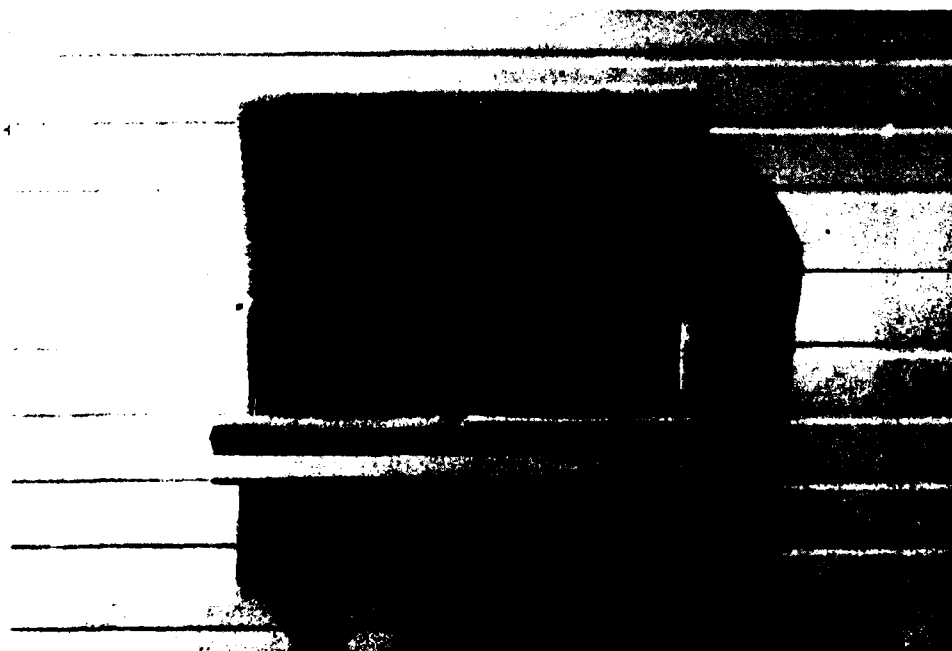


Figure 176. Trans-Aero flight attendant seat - front view.



Figure 177. Trans-Aero flight attendant seat - side view.

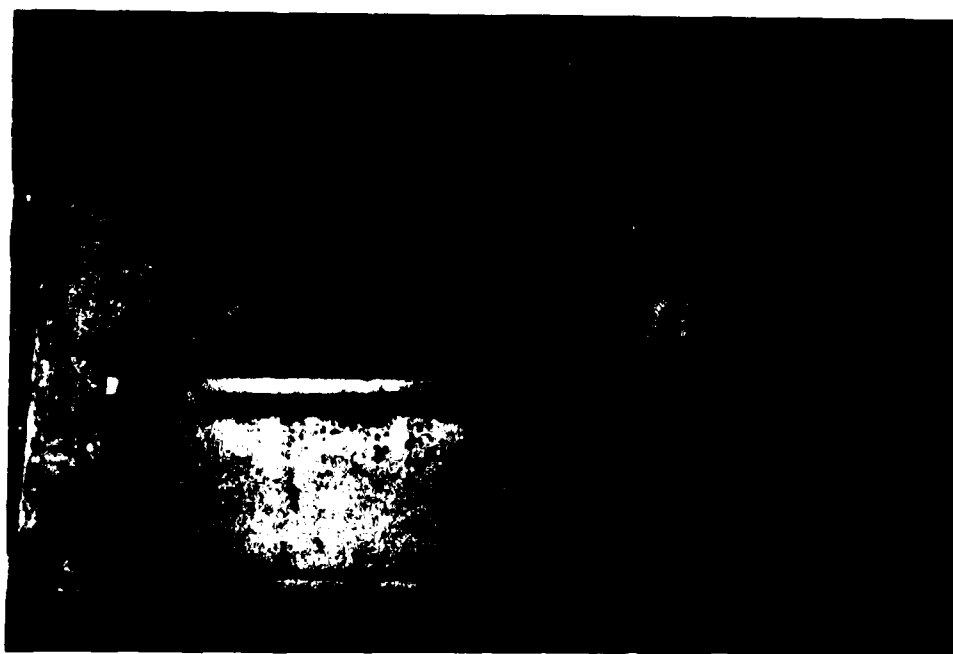


Figure 178. Framework of Trans-Aero flight attendant seat pan.

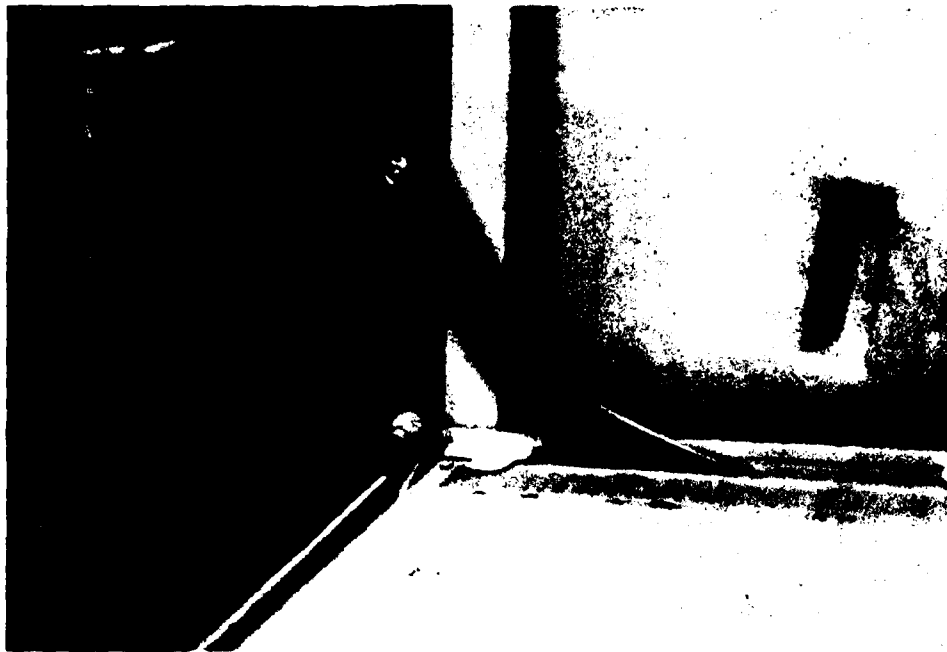


Figure 179. Pivot arm and roller bracket of Trans-Aero flight attendant seat.

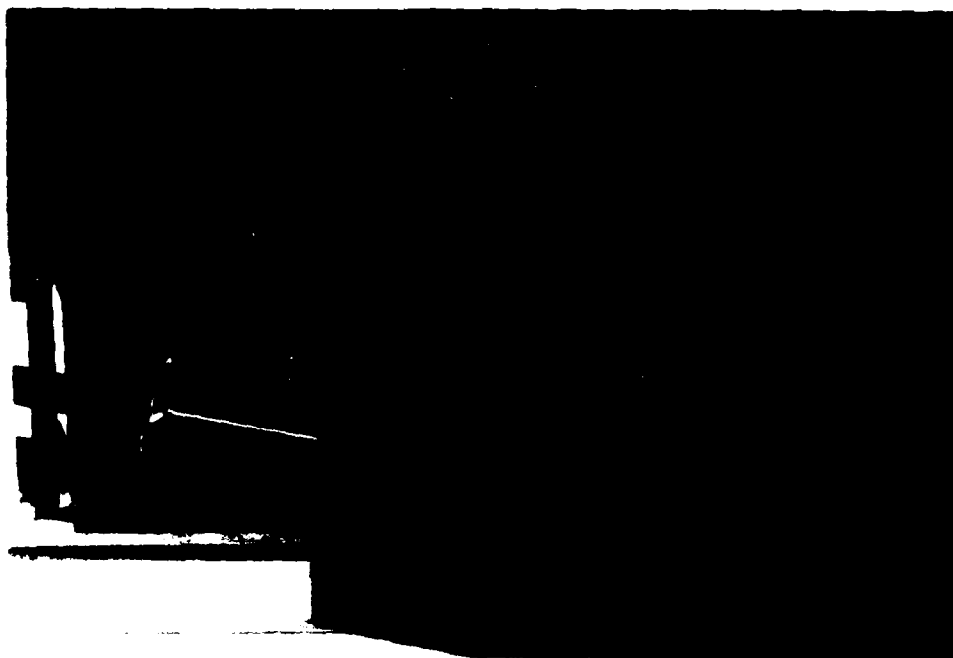


Figure 180. Downward test setup for the flight attendant seat.



Figure 181. Body blocks and framework for downward test.

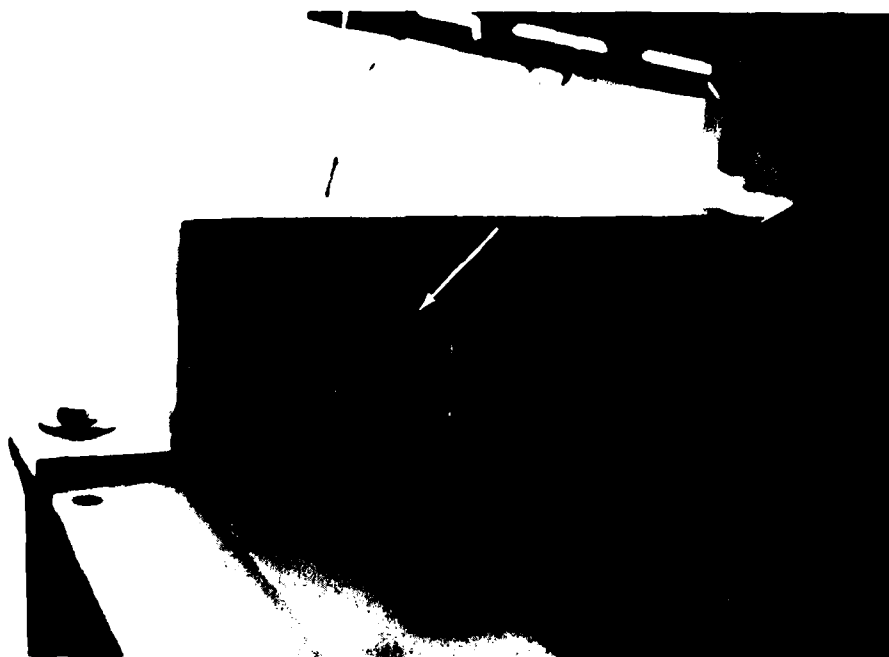


Figure 182. Posttest pivot bolt bracket failure of Trans-Aero flight attendant seat (Downward Test).

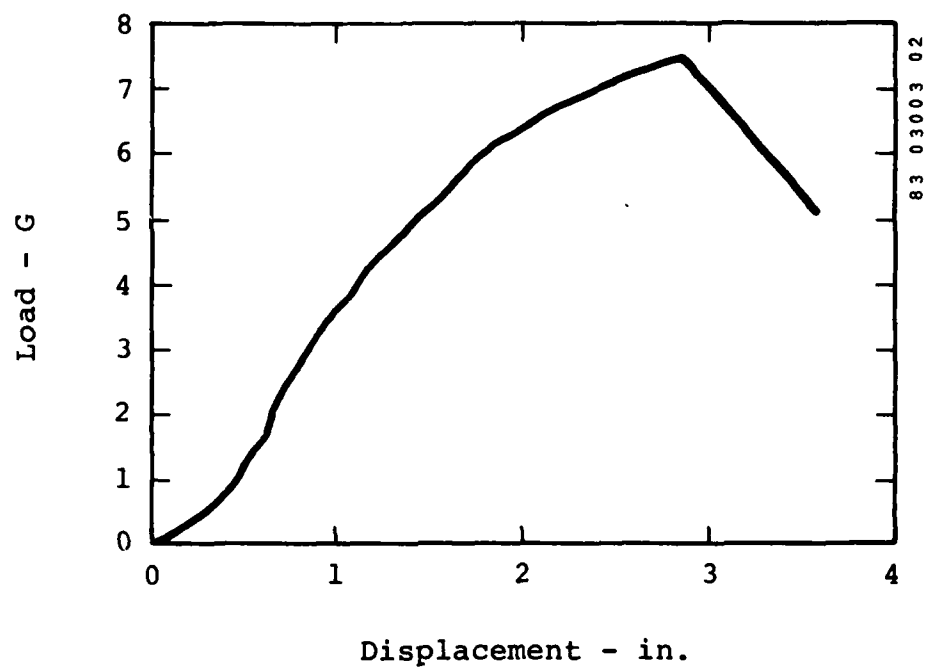


Figure 183. Load versus vertical displacement of Trans-Aero flight attendant seat left seat pan.



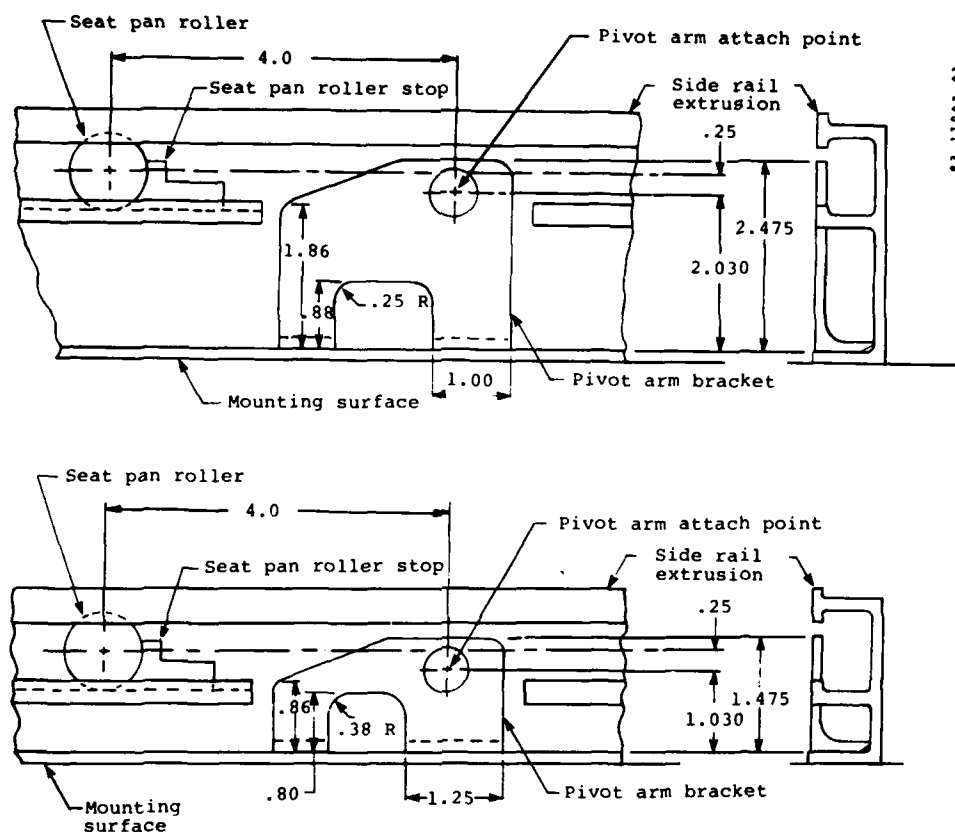


Figure 184. Dimensions of Trans-Aero Model 90835-6 flight attendant seat pivot arm bracket and side rail versus Model 90835-4 right-side pivot arm bracket and side rail.

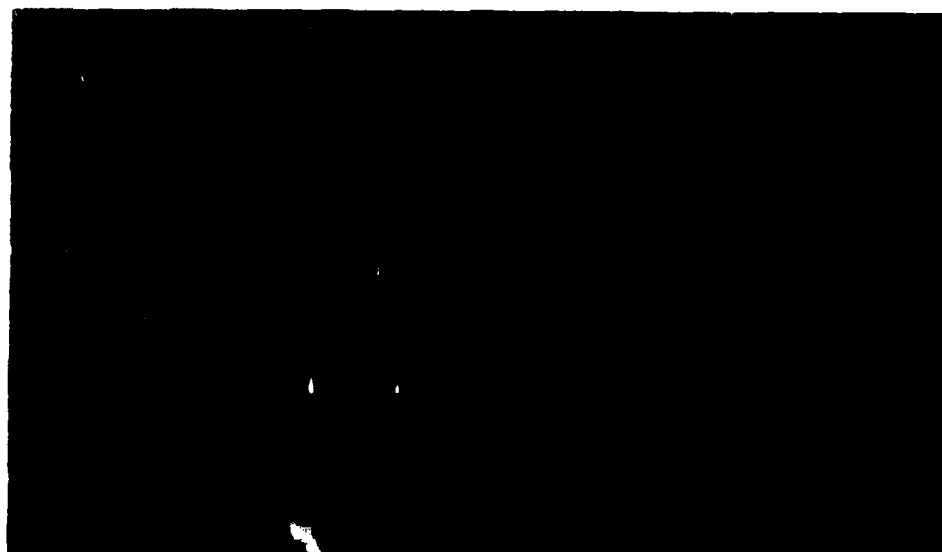
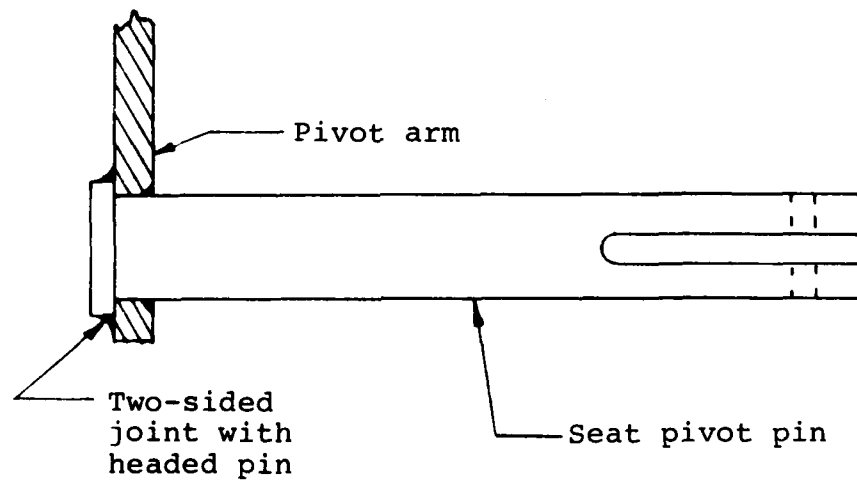
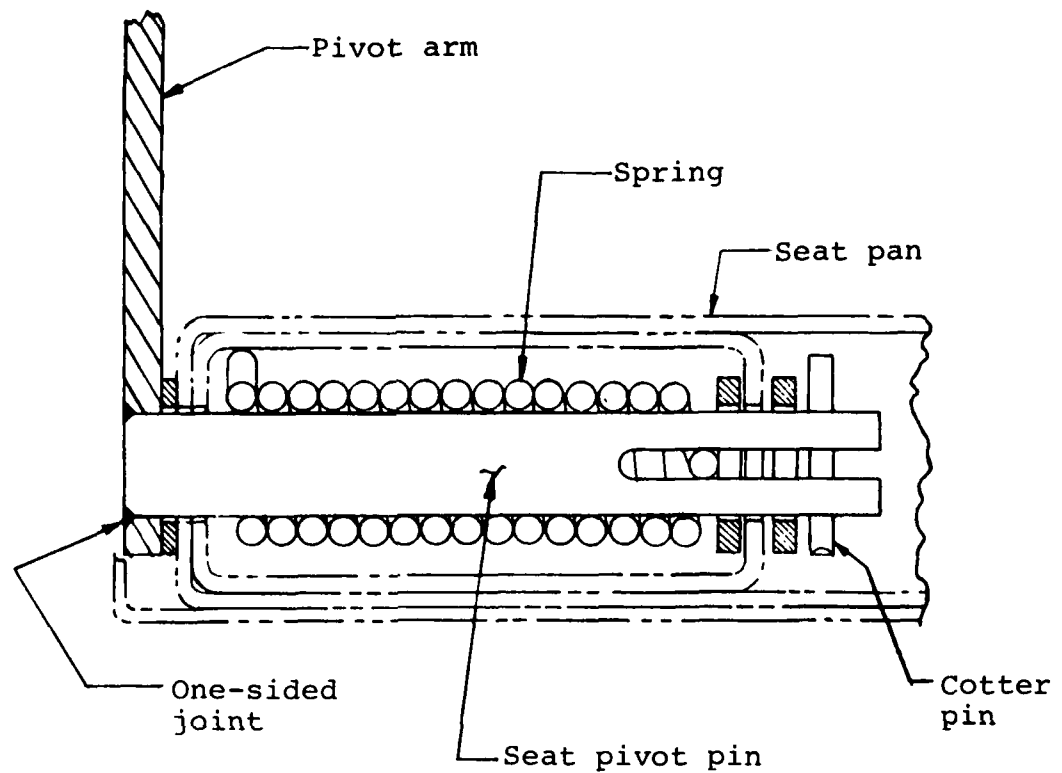


Figure 185. Comparison of modified (left) and standard pivot arm brackets.

STANDARD



MODIFIED

Figure 186. Comparison of modified and standard pivot arm assembly joints.

83 11003 02

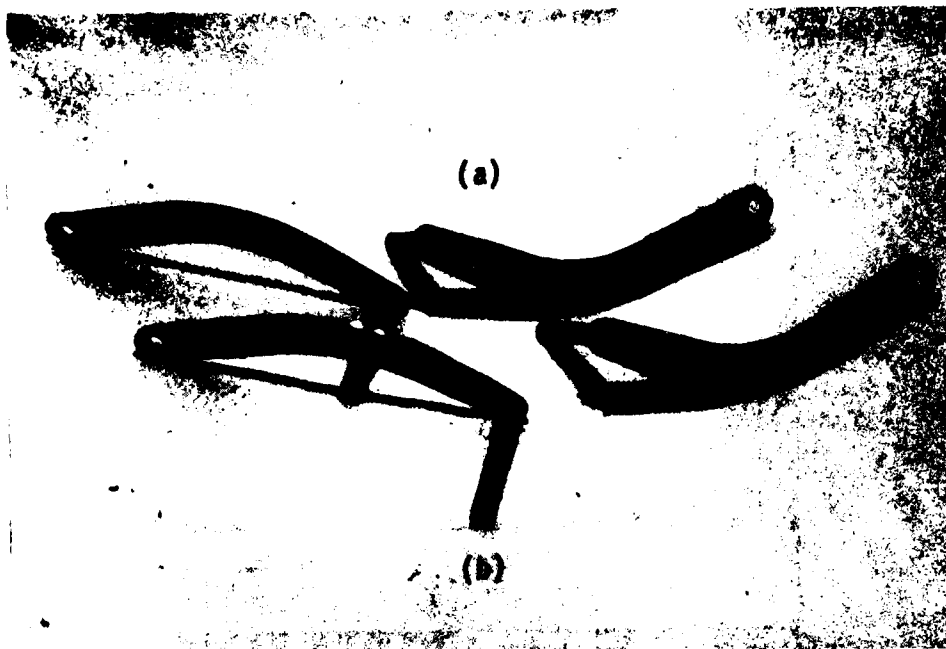


Figure 187. Comparison of modified (a) and standard (b) pivot arm assemblies.



Figure 188. Comparison of modified (a) and standard (b) seat pan roller brackets.

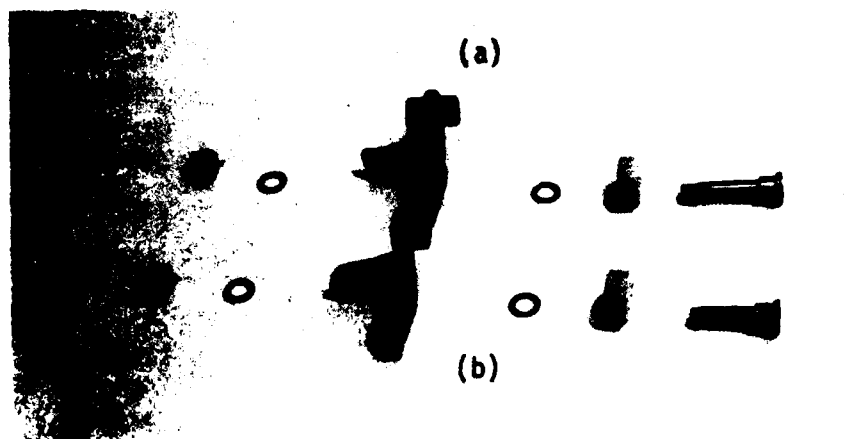


Figure 189. Comparison of modified (a) and standard (b) seat pan roller bracket assemblies.



Figure 190. Posttest Trans-Aero flight attendant seat MOD pivot arm bracket failure (Downward Test).

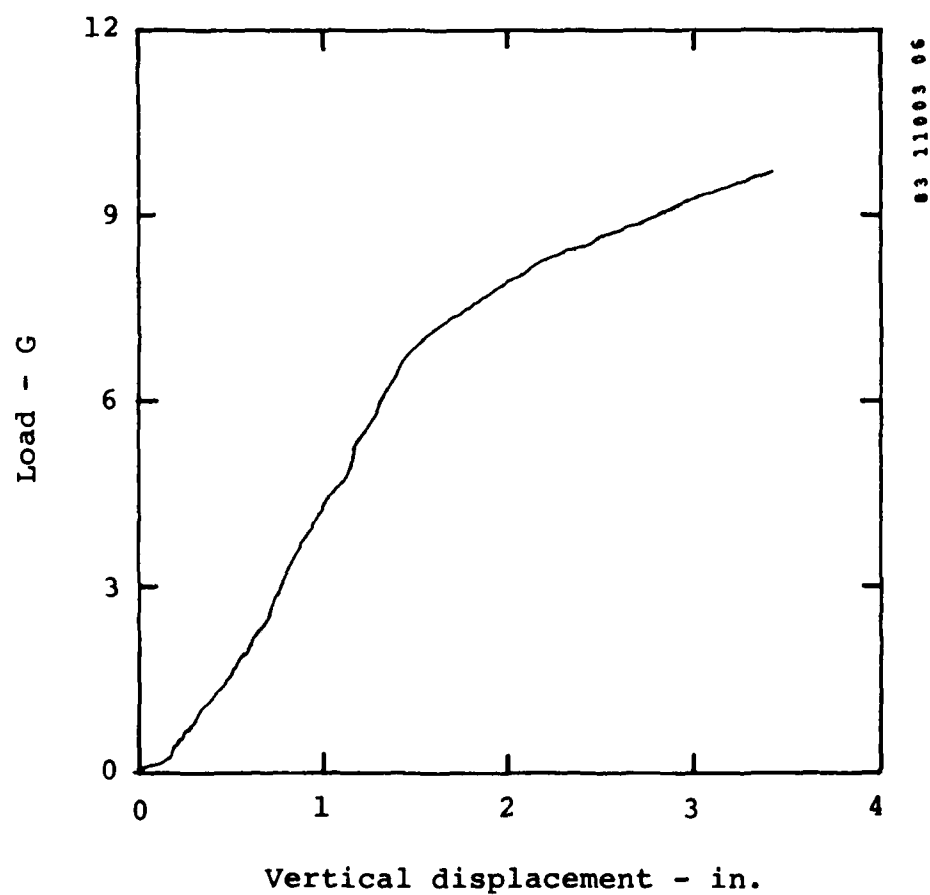


Figure 191. Load versus vertical displacement of Trans-Aero flight attendant seat MOD right seat pan.

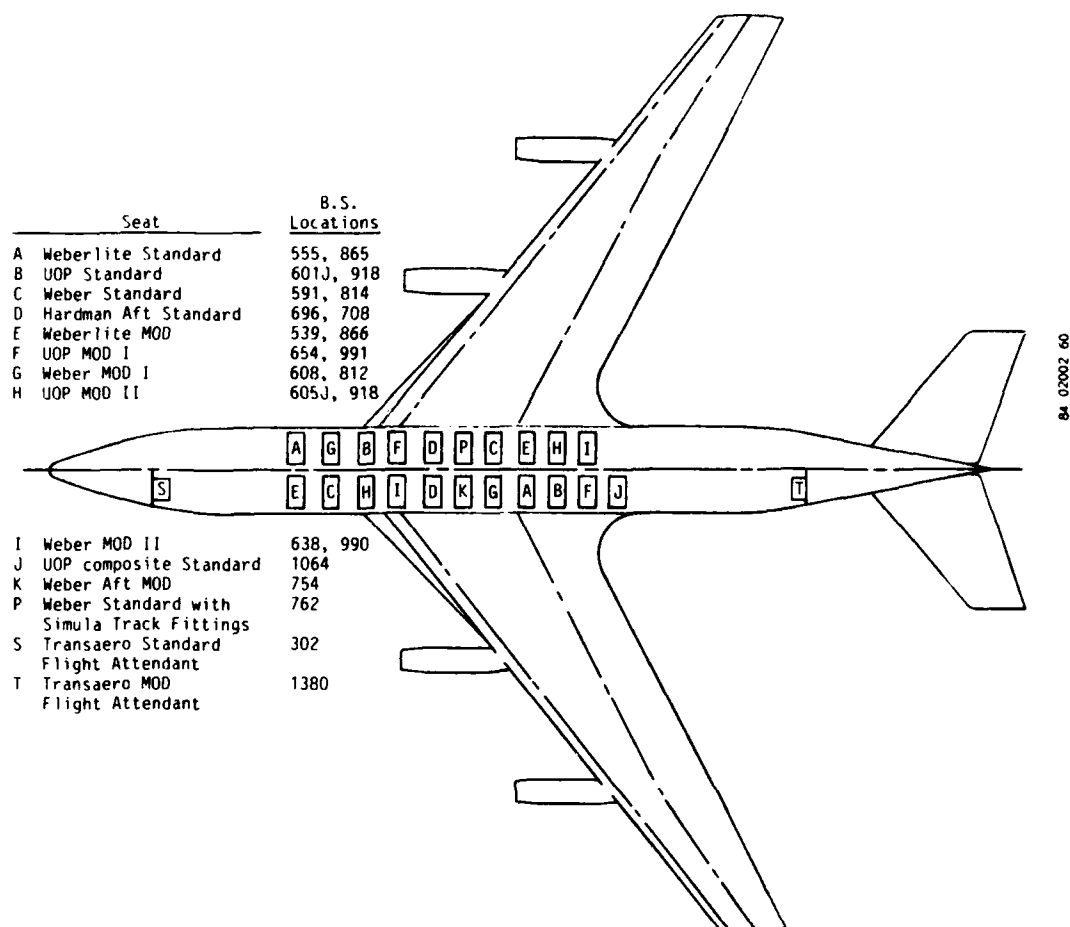


Figure 192. Position of seat experiments aboard aircraft.

TABLE B-1. WEBER (UNMODIFIED) SEAT, CORRELATION OF MSC/NASTRAN  
MODEL TO ACTUAL STRUCTURAL PARTS

Description of the Part	Model Element	From Node	To Node	Material
Front leg (right)	1	1	2	4130 STL
	2	2	3	
Front leg (left)	3	7	8	4130 STL
	4	8	9	
Rear leg (right)	5	4	5	4130 STL
	6	5	6	
Rear leg (left)	7	10	11	4130 STL
	8	11	12	
Diagonal strut between seat legs (right)	9	3	5	4130 STL
Diagonal strut between seat legs (left)	10	9	11	4130 STL
Longitudinal strut between seat legs (right)	11	2	5	4130 STL
Longitudinal strut between seat legs (left)	12	8	11	4130 STL
Front seat pan tube	13	13	3	2024-T3 AL
	14	3	14	
	15	14	9	
	16	9	15	
	17	15	16	
Rear seat pan tube	18	17	6	2024-T3 AL
	19	6	18	
	20	18	12	
	21	12	19	
	22	19	20	
Outboard spreaders under the seat pan	23	25	26	6061-T6 AL
	24	27	28	2024-T3 AL
	25	17	26	
	26	20	28	
	27	13	25	
	28	16	27	
Inboard spreaders under the seat pan	29	21	22	2024-T3 AL
	30	23	24	
	31	18	22	
	32	19	24	
	33	21	14	
	34	23	15	

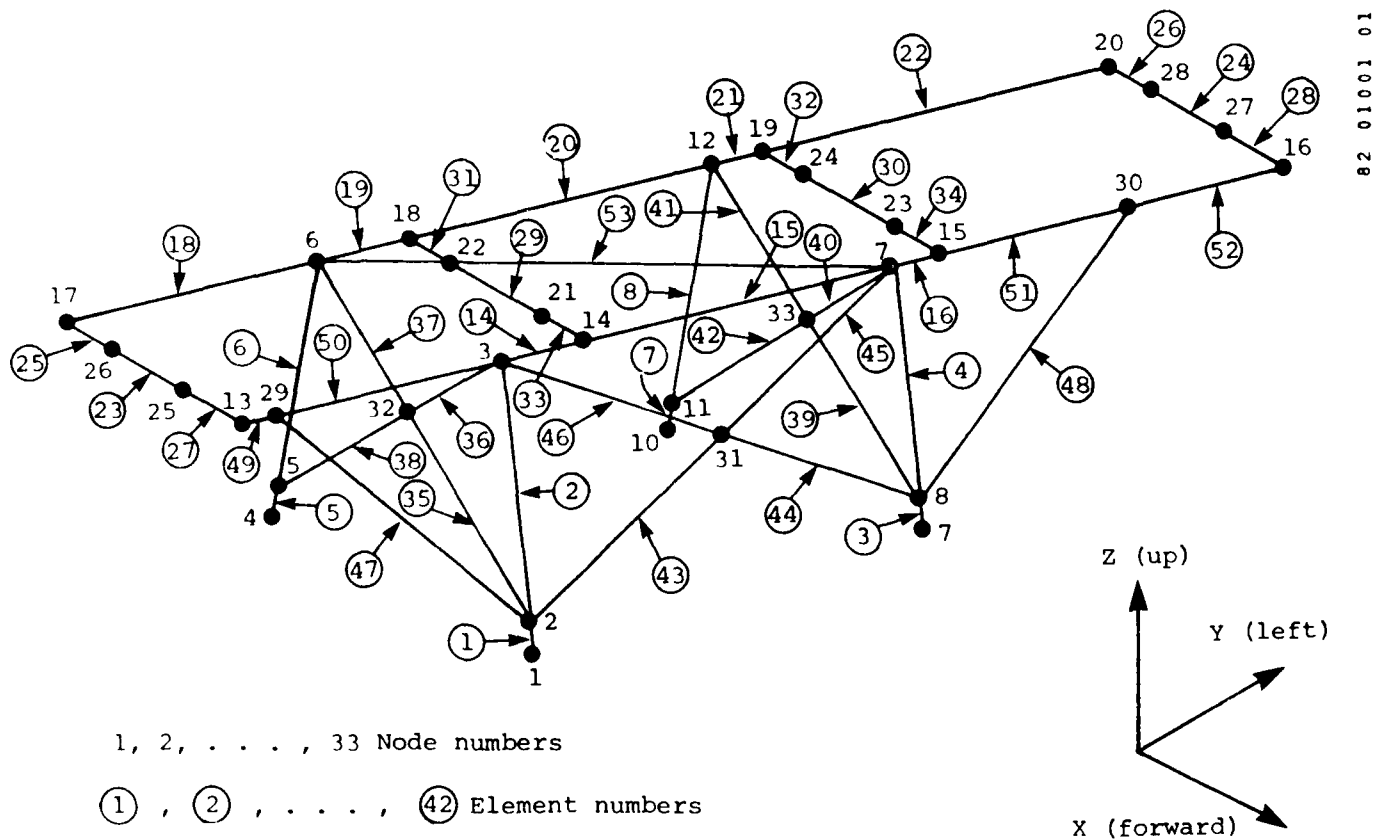


Figure B-2. Weber MOD I seat NASTRAN model.



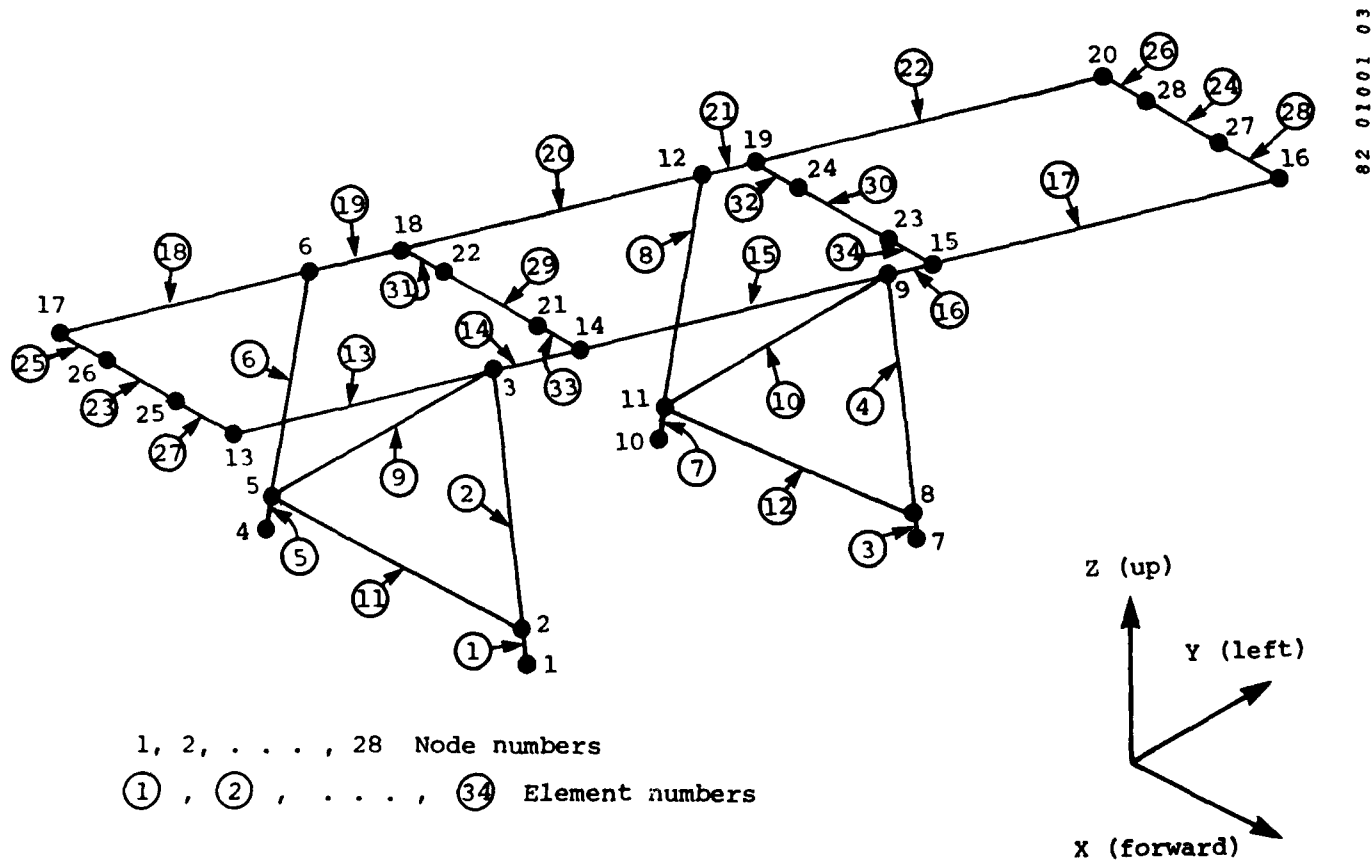


Figure B-1. Standard Weber seat NASTRAN model.

WEBER (MODIFICATION 1) SEAT-TRACK INTERFACE. The boundary conditions used for the Weber (Modification 1) seat consist of all the track fittings (nodes 1, 4, 7, and 10) which are restrained from translation in fore-and-aft, vertical, and lateral directions and from rotating about the vertical axis. Track fitting loads for 9-G forward, 7-G lateral, 10-G downward, and 9-G combined loads are presented in tables B-11 through B-14.

WEBER (MODIFICATION 1) SEAT STRESSES. The stresses for bar elements used in the seat model were calculated at four points on the cross section at each end of the elements. These stresses, when compared with the ultimate stresses for a given element, were used to predict the Margin of Safety (M.S.).

$$M.S. = \frac{F_{tu}}{\sigma_{max}} - 1$$

Tubular reinforcement braces were sized to take the compressive axial loads without buckling. The M.S. for these elements were computed by comparing the axial compressive load to the allowable load.

$$M.S. = \frac{P_{CALW}}{P_c} - 1$$

The maximum absolute values of stresses and axial loads, and the corresponding M.S. are tabulated in table B-15.

WEBER (UNMODIFIED) SEAT APPLIED LOADS. Applied concentrated loads at the nodal points corresponding to 1-G forward, 1-G lateral, 1-G downward, and 1-G combined loadings are presented in tables B-2 through B-5. These loads were determined from a free-body analysis of the occupant and the seat under static loads.

WEBER (UNMODIFIED) SEAT-TRACK INTERFACE. The boundary conditions used for the unmodified Weber seat model were as follows:

- a. Rear track fittings (nodes 4 and 10) were restrained from translation in fore-and-aft, vertical, and lateral directions and rotation about the vertical axis.
- b. Front track fittings (nodes 1 and 7) were restrained from translation in vertical and lateral directions.

Track fitting loads for 9-G forward, 10-G lateral, 10-G downward, and 9-G combined loads are presented in tables B-6 through B-9.

WEBER (UNMODIFIED SEAT STRESSES). The stresses for beam and bar elements used in the seat model were calculated at four points on the cross-section at each end of these elements. These stresses, when compared with the ultimate stresses for a given element, were used to predict the G factor to cause a failure in a given direction as follows:

$$G_{\text{failure}} = \frac{F_{tu}}{\sigma_{\text{max}}}$$

For the unmodified seat, this approach established the relative strength of various parts of the seat. The maximum absolute values of these stresses and corresponding G factor to cause failure are tabulated in table C-10.

WEBER (MODIFICATION 1) SEAT MODEL.

The finite element model of the Weber seat for Modification 1 is shown in figure B-2. The model is essentially the same as the unmodified Weber seat model, with the following exceptions:

- a. Bar elements 43 through 48 simulate tubular braces between the front legs.
- b. Bar elements 35, 37, 39, and 41 simulate additional tubular diagonal braces between the front and the rear legs.
- c. Bar element 53 simulates the strap under the seat pan.

WEBER (MODIFICATION 1) SEAT APPLIED LOADS. Applied concentrated loads at the nodal points corresponding to 9-G forward, 7-G lateral, 10-G downward, and 9-G combined loadings are obtained by multiplying the loads presented in tables B-2 through B-5 by the corresponding G factors.

## APPENDIX B

### FINITE ELEMENT STRUCTURAL ANALYSIS OF SEATS

#### INTRODUCTION.

This appendix describes the finite element structural analysis techniques used to analyze the seat structures. The loads and stresses predicted from the analyses of the existing seat designs were used to identify the modifications to the designs and to support the detailed design effort.

The sections on Program MSC/NASTRAN and the Weber (unmodified) seat model contain detailed descriptions of the seat model, applied loads, track reactions, and internal loads/stresses for the unmodified and MOD I Weber seats. Similar analyses were performed for other seat designs and modifications to those designs. The details of all analyses not included in Appendix C are on file at Simula Inc.

#### DESCRIPTION OF PROGRAM MSC/NASTRAN.

The seat assembly was analyzed using Finite Element Structural Analysis Program MSC/NASTRAN, which is a large digital computer program to analyze linear and nonlinear structural models.

The basic concept of finite element analysis is that every structure may be considered as a mathematical assemblage of individual structural components or elements. There must be a finite number of such elements, interconnected at a finite number of nodal points. The characteristics of a node point include position in space, movement in space (three translational  $x$ ,  $y$ ,  $z$ , and three rotational  $\theta_x$ ,  $\theta_y$ ,  $\theta_z$ ), and connectivity to other nodes via the finite elements. External forces may be assigned to each node. The solution procedure used (Rigid Format 24) consists of stiffness matrix formation followed by static analysis of the structure. The stiffness matrices of individual finite elements are first computed and then transformed from their local coordinate formulation to a form relating to the global coordinate system. Finally, the individual element stiffness contributing to each nodal point is superimposed to obtain the total assemblage stiffness matrix ( $K$ ). The static analysis phase is based on the Displacement Method and the results are in the realm of Small Displacement Theory.

#### WEBER (UNMODIFIED) SEAT MODEL.

The finite element model of the unmodified Weber seat consists of three-dimensional elastic bar elements as shown in figure B-1. The sheet metal pan was not incorporated into the seat model since it does not have significant effects on the seat structure strength. The correlations between elements are shown in figure B-1, and the correlation of the MSC/NASTRAN model to the actual structural parts is presented in table B-1. All structural parts were modeled using three-dimensional bar elements. Bar elements are prismatic: the neutral axis and shear center coincide, the cross-sectional properties do not vary along the length of the bar, and also include extension, torsion, bending in two perpendicular planes, and the associated shears.

For the dynamic test criteria, a drop test has been suggested only for small aircraft, because an impact with high vertical load components presents the greatest hazard in these aircraft. This test is to include longitudinal and lateral components as well as the vertical component, which is of primary interest. A longitudinal test is suggested for seat and restraint systems in all transport aircraft. A lateral component is to be included, to limit the amount of testing required and to assure that the system can sustain a condition of simultaneous loading in more than one direction.

In summary, the exact crash environment which occurs in present day transport aircraft is primarily of academic interest. Data suggest that G forces substantially greater than those specified in the current standards can be encountered in survivable crashes of transport aircraft. Weight and cost factors will undoubtedly limit the protection that can be provided for large numbers of passengers to less than this amount. Therefore, design improvements which reflect the highest level of protection consistent with human tolerance that can be provided in view of practical and economic considerations should be assessed. The selected test criteria, as provided under the subject project, is presented in accordance with this philosophy.

#### REFERENCES

- A-1 CRASH SURVIVAL DESIGN GUIDE, Dynamic Science, Division of Marshall Industries; USAAMRDL Technical Report 71-22, Fort Eustis Directorate, U.S. Army Air Mobility Research and Development Laboratory, Fort Eustis, Virginia, October 1971.
- A-2 Haley, J. L., et al., FLOOR ACCELERATIONS AND PASSENGER INJURIES IN TRANSPORT AIRCRAFT ACCIDENTS, Aviation Safety Engineering and Research (AvSER), Division of Flight Safety Foundation, Inc.; USAAVLABS Technical Report 67-16, U.S. Army Aviation Materiel Laboratories, Fort Eustis, Virginia, May 1967, AD815877.
- A-3 Laananen, D. H., AIRCRAFT CRASH SURVIVAL DESIGN GUIDE, Volume II, AIRCRAFT CRASH ENVIRONMENT AND HUMAN TOLERANCE, Simula Inc., Tempe, Arizona; USARTL Technical Report 79-22B, Applied Technology Laboratory, U.S. Army Research and Technology Laboratories (AVRADCOM), Fort Eustis, Virginia, January 1980.

the probability of survival at the higher G levels even if the seats were strong enough to support them.

- In an environment of rapidly increasing operating costs, considerable opposition can be expected to any requirements that would lead to increased weights. It is therefore evident that optimum crashworthiness will in all probability have to be compromised due to economic considerations.

As a result of these factors, improved test criteria were selected to provide protection for crash pulses of the magnitudes shown in table A-2.

TABLE A-2. DESIGN PULSES CORRESPONDING  
TO PROPOSED TEST CRITERIA

	Small (less than 50 passengers)		Medium (50-249 passengers)		Large (more than 250 passengers)	
	$\Delta v$ (ft/sec)	Peak (G)	$\Delta v$ (ft/sec)	Peak (G)	$\Delta v$ (ft/sec)	Peak (G)
Longitudinal	50	21	50	18	50	15
Vertical	42	19	35	10	35	8
Lateral	30	12	30	10	30	8

It is important to recognize that the selected criteria would not provide adequate protection in a 95th-percentile survivable crash. However, the improvement relative to existing criteria would be considerable. Based on the frequency of occurrence curves presented in reference A-1, these design pulses would provide adequate protection for at least the 50th-percentile survivable crashes.

An exception was made in the case of small aircraft. Since greater impact forces are transmitted to the occupant due to the minimum amount of crushable fuselage under the floor in these planes, the recommended design pulses are somewhat more severe than indicated by the previously cited data. Most notably, the velocity change in the vertical direction was increased from 35 ft/sec to 42 ft/sec. This increase was based on data for smaller aircraft in the current edition of Volume II of the Aircraft Crash Survival Design Guide (reference A-3).

The variations in the magnitude of the recommended pulses as a function of aircraft size is based purely on the engineering intuition of several very experienced people in the field of crash safety, as quantitative data are not presently available to support extrapolations from one size of aircraft to another.

Since longitudinal and vertical impacts can be expected to exert forces on the seat primarily in the forward and downward directions, no recommended test criteria have been made for the aftward and upward directions.

ences A-1 and A-2. The peak accelerations and velocity changes recommended therein equal or exceed those to be expected in 95 percent of the survivable crashes for transport category aircraft. While these recommendations are based on data gathered from the mid-1950's to the mid-1960's, there are no apparent reasons why they should not be reasonably valid for transport category aircraft in use today. Construction techniques have not changed to the extent that markedly different crash dynamics of the structures should be expected.

The recommended design pulses and supporting data for the transport cabin areas, taken from the Crash Survival Design Guide (reference A-1 and A-2), are presented in table A-1. However, it was not intended that seat and restraint systems be capable of protecting the occupant in the crash environments defined by table A-1; rather, environments of reduced severity were selected. The rationale for selecting the proposed, downgraded, test criteria considered the following factors:

TABLE A-1. TRIANGULAR DESIGN PULSES FOR  
95-TH PERCENTILE SURVIVABLE  
CRASHES OF TRANSPORT CATEGORY  
AIRCRAFT (FROM REFERENCE A-1)

	$\Delta v$ (ft/sec)	Peak (G)*	Duration (sec)
Longitudinal	64	20	0.200
Vertical	35	36	0.060
Lateral	30	16	0.116

\*Higher values are specified for cockpit seats.

- Because of the presence of additional structure capable of absorbing energy, very large transports can be expected to subject the seats and occupants to lesser crash loads than the smaller transports in crashes where sufficient livable space is maintained by the fuselage.
- The floor structure in very large transports is incapable of supporting the design pulse loads of reference A-1, so it would be pointless to design seats and restraints to that level.
- Vertical accelerations in excess of 14 G have a high probability of producing spinal fractures. Therefore, seat strength greater than 14 G in this direction is of limited value if the seat does not stroke and absorb energy.
- The use of lap-belts-only for restraint, and the presence of an adjacent row of seats in the head strike envelope, greatly diminish

## APPENDIX A

### CRASH ENVIRONMENT AND DESIGN PULSES FOR TRANSPORT CATEGORY AIRCRAFT

The crash environment that can be expected in transport category aircraft is discussed in Chapter 1 of the U.S. Army's TR-71-22 Crash Survival Design Guide, reference A-1 (This information is not included in the most recent revision of the Aircraft Crash Survival Design Guide, reference A-3) and in USAAVLABS' TR 67-16 (reference A-2). Both documents establish peak accelerations and velocity changes for the primary impact as a function of the probability of occurrence. These parameters were supported by crash test data, theoretical calculations, and studies of accident investigation reports. Although these data are published in Army documents, the preponderance of accidents and aircraft studied were civilian, as is discussed below.

Reference A-2 presents results of crash tests of C-46, C-82, DC-7, and L-1649 transport aircraft which were subjected to impacts at various angles and velocities. Longitudinal, vertical, and lateral floor accelerations were measured in both the cabin and cockpit areas. In the cabin, these measurements were made along the length of the fuselage.

Also discussed in TR 67-16 are theoretical calculations of maximum floor accelerations. These analyses considered the maximum possible longitudinal deceleration of the cabin floor based on the known mass distributions and the stiffness of the fuselage structure. The results were reasonably consistent with the crash test data.

Analysis of accident data is presented in both references A-1 and A-2, based on the same data sample (this information is not included in the most recent revision of the Aircraft Crash Survival Design Guide, reference A-3) which involved 43 civilian and 18 military crashes of many different types and sizes of transport aircraft, including the Lockheed Electra, Boeing 707, and the military C135 (B707) and C140.

The accidents selected for inclusion in the sample involved moderate to severe impact forces with decelerations in excess of 4 G but below human tolerance levels. Further criteria for inclusion in the study were that the aircraft be multi-engined with a minimum weight of 10 tons, that there be at least one injury requiring hospitalization, and that there be at least one survivor or conclusive evidence that survival would have been possible if adequate restraint had been provided. Hence, minor impacts were excluded, as were catastrophic, unsurvivable crashes.

As reported in TR 67-16, analysis of the crash test data indicated that a symmetrical, triangular pulse would adequately represent the measured pulses for the major impact in the majority of the tests. Therefore, this shape has been used as a design pulse for testing seats and restraints. The Crash Survival Design Guide (reference A-1) presents recommended design pulses for transport category aircraft, based on the analyses and tests discussed in both refer-



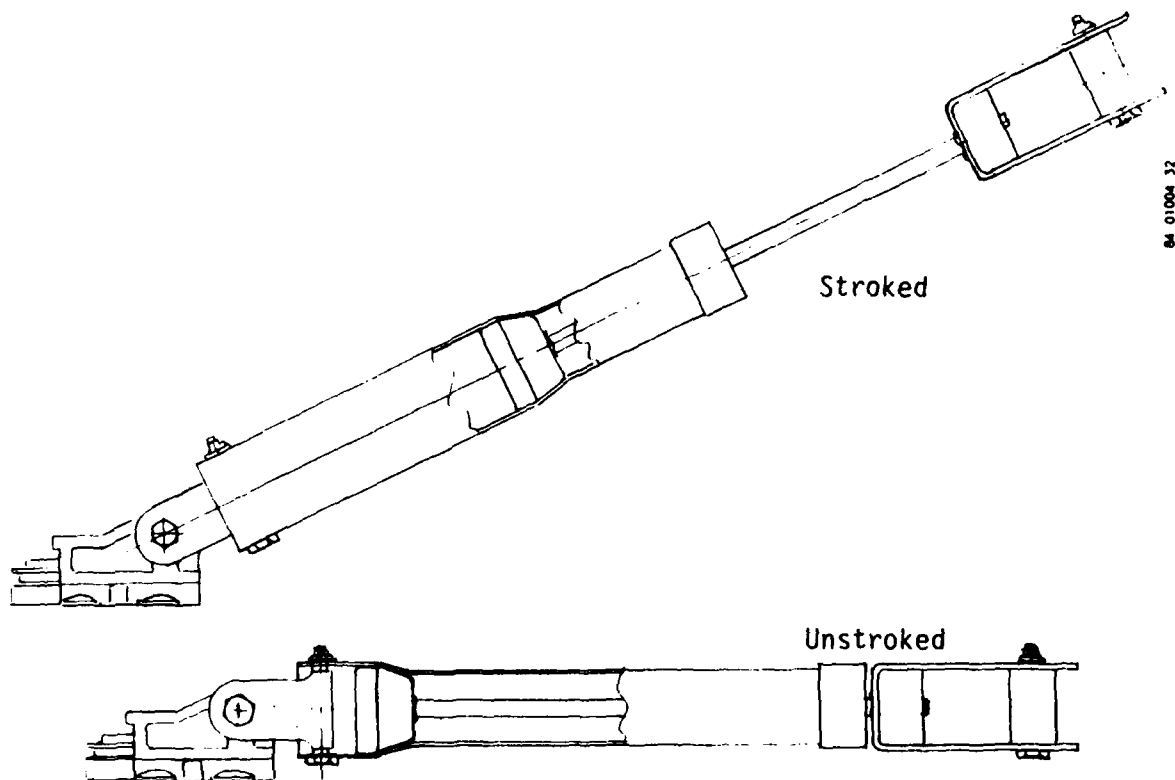


Figure 196. Secondary restraint system energy absorber.

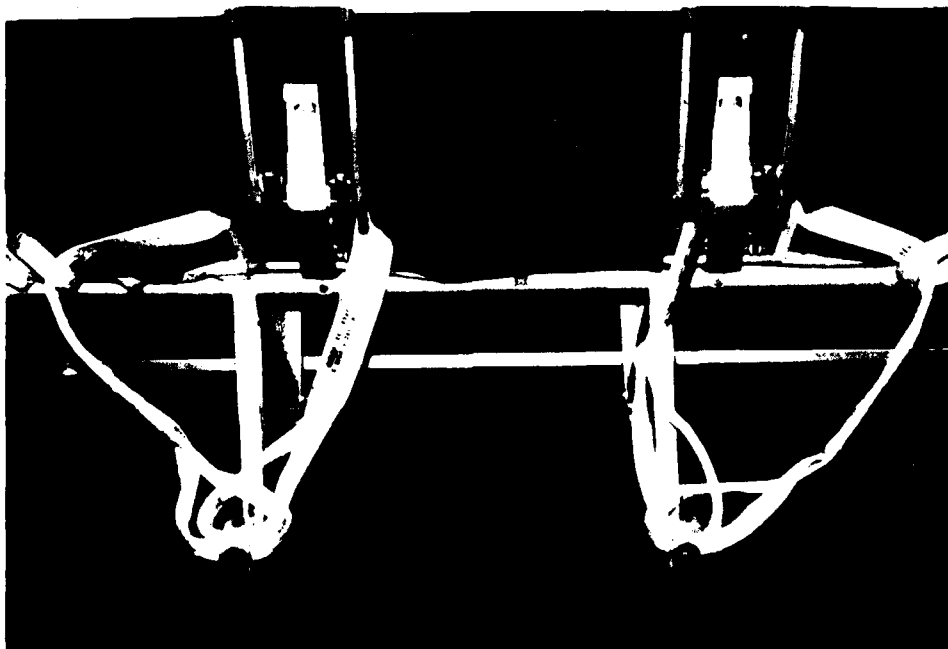
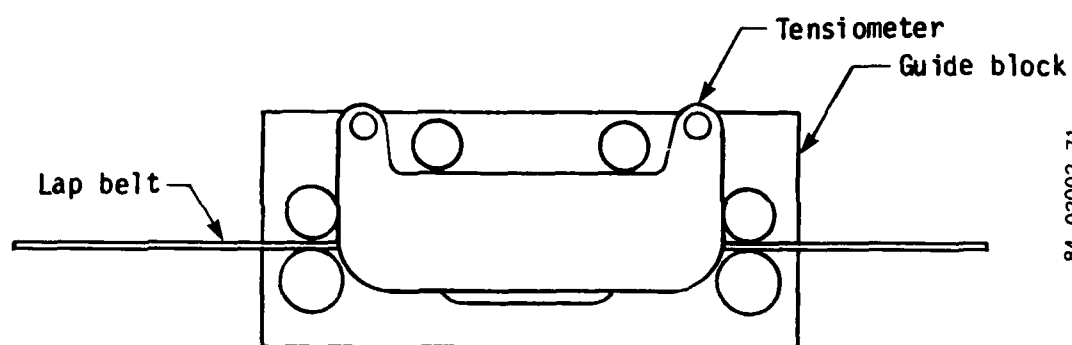
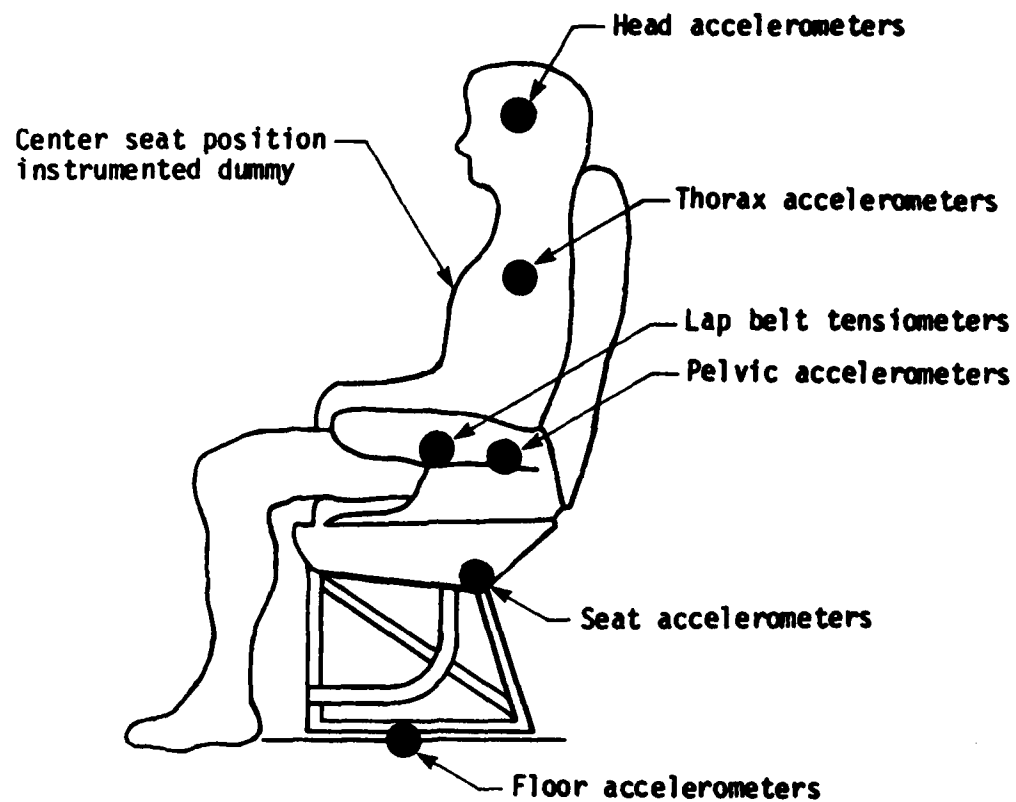


Figure 195. Secondary restraint system - side and rear views.



84 02002 71

Figure 194. Installation and sketch of lap belt tensiometer guide block.



BA 02002 70

Figure 193. Typical complete instrumentation setup for test aircraft seats.

TABLE B-2. WEBER (UNMODIFIED)  
SEAT APPLIED NODAL  
LOADS FOR 1-G  
FORWARD LOADING

Node No.	$F_X$ (1b)	$F_Y$ (1b)	$F_Z$ (1b)
13	-	-	-72
14	-	-	-144
15	-	-	-144
16	-	-	-72
17	100	-	72
18	200	-	144
19	200	-	144
20	100	-	72

TABLE B-3. WEBER (UNMODIFIED)  
SEAT APPLIED NODAL  
LOADS FOR 1-G  
LATERAL LOADING

Node No.	$F_X$ (1b)	$F_Y$ (1b)	$F_Z$ (1b)
13	-	-	-132
14	-	-	-132
15	-	-	-132
17	-222	-	-132
18	-	-200	132
19	-	-200	132
20	222	-200	264

TABLE B-4. WEBER (UNMODIFIED)  
SEAT APPLIED NODAL  
LOADS FOR 1-G  
DOWNWARD LOADING

Node No.	$F_x$ (lb)	$F_y$ (lb)	$F_z$ (lb)
13	-	-	-50
14	-	-	-100
15	-	-	-100
16	-	-	-50
17	-	-	-50
18	-	-	-100
19	-	-	-100
20	-	-	-50

TABLE B-5. WEBER (UNMODIFIED)  
SEAT APPLIED NODAL  
LOADS FOR 1-G COM-  
BINED LOADING (30°  
PITCH + 30° YAW)

Node No.	$F_x$ (lb)	$F_y$ (lb)	$F_z$ (lb)
13	-	-	-136
14	-	-	-215
15	-	-	-215
16	-	-	-78
17	-18	-	127
18	157	-87	127
19	157	-87	127
20	176	-87	150

TABLE B-6. WEBER (UNMODIFIED) SEAT TRACK FITTING  
LOADS FOR 9-G FORWARD LOADING

Location	$F_X$ (lb)	$F_Y$ (lb)	$F_Z$ (lb)	$M_X$ (in.-lb)	$M_Y$ (in.-lb)	$M_Z$ (in.-lb)
Right Front (Node 1)	-	-20	2210	-	-	-
Right Rear (Node 4)	-1940	-30	-2210	-	-	-140
Left Front (Node 7)	-	190	3490	-	-	-
Left Rear (Node 10)	-3460	-140	-3490	-	-	25

TABLE B-7. WEBER (UNMODIFIED) SEAT TRACK FITTING  
LOADS FOR 10-G LATERAL LOADING

Location	$F_X$ (lb)	$F_Y$ (lb)	$F_Z$ (lb)	$M_X$ (in.-lb)	$M_Y$ (in.-lb)	$M_Z$ (in.-lb)
Right Front (Node 1)	-	1660	4600	-	-	-
Right Rear (Node 4)	4110	1600	4920	-	-	5000
Left Front (Node 7)	-	1460	-1990	-	-	-
Left Rear (Node 10)	-4110	1280	-7530	-	-	3660

TABLE B-8. WEBER (UNMODIFIED) SEAT TRACK FITTING  
LOADS FOR 10-G DOWNWARD LOADING

Location	$F_X$ (lb)	$F_Y$ (lb)	$F_Z$ (lb)	$M_X$ (in.-lb)	$M_Y$ (in.-lb)	$M_Z$ (in.-lb)
Right Front (Node 1)	-	-290	1320	-	-	-
Right Rear (Node 4)	10	-250	670	-	-	-850
Left Front (Node 7)	-	290	2700	-	-	-
Left Rear (Node 10)	-10	250	1310	-	-	800

TABLE B-9. WEBER (UNMODIFIED) SEAT TRACK FITTING LOADS  
FOR 9-G COMBINED LOADING (30° PITCH + 30° YAW)

Location	$F_X$ (lb)	$F_Y$ (lb)	$F_Z$ (lb)	$M_X$ (in.-lb)	$M_Y$ (in.-lb)	$M_Z$ (in.-lb)
Right Front (Node 1)	-	520	4070	-	-	-
Right Rear (Node 4)	100	510	450	-	-	1520
Left Front (Node 7)	-	840	3030	-	-	-
Left Rear (Node 10)	-4350	490	-5190	-	-	1760



TABLE B-10. WEBER (UNMODIFIED) SEAT STRESSES FOR 1-G LOADING

Description of the Part	Model Element	$ \sigma_{\max} $	$G_{\text{failure}}$	Critical Loading
Front legs	2	56.67	2.4	Lateral
Rear legs	6	59.72	2.3	Lateral
Longitudinal strut between seat legs	11	8.60	11.0	Lateral
Diagonal strut between seat legs	9	11.92	8.0	Lateral
Front seat pan tube	14	26.50	2.6	Lateral
Rear seat pan tube	20	30.16	2.3	Lateral
Inboard spreaders under the seat pan	32	9.67	7.2	Lateral
Outboard spreaders under the seat pan	24	13.80	3.0	Lateral

TABLE B-11. WEBER (MODIFICATION 1) SEAT TRACK FITTING  
LOADS FOR 9-G FORWARD LOADING

Location	$F_X$ (lb)	$F_Y$ (lb)	$F_Z$ (lb)	$M_X$ (in.-lb)	$M_Y$ (in.-lb)	$M_Z$ (in.-lb)
Right Front (Node 1)	-130	20	2195	-	-	-500
Right Rear (Node 4)	-1795	40	-2185	-	-	50
Left Front (Node 7)	-660	110	3515	-	-	990
Left Rear (Node 10)	-2820	-170	-3515	-	-	-90

TABLE B-10. WEBER (UNMODIFIED) SEAT STRESSES FOR 1-G LOADING

Description of the Part	Model Element	$ \sigma_{\max} $	$G_{\text{failure}}$	Critical Loading
Front legs	2	56.67	2.4	Lateral
Rear legs	6	59.72	2.3	Lateral
Longitudinal strut between seat legs	11	8.60	11.0	Lateral
Diagonal strut between seat legs	9	11.92	8.0	Lateral
Front seat pan tube	14	26.50	2.6	Lateral
Rear seat pan tube	20	30.16	2.3	Lateral
Inboard spreaders under the seat pan	32	9.67	7.2	Lateral
Outboard spreaders under the seat pan	24	13.80	3.0	Lateral

TABLE B-11. WEBER (MODIFICATION 1) SEAT TRACK FITTING LOADS FOR 9-G FORWARD LOADING

Location	$F_X$ (lb)	$F_Y$ (lb)	$F_Z$ (lb)	$M_X$ (in.-lb)	$M_Y$ (in.-lb)	$M_Z$ (in.-lb)
Right Front (Node 1)	-130	20	2195	-	-	-500
Right Rear (Node 4)	-1795	40	-2185	-	-	50
Left Front (Node 7)	-660	110	3515	-	-	990
Left Rear (Node 10)	-2820	-170	-3515	-	-	-90

TABLE B-12. WEBER (MODIFICATION 1) SEAT TRACK FITTING  
LOADS FOR 7-G LATERAL LOADING

Location	$F_x$ (lb)	$F_y$ (lb)	$F_z$ (lb)	$M_x$ (in.-lb)	$M_y$ (in.-lb)	$M_z$ (in.-lb)
Right Front (Node 1)	35	2800	5680	-	-	1310
Right Rear (Node 4)	1040	-50	980	-	-	250
Left Front (Node 7)	790	1670	-3850	-	-	1020
Left Rear (Node 10)	-1860	-220	-2810	-	-	-320

TABLE B-13. WEBER (MODIFICATION 1) SEAT TRACK FITTING  
LOADS FOR 10-G DOWNWARD LOADING

Location	$F_x$ (lb)	$F_y$ (lb)	$F_z$ (lb)	$M_x$ (in.-lb)	$M_y$ (in.-lb)	$M_z$ (in.-lb)
Right Front (Node 1)	-460	-830	1130	-	-	-40
Right Rear (Node 4)	500	-60	860	-	-	-155
Left Front (Node 7)	-690	760	2890	-	-	105
Left Rear (Node 10)	645	130	1120	-	-	-

TABLE B-14. WEBER (MODIFICATION 1) SEAT TRACK FITTING  
LOADS FOR 9-G COMBINED LOADING (30° PITCH +  
30° YAW)

Location	$F_X$ (lb)	$F_Y$ (lb)	$F_Z$ (lb)	$M_X$ (in.-lb)	$M_Y$ (in.-lb)	$M_Z$ (in.-lb)
Right Front (Node 1)	-260	1260	5360	-	-	320
Right Rear (Node 4)	-630	-20	-840	-	-	120
Left Front (Node 7)	-350	1320	1740	-	-	1390
Left Rear (Node 10)	-3010	-200	-3900	-	-	-110

TABLE B-15. WEBER (MODIFICATION 1) SEAT STRESSES

Description of the Part	Model Element	$ \sigma_{max} $ / Axial Load	M.S.	Critical Loading
Front legs	3	98.2 ksi	0.37	7-G Lateral
Rear legs	8	149.7 ksi	-0.10	7-G Lateral
Diagonal tubular braces between the seat legs	42	2000 lb (T)	+0.28	9-G Combined
	39	1080 lb (C)	4.43	9-G Forward
Tubular braces between the front legs (center)	43	5040 lb (C)	+0.14	7-G Lateral
	44	4310 lb (T)	+1.04	7-G Lateral
Tubular braces between the front legs (outer)	47	1930 lb (C)	+0.81*	7-G Lateral
	48	2630 lb (T)	+1.43	
Front seat pan tube	51	72.8 ksi	-0.04	7-G Lateral
Rear seat pan tube	21	93.1 ksi	-0.25	7-G Lateral
Spreaders under the seat pan	32	62.5 ksi	0.12	9-G Combined
Diagonal strap under the seat pan	53	2300 lb (T)	+0.35	7-G Lateral

\* $P_{CALW}$  (3500 lb) is determined from Euler's formula for long columns.

## APPENDIX C

### FLOOR TRACK STRENGTH

This appendix summarizes information gathered relative to the strength of the floor tracks and supporting structure, and commonly used seat attachment fittings.

Boeing Documents D6-9012 (reference C-1) and D6-10881 (reference C-2), specify maximum allowable uploads for the floor tracks used in Boeing 707, 720, 727, and 737 aircraft. These are defined as follows:

With one stud: 4400 lb  
With two studs: 5360 lb

According to the documents, the single-stud limit is determined by the tear-out strength of the track lips, while the double-stud limit is based on bending of the track beam midway between two floor beams.

Brownline P/N 20864 is an extruded, 7075-T6 aluminum track made per MS33601 (reference C-3), with the same lip dimensions as the Boeing track. According to the Brownline Catalog (reference C-4), it has a single-stud capacity of 6000 lb. Since the Boeing track is made of 7178-T6511, which is a stronger material, it is assumed the 4400 lb maximum allowable upload includes a factor of safety, and the track can retain a load higher than 6000 lb before failing. It is reasonable to assume the same would apply to the 5360 lb allowable load.

The test loads and rated loads for several typical floor track fittings were also reviewed.

Brownline Part No. 21700-54 (reference C-4) is a track fitting that was used on the Hardman Model 8727 seats which were aboard the test aircraft. An illustration of the fitting is in figure 15 of this report. Brownline states a single load capacity for the fitting as 7500 lb applied 60 degrees from the horizontal and in the plane of the track. If it is assumed that a 33-percent fitting factor applies, then this part may be expected to support 9975 lb prior to ultimate failure. A similar fitting manufactured by Ancra and shown as drawing No. 42763 in reference C-5, lists a minimum ultimate load of 9600 lb applied at the same 60-degree angle. A similar load was attained at Simula by testing the Brownline fitting on the Brownline track. The results were equivalent to an ultimate load of 9496 lb at a 46-degree angle.

Several Ancra reports (references C-6 through C-8) and a Weber test report (reference D-9) were obtained. They gave the results of proof tests on Ancra fittings 40418, 40566, 40659, and 42810. These fittings are identical in their configuration and dimensioning of parts that interface and transfer loads to the track. The 40566 fitting is shown in figure 16 of this report. The proof tests were conducted in steel tracks and were performed to verify only the fitting strength. The Ancra tests held the fittings at the following loads and directions for two minutes.

<u>Direction</u>	<u>Load (lb)</u>
Z	7980
X	5320
Y	1330
Resultant	9700 @ 56 degrees

The Weber test held the fitting at 10,825 lb at 48 degrees for 10 seconds. The load was then increased until the fitting failed at 16,146 lb (averaged from three tests).

Another Ancra report (reference C-10) gives results of destructive tests on Ancra fitting 43387 in a 7075-T6511 aluminum track per MS33601. The fitting was pulled at an angle of 48 degrees until the track failed at 10,600 lb\*. Two more tests were performed at 53 degrees, where the track failed at an average load of 11,560 lb. These results corroborate those obtained by Simula, which showed the track failing at a load equivalent to 12,400 lb applied at 54 degrees.

Sabre Industries Part No. 500330 is illustrated in figure 17 of this report. This fitting is also designed for use on tracks per MS 33601, and is similar to the Ancra fittings. The ultimate loads specified for this fitting in the current Sabre catalog (reference C-11) are as follows:

<u>Direction</u>	<u>Ultimate Load (lb)</u>
±Z	9975
±X	9144
±Y	1662

This fitting is a 17-4PH CRES casting, and a 25 percent casting factor, as well as the 33 percent fitting factor, apply. When the 25 percent casting factor is considered, the loads applied in the Z and Y directions are equivalent to those applied in the Ancra tests. However, the X-direction loads are nearly 40 percent higher. The Z and X loads result in an equivalent load of 13,500 lb applied at an angle of 47.5 degrees.

Based on the published information, the maximum load capacities which can be anticipated for the retention of a double-studded fitting are approximately as follows:

Vertical (Z)	8000 lb
Longitudinal (X)	9000 lb
Lateral (Y)	1600 lb

While the fitting may remain attached to the track under an 8000-lb vertical load, the cited Boeing documents imply that the underfloor structure will yield, and perhaps fail, under such a load.

## REFERENCES

- C-1 Vale, B., et al., SEAT DESIGN AND INSTALLATION CRITERIA, Document No. D6-9012, Boeing Commercial Airplane Company, Seattle, Washington, December 11, 1962.
- C-2 Slater, C., et al., SEAT DESIGN AND INSTALLATION CRITERIA, Document No. D6-10881, Boeing Commercial Airplane Company, Seattle, Washington, July 22, 1982.
- C-3 Military Standard, MS 33601, TRACK AND STUD FITTING FOR CARGO TRANSPORT AIRCRAFT STANDARD DIMENSIONS FOR, Department of Defense, Washington, D.C., July 1983.
- C-4 CARGO RESTRAINT EQUIPMENT CATALOG, Brownline Catalog No. 206, Brownline, Torrance, California.
- C-5 AIRCRAFT TRACK FITTINGS AND ATTACHMENTS, Ancra Catalog No. 401 B, Ancra Corp., El Segundo, California.
- C-6 TEST REPORT FOR THE FITTING ASSEMBLY - REAR LEG, SEAT, ANCRA P/N 40418-10 AND -11, Report No. 1040, Ancra Corp., El Segundo, California, December 17, 1970.
- C-7 TEST REPORT FOR THE FITTING ASSEMBLY - REAR LEG, SEAT, ANCRA P/N 40566-10 AND -11, Report No. 1058, Ancra Corp., El Segundo, California, August 24, 1971.
- C-8 TEST REPORT FOR THE FITTING ASSEMBLY - REAR LEG, SEAT, ANCRA P/N 40659-10 AND -11, Report No. 1077, Ancra Corp., El Segundo, California, July 14, 1972.
- C-9 QUALIFICATION OF SEAT TRACK FITTING (ANCRA P/N 42810-11), Report No. TR 607, Weber Aircraft, Burbank, California, August 1978.
- C-10 TEST REPORT FOR 43387-11 FITTING ASSEMBLY-TRACK ATTACH, Test Report No. 1335-1, Ancra Corp., El Segundo, California, August 24, 1979.
- C-11 TAKE A LOOK AT SABRE, Sabre Industries Catalog, Sabre Industries, Burbank, California.

## APPENDIX D

### LONGITUDINAL LOAD LIMITING

The design criteria presented in this report specify an 18-G longitudinal acceleration pulse with a 50-ft/sec velocity change. This pulse is illustrated in figure D-1 along with a number of load-limited pulses having the same velocity change. Load-limited pulses are shown for 8, 9, 10, and 11 G, and the relative displacement between the seat and the floor structure is shown for each of these. As discussed in the report, only about 6 in. of forward stroke appears to be practical for a transport seat due to space limitations. A 6-in. stroke was also used on designs developed in the past. Since the spacing between transport seats has been reduced, a stroke in excess of 6 in. is probably impractical.

As shown by figure D-1, a 6-in. stroke allows load limiting at 11 G. If the level of load limiting is set at 9 G, the required stroking distance becomes 12.3 in. which is clearly more than is available. Thus, it is impossible to design a seat for the design pulse which will limit the floor loads to 9 G and only stroke 6 in.

This observation leads to the question of what input pulse can be sustained by a seat load-limited at 9 G with a 6-in. stroke. As there are any number of answers to this question, it is useful to examine the following:

1. What is the velocity change of a triangular input pulse with a peak of 18 G that can be sustained with a 6-in. stroke and a 9-G limit load?
2. What is the peak G for a triangular input pulse with a 50-ft/sec velocity change that can be sustained with a 6-in. stroke and a 9-G limit load?

In the first case, it can be shown that a velocity change of approximately 35 ft/sec is associated with the 18-G peak pulse under the stated conditions. Higher peak accelerations can be tolerated if the velocity change is reduced appropriately; for example, a 36-G pulse with a velocity change of approximately 23 ft/sec. This combination of parameters is of particular interest since it is very similar to the test pulse proposed by Aviation Crash Research of Cornell University over 20 years ago. The recommended pulse was a half sine with a 35-G peak and a 30-msec duration. This was therefore the pulse used by the Hardman Company in developing a 9-G load-limited restraint system with a 6-in. stroke. The alternate design pulses are illustrated in figure D-2.

In the second case, it can be shown that a 11-G peak corresponds to the stated conditions. Due to the very low value of the peak, this pulse is not particularly interesting for a design criteria.

In view of the above, a transport seat cannot be designed for an 18-G, 50-ft/sec input pulse if a load of 9-G or greater cannot be transmitted to the floor tracks. The velocity change of the input pulse must be reduced or the floor tracks must support more load.



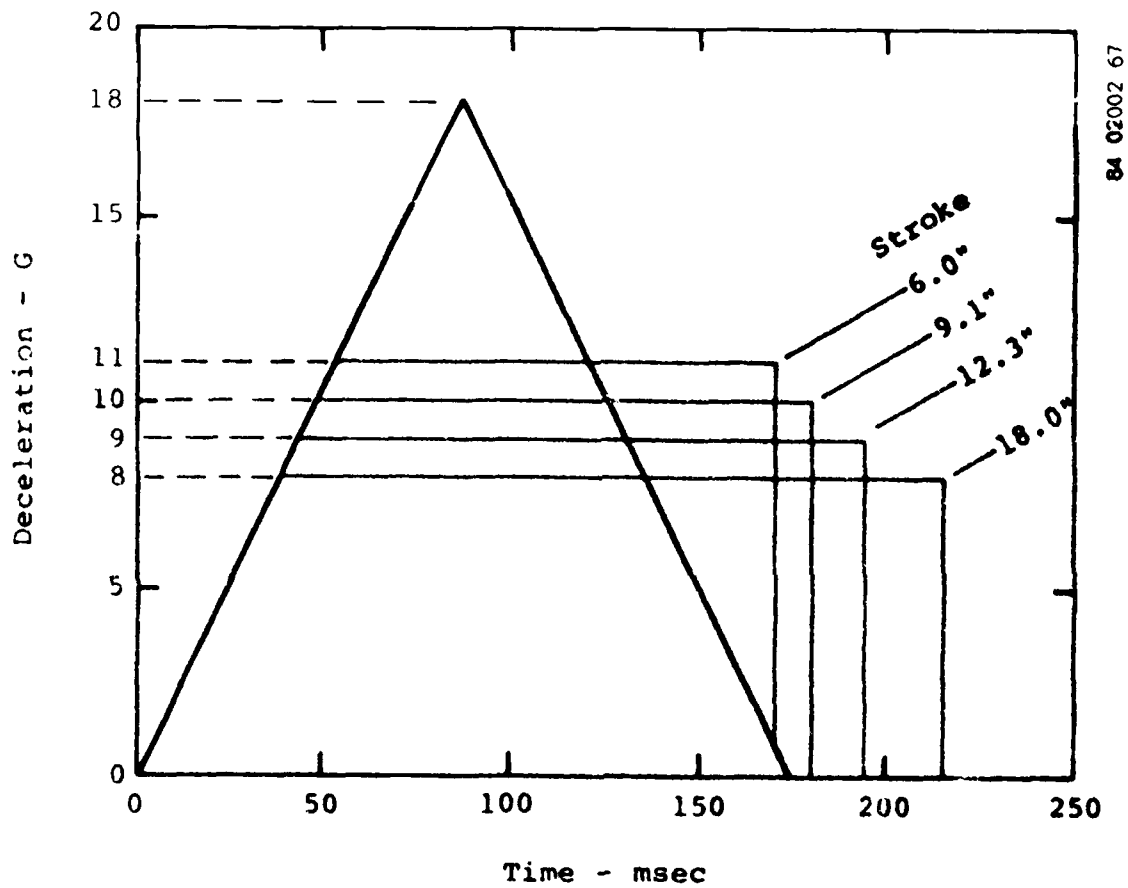


Figure D-1. Effects of various levels of load limiting.

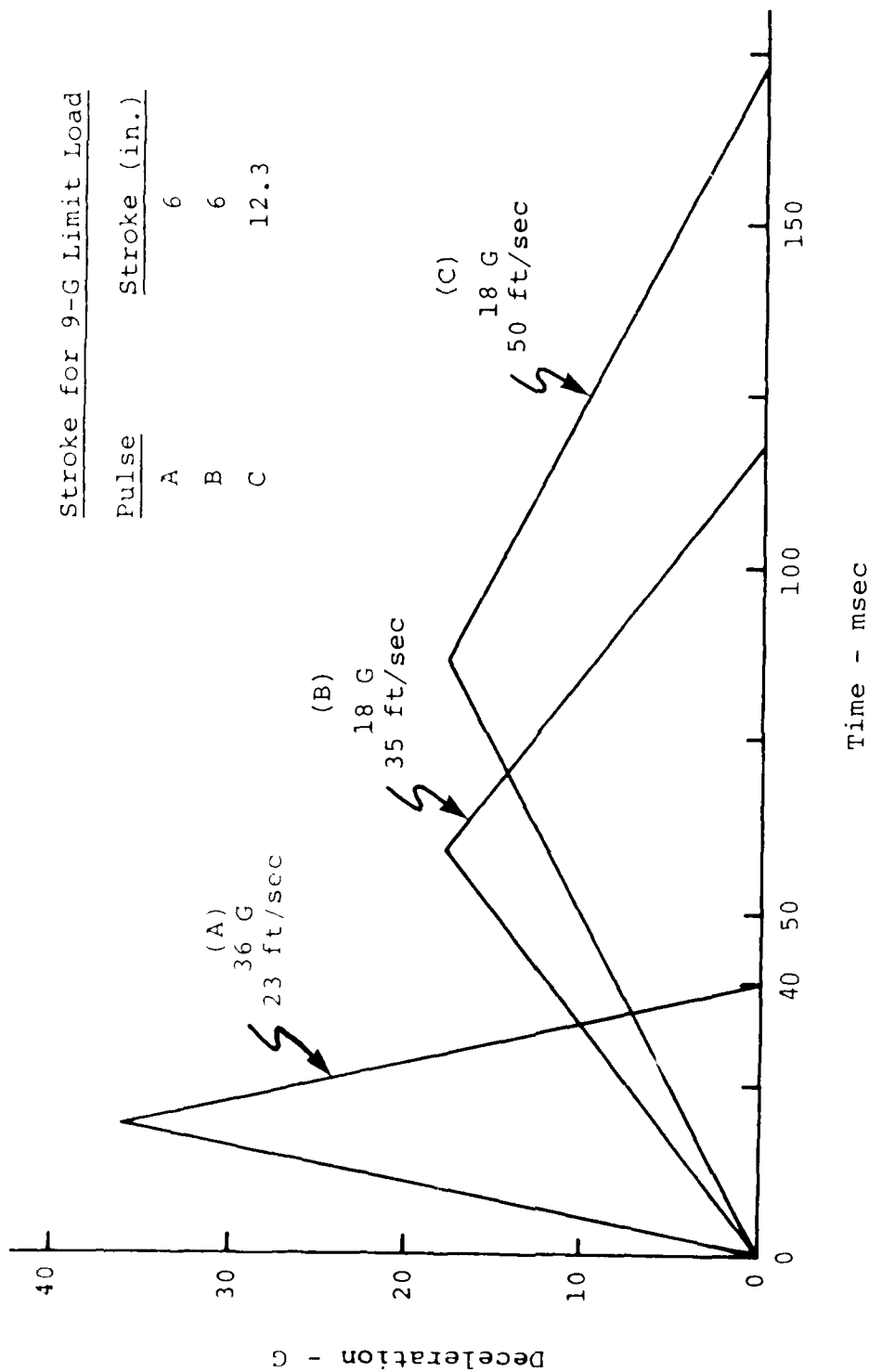


Figure D-2. Alternate design pulses.

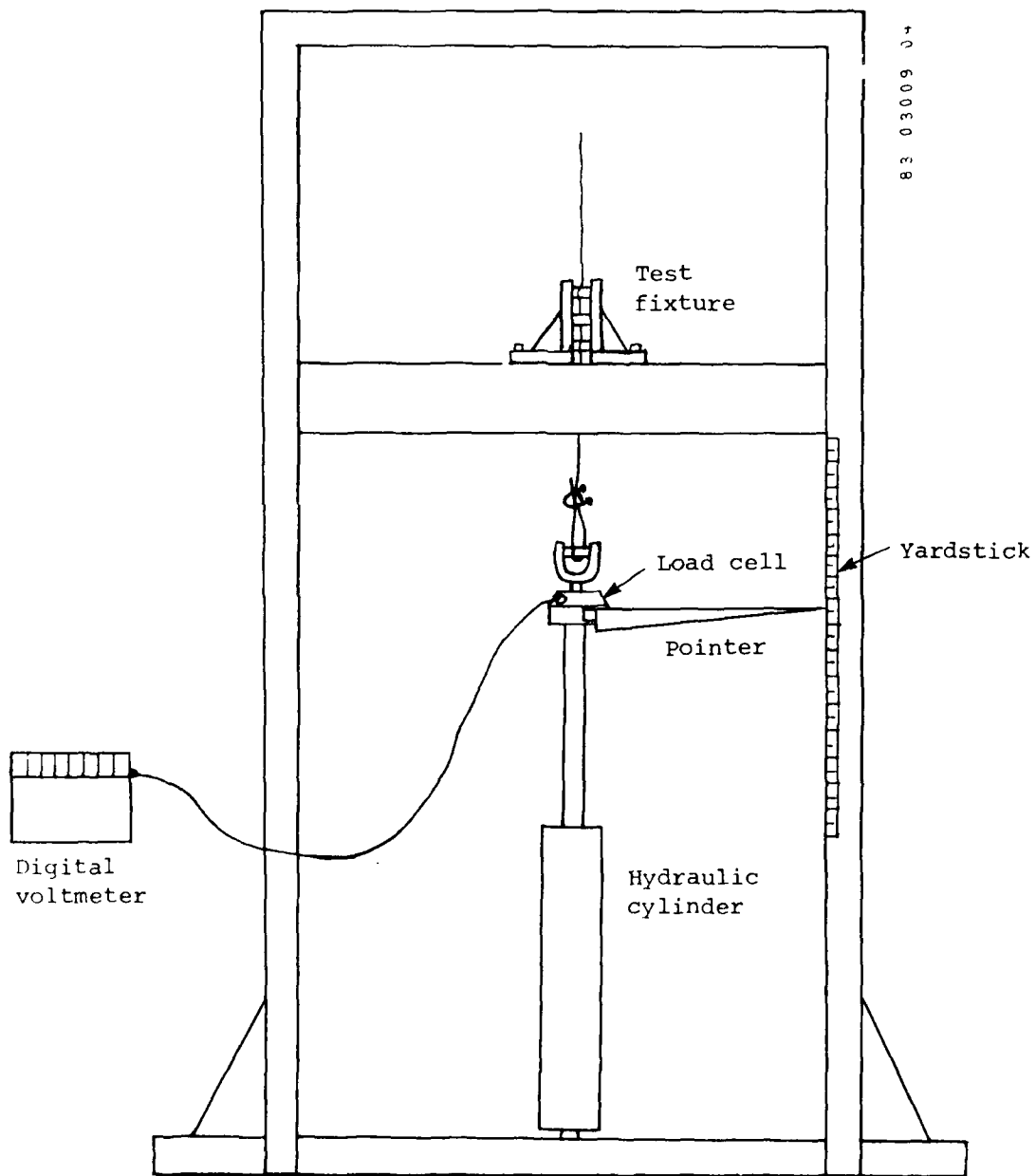


Figure G-2. Wire-pulling test apparatus.

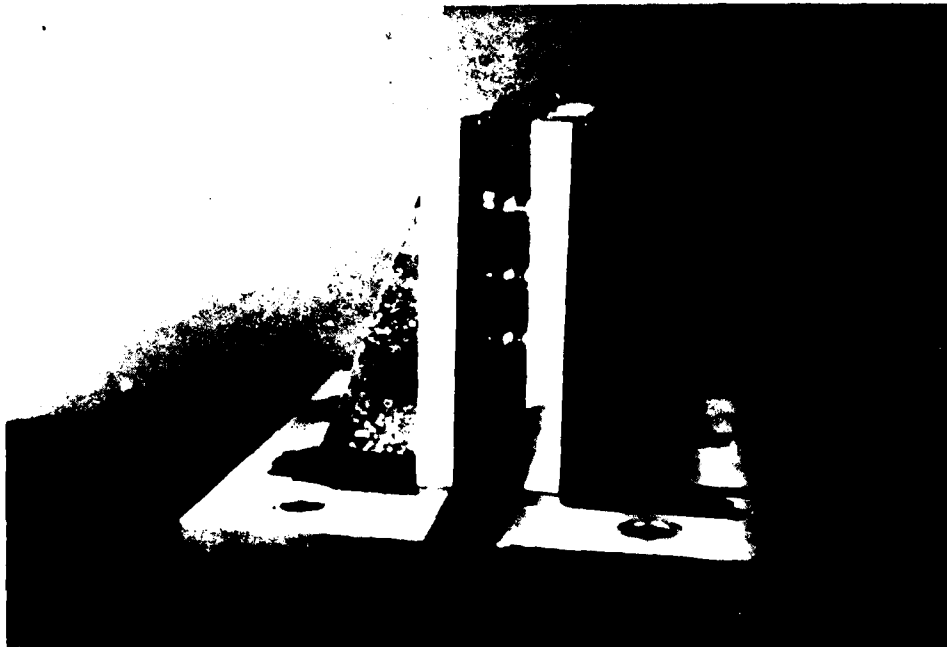


Figure G-1. Wire-pulling test fixture.

## APPENDIX G

### LAP BELT ENERGY ABSORBER COMPONENT TESTS

This appendix describes component tests associated with the lap belt energy absorbers to determine how certain parameters affected their load attenuating abilities.

In order to collect data on wire-pulling forces, the test fixture in figure G-1 was fabricated. The fixture was designed to allow the use of various wire diameters, various roller spacings, and either single or double wires. It consists of three identical aluminum rollers, 0.850 in. in length, which roll on 5/16-in., hardened steel pins. No lubrication is used. The center-line distance between the top and bottom rollers can be set between 1.70 and 2.70 in. The radius at which the wire bends around the rollers is 0.300 in. In an effort to keep the friction between the rollers and wires constant throughout the test, the wire was pulled at 2 in./min.

The complete test assembly is shown in figure G-2. A load cell was placed on the end of a hydraulic cylinder and used to measure the pulling force. Music wire was looped through the fixture and attached to the load cell. The test fixture was bolted to the top of two steel channels and aligned with the axis of the hydraulic cylinder. The pull rate of the wire was determined by using a pointer attached to the load cell and a yardstick attached to the test frame. A digital voltmeter connected to the load cell indicated the pulling force.

Tests were performed by first pulling slack out of the music wire. Next, the rate at which the wire was pulled was determined by comparing the distance the pointer moved along the yardstick to the sweep hand of a wristwatch. The hydraulic cylinder controls were adjusted until the rate was 2 in./min. When the rate became steady, the pulling load was read off the digital voltmeter and recorded. The test was then stopped and the distance between the top and bottom rollers was increased to the next increment. The test was run again for a new load reading and then repeated for successive roller distance increments. After the range of roller increments had been tested, the entire procedure was repeated for a different diameter of music wire.

Results from the tests are shown in table G-1. The column titled "No. of Wires" indicates whether single or double wires were pulled, "Roller Spacing" is the distance in inches between the top and bottom rollers (the middle roller is exactly between the two), and "Load" is the pulling force at 2 in./min.

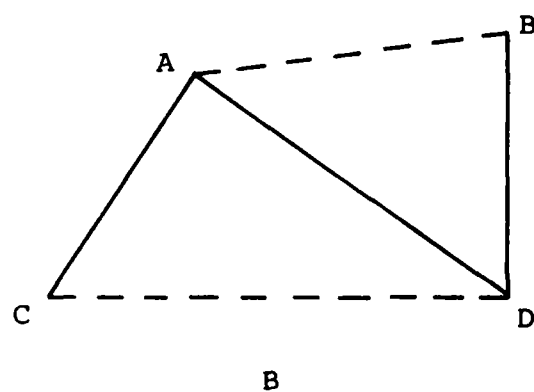
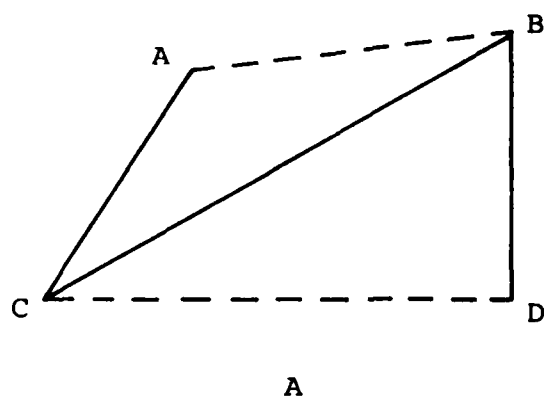
The load range that is applicable for the lap belt energy absorber is between 700 and 1,000 lb. Therefore, the wire diameters of interest are .094 and .125 in. The results from table G-1 for these diameters are plotted in figures G-3 and G-4. From these graphs, it is apparent that there is an approximate linear relationship between the roller spacing and the load. This characteristic facilitates the specific selection of wire diameter and roller spacing for a particular force that may be required for a specific lap belt energy absorber.

- The forward load on the highly-loaded rear track fitting is approximately 30 percent less, due to the direct transfer of forward load to the front track fitting (with all fittings assumed locked).
- No loads need to be carried between points A and B in order to transfer forward loads applied at point A to the floor track, i.e., no longitudinal brace is required between the top of the legs.

The tension brace offers an advantage that is not apparent from examination of the leg assembly itself. However, this advantage is quite apparent when the complete load path from lap belt anchorages to floor track is considered. Since the belt anchorages are not located in the plane of the leg assembly, the rear tube must carry the loads to point A on the leg assembly. This loads the rear tube in bending. If the front tube is restrained in the forward direction, as it is with the tension brace, these loads can be divided between the front and rear tubes. The existing seat pan structure will distribute the load very effectively since the lap belt anchorages are connected to the spreaders which run fore and aft between the front and rear tubes.

As a result of comparing the tension and compression brace arrangements, it is apparent that the redundant truss illustrated by figure F-1C is preferable for this application. The load carried by the various members will be dependent upon their sizing, but various benefits will be derived. The diagonal compression member transfers some forward load to the front track fitting, the compression load in the front leg will be less than it would if only the tension brace were used, and the front tube of the seat pan is supported by the tension brace, so that it can assist the rear tube in reacting the forward loads at the lap belt anchorages.

Either arrangement with a single diagonal would require at least a light member in position CD to maintain the proper leg spacing during installation on the floor tracks. The arrangement with both braces requires no member in this position. Since it also requires lighter members in position AB, there is no appreciable weight penalty associated with this design.



→  
Forward

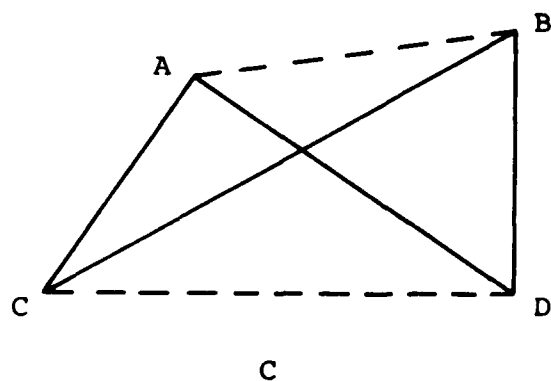


Figure F-1. Leg bracing option.

## APPENDIX F

### LEG BRACING OPTIONS

Several longitudinal bracing arrangements were examined for the leg assemblies. These included the tension brace (CB) (figure F-1A), the compression brace (AD) (figure F-1B), and the combination of the two braces (figure F-1C). The longitudinal members, AB and CD, could be either members in the leg assembly or load paths provided by existing seat pan and floor structure.

Initially, the tension and compression braces of figures F-1A and F-1B were compared. It was assumed that the leg assembly would have 3500-lb forward and upward loads applied at point A, and a 3500-lb downward load at point B. (Due to the position of the leg assemblies under the seat, the assembly on the window end must support approximately two-thirds of the loads applied in the forward direction. If the forward load is 9 G, each occupant weighs 170 lb, and the seat weighs approximately 80 lb, then two-thirds of the forward load is approximately 3500 lb. Since the c.g. of the occupants is about a foot above the seat pan, there is a moment acting on the leg assembly in addition to the forward load. Since the tops of the front and back legs are just over a foot apart, the moment is approximately equivalent to that formed by 3500-lb forces acting up on the rear leg and down on the front.) Under these conditions, the following loads must be carried by the members of the two configurations:

	<u>Figure F-1A</u>	<u>Figure F-1B</u>
AC (rear leg)	3500	4900
BD (front leg)	-4100	-3500
BC	2100	NA
AD	NA	-1300
AB	-1900	0

Due to the geometry of the seat, a compression brace (AD) would support only 60 percent of the load that a tension brace (BC) would. A compression brace would also be approximately 30 percent shorter. Therefore, the advantages usually associated with tension members are somewhat less significant in this case.

Advantages that can be attributed to the compression brace arrangement are as follows:

- The compressive loads in the front leg (BD) are not increased as they are in the case of the tension brace.
- Since other loading conditions will size the rear leg (AC), it can easily support a 4900-lb load with no more material than would be used to support a 3500-lb load. This leg is therefore used more efficiently with a compression brace, in the forward loading condition.



It would be extremely difficult to make an accurate assessment of the actual effect of all these factors. However, it is assumed, based on known characteristics of belt webbing and seat cushion foam, that these combined effects may cause the angle swept out by the lap belt on the Weber seat to be 55 to 40 degrees rather than 70 to 50 degrees. A system using the first method of lap belt energy absorption would experience a change of more than one-third the forward load component during 6 in. of forward stroke. This, combined with occupant retention considerations, seems to indicate the use of the second method.

There are additional factors to be considered in the design of such a system. One is that any energy-absorbing hardware added to an existing seat may raise the pivot point of the lap belt anchorage, in turn causing the angle change associated with 6 in. of forward motion to increase. Thus, the load variation cited in the paragraph above would be a function of the particular design but would be greater than one-third. Another consideration is that the mechanism used in method two need not be mounted horizontally. If it is tilted upward to the front, the perpendicular load acting on the device can be reduced in lieu of a slightly larger stroking load, and some weight savings can probably be achieved. Since the seat pan on the Weber seat is already at an angle of about 10 degrees, it is also desirable to place the energy-absorbing mechanism at an angle to prevent the belt from being effectively tightened as the occupant slides forward. A third consideration is that any friction between the occupant and the seat pan will increase the load on the seat over that applied by the energy-absorbing devices. The effects of friction are difficult to predict, and dynamic tests will be necessary to assess these effects. It is recognized that the second method of lap belt energy absorption, since it holds the occupant down to the seat, may increase this load component in relation to the first method. Also, all lap belt energy absorbers are affected by vertical inertial loads which change the frictional loads between the occupant and the seat.

The above discussion pertains to rather general considerations for lap belt energy-absorbing seat design and seat structure geometry. For the crash test program, there are some more specific concerns relating to interference with other hardware on the seat.

For example, on the Weber seat the location of the energy-absorbing devices causes an interference with the Hydrolock back adjustment mechanisms. It was decided to remove the Hydrolocks from the seat, if necessary, based on the following reasoning: the selected form of the energy-absorbing mechanisms will probably not represent a feasible seat retrofit, and they would probably be feasible only on a new seat designed to incorporate such a feature. Therefore, in this case, it is a concept for enhanced crash survival which is being tested rather than a feasible retrofit kit for an existing transport seat. The Weber seat is simply a test bed for evaluating a new concept in this modification, and it is more important to successfully demonstrate the effectiveness of the concept than it is to retain all of the comfort and convenience features found on the seat. In a new seat design, the adjustment mechanism could easily be moved to avoid interference with the lap belt energy absorbers.

#### REFERENCES

- E-1 Molony, G., THE INTERIOR DESIGN OF WIDE-BODIED AIRCRAFT, American Institute of Aeronautics and Astronautics, New York, N.Y.

at 9 G, the forward component of the stroking load will exceed the ultimate strength of the seat long before 6 in. of motion has occurred. On the other hand, if the energy absorber is designed so that the occupant begins stroking at 4-1/2 G (so that 9 G will not be exceeded at 6 in. of stroke) only two-thirds as much energy will be absorbed in the 6 in. of stroke. Therefore, the occupant will stroke further than necessary for any specific crash pulse and will be more susceptible to injury due to impact with the seat ahead of him. In a severe crash, he may exceed the capacity of the device and still be subjected to seat failure.

On a seat structure with the lap belt anchorage as far forward as it is on the Weber seat, the second method of lap belt energy absorption seems to be the only acceptable approach. The forward stroking load will then be a constant 9 G. However, very large lap belt angles cause high vertical load components and can cause the mechanisms to become relatively heavy. For a 70-degree lap belt angle, a 9-G forward load component with a 170-lb occupant results in a 2,100-lb vertical load on each belt anchorage  $((9 \times 170 \times \tan 70^\circ)/2)$ . Thus, large lap belt angles compromise the function of the first method of lap belt energy absorption and also introduce weight penalties in the second method.

It should be noted that, although relatively small lap belt angles, such as are found on the Hardman seat, simplify the design of a lap belt energy absorber, such small angles are not desirable from the standpoint of occupant retention. A shallow angle may permit the belt to slip over the pelvis so that the occupant "submarines" under the belt. This may cause crushed internal organs and fracture of the spine.

Therefore, neither of the belt angles found in these two seats is desirable. Small angles provide inadequate occupant retention, and large angles complicate the design of the lap belt energy absorber. From the standpoint of enhanced crash survival with a lap belt energy absorber, the ideal belt angle (under static conditions) would be 45 to 55 degrees. This would optimize occupant retention without introducing excessive weight penalties in the lap belt energy absorber. Unfortunately, the economic realities of present-day air travel prevent selecting the desired belt angle. The seating density requirement of a competitive air transport operation will probably always require large belt angles, such as are found on the Weber seat.

Another consideration for the design of a lap belt energy absorbing device is the actual angle of the belt at the time the inertial load reaches 9 G. Initial angles in the previous discussion were based on a 50th-percentile occupant seated under static conditions with the lap belt tightened snugly about his body. There are a number of factors which will cause the angle of the belt to decrease before the inertial loads of the crash reach 9 G. These include the following:

- Many occupants can be expected to wear the belt loosely.
- The belt is somewhat elastic and will stretch.
- The foam seat cushion under the occupant will be crushed due to the vertical load component in the belt and also due to any vertical component in the crash pulse.
- The occupant's body will deform.

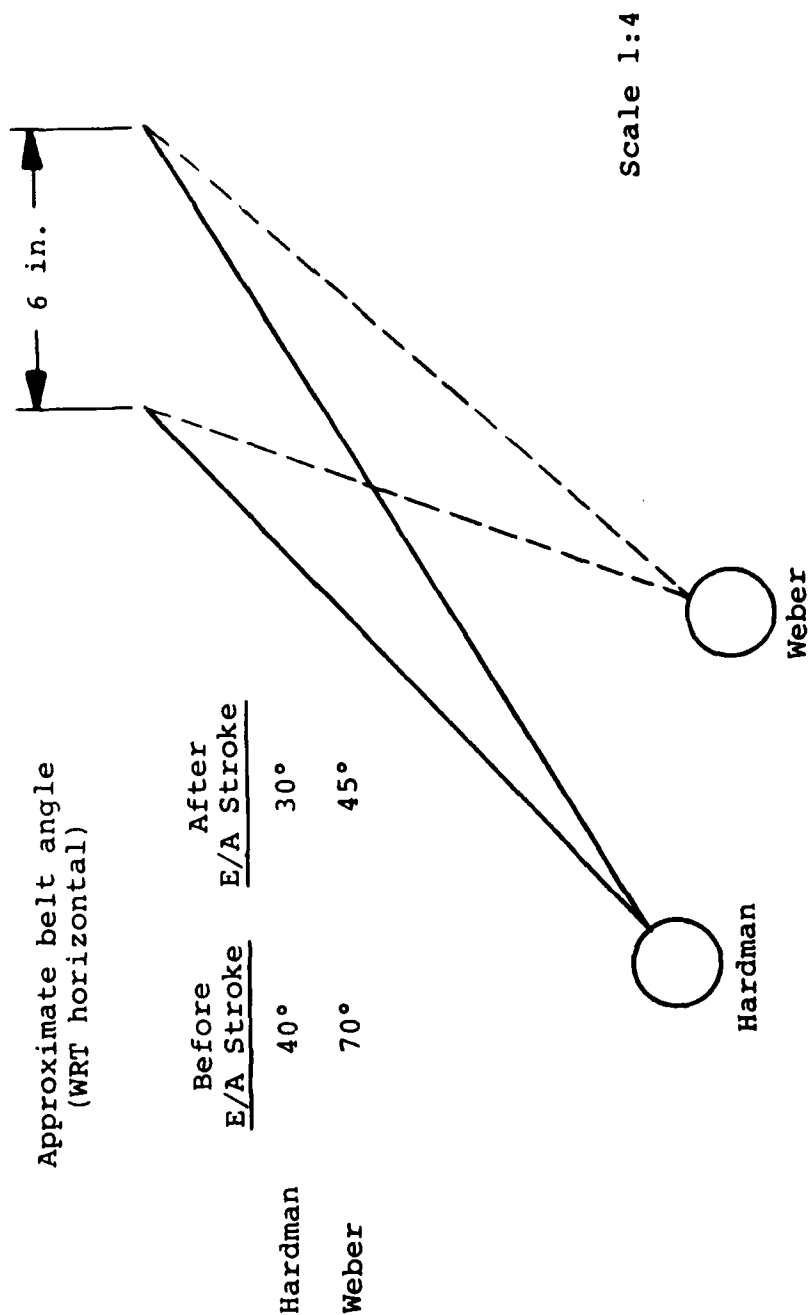
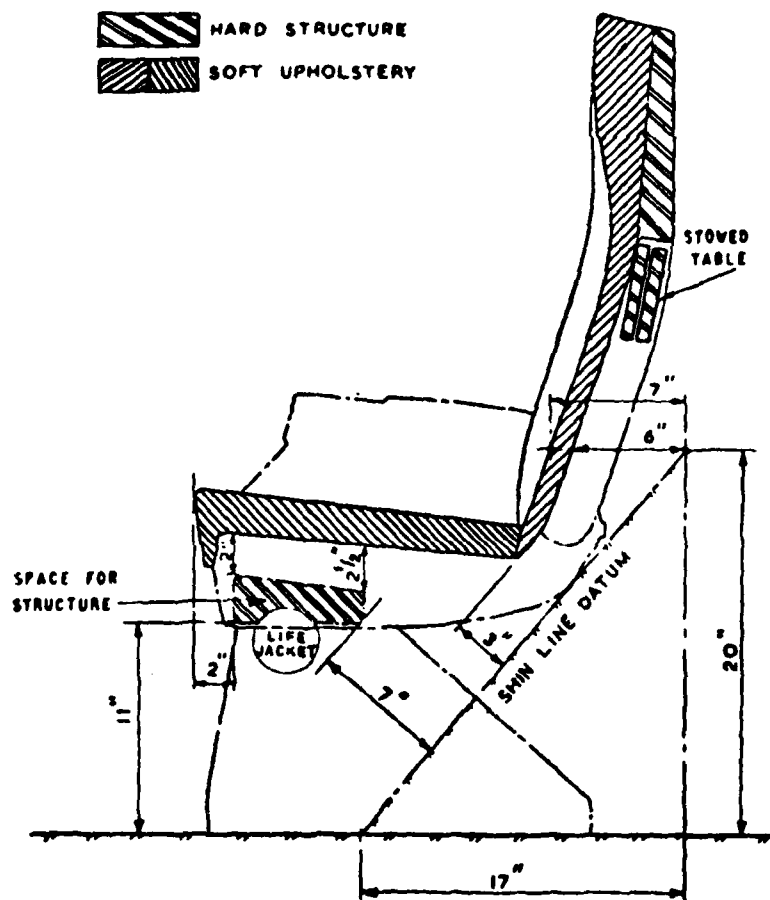
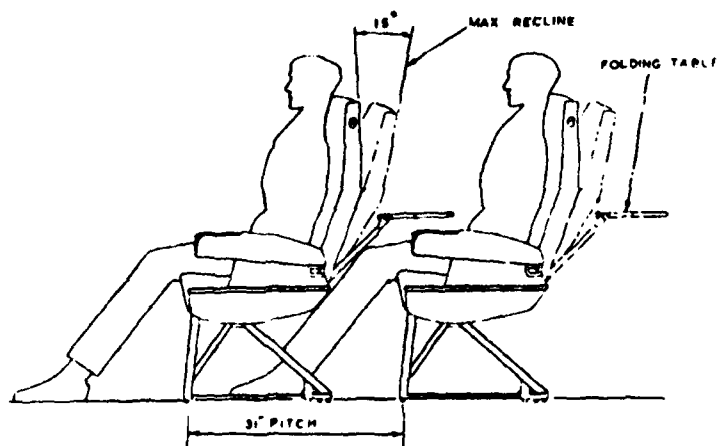


Figure E-4. Position of rear seat tubes and lap belts.



A. Seat basic envelope.



B. High density seating.

Figure E-3. Transport seat design criteria for a 31-in. pitch.

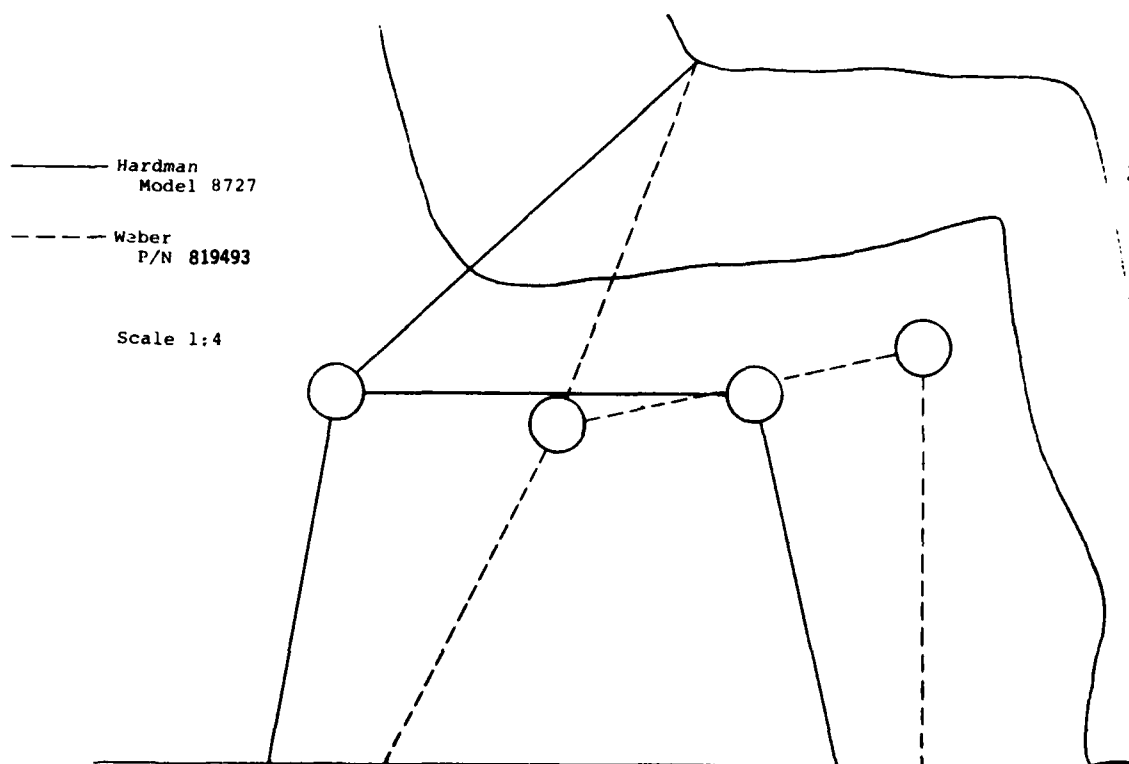


Figure E-2. Relative locations of structural components in Hardman and Weber seats.

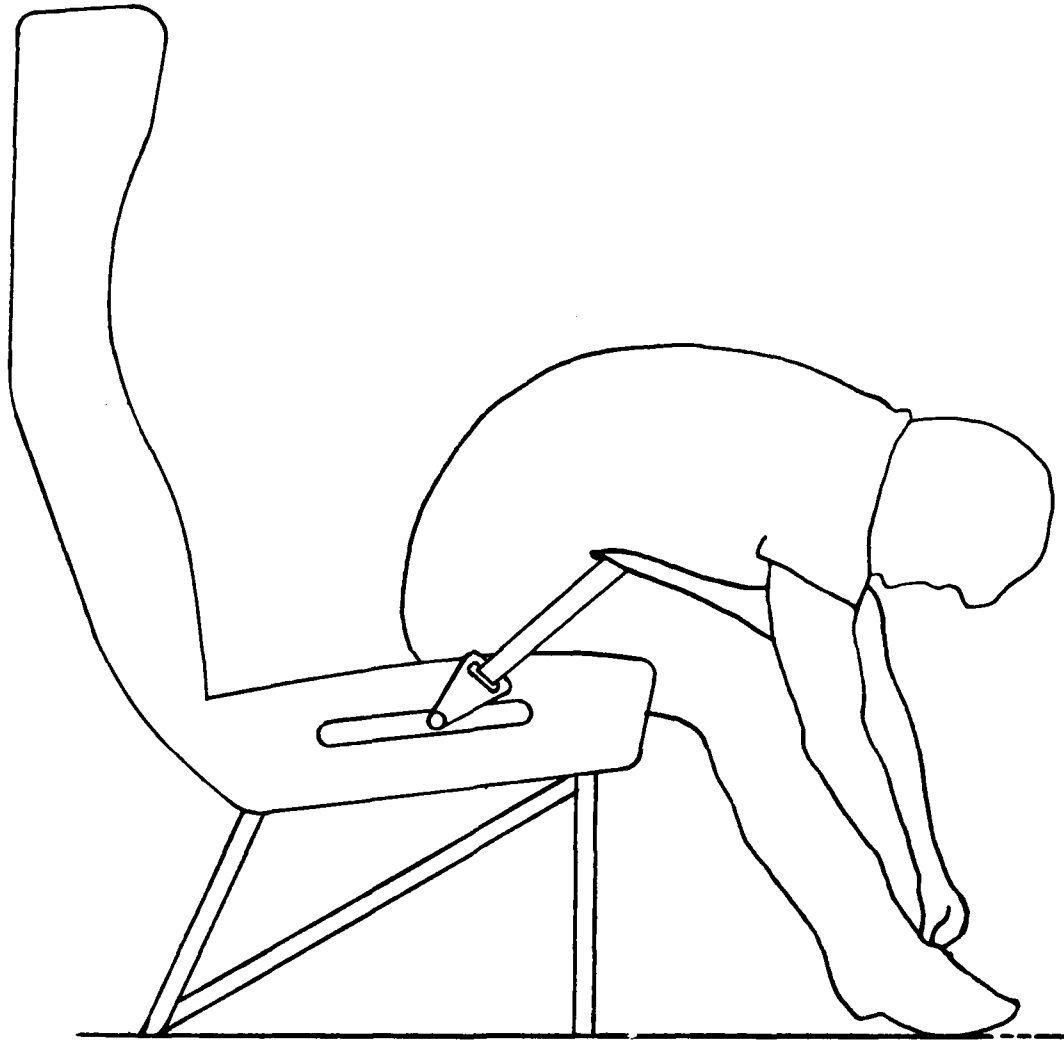


Figure E-1. Guided lap belt energy absorber.

The purpose of the lap belt energy absorbers is to limit the inertial loads that the occupant will apply to the seat structure in a crash, and thereby prevent ultimate failure of that structure. There are two methods for employing lap belt energy absorbers.

In the first, an energy-absorbing device is simply placed in series with the lap belt anchorage. As discussed in this report, this method was employed by the Hardman Company 20 years ago. A more efficient design for this method was planned for use in the crash test program.

The second method is illustrated in figure E-1. This involves using the energy-absorbing device to limit only the forward load component on the lap belt anchorage while the vertical load component is reacted by a sliding or rolling mechanism.

There are obvious tradeoffs between the two methods. The first method is the simpler and the more easily adapted to a seat retrofit program. The second requires less compromise of occupant retention since he is still held down against the seat pan even though he can slide forward.

Examination of the details of transport seat designs reveals there are also more subtle factors which affect the tradeoff between the two lap belt energy absorption methods. For example, the fore/aft position of the lap belt anchorage is a major factor influencing the effectiveness of the two methods. Figure E-2 shows the relative locations of the structural tubes in the Hardman Model 8727 and the Weber P/N 819493 seats. From this sketch, it is apparent that all structural components are moved forward on the Weber seat relative to the occupant and to the Hardman seat. As is illustrated by the discussion in reference E-1, the arrangement of the Weber seat is intended to allow an increase in seating density by creating more occupant leg room at the rear of the seat. Boeing Aircraft Drawing No. 65-14534 shows that the Hardman seats were placed at a 36-in. pitch in the Boeing 720. Later seat designs, such as the Weber P/N 819493, were spaced at a 30 to 32-in. pitch. Figures E-3a and E-3b, reproduced from a publication entitled (The Interior Design of Wide-Bodied Aircraft), show some transport seat design criteria for a pitch of 31 in.

The effect of the structural geometry of the seat on the function of a lap belt energy absorber is illustrated in figure E-4. On the Hardman seat, the initial lap belt angle is approximately 40 degrees (with respect to horizontal). After the occupant slides forward 6 in., it becomes approximately 30 degrees. For the Weber seat, it is initially 70 degrees and the 6 in. of forward stroke reduces it to approximately 45 degrees (assuming the occupant does not slide under the belt).

In-series lap belt energy absorbers will be more efficient on the Hardman seat. If the energy absorbers begin to stroke at 9-G forward load on the Hardman seat, it will require 10.18 G to stroke them the entire 6 in. ( $9 \times \cos 30^\circ / \cos 40^\circ$ ). Likewise, if they are designed to begin stroking at a 9-G forward load on the Weber seat, it will require 16.9 G to stroke them the full 6 in. Thus, the forward component of the stroking load changes 88 percent on the Weber seat but only 13 percent on the Hardman seat for a 6-in. forward motion.

For these reasons, the simple, in-series form of lap belt energy absorbers appears unsatisfactory for the Weber seat. If the energy absorber begins stroking

APPENDIX E

TI 83404

LAP BELT ENERGY ABSORBERS

A SUMMARY OF DESIGN CONSIDERATIONS  
FOR SEAT EXPERIMENTS FOR  
THE CRASH TEST AIRCRAFT

Simula Inc.

February, 1983



TABLE G-1. WIRE PULLING TEST RESULTS

Wire Diameter	No. of Wires	Roller Spacing (in.)	Load (lb)	Comments
.063	2	1.70	240	
.063	2	2.10	180	
.063	2	2.70	90	
.080	2	1.70	520	
.080	2	2.10	380	
.080	2	2.70	190	
.094	2	1.70	890	
.094	2	1.90	740	
.094	2	2.10	640	
.094	2	2.30	540	
.094	2	2.50	430	
.094	2	2.70	350	Two top rollers would not turn at 2 in./min. Began turning at 4 in./min. and load went to 380 lb.
.125	1	1.70	1100	
.125	1	1.90	1010	
.125	1	2.10	840	Bottom roller turned intermittently
.125	1	2.30	720	
.125	1	2.50	600	
.125	1	2.70	540	Only middle roller turned at 2 in./min.

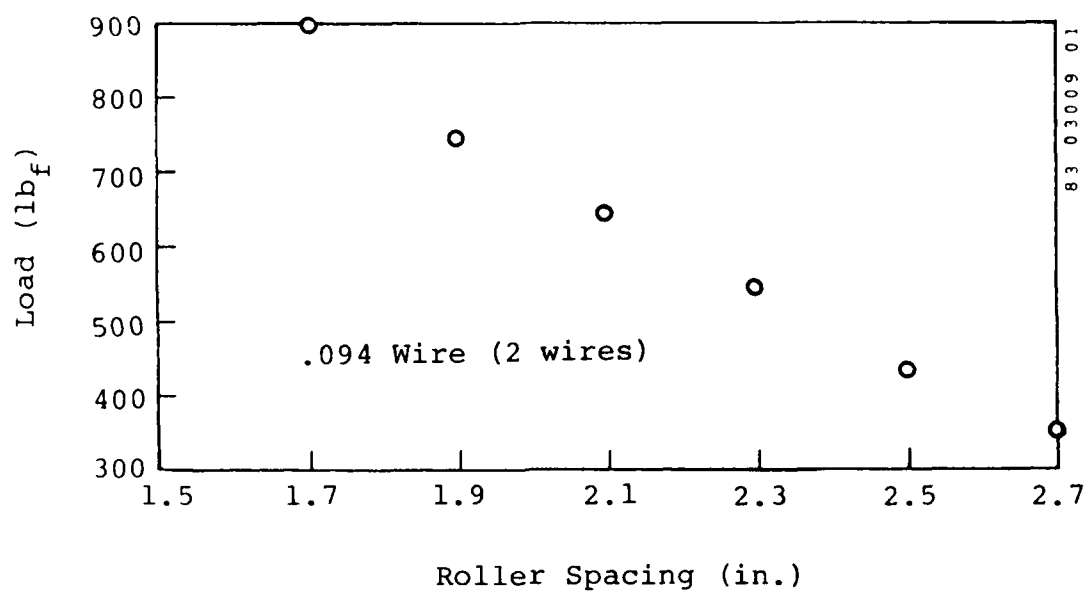


Figure G-3. Wire-pull results for .094 wire.

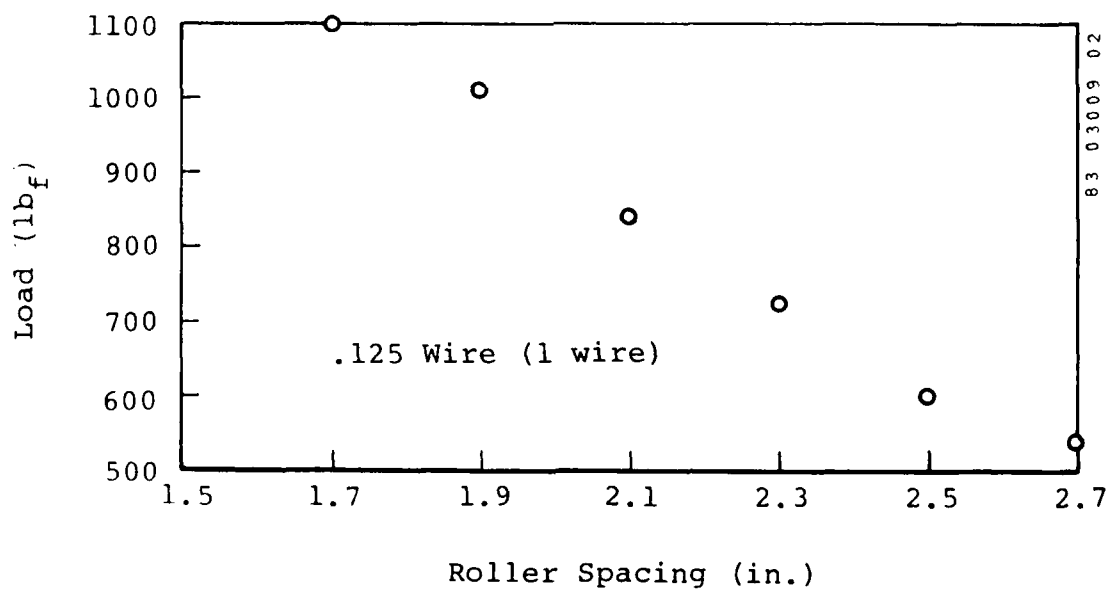


Figure G-4. Wire-pull results for .125 wire.

**END**

**FILMED**

**7-85**

**DTIC**